

STAT

AIR TECHNICAL INTELLIGENCE TRANSLATION

(Title Unclassified)
THEORY OF AVIATION GYROSCOPIC INSTRUMENTS
(Teoriya Aviatsionnykh Girokopeskikh Priborov)

Author: A. S. Kozlov

Source: State Publishing House For The
Defense Industry

Moscow

1956

256 Pages

STAT



STAT

A.S.KOZLOV

THEORY OF AVIATION GYROSCOPIC INSTRUMENTS

Approved by the Central Administration
of Higher Polytechnic and Machine-Building
Schools, Ministry of Higher Education USSR,
as a Text Book for Higher Aviation Schools

State Publishing House for the Defense Industry

Moscow 1956

STAT

This book gives the principles of the general theory of gyroscopes. The use of gyroscopes with displaced center of gravity to indicate the vertical and meridian is discussed. The principles of designing gyroscope correction systems are stated. The behavior of corrected gyroscopes on fixed and moving bases, and the theory of gyro horizons, gyroscopic course indicators and rate gyroscopes is discussed. Fundamental information is given on power gyroscope systems.

The book handles separately questions related to the principles of constructing correction systems and the behavior of corrected gyroscopes on fixed and moving bases, as questions common for all gyroscopic instruments. Particular attention is paid to questions connected with the use of gyroscopic instruments in flight: errors of instruments in flight, longitudinal accelerations, in turns and other maneuvers, as well as methods of diminishing these errors.

Reviewers: B.A.Ryabov, Doctor of Technical Sciences,
S.S.Tikhmenev, Doctor of Technical Sciences
Scientific Editor, M.S.Kozlov, Candidate in Technical
Sciences

Editor-in-chief,

Engineer A.I.Sokolov

STAT

PREFACE

The study of the aviation gyroscope has developed widely during the past 10-15 years. If we speak of the main trend of this development, it consists in the effort to increase the reliability of operation and increase the accuracy of gyroscopic instruments and units. This trend in development has been due to the continuous increase of the range, speed, and altitude of flight. As has been shown by experience, the most effective way of improving the reliability of operation and increasing the accuracy of gyro instruments and units is the development of the aviation electro-gyroscope, a fact that was well understood by our designers and production men, who, as far back as 1936-1937, produced in series production, completely electrified directional gyroscopes for use in autopilots, where the demands on the reliability of operation and accuracy of reading are particularly stringent.

The development of USSR aviation gyroscopy is based on the works of the Russian classical school of mechanics, Soviet scientists and specialists, who have created the theory of gyroscopic instruments, which has been formed today into an independent scientific discipline. First of all we must point out the fundamental works of Academician A.N.Krylov (Bibl.1) and B.V.Bulgakov (Bibl.2), corresponding member AN SSSR. These works, in the richness of their content and the combination of profound theoretical development of the questions with an engineering approach to the problems under consideration still remain unexcelled. It would not be an exaggeration to say that the modern Soviet school of gyroscopists has grown up and is developing precisely on the basis of the ideas that have been worked out and

developed in these works.

It must, however, be noted that a number of textbooks and manuals on aviation gyroscopy possess the shortcoming of being based on the description of individual gyroscopic instruments without an appropriate methodological generalization. This is all the more to be regretted because the above mentioned works by Krylov and Bulgakov and a large number of works by other Soviet authors, which will be cited in the present book, do provide adequate material for the generalizations and developments of the theory of aviation gyroscopic instruments that are necessary from the pedagogical and methodological point of view.

An attempt has been made in this book to fill in this lacuna.

In the compilation of this book the works of the late A.S.Kozlov on the theory of aviation gyroscopic instruments, published by VVIA imeni Zhukovskiy, have been utilized.

In connection with the development of the theory and technology of gyroscopic aviation instruments, during the last few years, it has become necessary to expand the theoretical point of the book and to include in it a number of questions devoted to the principles of operation of the most recent instruments. This work was done by H.S.Kozlov.

Professors V.A.Bodner, A.A.Krasovskiy, and G.O.Fridlender, together with instructor B.V.Komotskiy, took part in preparing this book for the press.

INTRODUCTION

Of the instruments based on the utilization of the properties of the gyroscope, the following are used in aviation:

1. Indicators of the aircraft position with respect to the earth, i.e., indicators of the angles formed by the aircraft axes with the corresponding axes bound to the earth. Such instruments include gyroscopic course indicators and gyrohorizons.

2. Indicators and devices for measuring angular velocities and rotary accelerations of an aircraft about its axes. These instruments include the widely known "turn indicator", that is, an indicator of angular velocity of rotation of an aircraft about its normal axis. This group also includes devices for measuring angular velocities and angular accelerations of the rotation of an aircraft about its axes, which are used in autopilots.

Common to all gyroscopic instruments is the presence in each of them of a rotor, rapidly rotating or vibrating, and possessing a sufficiently high moment of inertia with respect to its axis of rotation or vibration. The properties inherent in an instrument with such a rotor, and the phenomena thereby caused, will be termed gyroscopic, and the rotor itself a gyroscope.

The rotor is caused to rotate either by means of an air jet, or by electrical energy. Accordingly, gyroscopes are divided into pneumatic and electrical.

The rotors used in gyro instruments usually have three or two degrees of freedom, which are provided by the corresponding gimbal suspension with two frames or

STAT

with a single frame.

In instruments of the former group, that is, in gyro angle-measuring instruments, the frame of the gimbals, which serve as bearings for the rotor spindle, is called the inner frame, while the frame serving as the bearing for the spindle of the inner frame is termed the outer frame of the suspension. By adding to the number of degrees of freedom of the gimbals, still another degree of freedom of rotation about the axis of the rotor, we obtain the total number of degrees of freedom for the material parts of the rotor equal to three.

A rotor in gimbals is therefore usually called a gyroscope with three degrees of freedom.

If in such a gyroscope the center of gravity of the system coincides with the center of the bearing, then in this case it is called astatic, since the force of gravity will have no effect on the position of the axis of its rotor. If in addition we assume the absence of friction in the bearings of the gimbals, and the absence of systems imposing moments on the gyroscope as its position varies, then we get a gyroscope that is usually called a "free" gyroscope, since such an instrument will remain free from the influence of any forces and moments, not only in any position of the rotor axis, but also under any variation of the position of the base of the suspension.

In instruments of the second group, which are designed to determine angular velocities or to measure them, the suspension of rotor has one gimbal, the displacement of which is resisted by a spring. We shall term such gyroscopes, gyroscopes with two degree of freedom*.

In an instrument designed for the simultaneous measurement of angular velocity and angular acceleration, which are used in autopilots, the rotor gimbals have two

*They are sometimes called "precessional", but we shall not use this term, since every gyroscope is, in fact, "precessional".

STAT

frames, the displacement of which is resisted by a spring.

In instruments designed for the measurements of angles, moments are imposed on the gyroscope with the object of giving the rotor axis selectivity with respect to the direction to be determined by means of the given instrument.

This object is accomplished either by using the force of gravity of the gyroscope, i.e., by a corresponding displacement of the center of gravity with respect to the point of support, or else by means of a system specially added to the gyroscope, which is termed a correction system.

According to the type of energy used in the correction system with the object of producing the positional moments, these systems are divided into mechanical, aerial, and electrical.

The problem of aviation gyroscopy has been and still remains, primarily connected with the need for determining the position of an aircraft with respect to the earth axes, the geographic meridian and the vertical of the place, whether for visual purposes or to make piloting automatic. In other words, this is the problem of the artificial gyro horizon, i.e., of an instrument indicating the direction of the geographic meridian.

Long before the need of such instruments for aviation was first felt, instruments used for this purpose existed and were employed in marine navigation. But the principles on which the marine gyrocompass (pendulum gyrocompass) and the marine gyrohorizon (gyro-pendulum vertical) were based proved inapplicable for aviation.

This was due to three circumstances: the great accelerations in aircraft, the unsuitability for the conditions of installation on an aircraft, of the dimensions and weights of the pendulum gyrocompass and the gyro-pendulum vertical, and the duration of the transient states inherent in these instruments, a duration that made them inapplicable to aviation conditions.

Other methods of determining the direction of the vertical and meridian also exist. They are the use of a physical pendulum of one form or another to determine

STAT

the vertical, and the use of the magnetic needle to determine the course. It must be noted that the application of the magnetic needle, that is, of the magnetic compass, has found its place in aviation, and has not lost its importance down to the present day. But by itself it does not exhaustibly solve the problems of the aviation compass. The inadequate stability of the compass card, the strong influence on magnetic compass of turns, and of acceleration in general, the influence of units with steel parts, varying their position with respect to the compass card with varying course of the aircraft, as well as the influence of stray magnetic fields due to electrical and radio equipment, all these lead to the necessity either of replacing or of supplementing the magnetic compass by a gyroscopic instrument free from the above enumerated shortcomings of the magnetic compass. As for the use of the physical pendulum on the aircraft to determine the direction of the vertical, this did not give a good account of itself at all, although attempts of this nature were, indeed, made; in other words, the solution of the problem of building a gyroscopic artificial horizon suitable for aviation practice was the only method of solving the problem of determining the direction of the vertical on aircraft.

The necessary solution of this problem and of the problem of the aviation gyrocompass was found by using systems of correction for directional gyroscopes.

This path assured, first of all, the procurement of accuracy that was satisfactory enough with the incomparably smaller weights and dimensions than are demanded by the pendulum gyrocompass and the gyropendulum vertical. The question of the duration of the transient states was also solved satisfactorily by this method. For this reason gyro horizons (aviation horizons) with a correction system, and gyrocompasses (course compasses) with a correction system, became parts of the indispensable set of aircraft equipment and constitute the basis of the sensing system in automatic pilots.

It is therefore natural that the theory of such gyroscopic instruments should be particularly important for aviation technology. It may be said in general that

STAT

the theory of aviation gyro instruments is primarily the theory of directional gyroscopes with correction systems.

It is the exposition of questions of this theory that constitutes the task of this textbook. While during the first stage rigorous demands were not made on the accuracy of the readings of gyroscopic directional instruments, as the range and speed of flight increased, and as certain new problems appeared, these requirements did increase.

The use of electric power to maintain the rotation of the rotor and for the purposes of correction only partially satisfies the increased demands on the accuracy of the readings of gyroscopic directional instruments. The point is that the loads that are taken by directional gyroscopes have an unfavorable effect on them. It is necessary to watch out for possible reduction of the reactions in such gyroscopes, owing to the unavoidable connection with the indicating system or with the automatic control system. And yet we have not been able to eliminate the harmful action of these connections entirely.

As has been shown by the works of Soviet scientists, and, first of all, by B.V. Bulgakov and his pupils (Bibl.13), a radical solution of this problem may be provided by the power-stabilized multigyro systems now beginning to occupy a prominent position in gyroscopic aviation engineering. We have therefore found it necessary to dwell on a number of questions connected with such systems.

Gyroscopic measuring systems for the angular velocities of rotation of an aircraft, termed by us gyroscopes, play a very important role in aviation.

A representative of this type of instruments is the widely known "turn indicator". In reacting to the angular velocity of rotation of an aircraft, this instrument, as it were, might be said to warn the pilot that the aircraft is entering a state of violation. Such instruments are of no less importance for automatic piloting devices. Their use as auxiliary sensing elements in automatic pilots makes it possible to obtain artificial damping of the motions of the aircraft, which is of

very essential importance from the point of view of assuring the necessary quality of automatic piloting.

The acceleration-velocity gyroscope, which measures the angular velocity and the angular acceleration of rotation of an aircraft, is also very important for the automatic pilot.

This book also gives the principles of the theory of velocity and acceleration-velocity gyroscopic instruments.

We shall now discuss certain historic moments in the development of aviation gyroscopy of the USSR.

At the time when the problem of aviation gyroscopy had sufficiently matured, the USSR already possessed the necessary cadres for the solution of that problem. The reason for this was that although there was no gyroscope industry, in the strict sense of the word, in pre-revolutionary Russia, still the problems of gyroscopy (and in particular of aviation gyroscopy) even then had attracted the attention of a number of Russian scientists and inventors.

We might mention that as early as 1911 N.Ye.Zhukovskiy occupied himself with these problems, and precisely in the interests of aviation (Bibl.6).

The first aviation gyroscopes, in which the rotation of the rotor and the correction were accomplished by pneumatic action, were developed and built in 1926-1929 in the USSR for use in the automatic pilot.

The creation in 1936-1937 of completely electrified directional gyroscopes with a correction system was a substantial achievement of Soviet designing thought and of its aviation instrument industry. This work was performed in connection with the creation of a completely electric automatic pilot in these years, and it was the principal element in the solution of the problem of the electric automatic pilot. In the problem of the all-electric positional gyroscopes itself, the principal question was that of the electrical correction system. This question was solved on the principles of the inductive correction mechanism proposed by Soviet inventors.

The recent work of Soviet gyroscopists in the field of electric aviation gyroscopes has been particularly successful, and as a result we now possess a full set of USSR electrogyroscopic board instruments.

STAT

CHAPTER I

GYROSCOPIC PHENOMENA AND PROPERTIES

Section 1.1. Visible Gyroscopic Phenomena

Consider the astatic gyroscope (Fig.1.1). The rotor, in the gimbals consisting of the inner frame 3 and the outer frame 4, is called a gyroscope; in the astatic gyroscope the center of gravity of the gyroscope coincides with the center O, the point of intersection of the axes of the gimbal frames.

So long as the rotor of the gyroscope is not rotating, we observe no phenomena in this instrument that distinguish it from an ordinary nongyroscopic body, by which we shall here and hereafter understand a body that does not possess a moment of momentum before it is subjected to an experiment.

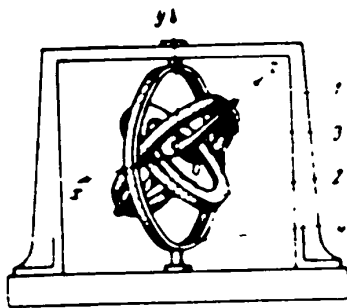


Fig.1.1 - Astatic Gyroscope

Thus the rotation of the base of the gyroscope suspension 1 leads to the variation in the position of the polar axis of its rotor Oz , owing to the influence of friction in the suspension. A moment applied to any of the frames of the Cardan suspension leads to the rotation of that frame about its axis of rotation. A tap on the frame also

causes it to rotate in the direction of the tap.

Let us put the rotor of the astatic gyroscope in sufficiently rapid rotation

STAT

about its polar axis Oz . We shall call this rotation the spin of the gyroscope rotor. It is the presence of this spin that marks the transformation of this device from a nongyroscopic body into a gyroscopic one. Let us then repeat all the operations that we performed with the rotor at rest. We shall now find the following phenomena.

The Phenomenon Gyroscopic Rigidity

The gyroscope rotor axis acquires "rigidity": when the base of the suspension rotates, the variation in the position of the polar axis Oz is unnoticeable, although the friction in the axes of the gimbals, which have already varied its position, still continues to act. Similarly, a tap on the gyroscope frame, with force that would have been sufficient formerly to make that frame rotate several times, now produces no visible effect.

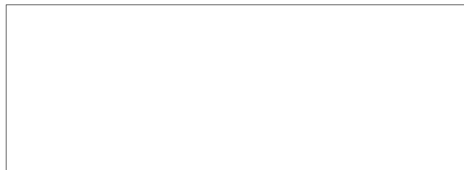
The Phenomenon of Precession

The character of the motion of the gyroscope under the action of an applied moment now changes: a moment applied to the outer frame of the gyroscope causes it to rotate about the axis of the inner frame, and, on the other hand, a moment applied to the inner frame, causes the gyroscope to rotate about the axis of the outer frame. When the direction of the applied moment is reversed, the sense of rotation of the frames is likewise reversed.

This rotation of the gyroscope about the axes of its frames is called the precession of the gyroscope.

If we study the sense of the gyroscope rotor spin and the sense of the applied moment, we obtain the following law of the sense of precession of the gyroscope: the precession of the gyroscope ω_{pr} tends to make the vector of angular velocity of the rotor spin $\vec{\omega}$ coincide with the vector of external moment \vec{L} causing this precession (Fig.1.2).

It is easy to establish by further observation that, in addition to the



.STAT

"extraordinary" relation between the applied moment and the sense of rotation, precession also possesses other properties distinguishing it from the motions inherent in nongyroscopic bodies.

These peculiarities are as follows:

1. To a definite magnitude of the applied moment, at a definite angular velocity of spin, corresponds a definite value of the angular velocity of precession. In nongyroscopic bodies, to a definite value of the applied moment there corresponds a definite value of the angular acceleration.

As a consequence of this, with constant applied moment and constant angular velocity of the spin, the angular velocity of precession will also be constant. In nongyroscopic bodies, with a constant applied moment, the angular velocity of rotation will increase.

But from this it follows in turn that, in spite of the presence of a constant applied moment, the energy of the gyroscopic system in the latter case still remains unchanged, and this is natural enough: the plane of precession produced by the applied moment is perpendicular to the plane in which this moment acts. In other words, the applied moment causing the precession does no work, that is, precession is a motion performed without the expenditure of energy.

2. With constant value of the applied moment, the angular velocity of precession diminishes with increasing angular velocity of the rotor spin, and increases with decrease in that angular velocity.

At constant angular velocity of rotor spin, the angular velocity of precession increases with increase in the applied moment, and decreases with decrease in the applied moment.

3. The value of the angular velocity of precession corresponding to given values of the applied moment and angular velocity of the rotor spin appears instantaneously, with a jump, on application of the moment; and in the same way, instantaneously and with a jump, it disappears when the moment is removed.

STAT

In this way, on variation of the value of the moment, the corresponding variation in the angular velocity of precession takes place without a lag.

In other words, precession is "inertialess".

This peculiarity of precession is, however, in contradiction to the argument that the energy of the system cannot vary instantaneously on application of a moment, although the observed appearance of precession in this case means precisely the instantaneous variation in the energy of the system.

It follows from this that the "inertialessness" of precession is only an apparent phenomenon, and that, in addition to precession, the applied moment must cause some other motion as well, which is not perceptible by observation, during which the moment does perform work assuring the increase of the energy of the system by the value of the energy of precession. This motion, which is termed nutation, will be considered in Sections 2.5, 2.6, and 2.7.

Consider the behavior of a wheel with a handle, so constructed that its shaft is attached on bearings to the handle.

Let us impart a spin to the wheel, thus converting it into a gyroscopic body. On the basis of the phenomenon of gyroscopic precession, established by observations, these motions would be expected to take place in a plane perpendicular to the plane of action of the moment \bar{L} of the force of gravity \bar{G} (Fig.1.3). And this actually does take place: when suspended on a thread attached to the handle, the wheel does not fall, but rotates in a horizontal plane, and exactly in the same way, when the handle is placed on a table, the wheel does not fall, but rotates, with its axis describing a cone in space.

The Phenomenon of Gyroscopic Reaction

As we have seen above, an external moment causes a precessional moment in a plane perpendicular to the plane in which the moment acts. According to the D'Alembert principle, a system of external forces or moments acting on a body causes

with accelerations such that the system of inertial forces or STAT

moments is equal and opposite to the system of external forces and moments.

It follows from this that in precessional motion, the points of a body also



Fig.1.2 - Precession of Gyroscope

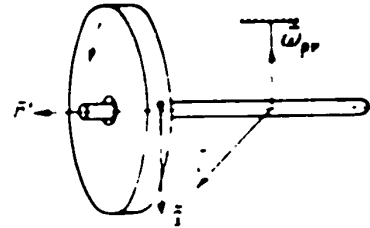


Fig.1.3 - Precession under the Action of the Moment of the Force of Gravity

move with accelerations. The moment of the forces of inertia due to these accelerations is called the gyroscopic moment or moment of the gyroscopic reaction \bar{L}_j (Fig.1.4).

Section 1.2. Relation between the Visible Gyroscopic Phenomena

The moments of friction in the suspension produce in the gyroscope at sufficiently high spinning speeds so small a rate of precession that the deflection of the rotor axis of the gyroscope rotor during a short time of observation is practically unnoticeable.

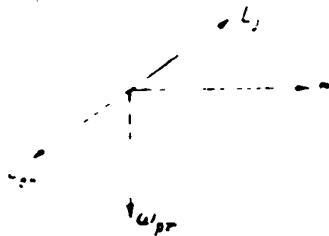


Fig.1.4 - Relation between Precession and Gyroscopic Reaction

The angular velocity of precession arising as a result of a tap on the gyroscope, or, what is the same thing, of the application to the gyroscope of a finite external moment during a negligibly short interval of time, may have a considerable value, but the angle of deviation of the rotor axis

due to this precessional motion will be practically imperceptible, since the time of precession under the shock is negligibly small and equal to the time of applica-

STAT

tion of the external moment.

Section 1.3. Physical Origin of the Gyroscopic Reaction

As already remarked, the gyroscopic moment is the moment of the inertial forces due to the accelerations that appear on the simultaneous existence of two rotations of the gyroscope, rotation about the polar axis of the rotor, and rotation of the axis itself.

Let us find these accelerations.

Let us take a rotor rotating about its polar axis at angular velocity \bar{r}' .

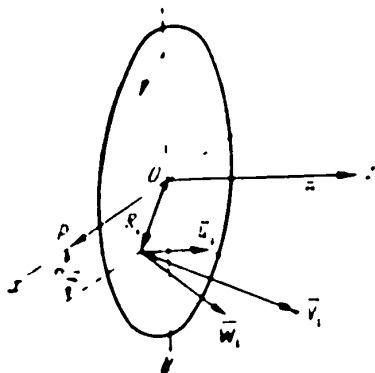


Fig.1.5 - Velocity of Particles
of Rotor

Let us reproduce on the drawing (Fig.1.5) the equatorial plane of this rotor, by which we mean the plane perpendicular to the polar axis of the rotor and passing through the center of the support, that is, through the fixed point of the gyroscope. Let Ox and Oy be the mutually perpendicular axes lying in the equatorial plane, but not taking part in the spin \bar{r}' . Let there be, simultaneously with the rota-

tion \bar{r}' , a rotation about the axis Ox at angular velocity p. Let us consider whether the particles of the rotor, in this case, will move with any acceleration due to the gyroscopic moment. Let us assume, for simplicity of the reasoning, that $r' = \text{const}$ and $p = \text{const}$, that is, let us take a case when angular accelerations are known to be absent.

The velocity \bar{V}_i of any of the material points of the rotor is made up of the component \bar{u}_i , perpendicular to the equatorial plane of the rotor, and the component \bar{w}_i , which lies in this plane (Fig.1.5).

Consider the behavior of the component \bar{u}_i , under the combined rotation of the

STAT

gyroscope about the axes Oz and Ox.

At a given value of \bar{p} , the magnitude of this component is determined, for each material particle of the rotor, by the distance of that particle from the axis Ox.

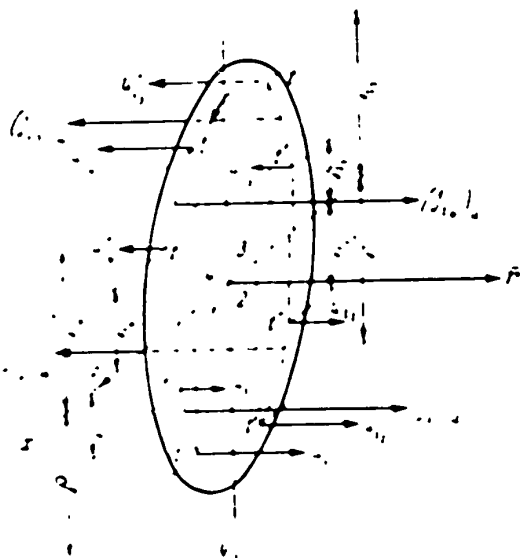


Fig.1.6 - Behavior of Components of Velocity caused by Rotation about the Equatorial Axis

This distance, under the influence of the spin \bar{r}' , increases in the first and third quadrants (Fig.1.6), and decreases in the second and fourth quadrants.

Therefore, during the interval of time $\Delta t = t'' - t'$, the velocities of the material particles traveling over certain areas in the first and third quadrants, will increase in modulus from the values u_{i1}' and u_{i3}' to the values u_{i1}'' and u_{i3}'' respectively.

This means that the particles moving in the first and third quadrants will move at accelerations $(\bar{j}_{i1})_u$ and $(\bar{j}_{i3})_u$, directed, as indicated in Fig.1.7, that is, in the same sense in which the velocities \bar{u}_i are directed in these quadrants.

During the same interval of time, the velocities u_i of the material particles passing over certain areas in the second and fourth quadrants will decrease in modulus from the values u_{i2}' and u_{i4}' to the values u_{i2}'' and u_{i4}'' respectively. This means that the particles traveling in the second and fourth quadrants will move at accelerations $(\bar{j}_{i2})_u$ and $(\bar{j}_{i4})_u$ directed opposite to the velocity \bar{u}_i in these quadrants.

Starting out from this, we get the result that in this case the accelerations $\bar{j}_{i,u}$ will be directed to the right in the first and fourth quadrants and to the

STAT

left in the second and third.

Consider the behavior of the component \bar{w}_i when the gyroscope rotates simultaneously about the axes Oz and Ox.

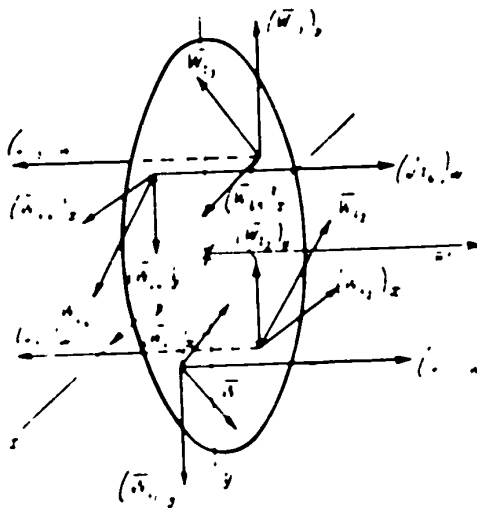


Fig.1.7 - Behavior of the Components of Velocity Due to Rotation about the Polar Axis

Under the influence of \bar{p} , the component \bar{w}_i reverses its direction. In order to represent more distinctly the result of this change, let us resolve \bar{w}_i with respect to the axes Ox and Oy (cf. Fig.1.7). It is easy to see that the component \bar{w}_{ix} of any particle does not change its direction under the influence of \bar{p} , which direction remains parallel to itself, but that the component \bar{w}_{iy} receives an increment under the influence of \bar{p} , causing a change in the direction of the components \bar{w}_{iy} , these increments being directed toward

the right in the first and fourth quadrants, and to the left in the second and third quadrants. The accelerations j_{iw} with which the particles move will be directed in the same way, that is, the accelerations j_{iw} are in the same sense as the accelerations j_{iu} for all particles of the rotor (cf. Fig.1.7 and 1.8). Whence the total acceleration j_i with which the particles move, will be determined by the expression

$$j_i = j_{iu} + j_{iw}$$

Both these components appear, as we see, as a result of the simultaneous rotation of the rotor about two axes, the polar axis and one of the equatorial axes; one of these rotations gives rise to the corresponding component of the velocity of the particles, while the other one produces the variation of this component in

STAT

magnitude and direction.

Consequently the total acceleration is also the result of the simultaneous rotation of the rotor about the two axes, the polar axis and one of the equatorial axis.

It is commonly known that accelerations of this kind are termed rotational (Coriolis force). These accelerations produce the forces of inertia f_i directed

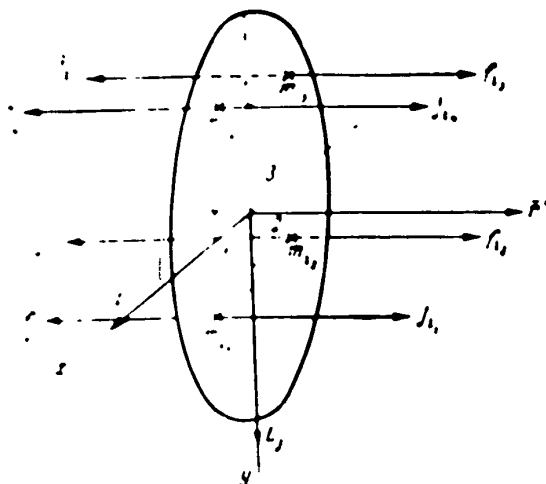


Fig.1.8 - Direction of the Rotational Accelerations and Forces of Inertia

opposite to these accelerations (cf. Fig.1.8). These forces of inertia produce a moment of inertia directed, as indicated on Fig.1.8. It is easy to see that this direction coincides exactly with the direction of the gyroscopic moment. It may be asserted, on this basis, that the gyroscopic moment is the moment of the forces of inertia due to the rotational accelerations with which the particles of the gyroscope rotor move when it rotates simultaneously about two axes, the polar axis and one of the equatorial axes.

taneously about two axes, the polar axis and one of the equatorial axes.

Section 1.4. Magnitude of the Gyroscopic Moment

The component of the velocity of the particles u_i (Fig.1.9) may be represented by the expression

$$u_i = \rho R_i \sin \gamma_i$$

where R_i = radius-vector of the i -th particle;

γ_i = angle made by radius vector of i -th particle with the Ox axis at the given instant of time.

But

$$\gamma_i = r' t + \gamma_{i0}$$

where γ_{i0} = angle made by radius vector of i -th particle with Ox axis at initial instant of time.

Whence we have:

$$\frac{du_i}{dt} = \frac{dp}{dt} R_i \sin \gamma_i + p R_i \cos \gamma_i r'$$

Or, taking $p = \text{const}$ and bearing in mind that $R_i \cos \gamma_i = x_i$, we get

$$f_{iu} = \left(\frac{du_i}{dt} \right)_{p = \text{const}} = p r' x_i$$

Since the acceleration \bar{j}_{iw} is obtained on account of rotation of the vector \bar{w}_{iy} about the axis Ox at angular velocity \bar{p} , then, consequently it may be represented by the expression

$$\bar{j}_{iw} = \frac{d(\bar{w}_{iy})}{dt} = [\bar{p} \times \bar{w}_{iy}]$$

whence, for the quantity j_{iw} , bearing in mind that $w_{iy} = R_i r' \cos \gamma_i = r' x_i$, $\bar{p} \perp \bar{w}_{iy}$, we get (Fig.1.10);

$$j_{iw} = p r' x_i$$

i.e., an expression identical with the expression for j_{iu} .

Thus we have

$$f_{iu} = f_{iw} = -2 p r' x_i$$

whence, for f_{ji} we get

$$f_{ji} = -2 m_i p r' x_i$$

The resultant moment L_{jz} of the inertial forces due to these accelerations about the axis Ox will be zero under the condition of the symmetry of the rotor with respect to either of the equatorial axes. L_{iy} , the resultant moment of these forces about the axis Oy , will be directed as indicated on Fig.1.11, and will equal:

$$L_{iy} = \sum m_i r_i^2 \dot{\varphi}.$$

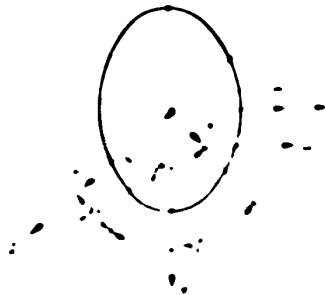


Fig.1.9 - Magnitude of the Component of the Velocities Due to Rotation about the Equatorial Axis

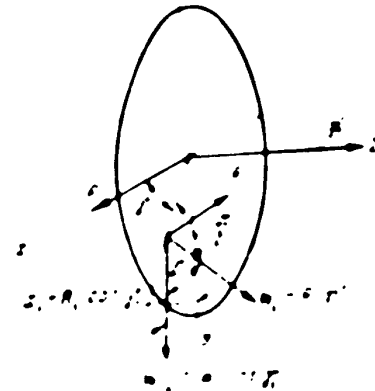


Fig.1.10 - Resolution of the Components of the Velocity Due to Rotation about the Polar Axis

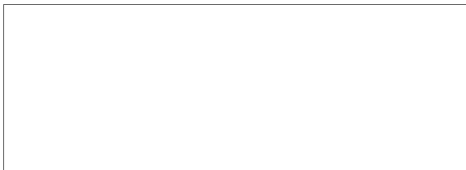
Since, under the condition of the symmetry of the rotor with respect to the polar axis:

$$\sum m_i x_i^2 = \sum m_i (x_i^2 + y_i^2) = \sum m_i R^2$$

and since neither ρ nor r^2 depend on \bar{x}_i , we get

$$L_{jz} = J_j \dot{\varphi} \tag{1.1}$$

where $J_j = \sum_{i=1}^n m_i l_i^2$ - polar moment of inertia of rotor.



STAT

CHAPTER II

DERIVATION OF THE FUNDAMENTAL EQUATIONS OF MOTION OF THE
GYROSCOPE AND THEIR ANALYSISSection 2.1. The Kinetic Moment of the Symmetrical Gyroscope

Let a gyroscope possessing symmetry about both the polar axis and any of the equatorial axes, rotate at angular velocity $\bar{\Omega}_1$ about a certain arbitrary axis. In connection with this rotation, the particles of the gyroscope will have the corre-

sponding velocities and momenta. The sum of the moments of these momenta with respect to the fixed point of the gyroscope is termed its kinetic moment.

Let us bind to the gyroscope the system of coordinates $Oxyz$, by placing its origin at the fixed point of the gyroscope, and matching the axis Oz with the polar axis of the rotor.

Let us resolve the angular velocity $\bar{\Omega}_1$ into the polar component $\bar{\Omega}$ and the equatorial component $\bar{\omega}$. Let the velocity of the i -th particle of

the gyroscope with radius vector \bar{R}_i and mass m_i be equal to \bar{V}_i (Fig.2.1). The kinetic moment of the gyroscope \bar{G} will then be represented by the expression

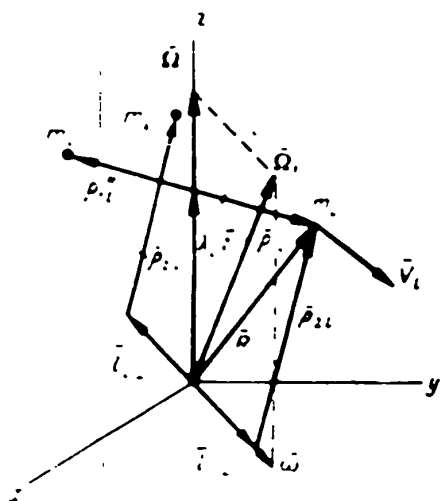


Fig.2.1 - Kinetic Moment of a
Symmetrical Gyroscope

STAT

$$G = \sum_{i=1}^n R_i \cdot m_i V_i \quad (2.1)$$

Or, in view of the fact that

$$V_i = \omega_i R_i \quad (\omega = \omega_i) R_i,$$

we get

$$G = G_2 \cdot G_1,$$

where

$$G_2 = \sum_{i=1}^n R_i \cdot [m_i \omega_i R_i],$$

$$G_1 = \sum_{i=1}^n \bar{R}_i \cdot [m_i \omega_i R_i].$$

Let us resolve \bar{R}_i into $\lambda_i \bar{z}_0$, the component along the Oz axis, and ρ_{1i} , the component perpendicular to this axis, i.e., let us represent

$$R_i = \lambda_i \bar{z}_0 + \rho_{1i}.$$

where \bar{z}_0 is the orthogonal axis Oz and λ_i the projection of the vector \bar{R}_i on the axis Oz.

Then the expression for G_2 is rewritten in the following form:

$$G_2 = \sum_{i=1}^n (\lambda_i z_0 + \rho_{1i}) \cdot [m_i \omega_i (\lambda_i z_0 + \rho_{1i})].$$

or

$$G_2 = \sum_{i=1}^n \lambda_i z_0 \cdot [m_i \omega_i \times \rho_{1i}] + \sum_{i=1}^n \rho_{1i} \cdot [m_i \omega_i \cdot \rho_{1i}].$$

since $[m_i \omega_i \times \lambda_i z_0] = 0$ is in essence a vector product.

STAT

Making use, further, of the formula for a double vector product, we get

$$G_z = \sum_{i=1}^{i=N} m_i [\omega (\lambda_i z_{0i} \rho_{1i}) - \rho_{1i} (\lambda_i z_{0i} \omega)] \cdot \sum_{i=1}^{i=N} m_i [\omega (\rho_{1i} z_{1i}) - \rho_{1i} (\rho_{1i} \omega)]$$

The first sum of the expression so obtained is equal to zero since $(\lambda_i z_{0i}, \rho_{1i}) = 0$ from the property of a scalar product;

$$\sum_{i=1}^{i=N} m_i \lambda_i z_{0i} \rho_{1i} = 0$$

by the condition of symmetry with respect to the polar axis, since by virtue of the symmetry for each particle m_i at the distance \bar{P}_{1i} from the axis Oz the opposite point m_i' is found, which is the distance

$$z_{1i} = -\rho_{1i}$$

from the axis Oz.

Moreover, in view of the fact that the second term in the second sum is also equal to zero from the property of a scalar product, we get

$$G_z = J\omega$$

where $J = \sum_{i=1}^{i=N} m_i \rho_{1i}^2$ - polar moment of inertia.

Solve \bar{R}_i into the equatorial component \bar{l}_{i0} , directed along $\bar{\omega}$, and the component $\bar{\rho}_{2i}$, perpendicular to $\bar{\omega}$, i.e., represent:

$$R_i = l_{i0} + \rho_{2i}$$

Then the expression for \bar{G}_{eq} is rewritten in the following form:

$$G_z = \sum_{i=1}^{i=N} (l_{i0} + \rho_{2i}) [m_i \omega \cdot (l_{i0} + \rho_{2i})]$$

or

STAT

$$G_e = \sum_{i=1}^l \bar{l}_{i\omega} \cdot |m_i \omega \cdot \rho_{2i}| + \sum_{i=1}^l \rho_{2i} \cdot |m_i \omega \cdot \rho_{2i}|$$

Using the formula for a double vector product, we get

$$G_e = \sum_{i=1}^l m_i [(\omega \cdot \rho_{2i}) - \rho_{2i} (\omega \cdot \omega)] + \sum_{i=1}^l m_i [(\rho_{2i} \cdot \rho_{2i}) - \rho_{2i} (\rho_{2i} \cdot \omega)]$$

The first sum in this expression is equal to zero, since $(\bar{l}_{i\omega}, \bar{\rho}_{2i}) = 0$ by the property of a scalar product; $\sum_{i=1}^l \rho_{2i} (\omega \cdot \omega) = 0$ by the condition of the same symmetry with respect to the polar axis, since by virtue of the symmetry for each particle m_i , the radius vector of which has the component $\bar{l}_{i\omega}$, the opposite point m_i'' is found, the radius vector of which has the component $\bar{l}_{i\omega} = -\bar{l}_{i\omega}$. In view also of the fact that one of the terms entering into the second sum is likewise equal to zero from the property of a scalar product, we get

$$G_e = J_e \omega,$$

where $J_e = \sum_{i=1}^l m_i \rho_{2i}^2 =$ equatorial moment of inertia.

Thus we have

$$G = G_z + G_e = I \Omega + J_e \omega \quad (2.2)$$

Section 2.2. The Resal Theorem

Let us find the derivative of the expression for the kinetic moment, taken in the general form eq.(2.1).

Differentiating eq.(2.1), we get

$$\frac{dG}{dt} = \sum_{i=1}^l \frac{dK_i}{dt} \times m_i V_i + \sum_{i=1}^l K_i \times m_i \frac{dV_i}{dt}$$

Let us write a number of obvious equalities:

$$\frac{dR_i}{dt} = v_i$$

$$v_i \cdot v_i = 0$$

by the property of a vector product;

$$m_i \frac{d^2 r_i}{dt^2} = (F_i)_{\text{external}} + (F_i)_{\text{internal}}$$

where $(\bar{F})_{\text{external}}$ is the resultant vector of external forces;

where $(\bar{F}_i)_{\text{internal}}$ is the resultant vector of the internal forces acting on the i-th particle

$$r_i \times ((F_i)_{\text{external}} + (F_i)_{\text{internal}}) = (L_i)_{\text{external}} + (L_i)_{\text{internal}}$$

where $(\bar{L}_i)_{\text{external}}$ is the resultant moment of the external forces acting on the i-th particle;

$(\bar{L}_i)_{\text{internal}}$ resultant moment of internal forces acting on the i-th particle

$$\sum_i (L_i)_{\text{internal}} = \sum_i (L_i)_{\text{external}} = \bar{L}$$

where \bar{L} - resultant moment of external forces acting on the body.

Making use of these equations, we get

$$\frac{d\bar{G}}{dt} = \bar{L} \quad (2.3)$$

But $\frac{d\bar{G}}{dt} = v_G$ is the velocity of the end of the vector of the kinetic moment \bar{G} .

Thus,

$$v_G = \bar{L}$$

STAT

i.e., the velocity of the end of the vector of kinetic moment \bar{G} is equal in magnitude and direction to the moment of the external forces.

The relation so obtained is called the Resal theorem.

Let us apply the Resal theorem to the gyroscope.

At a sufficiently rapid proper rotation of the rotor, the equatorial component of the kinetic moment of the gyroscope \bar{G} , is usually negligibly small by comparison to its polar component \bar{G}_z . In other words, it may be considered that the kinetic moment of the gyroscope \bar{G} coincides in direction with the polar axis of rotation of the gyroscope rotor.

Let us assume that the external moment \bar{L} , directed as indicated in Fig.2.2, is applied to a gyroscope having the kinetic moment \bar{G} , which we shall consider as coinciding with the axis of rotation of the rotor.

According to the Resal theorem, under the influence of this moment, the point on the axis of the rotor corresponding to the end of the vector G , receives the

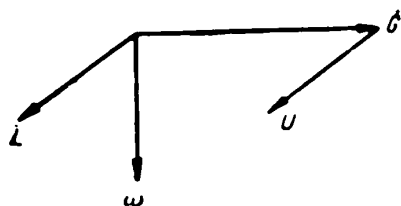


Fig.2.2 - The Theorem of Moments

velocity \bar{U}_G , equal in magnitude and direction to \bar{L} . This velocity can be obtained only under the condition that the gyroscope is rotating with respect to a fixed point at the angular velocity $\bar{\omega}$, directed as indicated in Fig.2.2.

It will be easily seen that this direction coincides with the direction of the angular velocity of precession described above and explained starting out from the fact that the simultaneous existence of two rotations of the gyroscope about the polar and equatorial axes produces the corresponding external moment.

Section 2.3. Derivation of Approximate Equations of Motion
of the Gyroscope in the Vector Form

As already stated, the equatorial component of the kinetic moment \bar{G}_{eq} of the gyroscope is negligibly small by comparison with its polar component \bar{G}_z . For those technical applications with which we shall deal, the modulus G_{eq} will be tens and hundreds of thousands of times smaller than the modulus G_z . On this basis, let us neglect the equatorial component in the expression for the kinetic moment (2.2). Then the expression (2.2) is rewritten in the following form:

$$\bar{l} = J\Omega \bar{z}_0 \quad (2.4)$$

where \bar{z}_0 is the orthogonal coinciding with the polar axis of the rotor.

Differentiating eq.(2.4), we get

$$\frac{d\bar{l}}{dt} = J \frac{d\Omega}{dt} \bar{z}_0 + J\Omega \frac{d\bar{z}_0}{dt}$$

Thus, on the basis of eq.(2.3)

$$l = J \frac{d\Omega}{dt} \bar{z}_0 + J\Omega \frac{d\bar{z}_0}{dt}$$

Let us consider $\Omega = \text{const}$. Then we get

$$l = J\Omega \frac{d\bar{z}_0}{dt}$$

where $\frac{d\bar{z}_0}{dt}$ = the velocity of the end of a unit vector bound to the polar axis of rotation of the rotor.

It is clear that the velocity $\frac{d\bar{z}_0}{dt}$ can be obtained only as a result of the rotation of the orth, i.e., of the rotation of the polar axis of the rotor about an axis not coinciding with the orth itself. Such a rotation is the equatorial compo-

ment of the rotations of the gyroscope $\bar{\omega}$. It follows from this that $\frac{d\bar{z}_0}{dt}$ may be represented by the expression

$$\frac{d\bar{z}_0}{dt} = \bar{\omega} \times \bar{z}_0.$$

Making use of this expression, we get

$$I \bar{\Omega} (\bar{\omega} \times \bar{z}_0) = J (\bar{\omega} \times \bar{z}_0). \quad (2.5)$$

The relation so obtained is the vector form of the approximate equation of motion of the gyroscope for the special case when the rotor spin may be taken as constant. This special case is the principal case in the technical applications.

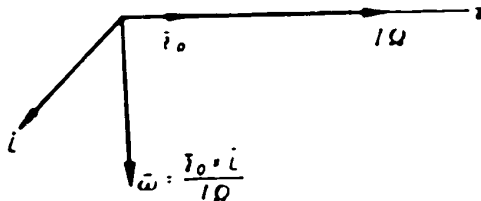


Fig.2.3 - The Law of Precession

On the other hand, even the approximation, from the point of view of the technical applications, is of very high accuracy, since it is based on neglecting a quantity whose share is measured in thousandths of a percent.

On this basis we may conclude that the equation of motion of the gyroscope, eq.(2.5), describes these motions with sufficient completeness.

It follows from eq.(2.5) that the motion of the gyroscope under the application of the external moment \bar{L} to it will be a rotation of the polar axis of the rotor of the gyroscope about its equatorial axis at angular velocity ω .

Let us solve eq.(2.5) with respect to $\bar{\omega}$. For this purpose let us vectorially multiply its right and left sides by \bar{z}_0 , that is, let us represent it in the following form:

$$\bar{z}_0 \times \bar{L} = \bar{z}_0 \times (I \bar{\omega} \times J \bar{z}_0)$$

Applying the formula for a double vector product to the right side of the formula, we get

$$\mathbf{z}_0 \times L = \omega (z_0 \cdot J\Omega) - J\Omega (z_0 \cdot \omega),$$

or

$$\omega = \frac{z_0 \cdot L}{J\Omega} \bar{\omega}, \quad (2.6)$$

since $(\bar{z}_0, J\bar{\Omega}) = J\bar{z}_0\bar{\Omega}$, by virtue of the fact that z_0 and Ω are parallel, and $\Omega (\bar{z}_0\bar{\omega}) = 0$ by virtue of the fact that \bar{z}_0 and $\bar{\omega}$ are perpendicular.

As follows from Fig.2.3, the direction of $\bar{\omega}$ coincides exactly with the sense of precession of the gyroscope, the sense which we observed on application of an external moment and which was explained above from the rotational accelerations.

In this connection, we shall call the relation (2.6) the law of precession.

For the modulus $\bar{\omega}$, we obtain, on the basis of eq.(2.6),

$$\bar{\omega} = \frac{L \sin(\alpha, l)}{J\Omega} = \frac{L \sin(\alpha, l)}{J\Omega}. \quad (2.7)$$

In other words, the magnitude of the angular velocity of precession is proportional to the equatorial component of the applied moment and inversely proportional to the kinetic moment of the gyroscope.

Let us illustrate, starting out from the relations (2.7), for the law of precession, the "insensitivity" of the gyroscope with respect to friction in the gimbals.

Let us take $J\Omega = 4000$ g-cm/sec, a value corresponding to the kinetic moment of the gyroscope of the gyrohorizon. Let the moment of friction in the gimbals be equal to 1 g-cm, a value that is in general exaggerated: according to the standards, the moment of friction in the gimbals must not exceed 0.5 g-cm for aviation gyroscopes.

Since it may be considered that the moment of friction in the gimbals lies in the equatorial plane, we obtain, for the angular velocity of precession under the influence of this moment, with the data taken by us:

$$\omega = 1/4000 \text{ rad/sec} = 0.9 \text{ degree/min.}$$

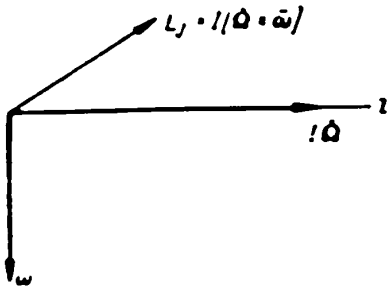


Fig.2.4 - Law of Gyroscopic Reaction

It is clear that such a rate of rotation cannot be detected by simple observation. The rotation of the gyroscope as a result of such a rate of rotation when the base of the suspension is rotated is likewise not detected, since in this rotation the application of the moments of friction in any direction continues for a few seconds, in any case, not longer than a few tens of seconds. For this reason the axis of the gyroscope appears to maintain its position invariant in space.

The inertial moment \bar{L}_j , arising as a result of the rotation of the gyroscope about the equatorial axis of the rotor at angular velocity ω with simultaneous rotation of the rotor about the polar axis, and as a result of what we have called gyroscopic moment, is equal in magnitude to the external moment and is directed in the opposite sense.

On the basis of what has been said, and of eq.(2.5), we obtain

$$L_j = - I \cdot J |\Omega \times \omega|.$$

As follows from Fig.2.4, the sense of the gyroscopic moment of inertia \bar{L}_j , according to eq.(2.8), exactly coincides with the sense for this moment fixed by us, on the basis of the rotational accelerations.

We shall call the relation (2.8) the law of gyroscopic reaction.

For the modulus L_j , we get, on the basis of eq.(2.8):

STAT

$$L_y = J\Omega \omega.$$

since

$$\sin(\Omega, \omega) = 1$$

since $\bar{\omega}$ = the equatorial component of $\bar{\Omega}_1$.

Thus, starting out from the approximate equation, the motions of the gyroscope may be treated as follows: on the application of an external moment to the gyroscope, there arises a precession of the gyroscope, whose law is defined by eq.(2.6); in this case there develops the gyroscopic moment of inertia defined by eq.(2.8).

Section 2.4. Analytic Form of Approximate Equations of Motions of the Gyroscope

Physically, the complete rotation of the gyroscope $\bar{\Omega}_1$ is made up of the rotor spin \bar{r} , by which we mean the rotation of the rotor about its polar axis with respect to the inner frame of the gimbals, of the rotation of the gyroscope in the

axes of the gimbals, and of the rotation of the base of the gimbals.

Let the resultant angular velocity of the two latter rotations be equal to $\bar{\omega}$. Then $\bar{\Omega}_1$, which was represented by us earlier in the form

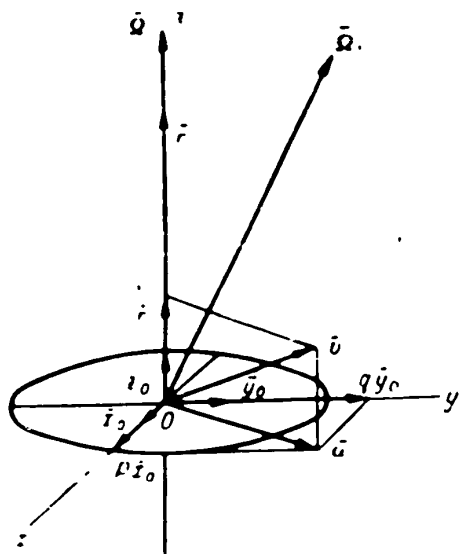


Fig.2.5 - Components of the Rotations of the Gyroscope

may now be represented as:

By resolving $\bar{\omega}$ into an equatorial component $\bar{\omega}$ and a on it with respect to the polar axis of the rotor \bar{r} , we get

Then, for the total polar component $\bar{\Omega}_1$, which we denote by $\bar{\Omega}$, we get

$$\bar{\Omega} = \Omega + \Omega'$$

Let us connect with the gyroscope (Fig.2.5) the system of coordinates $Oxyz$, by matching the axis Oz with the polar axis of the rotor and placing the axes Ox , Oy in the equatorial plane in such a way that they shall not take part in the proper rotation of the rotor \bar{R}' .

Such a system of axes is called Resal axes. It is easy to convince oneself that the axis of the inner frame of the gimbals may serve as one of the equatorial axes of Resal, since this axis, like the axis of the gimbals, passes through the fixed point of the gyroscope and at the same time lies in the equatorial plane.

Let us set up, starting out from eq.(2.5), approximate equations of motion of the gyroscope in the analytic form, applicable to the system of Resal coordinate axes selected by us.

On resolving the equatorial component of the end of the velocity of the rotation of the gyroscope on Resal axes, we get

$$\omega = p x_0 + q y_0$$

Substituting this expression in eq.(2.5), we get

$$i = p x_0 \setminus J \Omega z_0 + q y_0 \setminus J \Omega z_0$$

Whence we have

$$l_x = J \Omega q \tag{2.9}$$

$$l_y = J \Omega p \tag{2.10}$$

for

$$\begin{aligned} (\bar{x}_0 \setminus \bar{z}_0) &= \bar{y}_0 \\ (\bar{y}_0 \setminus \bar{z}_0) &= \bar{x}_0 \end{aligned}$$

The equations for the gyroscopic moment in the analytic form will be respectively of the form:

$$L_{\rho} = -J\Omega q; \quad (2.11)$$

$$L_{\eta} = J\Omega p. \quad (2.12)$$

Section 2.5. Complete Form of the Equations of Motion of the Gyroscope

Let us take the complete expression for the kinetic moment of a symmetrical gyroscope, representing the equatorial component in this expression as resolved according to the Resal axes:

$$G = J\Omega \bar{z}_0 + J_c p x_0 + J_c q \bar{y}_0.$$

Differentiating this expression and bearing eq.(2.3) in mind, we get

$$\begin{aligned} L = J \frac{d\Omega}{dt} z_0 + J_c \frac{dp}{dt} x_0 + J_c \frac{dq}{dt} y_0 + J\Omega \frac{dz_0}{dt} + \\ + J_c p \frac{dx_0}{dt} + J_c q \frac{dy_0}{dt}. \end{aligned} \quad (2.13)$$

The derivatives of the orths are found from the considerations that all these derivatives will be the velocities of the ends of these orths, which may be obtained only on account of the rotations of the orths about axes not coinciding with them. Since the system of coordinates selected, and therefore also the system of orths of the coordinate axes rotate at angular velocity $\bar{\Omega}$, equal to

$$\bar{\Omega} = p x_0 + q y_0 + r z_0.$$

we obtain, on the basis of the above, the following expressions for the derivatives of the orths

$$\frac{dz_0}{dt} = (p x_0 + q y_0) \times z_0 = -p y_0 + q x_0.$$

$$\frac{dx_0}{dt} = (r z_0 + q y_0) \times x_0 = r y_0 - q z_0.$$

STAT

$$\frac{dy_0}{dt} = (rx_0 + px_0) \times y_0 = -rx_0 + pz_0.$$

On substituting these relations in eq.(2.19), then resolving L into components along the Resal axes, we get the following system of equations by equating the coefficients of the same orths:

$$L_x = J_e \frac{dp}{dt} + J\Omega q - J_c qr, \quad (2.14)$$

$$L_y = J_e \frac{dq}{dt} - J\Omega p + J_c pr. \quad (2.15)$$

$$L_z = J \frac{d\Omega}{dt}. \quad (2.16)$$

The equation so obtained are called modified Euler equations for the symmetrical gyroscope to distinguish them from the classical Euler equations, introduced with reference to the system of coordinates rigidly bound to the gyroscope.

This form of complete equations of motion of the gyroscope is the one which is usually employed in gyroscope theory, and has the advantage that it allows a graphically clear representation of the consequences of the presence in the gyroscope of the proper rotation \bar{r} , that is, of the factor that transforms a nongyroscopic body into a gyroscope.

Bearing in mind that the complete polar component of the angular velocity of rotation of the gyroscope $\Omega = r + r'$, let us rewrite eq.(2.11) - eq.(2.16) in the following form:

$$L_x = J_e \frac{dp}{dt} + (J - J_c) qr + Hq, \quad (2.17)$$

$$L_y = J_e \frac{dq}{dt} - (J - J_c) pr - Hp, \quad (2.18)$$

$$L_z = J \left(\frac{dr'}{dt} + \frac{dr}{dt} \right), \quad (2.19)$$

where $H = Jr'$ = proper kinetic moment of gyroscope.

The first and second terms of eq.(2.17) and (2.18) would remain the same, even

STAT

in the absence of the rotor spin, i.e., in the absence of the conditions transforming a solid body into a gyroscope in the real sense of this word. From their first terms we determine, as is clear, the moments of inertia from the angular accelerations about the axis of action of the moment, from their second terms, the moments of inertia from the centripetal accelerations taking place as a result of the rotation of the gyroscope and angular velocity $\bar{\omega}$.

The last terms of these equations are obtained only when the gyroscope rotor is spinning. They give, as will be clear, the velocity of rotation about an axis perpendicular to the direction of the component of external moment standing on the left side of the equations.

The role of the centripetal accelerations in all cases of interest to us will be negligibly small, since the co-factors in the corresponding terms will be products of the small angular velocities p , q and r . By rejecting them we find that in the absence of rotor spin, the external moment is expended only in imparting angular accelerations about the axis of its action, as it should be for a nongyroscopic body.

If, however, a rotor spin r' does occur, then, in addition to the angular accelerations about its axis of action, the external moment applied to the gyroscope will also produce an angular velocity about the actions perpendicular in its direction to the motion termed by us the precession of the gyroscope. Thus the complete motion of the gyroscope consists of two motions, one an "ordinary", inherent in all bodies in general, including nongyroscopic bodies, and the second one, precession, which is peculiar to gyroscopes alone.

Turning to the approximate equations of motion (2.9) and (2.10), we note that, according to these equations, the external moment produces only precession, and with the same practically quantitative characteristics as the precession entering into as a component of motion in the complete equations, since, owing to the smallness of r in comparison to r' , we may put:

$$J\Omega - J(r \cdot r') \approx Jr' - H.$$

i.e., the approximate equations cover only the motions specifically inherent in gyroscopes and not inherent in other bodies.

But we have already noted above that the degree of accuracy of the approximate equations of motions of the gyroscope is very high for a sufficiently rapid rotor spin.

If this is true, then it follows that the "ordinary" component of the motions of the gyroscopes, inherent in a gyroscope as in any nongyroscopic body, play a very small role in comparison to the "gyroscopic" component of this motion, which is inherent only to the gyroscope in the proper sense of this word.

The equations for the moment of inertia are written on the basis of eq.(2.17)-(2.19) in the following form:

$$L_{ix} = -L_i = -J_x \frac{dp}{dt} - (J - J_x)qr - Hq; \quad (2.20)$$

$$L_{iy} = -L_y = -J_y \frac{dq}{dt} + (J - J_y)pr + Hp.$$

$$L_{iz} = -L_z = -\left(\frac{dH}{dt} + J \frac{dr}{dt}\right). \quad (2.21)$$

Rejecting the second terms of the right sides of eq.(2.20) and (2.21) as negligibly small, we find that, in the absence of rotor spin, the external moment is equal to the "ordinary" moment of inertia, that is, to the moment which any rotating body, including a nongyroscopic body, is able to develop. In the presence of proper rotation of the gyroscope rotor, the external moment is equal to the sum of the "ordinary" moment of inertia and the gyroscopic moment of inertia, which can be developed only by a rotor possessing a considerable moment of momentum.

According to the approximate equations for the moment of inertia (2.11) and (2.12), the external moment is equal only to the gyroscopic moment. Consequently, it follows from the high accuracy of the approximate equations that it is precisely

to the gyroscopic moment of inertia that we must attribute the total moment of inertia developed by the gyroscope.

Section 2.6. Motion of Gyroscope under the Influence
of an Equatorial External Moment

Consider the character of the motion of the gyroscope when an external moment L , acting, let us assume, about the axis of the inner frame, with which we match the axis Ox , is applied to it. We shall consider that in this case $L_y = 0$, $L_z = 0$, $r = 0$. The restrictions adopted simplify the character of the subsequent calculations, without substantially impairing the generality of the basic conclusions that can be obtained.

For the case we have taken, the equations of motions of the gyroscope, (2.14) and (2.15), will take the following form:

$$\frac{dp}{dt} + \mu q = \mu \frac{L}{H}, \quad (2.22)$$

$$\frac{dq}{dt} - \mu p = 0. \quad (2.23)$$

where $\mu = \frac{H}{J_{eq}} = \frac{Jr'}{J_{eq}} > r'$, since $J > J_{eq}$ is always true. On differentiating once eq.(2.22) and substituting in it $\frac{dq}{dt}$ from eq.(2.23), we get

$$\frac{d^2 p}{dt^2} + \mu^2 p = 0.$$

The solution of this equation, as is commonly known, is of the form:

$$p = A \sin \mu t + B \cos \mu t$$

Making use further of eq.(2.22), we get

$$q = -A \cos \mu t + B \sin \mu t + \frac{L}{H}.$$

Pseudoregular Precession

Let us take initial conditions corresponding to the gyroscope at "rest" under

STAT

the application of an external moment, i.e., let us assume that, at $t = 0$, $p = 0$, $q = 0$. Under these initial conditions we obtain for the arbitrary constants

$$B = 0, \quad A = \frac{L}{H}.$$

As a result, the solution takes the following form:

$$p = \frac{L}{H} \sin \mu t. \quad (2.24)$$

$$q = \frac{L}{H} (1 - \cos \mu t). \quad (2.25)$$

which is represented by the graphs of $p(t)$ and $q(t)$ that are presented in Fig. 2.6. On considering the same case on the basis of the approximate equations of motion (2.9) and (2.10), we put in them $J\Omega = H$, or, what is the same thing, from the complete equations (2.17) and (2.18), rejecting the terms representing the "ordinary" motion in them, and leaving only the terms representing the precession of the gyroscope, we obtain

$$p_{approx} = 0. \quad (2.26)$$

$$q_{approx} = \frac{L}{H}. \quad (2.27)$$

On comparing the approximate formulas of motion according to eq. (2.26) and (2.27) with the more exact formulas for (2.24) and (2.25), we convince ourselves that the first two yield the constant component of the second two.

Denoting the angle of rotation of the polar axis of the gyroscope about the equatorial axis Oy by α , and about the equatorial axis Ox by β , we get, by eqs. (2.24) and (2.25), the following:

$$\alpha = \frac{L}{H} t - \frac{LJ}{H^2} \sin \mu t + C_1.$$

$$\beta = -\frac{LJ}{H^2} \cos \mu t + C_2.$$

STAT

Let the initial conditions in the relation of angles α and β be likewise zero, i.e., let, at $t = 0$, $\alpha = 0$, $\beta = 0$. Then we shall have

$$C_1 = 0; \quad C_2 = \frac{I J_0}{H}.$$

and as a result

$$\alpha = \psi_m (\omega t - \sin \omega t), \quad (2.28)$$

$$\beta = \psi_m (1 - \cos \omega t), \quad (2.29)$$

where

$$\psi_m = \frac{I J_0}{H^2}.$$

Thus the motion of the gyroscope in the system under study will consist of two different components:

a) the first $\alpha = \omega_m \mu t$, of motion with a constant angular velocity about the equatorial axis perpendicular to the direction of the applied moment; this component is called by us the precession of the gyroscope;

b) the second: $\alpha = -\psi_m \sin \mu t$, $\beta = \psi_m (1 - \cos \mu t)$, being the periodic oscillations both about the axis, coinciding with the direction of the applied moment, and about the axis perpendicular to this direction, with a phase shift between these oscillations equal to $\pi/2$. We shall call the second component of total motion the rotation of the gyroscope. It is obtained as a result of the influence of terms of the complete equations of motion of the gyroscope, which consist of angular accelerations caused in the gyroscope by the application of a moment to it. We have termed their terms representing the "ordinary" motion of the gyroscope in the sense that they would remain, even in the absence of rotor spin, i.e., in the sense that they are inherent in any nongyroscopic body. In the gyroscope, however, the effect caused by these terms, as we have seen, is not at all "ordinary": instead of a definite rotation in the direction of action of the moment, as would occur in a non-gyroscopic body, they cause periodic oscillations, both about the axis coinciding

STAT

with the direction of the applied moment, and about the axis perpendicular to this direction.

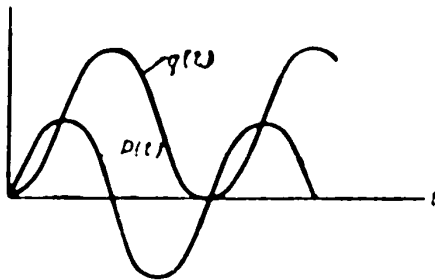


Fig.2.6 - Pseudoregular Precession
of Gyroscope

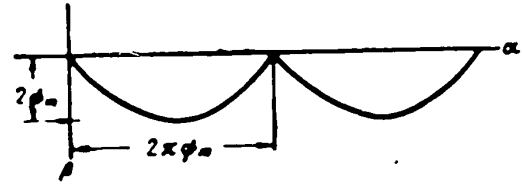


Fig.2.7 - Path of End of Gyroscope Axis
in Pseudoregular Precession

As a result of the motions defined by eqs. (2.28) and (2.29), the axis of the gyroscope will describe a certain path on a plane perpendicular to the original position of the axis of the gyroscope, and located at unit distance from the center of the suspension of the gyroscope. For the beginning of motion, when $\sin \alpha \approx \alpha$ and $\sin \beta \approx \beta$, this path may be described with sufficient accuracy by eq.(2.28) and (2.29) in the rectangular system of the coordinates $O\alpha\beta$, the axis $O\alpha$ of which is parallel to the axis Ox , while the axis $O\beta$ is parallel to the axis Oy .

It is easy to see that this curve will be a cycloid with a radius equal to ψ_m , i.e., that it will be equal to the amplitude of nutation (Fig.2.7).

Let us take for L a magnitude corresponding to the maximum value of the correcting moment of the autopilot, amounting to 8 g-cm , and the other data corresponding to the characteristics of the gyrohorizon, i.e., let $J_{eq} \approx 1.0 \text{ g-cm-sec}^2$, $H = 4000 \text{ g-cm-sec}^2$. As a result we get the following expression for the amplitude of the nutation ψ_m

$$\psi_m = \frac{8}{16 \cdot 10^6} \text{ rad} = \frac{1}{2} 10^{-6} \text{ rad} \approx 0.1''.$$

i.e., a quantity of no practical importance.

In other words, the cycloid traced by the rotor axis will under normal conditions have a radius so small that with a very high degree of accuracy it may be taken as a straight line.

The frequency of the periodic oscillations of the axis of the gyroscope rotor, μ , is measured in hundreds and thousands per sec. As a result of the negligible value of the amplitude and of the high frequency, these periodic oscillations are imperceptible.

The motions of the gyroscope that have just been studied bears the name pseudo-regular precession. In this term, the word "regular" emphasizes the fact that from the practical point of view, the motion reduces in essence to a regular motion, that is of uniform precession, while the word "pseudo" emphasizes the fact that from the theoretical point of view this motion contains not only precession but also nutation.

It should be added to all that has been said that nutation dies away relatively fast on account of friction in the suspension and of other resistances, after which only precession remains, the existence of which is assured by the external moment applied to the gyroscope.

Regular Precession

Let us take for the same case of the application of an external moment, the following initial conditions: at $t = 0$, let $p = 0$, $q = L/H$, i.e., let us assume that about the axis the action of the applied moment there is a state of rest, and about the axis perpendicular to the applied moment, rotation already takes place at an angular velocity equal to the constant component of the angular velocity of pseudoregular precession due to that external moment.

For these initial conditions we have

$$\dot{\lambda} = 0; \dot{\tau} = 0$$

and, consequently,

$$p = 0,$$

STAT

$$q = \frac{L}{H}$$

that is, the motion will consist only of precession without nutation. Such a motion is called regular precession.

As we see, by varying the initial conditions, that is, by taking them to correspond to that motion of the gyroscope which is obtained after the damping of the nutation, we obtain a motion which is without nutation from the very beginning.

It follows from this that nutation is the component of the motions of the gyroscope which, according to the initial conditions, may either occur or not occur. If it does occur, then pseudoregular precession takes place. But in connection with the damping of the nutation, this pseudoregular precession may be treated as a motion passing over into regular precession and it is only this type of precession that can exist for an indefinitely long time.

On applying the approximate equations of motion to this case, we obtain the same result that was given in this case by the complete equations. This is natural enough, since the nutation, which distinguishes the complete motion from the approximate motion, has disappeared in this case in connection with a certain choice of the initial conditions.

Influence of a Shock

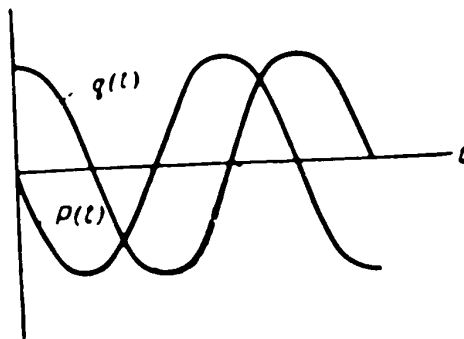


Fig. 2.8 - Nutation after a Blow

Let us assume that as a result of a blow in the neighborhood of the axis Oy , the initial angular velocity q_0 arises. In this case let $p = 0$. Putting $L = 0$ in eq.(2.25), we obtain for these initial conditions:

$$A = -q_0; B = 0$$

And, consequently,

$$p = -q_0 \sin \mu t,$$

STAT

$$q = q_0 \cos \mu t.$$

Thus in this case the motion will consist of nutation alone (Fig. 2.2) without precession, but this is understandable, since in this case the external moment, on account of which precession may exist, is absent.

Section 2.7. Energetic Balance of Motions of the Gyroscope

With regular precession, the motion during the course of all the time after the initial instant will remain exactly the same as it was at that initial instant.

Although regular precession still exists on account of the action of an applied external moment, this action nevertheless does not change the energy of the system by comparison with the energy possessed by the system on the application of the external moment.

As already remarked, this is explained by the fact that in this case the external moment causes motion in a plane perpendicular to the plane in which it acts. Consequently, in assuming the existence of precession, the external moment does not perform work, and in this connection it cannot be a source of variation of the energy of the system. But since there are likewise no other sources of energy of any kind in this case, it is understandable that the energy of the system should remain unchanged during the existence, for as long a period as may be desired, of regular precession and of the action of an external moment, that is, that it should remain as it was at the initial instant of time. At the initial instant of time, however, the initial angular velocity $q = \frac{L}{I_1}$, was imparted to the gyroscope, which meant the introduction of energy into the system that was exactly equal to the energy of precession which this given external moment is able to provide.

In contrast to the initial conditions leading to the appearance of regular precession, the initial conditions leading to the appearance of pseudoregular precession do not involve the introduction of additional initial energy into the system. Consequently the energy of pseudoregular precession can be formed only on account of

l. moment.

STAT

Such work is actually performed by the external moment in pseudoregular precession in connection with the existence of a rotation about the axis of its action. The magnitude of this work may be characterized by the angle of this shift, since the external moment is constant.

As follows from eq.(2.27), this angle, which always retains a positive sign, varies from zero to a value equal to $2\psi_m = 2\frac{LJ_{eq}}{H^2}$, and has a constant component equal to $\psi_m = \frac{LJ_{eq}}{H^2}$. Consequently, the work of the external moment $U_L = L\beta$ varies from zero to a value equal to $2\frac{L^2J_{eq}}{H^2}$ for a constant component equal to $U_{Lc} = \frac{L^2J_{eq}}{H^2}$. This work, at each given instant, according to the law of conservation of energy, must be equal to the energy of pseudoregular precession $U_{pr} = \frac{J_{eq}}{2}(p^2 + q^2)$.

Using the expression eq.(2.24) and (2.25), we get for U_{pr} :

$$U_{pr} = \frac{J_{eq}L^2}{H^2} (1 - \cos \psi t).$$

i.e., an expression identical with the expression for $U_L = L\beta$, if β is taken according to eq.(2.29).

The constant component of the energy of pseudoregular precession may in turn be divided into the energy of precession proper and the energy of nutation. These energies in our case will be equal to each other, and it is easy to convince oneself of this. In fact, the energy of precession equals

$$J_{eq} \psi_{pr}^2 = \frac{J_{eq}L^2}{2H^2}$$

this corresponds to half the constant component of the work of the external moment. On the damping of the nutation, the energy of nutation is dissipated, and the gyroscope now retains only the energy of proper precession equal to $\frac{J_{eq}L^2}{2H^2}$.

The initial conditions corresponding to a blow mean the introduction of the initial energy $U_0 = \frac{J_{eq}q_0^2}{2}$ into the system. Since the subsequent motion is performed without participation of external forces, it follows that the energy of the

STAT

system must remain invariant during the nutation following the blow and must remain equal to $\frac{J_c \omega^2}{2}$, which, in reality, it does.

Section 2.8. Transition to the Equations of Motion with Respect to Terrestrial Coordinate Axes

The basic content of the theory of aviation gyro instruments reduces down to the determination of the laws of the establishment of the gyroscope in a position of stable equilibrium in one system or the other of terrestrial coordinate axes. A knowledge of these laws allows us to determine the conditions under which a gyro instrument is able to indicate the direction of these terrestrial coordinate axes or to determine the rotary velocity of the aircraft with respect to the earth.

In both cases, to solve the problems so formulated, we must pass from the equations of motion in the mesal axes to the equations of motion in terrestrial axes.

Let us take the system of terrestrial coordinate axes $O\xi\eta$ (Fig.2.9). Let us match one of these axes, let us say $O\xi$, with the direction to be determined by the aid of this gyro instrument: for gyro horizons, it will be the direction of the true vertical, for course-indicating gyro instruments, the direction of the meridian. Let us call this axis the principal terrestrial axis. Let us match, to other axis, let us say the axis $O\eta$, the axis of rotation of the outer frame of the gimbals, which is always located parallel to some one of the aircraft axes in horizontal flight. The direction of the third axis will then be determined according to a right-hand system of coordinates.

Let us match with the origin of coordinates $O\xi\eta$ the origin of the system of coordinates $Oxyz$. We recall that the axis Oz of this system of coordinates has been matched with the polar axis of the rotor, and that the axes Ox and Oy lie on the equatorial plane and do not participate in the rotor spin. As has been stated above, the axis of rotation of the inner frame of the gimbals lies in the equatorial plane of the gyroscope, as the axis passing through the center of the suspension of the axis Oz . On the other hand, this axis will not participate

STAT

in the proper rotation of the rotor, but it will participate in the other rotations of the gyroscope, for example, about the axis of rotation of the frame of the suspension, or in the rotations together with the base of the suspension. Consequently the axis of the inner frame will satisfy the condition imposed on the equatorial Resal axes and may be selected as one of such axes. Let it be the equatorial axis Ox . The second equatorial axis Oy is then determined according to a right-hand system of coordinates.

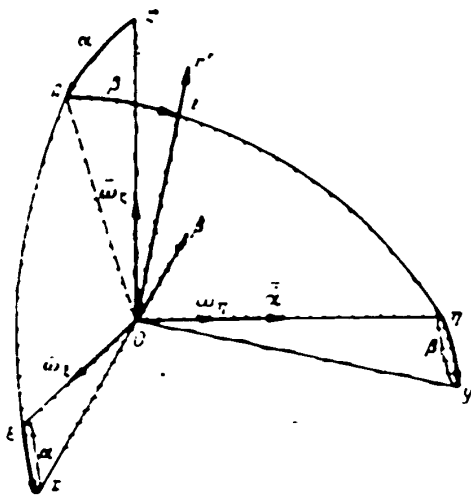


Fig.2.9 - The Euler Angles

Draw the plane $zO\eta$. Let this plane, in a given position of the axis Oz intersect the coordinate plane $EO\zeta$ in the line OA . Let us denote by α the angle between the principal axis $O\zeta$ and the line OA , and by β the angle between the line OA and the axis Oz , selecting the positive sense of these angles by the arrows shown in Fig.2.9. It is not hard to see that these two angles will completely determine the position of the axis Oz and the system of coordi-

nates $O\zeta\eta\zeta$, since the axis Oz may be brought into an assigned position by a rotation first in the plane $EO\zeta$ about the axis $O\eta$ by the angle α , followed by a rotation in the plane $zO\eta$ about the axis Ox by the angle β . By associating to the angles α and β the angle of rotation of the rotor in the equatorial plane on account of its spin, we obtain three degrees of freedom of the gyroscope.

The angles α and β are, as is commonly known, called Euler angles. They are selected by various methods, according to the form of the problem to be solved. The selection made by us is convenient in that a rotation in the planes $EO\zeta$ and $zO\eta$ is identical with a rotation about the axes of rotation of the outer and inner frames

STAT

of the gyroscope suspension, respectively. The former results directly from the fact that we have matched the axis of rotation of the inner frame with the axis $O\eta$, perpendicular to the plane zOz' , while the latter results from the fact that we have matched the axis of rotation of the inner frame with the axis Ox , which is perpendicular to the plane zOz' .

It follows from this that the angle α is the angle of rotation of the gyroscope about the axis of rotation of the outer frame, while the angle β is the angle of shift of the gyroscope about the angle of rotation of the inner frame.

The positive values of α and β are directed, as shown in Fig. 2.9, that is, α , along the positive semiaxis $O\eta$, β along the negative semiaxis Ox .

The system of coordinates $O\xi\eta\zeta$ always participates in the rotation of the earth, and, in addition, may also receive additional rotations on account of the displacement of the aircraft with respect to the earth surface, since the direction of the vertical or meridian is different for different points of the earth. Let, in the aggregate, the angular velocities of all these rotations of the system of coordinates $O\xi\eta\zeta$ have components along the axes $O\xi$, $O\eta$, $O\zeta$, equal respectively to ω_ξ , ω_η , ω_ζ . Then the angular velocities of rotation of the gyroscope, p and q , with respect to the axes Ox and Oy , are determined by the expressions

$$p = -\dot{\beta} + \omega_\xi \cos(\zeta, x) + \omega_\eta \cos(\eta, x) + \omega_\zeta \cos(\xi, x), \quad (2.30)$$

$$q = \dot{\alpha} + \omega_\xi \cos(\zeta, y) + \omega_\eta \cos(\eta, y) + \omega_\zeta \cos(\xi, y). \quad (2.31)$$

The cosines of the angles entering into these expressions are given in the following table:

Table I

	ξ	η	ζ
x	$\cos \alpha$	0	$-\sin \alpha$
y	$-\sin \alpha \sin \beta$	$\cos \beta$	$-\cos \alpha \sin \beta$

STAT

For small values of the angles α and β , with which we shall for the most part be dealing, this table is transformed into the following one:

Table II

$$\begin{array}{l} \xi \quad \eta \quad \zeta \\ x \quad 1 \quad 0 \quad -\alpha \\ y \quad 0 \quad 1 \quad -\beta \end{array}$$

On the basis of the last table, for small angles α and β , the expressions for p and q , taking account of the mobility of the system of coordinates $O\xi\eta\zeta$, will take the following form:

$$p = -\dot{\beta} + \omega_x - \omega_z \alpha. \quad (2.32)$$

$$q = \dot{\alpha} + \omega_y - \omega_z \beta. \quad (2.33)$$

The expression for L_x and L_y in the general case may be represented in the following form:

$$L_x = L_{kx} + L_{\rho x},$$

$$L_y = L_{ky} + L_{\rho y},$$

where L_{kx} , L_{ky} = moments produced by the correction system or the systems of springs and damper devices;

$L_{\rho x}$, $L_{\rho y}$ = moments of forces of friction in the axis of rotation of the inner and outer frames respectively.

Section 2.9. Influence of Earth Rotation and of the Displacement of the Aircraft with Respect to the Earth

The essence of these phenomena, taken into account according to eqs.(2.30), (2.31), or eqs.(2.32), (2.33), reduces to the following: the principal axis $O\xi$ of the system of coordinates $O\xi\eta\zeta$, which can be matched, as has been shown, either with the meridian of the place, varies its direction in s-STAT

This variation occurs, on the one hand, as a result of the fact that the true vertical and the local meridian also participate in the rotation of the earth, and on the other hand, a result of the fact that with the displacement of the aircraft with respect to the earth, the true vertical and the local meridian, whose direction must be determined by the aid of the gyro instruments, also vary their position.

It is commonly known that the expression true local vertical is the term applied to the direction of the action of the force of gravity which practically coincides with the direction of the earth radius OM (Fig.2.10). The deflec-

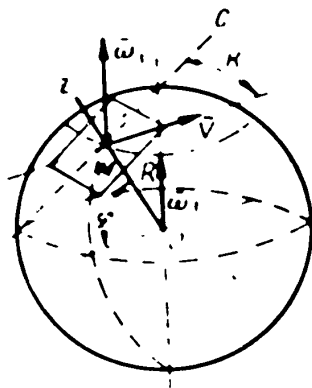


Fig.2.10 - Rotation of Plane of the Horizon

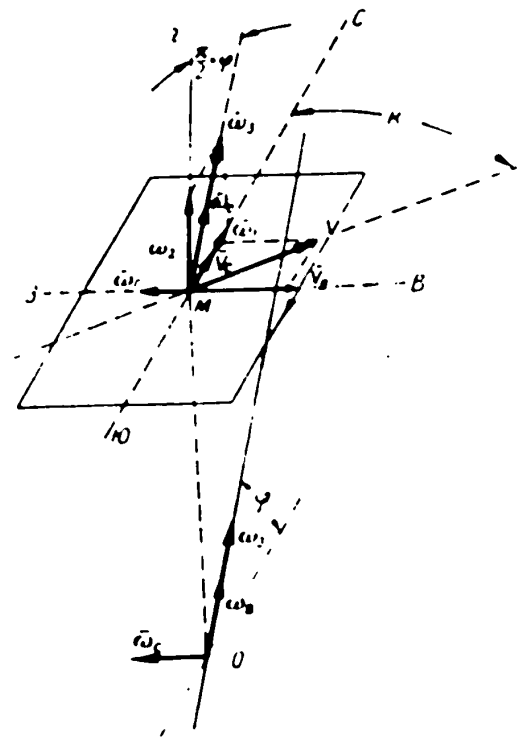


Fig.2.11 - Components of the Rotation of the Plane of the Horizon

tion of the vertical from the direction of the radius does not exceed units of minutes of arc. The prolongation of the vertical above Mz is called the zenith line. The plane perpendicular to the true vertical is called the plane of the horizon. The plane passing through the point of the place l and the axis of rotation of the earth, is called the plane of the local meridian. The intersection between the plane of the horizon and the plane of the meridian is called the meridian, or meri-

STAT

The planes perpendicular to the axis of rotation of the earth are called planes of the parallels. Of them, the plane of the parallel passing through the center of the earth O is called the plane of the equator. The angle between the true vertical and the plane of the equator is called the local latitude.

As follows from Fig.2.10, the rotation of the plane of the horizon, and, with it, of the vertical and meridian of the local vertical and local meridian in connection with the rotation of the earth, may be represented as the result of two rotations, first, the rotation about the true vertical, during which the north point of the meridian is shifted at first to the left, if viewed from the north when looking northward (in the northern hemisphere), and second, the rotation about the meridian, during which the eastern half of the plane of the horizon sinks while the western half rises.

The angular velocity of the former rotation $\omega_2 = \omega_e \sin \varphi$ will be called the vertical component of the earth rotation, while the angular velocity of the second rotation $\omega_1 = \omega_e \cos \varphi$ will be called the horizontal component of the earth rotation.

On resolving the speed of the aircraft V into its components along the meridian $V_c = V \cos K$ and along the parallel $V_B = V \sin K$, where K is the course angle, it becomes possible to treat the result of the flight of the aircraft as an additional rotation of the plane of the horizon, first about the axis of rotation of the earth at angular velocity $\omega_B = \frac{V_B}{R \cos \varphi}$ (R = distance from aircraft to center of earth), and second of angular velocity $\omega_c = \frac{V_c}{R}$ about the equatorial diameter of the earth, perpendicular to the plane of the meridian of the given place (Fig.2.11).

Estimation of the Influence of Rotation of the Earth and the Speed of Flight with Respect to the Vertical Position of the Principal Axis of the Gyroscope

In this case the principal axis Oz of the system of coordinates $O\xi\eta\zeta$ is matched with the true vertical Mz . The axis $O\eta$, with which the axis rotation of the outer

STAT

frame is matched, will either coincide with the direction of the velocity of flight V , or will be perpendicular to it, depending on whether the axis of rotation of the outer frame is parallel to the longitudinal axis of the aircraft or to its

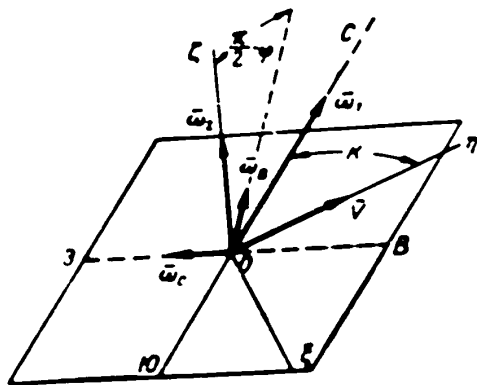


Fig.2.12 - allowing for the rotation of the Plane of the Horizon with respect to the Gyro Horizon

transverse axis. Here we shall consider the angle of drift of the aircraft as equal to zero, that is, we shall consider the course equal to the route angle. It is not hard to see (Fig.2.12) that if we take, let us say, the former case as our basis, then we obtain the latter case from the former by increasing the course angle of the aircraft by the angle $\frac{\pi}{2}$.

On projecting the corresponding components (Fig.2.12) onto the axis of

the system $Ox^0y^0z^0$, we obtain the following equations for the case when the axis of the outer frame of the gyroscope is parallel to the longitudinal axis of the aircraft:

$$\begin{aligned} \omega_x &= -\omega_1 \sin K - \omega_H \cos \varphi \sin K - \omega_c \cos K = -\omega_1 \sin K - \\ &\quad - \frac{V}{R} \sin^2 K - \frac{V}{R} \cos^2 K, \\ \omega_y &= \omega_1 \cos K + \omega_H \cos \varphi \cos K - \omega_c \sin K = \omega_1 \cos K + \\ &\quad + \frac{V}{R} \sin K \cos K - \frac{V}{R} \cos K \sin K, \\ \omega_z &= \omega_2; \quad \omega_H \sin \varphi = \omega_2 + \frac{V}{R} \sin K \operatorname{tg} \varphi \end{aligned}$$

01

$$\begin{aligned} \omega_x &= -\omega_1 \sin K - \frac{V}{R}, \\ \omega_y &= \omega_1 \cos K, \\ \omega_z &= \omega_2 + \frac{V}{R} \sin K \operatorname{tg} \varphi. \end{aligned}$$

STAT

On substituting the relations so obtained in eqs.(2.32) and (2.33), we get

$$p = -\dot{\beta} - \left(\omega_2 + \frac{V}{R} \sin K \operatorname{tg} \varphi \right) \alpha - \omega_1 \sin K - \frac{V}{R}, \quad (2.34)$$

$$q = \dot{\alpha} - \left(\omega_2 + \frac{V}{R} \sin K \operatorname{tg} \varphi \right) \beta + \omega_1 \cos K. \quad (2.35)$$

Allowing for the Influence of the Earth Rotation and of the Flight Speed
With Horizontal Position of the Principal Axis of the Rotor, Parallel to
the Meridian

In this case the axis $O\zeta$ is matched with the meridian; the axis On with which we shall consider the axis of rotation of the outer frame to be matched, will be parallel to the normal axis of the aircraft. Consequently, for horizontal flight (and it is for this that we are setting up the corresponding expressions) it will coincide with the zenith line Mz (Fig.2.13).

On projecting the same components of the rotation as in the preceding case, onto the axes of the system $O\xi\eta\zeta$ for a given arrangement of those axes, we get:

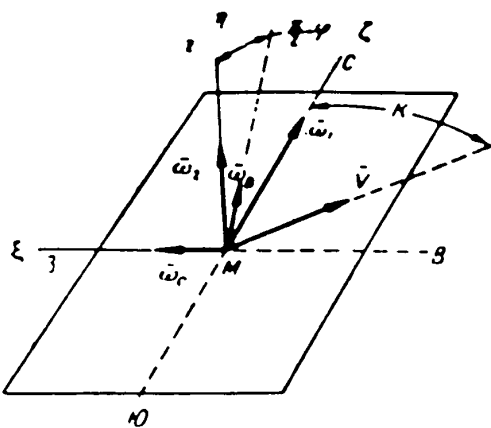


Fig.2.13 - Allowing for the Rotation of
the Plane of the Horizon with Respect
to the Gyroscopic Course Indicator

$$\begin{aligned} \omega_3 &= \omega_3 = \frac{V}{R} \cos K; \\ \omega_1 &= \omega_2 + \omega_3 \sin \varphi = \omega_2 + \\ &+ \frac{V}{R} \frac{\sin K}{\cos K} \sin \varphi, \\ \omega_2 &= \omega_1 + \omega_3 \cos \varphi = \omega_1 + \\ &+ \frac{V}{R} \frac{\sin K}{\cos \varphi} \cos \varphi \end{aligned}$$

or

$$\begin{aligned} \omega_3 &= \frac{V}{R} \cos K, \\ \omega_1 &= \left(\omega_2 + \frac{V}{R} \frac{\sin K}{\cos \varphi} \right) \sin \varphi, \\ \omega_2 &= \omega_1 + \frac{V}{R} \sin K. \end{aligned}$$

STAT

Substituting the relations so found in eqs. (2.32) and (2.33), we get

$$p = -\dot{\beta} - \left(\omega_1 + \frac{V}{R} \sin K \right) \alpha + \frac{V}{R} \cos K, \quad (2.36)$$

$$q = \dot{\alpha} - \left(\omega_1 + \frac{V}{R} \sin K \right) \beta + \left(\omega_2 + \frac{V}{R} \frac{\sin K}{\cos \varphi} \right) \sin \varphi. \quad (2.37)$$

Allowing for the Effect of a Turn on the Gyro Horizon

In this case we may consider that the system of coordinates $O\xi\eta\zeta$ possesses only a rotation about the true vertical at angular velocity $\omega_B = \frac{V}{\rho}$, where ρ = radius of turn.

In other words, we need not reckon with the variation of the position of the true vertical during the time of the turn, owing to the earth rotation.

Assuming this, we have

$$\omega_1 = \omega_2 = 0,$$

$$\omega_3 = \pm \omega_B,$$

where the upper sign corresponds to a right turn and the lower sign to a left.

Subsequently,

$$p = \dot{\beta} \pm \omega_B \alpha, \quad (2.38)$$

$$q = \dot{\alpha} \pm \omega_B \beta, \quad (2.39)$$

with the same rule for the selection of the signs.

CHAPTER III

BRIEF SURVEY OF PRINCIPLES OF ACTION OF POSITIONAL
GYROSCOPESSection 3.1. Astatic Gyroscopes

The principal advantage of gyroscopic positional instruments is their great rigidity produced by the rapidly spinning rotor, usually mounted in the gimbals. The motions of this rotor about the axis of the suspension may be sufficiently slow owing to the increased proper kinetic moment of the rotor.

As a result of this the axis of the gyroscope rotor acquires stability with respect to the action of disturbing forces. In this respect it is completely incomparable to the sensitive systems of positional instruments based on the use of other nongyroscopic principles, for instance, with a magnetic needle or pendulum.

But, in contrast to the latter, gyroscopic positional instruments make it necessary to take special measures to give them selectivity with respect to the direction which they must indicate. The selectivity of one positional instrument or another with respect to some position means the presence in that instrument of properties by virtue of which, when the sensitive system of the instrument deviates from this position, a certain moment, called the positional moment, is applied to it and returns it to the indicated position. A positional instrument thus possesses selectivity with respect to that position which constitutes the position of stable equilibrium for its sensitive system.

STAT

The center of gravity of the astatic gyroscope is matched with the center of the suspension, and, owing to this, the action of the force of gravity on the gyroscope is eliminated.

Thus any position of the astatic gyroscope is an equilibrium position.

It is of substantial importance that the position of the gyroscope will vary, during motion of the base of the suspension, owing to the action on the gyroscope of the forces of friction in the axis of the suspension, and owing to a certain unavoidable residual imbalance of the gyroscope.

It is true that the rate of this change, at a proper value of the kinetic moment of the gyroscope, will be small. In this connection, in those cases where a definite direction must be indicated for 2-3 min, it is entirely possible to use an astatic gyroscope for these purposes, although in practice this is not done.

In this case, the fact that an astatic gyroscope is indifferent to the position in which it is installed, is a substantial merit for this use, since, in this connection, an astatic gyroscope may be utilized for the brief designation of any direction with respect to the earth surface.

It must, however, be noted, that in this case the astatic gyroscope must initially be set in the required direction, since the gyroscope itself is unable to "find" this direction.

Section 3.2. Position Gyroscopes with Displaced Center of Gravity

Two methods are used for giving gyroscopic position instruments the necessary selectivity.

The first method, on which we shall dwell in this Section, is based on obtaining the necessary positional moment by means of a definite displacement of the center of gravity of the gyroscope with respect to the center of the suspension, that is, by eliminating the astatic nature of the gyroscope.

In this case, when the gyroscope departs from the assigned direction, a positional moment, which will return the gyroscope to the assigned direction, will

develop on account of the activity of gravity.

In technology two types of positional gyroscopes are in use, in which this same method of obtaining selectivity, the gyroendulum and gyrocompass, are used.

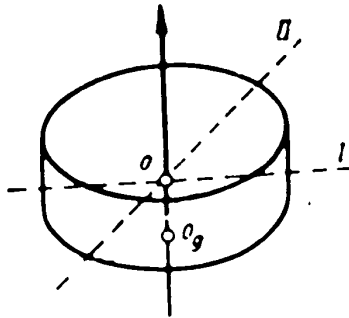


Fig.3.1 - Gyroendulum

I - Axis of inner frame; II - Axis of outer frame; O - Center of suspension; O_g - Center of gravity

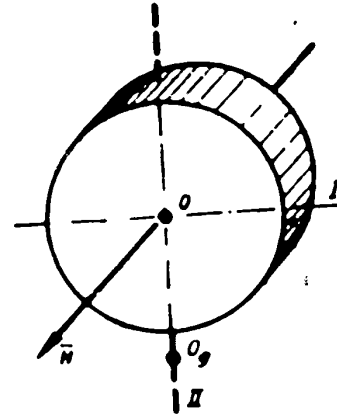


Fig.3.2 - The Magnetic Gyrocompass

I - Axis of inner frame; II - Axis of outer frame; O - Center of suspension; O_g - Center of gravity

Gyroendulums serve to indicate the vertical. The axis of the gyroendulum rotor is held in the vertical direction by means of the downward displacement of the center of gravity of the gyroscope O_g (Fig.3.1) along the spin axis from the center of suspension O. The gyrocompass serves to indicate the geographic meridian. The axis of the gyroscope rotor is held in the direction of the meridian by the displacement of the center of gravity of the gyroscope O_g below the center of the suspension O (Fig.3.2) in the equatorial plane of the gyroscope.

A brief theory of the gyroendulum and gyrocompass is given in the following Chapters, and here we have no intention of touching on this subject in any way. We confine ourselves mainly to a few remarks of fundamental nature.

The equilibrium position for the spin axis of the gyroendulum will be the

vertical of the locality (without taking account of the error owing to the earth rotation and the displacement of the base of the gyroscope suspension).

The position of equilibrium for the rotor axis of the gyropendulum will be the local vertical (not taking into account the errors due to the rotation of the earth and the displacement of the base of the gyroscope suspension).

On deviation of the axis of the rotor from the vertical, the positional moment of the force of gravity begins to act on the gyroscope. This force tends to restore the rotor axis to the plane preceding the deviation, by moving it toward the vertical. But under the action of this moment, the motion of the gyropendulum, according to the law of precession, begins not in the plane of the deviation that has taken place, but perpendicular to it.

Thus we get the result that the action of the positional moment in the gyropendulum leads it to the liquidation of any violations that arise, and to the transfer of such violation to a different plane. In the last analysis the spin axis of the gyropendulum, instead of returning to the position of equilibrium, will undergo oscillations, describing a cone about the equilibrium position, having its vertex at the fixed point. Under the influence of friction in the suspensions, the radius of this cone will diminish more and more, and ultimately the spin axis of the gyro rotor will be matched with the angle of repose relative to the vertical. From the technical aspect, however, this circumstance cannot be utilized, since by the conditions of accuracy for the operation of the instrument, a more or less considerable friction in the suspension must not be allowed, and at such friction as may be allowed, too much time is required for damping of the precessional oscillations of the gyrocompass to take place on that account. In other words, in order to transform the gyropendulum into a positional instrument, it must be provided with some means capable of assuring the effective damping of its oscillations. Such methods have indeed been worked out, but they considerably complicate the design of the instrument. And in a gyrocompass that does not use these special damping devices, the

STAT

axis of the rotor, while it is returned to the meridian in case of its departure from it, will also perform oscillations around that meridian of only a slightly more complex form.

The equilibrium position of the rotor axis in the gyrocompass having a fixed base with respect to the earth, is a direction in the plane of the meridian with a certain entirely definite inclination to the plane of the horizon. On account of this inclination, there develops a positional moment of the force of gravity, which assures the precession of the gyroscope equal to the vertical component of the earth rotation. In this case, the rotor axis of the gyroscope and the plane of the meridian will both be rotating at constant speed and will remain matched.

If the axis of the rotor of the gyrocompass, however, leaves the plane of the meridian, the center of gravity of the gyrocompass will also leave this plane. In this case the rotation of the plane of the horizon due to the horizontal component of the velocity of rotation of the earth will vary the angle between the gyroscope axis and the horizon plane, which will lead to a change in the magnitude and direction of the positional moment due to gravity. When the rotor axis leaves the meridian plane, the angle between the gyroscope axis and the horizon plane increases, thus causing an increase in the rate of precession. This increase in the rate of precession returns the rotor axis to the meridian plane. Owing to the fact that the rate of precession of the gyroscope exceeds the rate of rotation of the meridian, the rotor axis of the gyroscope will catch up with the meridian. As the meridian advances, the angle between the gyroscope rotor axis and the horizon plane will diminish, which will cause a corresponding reduction in the rate of precession and will again return the rotor axis to the meridian plane.

Thus, in the gyrocompass as well, the gyroscope axis will describe a cone whose center coincides with the center of the suspension, and whose axis coincides with the equilibrium position of the gyroscope axis.

In exactly the same way as in the gyropendulum, by using damping devices of one

STAT.

kind or another, the damping of these oscillations of the gyrocompass can be assured, but exactly as in that case, this implies a substantial complication of the instrument design.

Another substantial disadvantage of both the gyropendulum and the gyrocompass is that, owing to loss of astaticity, they become particularly subject to the action of inertial disturbing forces. It must, finally, be recalled that these instruments (especially the gyrocompass) possess considerable errors owing to the influence of the earth rotation on them and owing to the displacements, with respect to the earth, of the object on which they are installed.

What had been said will explain sufficiently why this method has not found widespread use in aviation practice.

Section 3.3. Positional Gyroscopes with Correction System

Let us now dwell on the second method of giving gyroscopic positional instruments the necessary selectivity, based on the gyroscope itself remaining astatic, but being supplemented by what is called a correction system.

The operation of the correction system is based on the application of a positional moment to the gyroscope, when any deviation from its position takes place, in such a way as to cause its spin axis to move (Fig.3.3).

The question whether deviation exists is answered, and its amount evaluated, by comparing the position actually occupied by the gyro with the position of some other element having selectivity with respect to the direction which is to be indicated in this case. For example, the position of the spin axis of a gyroscope indicating the vertical is compared for this purpose with the position of a pendulum; the position of the spin axis of a gyro indicating the meridian, with a magnetic needle, etc.

We shall henceforth term an element whose position is compared with the position of the gyro the sensitive element of the correction system.

It is easy to see that in essence, a gyro correction system may be treated as a feedback regulator of its position, and that in this sense it may be said that

the method of making gyroscopic position instruments selective by means of a correction system is a method of automatic control of the position of an astatic gyro not possessing selectivity, by the aid of a special element that does possess such selectivity.

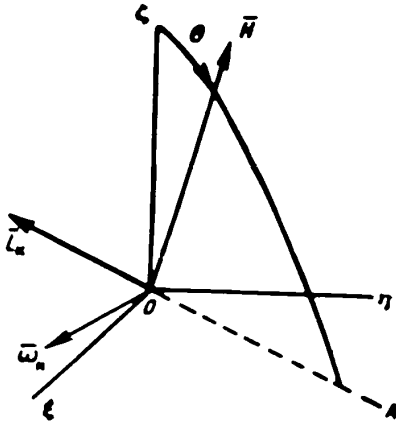


Fig.3.3 - Principle of Operation of
Radial Correction System

OCA - Plane of deviation; θ - Angle of deviation; L_K - Moment of correction; ω_K - Angular velocity of correcting precession.

In what does the technical meaning of such a method of indicating an assigned direction reside? Would it not be simpler to use directly, as the positional instrument, the very same element possessing selectivity by means of which the correction is effected, or, in other words, by means of which the automatic regulation of the gyro position is effected?

The answer to this question is that when we use a radial correction system for a gyroscope we get a system

that combines not only the selectivity of the element by which the correction is effected, but also the high rigidity or inertia inherent in the gyroscopes. This means that the system as a whole will react much more weakly to disturbances than the element effecting the correction itself.

Now let us consider, to be concrete, the system of a gyro-vertical indicator in which a pendulum is used as the sensitive correcting member.

We remark that during the initial period of the development of aviation there were attempts to utilize pendulums of one kind or another to indicate the vertical, but these attempts were unsuccessful, mainly owing to the fact that even the

so-called uniform flight of an aircraft still involves accelerations that vary in

STAT

magnitude and sign in a more or less random manner. Maneuvers involve such accelerations even more. As a result, the pendulum in flight is always under the influence of various disturbing inertial forces differing in direction and magnitude, and

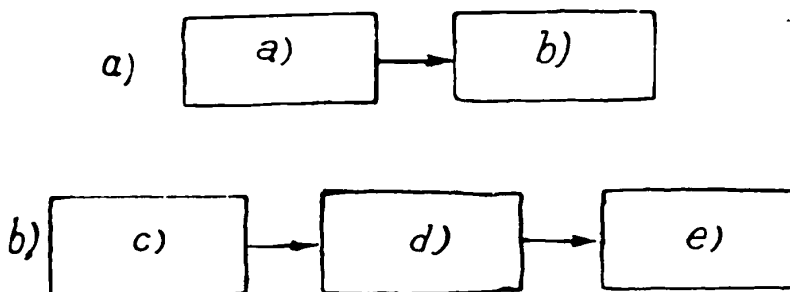


Fig.3.4 - Diagram of Formation of the Errors of Indicating System
without Gyro (a) and with Gyro (b)

- a) Disturbing forces; b) Errors of indicating system; c) Disturbing forces;
d) Errors of corrector; e) Errors of indicating system

since the rigidity or inertness of the pendulum is relatively small, these forces disturb its position rather substantially.

If the pendulum is used directly as an indicator of the vertical, then the disturbances in its position will mean the appearance of corresponding errors in its readings. But if the pendulum serves instead as the sensitive member of a correction system, then the disturbances in this position will mean, from the very beginning, only the application of the corresponding forces to the gyro.

In other words, while, in the former case, the chain of phenomena leading to the appearance of errors due to the action of disturbing forces will consist of two links, it will consist in the latter case of three links (Fig.3.4), of which the third link, the gyroscope, involves a high degree of inertness.

Thus, although there will still be an ultimate disturbance in the position of the gyro, that disturbance will be considerably less than the disturbances in the
than the disturbances of the pendulum.

STAT

We shall illustrate this by an example.

On account of the disturbed oscillations of a pendulum, defined by the functions $\gamma(t)$, let a disturbing moment proportional to these oscillations, i.e., equal

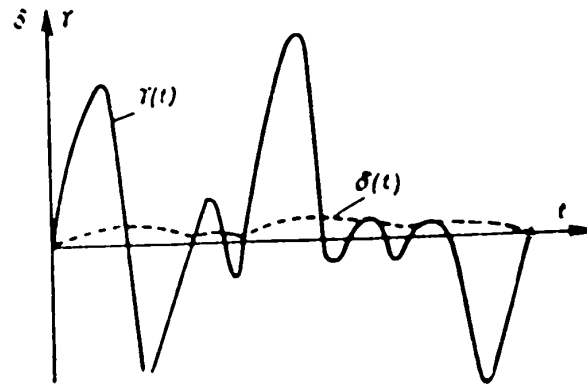


Fig.3.5 - Influence of Disturbances of Corrector

$\gamma(t)$ - Disturbances of corrector; $\delta(t)$ - Disturbances of gyroscope

to $k\gamma(t)$, where k is a factor of proportionality, act on the gyro in connection with the disturbances of the correction system. According to the law of precession for the disturbances of position of the gyro δ under the influence of this moment, we get

$$\delta = \frac{k}{H} \int_0^t \gamma(t) dt,$$

where H = kinetic moment of gyro.

Assume that $\gamma(t)$ varies with time according to the diagram in Fig.3.5. Then δ will be determined by the mean area of the diagram of $\gamma(t)$, multiplied by the quantity $\frac{k}{H}$, which may be made sufficiently small, on account of the sufficient value of the kinetic moment of the gyro H_0 .

STAT

CHAPTER IV

THEORY OF THE GYROPENDULUM

Section 4.1. Behavior of Undamped Gyro pendulum on Fixed Base
without Allowing for the Earth Rotation

Equations of Motion

We shall apply the term undamped gyro pendulum to a gyroscope with three degrees of freedom, whose polar axis is directed along the vertical, and whose center of

gravity is displaced upward or downward along the polar axis of the rotor Oz , with respect to the center of the support.

We shall restrict our problem to the study of the precessional motions of a gyro pendulum, disregarding the rotation as a component of the motion which is of no practical importance in this application, i.e., we shall take, as our basis, the equations of motion in the following form:

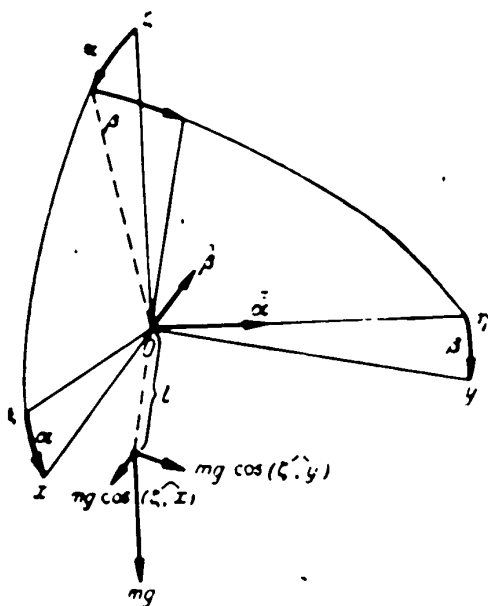


Fig. 4.1 - Gyro pendulum on Fixed Base

$$Hq = I_{\omega} \quad (4.1)$$

$$Hp = I_{\omega} \quad (4.2)$$

Putting, in eqs.(2.34) and (2.35), the terms allowing for the influence of the earth rotation and the flight speed as equal to zero, we get

$$q = \dot{\alpha}; \quad (4.3)$$

$$p = -\dot{\beta}. \quad (4.4)$$

For the moments L_x and L_y , when the center of gravity is displaced downward according to Fig.4.1, we have:

$$\begin{aligned} L_x &= -mgl \cos(\zeta, y) + L_{\rho\dot{\alpha}}, \\ L_y &= mgl \cos(\zeta, x) + L_{\rho\dot{\beta}}. \end{aligned}$$

where the first terms are the positional moments due to the displacement of the center of gravity; $L_{\rho\dot{\alpha}}$ and $L_{\rho\dot{\beta}}$ are moments of friction about the axis of rotation of the inner and outer frames of the gimbals respectively. We shall take these moments of friction as constant. To the upper signs correspond positive values of $\dot{\beta}$, $\dot{\alpha}$ and to the lower signs, negative values.

Making use of the values of $\cos(\zeta, y)$ and $\cos(\zeta, x)$ according to Table II of Chapter 2, and taking $\cos \beta = 1$, we get

$$\begin{aligned} L_x &= mgl\beta \pm L_{\rho\dot{\alpha}}, \\ L_y &= -mgl\alpha + L_{\rho\dot{\beta}}. \end{aligned}$$

As a result, the equations of motion (4.1) and (4.2) for the gyropendulum, in the case taken by us of a downward displacement of the center of gravity, take the form

$$\ddot{\alpha} - \lambda\beta = \pm \lambda\rho_{\dot{\alpha}}, \quad (4.5)$$

$$\ddot{\beta} + \lambda\alpha = \mp \lambda\rho_{\dot{\beta}}. \quad (4.6)$$

where

$$\lambda = \frac{mgl}{H},$$

$$\rho_{\dot{\beta}} = \frac{L_{\dot{\beta}}}{mgl},$$

$$\rho_{\dot{\alpha}} = \frac{L_{\dot{\alpha}}}{mgl}.$$

The signs of $\rho_{\dot{\beta}}$ and $\rho_{\dot{\alpha}}$ are selected by the rule formulated for the selection of signs for moments of friction.

Law of Motion of the Gyro- Pendulum without Allowing for Friction in the Gimbals

Putting $\rho_{\dot{\alpha}} = \rho_{\dot{\beta}} = 0$ in eqs.(4.5) and (4.6), we rewrite these equations in the following form:

$$\frac{d\alpha}{dt} = \lambda\beta, \quad (4.7)$$

$$\frac{d\beta}{dt} = -\lambda\alpha. \quad (4.8)$$

Let us draw a sphere of radius equal to unit length about the fixed point of the gyroscope. In its motion, the end of the spin axis will describe a certain path on this sphere. It is the form of this path that will determine the law of motion of the gyro.

Let us take a part of this sphere near the intersection of its surface with the axis Oz . Let us take, further, the line of intersection between this sphere and the coordinate plane zOx as the coordinate axis $O\alpha$, and the line of its intersection with the coordinate plane zOy as the coordinate axis $O\beta$. Such assumptions may be considered correct only for small values of α and β .

As a result, the path described by the end of the spin axis on the sphere may be approximately treated as the curve $F(\alpha, \beta) = 0$ in the coordinate plane $O\alpha\beta$, defined by the solution of eqs.(4.7), (4.8).

By dividing eq.(4.7) by eq.(4.8) to eliminate dt , we get the following differential equation:

STAT

$$\frac{d\alpha}{dt} = -\frac{\beta}{a}$$

whence, separating the variables and integrating, we have

$$\alpha^2 + \beta^2 = \theta_0^2$$

where θ_0^2 is an arbitrary constant.

Assume that for $t = 0$, $\alpha = \alpha_0$, $\beta = \beta_0$. Then for θ_0 we get

$$\theta_0 = \sqrt{\alpha_0^2 + \beta_0^2}$$

Thus the path sought is a circle with its center at the origin of coordinates, and a radius equal to the initial disturbance. (Fig.4.2).

In other words, if, at the initial instant, the spin axis of the gyropendulum

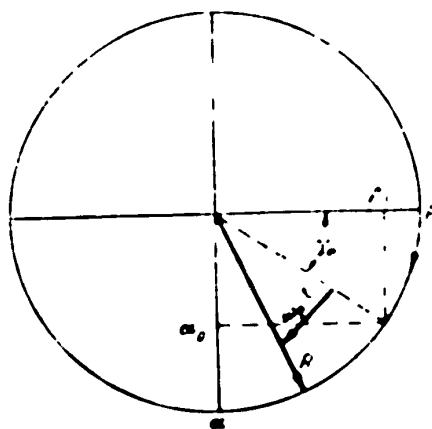


Fig.4.2 - Path of the End of the Spin axis of Gyropendulum, Neglecting Friction in the Gimbals

was on true vertical, it will remain on it. If, however, at the initial instant, the spin axis of the gyropendulum was deflected from the true vertical by a certain angle θ_0 , different from 0, then it will rotate about the true vertical in such a way that its end describes a circle in the coordinate plane $O\alpha\beta$, while the axis itself describes a cone with vertex at the fixed point of the gyro.

It follows from eq.(4.7) that, for the case we are investigating,

positive values of β correspond to positive values of $\frac{d\alpha}{dt}$, while negative values of β correspond to negative values of $\frac{d\alpha}{dt}$, that is, for all $\beta > 0$, α increases, while for all $\beta < 0$, α decreases.

This means that the end of the spin axis of the gyropendulum is displaced clockwise along the path we have found.

The law of motion of the end of the spin axis so found may be treated as precession about the true vertical. The rate of this precession, which we shall denote by ω_p , will obviously be equal to the angular velocity of rotation of the radius vector of the end of the spin axis in the coordinate plane $O\alpha\beta$.

On eliminating β from eqs.(4.7) and (4.8), we get

$$\frac{d^2\alpha}{dt^2} + \lambda^2\alpha = 0,$$

and on eliminating α from them, we get

$$\frac{d^2\beta}{dt^2} + \lambda^2\beta = 0.$$

The solutions of these equations will be:

$$\alpha = \eta_0 \sin(\omega_p t + \gamma_0),$$

$$\beta = \eta_0 \cos(\omega_p t + \gamma_0),$$

where γ_0 equals the initial angle of the radius vector of the end of the spin axis

$$\frac{d\alpha}{dt} = \eta_0 \omega_p \cos(\omega_p t + \gamma_0) = \omega_p \beta,$$

$$\frac{d\beta}{dt} = -\eta_0 \omega_p \sin(\omega_p t + \gamma_0) = -\omega_p \alpha.$$

It follows from a comparison of the expressions so obtained with eqs.(4.7), (4.8) that

$$\omega_p = \lambda$$

Thus the rate of regular precession is numerically equal to λ , and it is directed downward from the fixed point of the gyro.

On investigating this case on the basis of the complete equations of motion, we would obtain, for the initial conditions adopted, one of the partial cases of regular precession (cf. F.V.Bulgakov (Bibl. 1, pages 18-22), with a nuta-

STAT

tion frequency $\mu = \frac{H}{J_{eq}}$ and with an amplitude smaller than the initial deviation θ_0 by a factor of $\frac{\mu}{\lambda}$. For one of the gyro horizons of the gyropendulum type, the quantity $\frac{\mu}{\lambda}$ is of the order of 5×10^5 . If we add the fact that nutation is very rapidly damped, even by the resistance of the air without considering other factors, then we reach the conclusions that it is entirely correct to neglect it.

On repeating the same study for an upward displacement of the center of gravity, we get the same general result, with a single difference that in this case the rotation of the spin axis will be counterclockwise.

This results from the fact that when the center of gravity is displaced upward, the signs are reversed in the left sides of eqs.(4.7) and (4.8), and therefore α will increase for all $\beta < 0$, while β will decrease for all $\alpha > 0$.

Law of Motion of Gyropendulum Allowing for Friction in the Gimbals

Let us rewrite the equations of motion (4.5) and (4.6) in the following form:

$$\frac{d\alpha}{dt} = \lambda(\beta + \rho_\beta) \quad (4.9)$$

$$\frac{d\beta}{dt} = -\lambda(\alpha + \rho_\alpha) \quad (4.10)$$

Let us introduce the new variables:

$$\tilde{\beta}_{1,2} = \beta + \rho_\beta$$

$$\tilde{\alpha}_{1,2} = \alpha + \rho_\alpha$$

where the index "1" corresponds to the upper sign on the right side, and the index (2) to the lower sign. It is easy to see that for all points except those at which ρ_α and ρ_β change their signs, we may write

$$d\tilde{\beta}_{1,2} = d\beta \quad (4.11)$$

$$d\tilde{\alpha}_{1,2} = d\alpha \quad (4.12)$$

On dividing eqs.(4.9) and (4.10) by each other and using (4.11) and (4.12), we

STAT

get

$$\frac{d\tilde{\alpha}_{1,2}}{d\tilde{\beta}_{1,2}} = -\frac{\tilde{\beta}_{1,2}}{\tilde{\alpha}_{1,2}}$$

Or, on separating the variables and integrating:

$$\tilde{\alpha}_{1,2}^2 + \tilde{\beta}_{1,2}^2 = \theta_0^2 \tag{4.13}$$

The equation of path so obtained is real for all values of α and β except for those values at which $\rho_{\dot{\beta}}$ and $\rho_{\dot{\alpha}}$ change their signs, i.e., at which $\tilde{\alpha}_1, \tilde{\beta}_1$, pass into $\tilde{\alpha}_2, \tilde{\beta}_2$ respectively, or vice versa. At each such transition, we will leave the equation of path corresponding to the course of time before the transition, and find a new one, selecting as the initial conditions for each successive piece of the path, the terminal values of the preceding one, i.e., in essence, adjusting each successive piece of the path to the preceding piece.

This change of sign and transition takes place when $\dot{\alpha}$ or $\dot{\beta}$ pass through the 0 value, which takes place, according to (4.9) and (4.10), at $\beta^+ \rho_{\dot{\beta}} = 0$ and $\alpha^+ \rho_{\dot{\alpha}} = 0$ respectively. Consequently the boundaries of transition from $\tilde{\alpha}_1$ to $\tilde{\alpha}_2$, or vice versa, are the straight lines $\beta = \pm \rho_{\dot{\beta}}$, and the boundaries (Fig.4.3) of the transition from $\tilde{\beta}_1$ to $\tilde{\beta}_2$ or the reverse are the straight lines $\alpha = \pm \rho_{\dot{\alpha}}$.

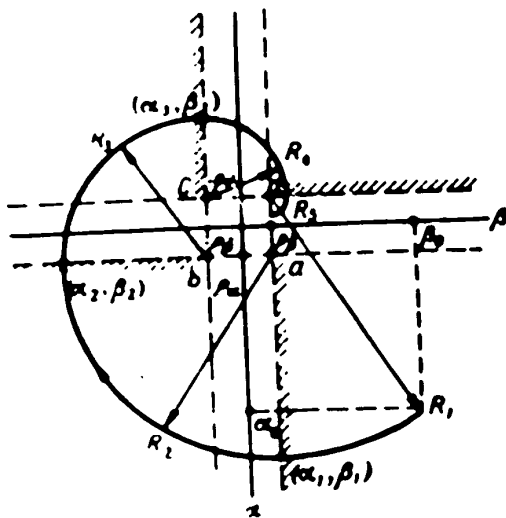


Fig.4.3 - Path of End of Axis of a Gyro-
pendulum with Downward Displacement of
Center of Gravity, Allowing for Friction
in the Gimbals

We remark that the motion of the end of the spin axis through all the pieces of the path is clockwise in the case under study.

STAT

This results from the fact that, by (4.9), α increases at positive β exceeding $\rho_{\dot{\beta}}$, while for negative β exceeding $\rho_{\dot{\beta}}$ in modulus, α decreases.

If for $|\beta| \leq \rho_{\dot{\beta}}$, $|\alpha| > \rho_{\dot{\alpha}}$, then, turning to (4.10), we have a decrease in β at positive α exceeding $\rho_{\dot{\alpha}}$, and an increase of β at negative α exceeding $\rho_{\dot{\alpha}}$ modulo. It is not hard to see that all this means that the motion of the end of the spin axis is clockwise on the path, and this is the motion of the spin axis along the path even in the absence of all friction in the gimbals.

If, for $|\beta| \leq \rho_{\dot{\beta}}$, $|\alpha| \leq \rho_{\dot{\alpha}}$, then this means that the moment of friction exceeds the moments due to the displacement of the center of gravity, and, consequently, motion of the gyro is impossible.

Assume that at $t = 0$, $\alpha = \alpha_0 > |\rho_{\dot{\alpha}}| > 0$, $\beta = \beta_0 > |\rho_{\dot{\beta}}| > 0$ (cf. Fig.4.3). By (4.9) and (4.10) we have for these cases $\dot{\alpha} > 0$; $\dot{\beta} < 0$. Consequently the upper sign must be taken for $\rho_{\dot{\alpha}}$, and the lower sign for $\rho_{\dot{\beta}}$, while the equation of the path eq.(4.13) is written in the following form:

$$(\alpha + \rho_{\dot{\alpha}})^2 + (\beta - \rho_{\dot{\beta}})^2 = (\alpha_0 + \rho_{\dot{\alpha}})^2 + (\beta_0 - \rho_{\dot{\beta}})^2,$$

which is the equation of the circle with center at the point $(-\rho_{\dot{\alpha}}, \rho_{\dot{\beta}})$ and the radius $R_1 = \sqrt{(\alpha_0 + \rho_{\dot{\alpha}})^2 + (\beta_0 - \rho_{\dot{\beta}})^2}$.

For $\beta = \rho_{\dot{\beta}}$, $\dot{\alpha}$ passes through 0, and (3.13) ceases to be real. For the following piece of the path $\tilde{\alpha}_1 = \alpha + \rho_{\dot{\alpha}}$, must be replaced by $\tilde{\alpha}_2 = \alpha - \rho_{\dot{\alpha}}$ in connection with the change of sign of $\rho_{\dot{\alpha}}$. Taking as initial conditions for the new piece of path, the terminal values of the latter, i.e., taking for $t = t_1$, $\alpha = \alpha_1$, and $\beta = \rho_{\dot{\beta}}$, we get

$$(\alpha - \rho_{\dot{\alpha}})^2 + (\beta - \rho_{\dot{\beta}})^2 = (\alpha_1 - \rho_{\dot{\alpha}})^2 \quad (4.14)$$

which is the equation of a circle with center at point $(\rho_{\dot{\alpha}}, \rho_{\dot{\beta}})$ and with radius $R_2 = \alpha_1 - \rho_{\dot{\alpha}}$ (cf. Fig.4.3).

At $\alpha = \rho_{\dot{\alpha}}$, $\dot{\beta}$ passes through zero, and eq.(4.14) ceases to be real. For the following new solution $\tilde{\beta}_2 = \beta - \rho_{\dot{\beta}}$ must be replaced by $\tilde{\beta}_1 = \beta + \rho_{\dot{\beta}}$, in view of the

change of sign of ρ_{β} . Then, selecting the initial conditions at finite values of the solution (4.14), i.e., taking for $t = t_2$, $\alpha = \rho_{\alpha}$, $\beta = \beta_2$, we get

$$(\alpha - \rho_{\alpha})^2 + (\beta + \rho_{\beta})^2 = (\beta_2 + \rho_{\beta})^2 \quad (4.15)$$

which is the equation of a circle with center at the point $(\rho_{\alpha}, -\rho_{\beta})$, $R_3 = R_2 + \rho_{\beta}$ (cf. Fig.4.3).

At $\beta = -\rho_{\beta}$, $\dot{\alpha}$ passes again through zero. On replacing in connection with this $\tilde{\alpha}_2 = \alpha - \rho_{\alpha}$ by $\tilde{\alpha}_1 = \alpha + \rho_{\alpha}$ and taking, as the new initial conditions, finite values of eq.(4.15), that is, taking, for $t = t_3$, $\alpha = \alpha_3$ and $\beta = -\rho_{\beta}$, we get

$$(\alpha + \rho_{\alpha})^2 + (\beta + \rho_{\beta})^2 = (\alpha_3 + \rho_{\alpha})^2$$

which is the equation of a circle with center at the point $(\alpha - \rho_{\alpha}, -\rho_{\beta})$ etc.

Thus, for each transition to the following piece of the path, the center of the circle, whose arc represents this piece, jumped clockwise to the adjacent angle of the rectangle abcd (cf. Fig.4.3).

We shall call this rectangle the rectangle of repose, and the angles ρ_{α} and ρ_{β} the angles of repose respectively of the outer and inner frames of the suspension.

As a result of this, the transition of the radius of the next circle will be less than the radius of the preceding circle by twice the angle of repose of the outer or inner frames, depending on whether the center of the circle is displaced parallel to axis of $O\alpha$ or $O\beta$.

In consequence, the resultant curve is represented by an involutorial spiral (cf. Fig.4.3), consisting of arcs of circles of steadily diminishing radius, fitted to each other.

The straight lines on which the fitting is performed are marked by dashed lines on Fig.4.3.

This process will be continued until the finite state of some piece of the trajectory is in accordance with the conditions $|\alpha| \leq \rho_{\alpha}$, $|\beta| \leq \rho_{\beta}$, which will mean the impossibility of further motion.

STAT

Thus the spiral will end at some point on the sides of the rectangle of repose.

For a gyropendulum with an upward displacement of the center of gravity, the equations of motion will take the following form:

$$\frac{d\alpha}{dt} = -\nu (\beta + \beta_0),$$

$$\frac{d\beta}{dt} = \nu (\alpha + \alpha_0).$$

On performing an analogous study, we may convince ourselves that the motion of the end of the axis of the gyroscope over all the pieces of the path, will be counterclockwise in this case. The centers of the circles whose arcs represent pieces

of the path will also be displaced counterclockwise at the corners of the rectangle of repose.

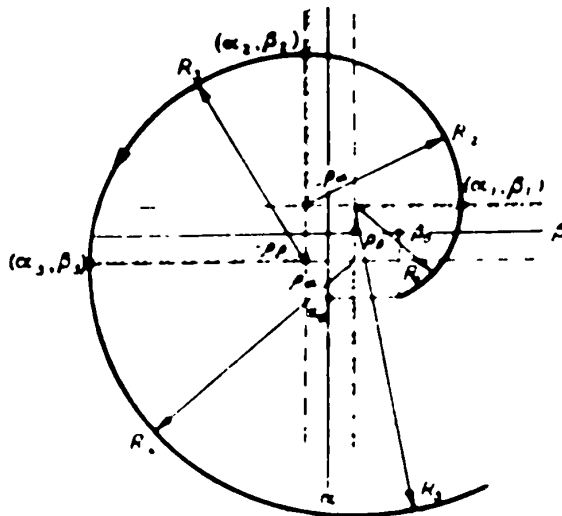
As a result, at each transition, the radius of the next circle will not decrease, but will increase by comparison with the radius of the preceding circle at two angles of repose.

In this connection, the path, composed of the pieces, will not be an involutational but an evolutational spiral (Fig.4.4), that is, with an upward displacement of the center of gravity, the deflection of the gyropendulum axis under the influence of dry friction will increase.

Fig.4.4 - Fate of End of Spin Axis of Gyropendulum with Upward Displacement of the Center of Gravity, Allowing for the Friction in the Gimbals

will increase.

With the passage of time, the spin axis may occupy a horizontal position, and then the upper gyropendulum may pass over into a lower gyropendulum.



Section 4.2. Behavior of Gyropendulum in the Presence of a Hydraulic Arrester

The material such as given in this paragraph is taken with insubstantial modifications from the book by B.V. Bulgakov.

Figure 4.5 gives a diagram of the gyropendulum with hydraulic arrester in one plane of oscillation.

As follows from its name, the hydraulic arrester is used to extinguish the precessional oscillations that can arise in the system under the action of disturbing moments.

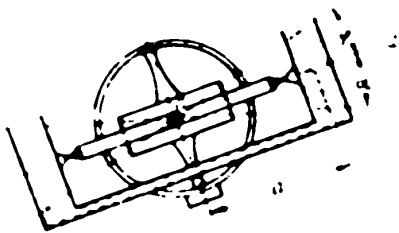


Fig.4.5 - Diagram of Gyropendulum
with Hydraulic Arrester

As will be seen from the diagram, the hydraulic arrester consists of two vessels filled with liquid and connected by a capillary tube. The limited rate of flow of the liquid through this tube leads to its nonuniform distribution between the vessels, which produces the moment N about the axis of

rotation of that frame of the gimbals with which these vessels are connected.

On the diagram of Fig.4.5, this frame happens to be the outer one. Its axis is perpendicular to the plane of the drawing, and Ox is the axis of the inner frame. As follows from this diagram, the moment may be represented by the expression:

$$N = c_1 \gamma \cdot 2a^2 S \gamma.$$

where a = distance between center of gravity of vessels and the axis of rotation;

S = cross-sectional area of vessels;

γ = specific weight of liquid.

The pressure assuring the flow of the liquid through the capillary tube will be equal to the difference between the levels of the liquid over the true horizontal

STAT

zon in the tubes. If we take Poisseuille law that the rate of flow of a liquid is proportional to this pressure, we get

$$\dot{z} = -c_2(z + \varphi). \quad (4.16)$$

Thus, in the presence of a hydraulic arrester, the expression for the moments L_x, L_y , will be of the following form, if the moments of friction in the gimbals are neglected:

$$\begin{aligned} L_x &= mgl\beta, \\ L_y &= mglz + c_1\varphi. \end{aligned}$$

On substituting these expressions in (4.1) and (4.2), likewise bearing in mind (4.3) and (4.4), and associating them with the equations of motion (4.16), we get

$$\begin{aligned} H\ddot{\alpha} &= mglz + c_1\dot{\varphi}, \\ H\ddot{\alpha} &= mglz, \\ \dot{z} &= -c_2(z + \varphi). \end{aligned}$$

or

$$\left. \begin{aligned} \ddot{\alpha} - \lambda\beta &= 0, \\ \ddot{\beta} + \lambda\alpha + (1-k)\lambda\dot{\varphi} &= 0, \\ \dot{\varphi} + c_2(z + \varphi) &= 0. \end{aligned} \right\} \quad (4.17)$$

where

$$\begin{aligned} \lambda &= \frac{mgl}{H}, \\ k &= 1 - \frac{c_1}{mgl}. \end{aligned}$$

On eliminating the variables β and φ , we now obtain

$$\ddot{\alpha} + c_2\alpha + c_2\lambda^2k\alpha = 0. \quad (4.18)$$

The functions which together make up the solution of eq.(4.18), will die away in the course of time if the roots of the characteristic equation (4.18) have a negative real part. The satisfaction of this condition may be checked by means of

the Routh-Hurwitz criterion, without actually having to solve these equations.

STAT

According to this criterion, in an equation of the third order, all the roots of the characteristic equation will have a negative real part if all the coefficients of the equation are positive and if the following inequality is satisfied

$$AB - C > 0. \quad (4.19)$$

where A, B, and C are respectively the coefficients of the second, first, and zero-th derivative of the equation. In our case, the condition that the coefficients shall be positive is always satisfied for $k > 0$. As for inequality (4.19), it will take the form:

$$1 - k > 0$$

From the latter inequality and from the inequality $k > 0$ it follows that the damping of the solution is assured by the condition

$$0 < 2\alpha S \gamma \quad \text{mgl} \quad (4.20)$$

But if, in connection with the damping of the motion, assured by the condition (4.20), α tends with the passage of time to approach zero, then β and φ will also approach zero, since the differential equations for these functions, which were constructed starting from system (4.17), will be entirely the same in structure and coefficients as eq.(4.18) for α .

As a result, the path of the end of the spin axis is transformed from the circle that it was with an undamped pendulum into an involutorial spiral, with its end at the origin of coordinates, that is, in the true vertical.

Section 4.3. Deviations of the Gyro-pendulum

The equilibrium position of the spin axis of the gyro-pendulum, allowing for the earth rotation and the displacement of the point of suspension along the earth surface, will not coincide, as will be shown below, with the true vertical. We shall term the deflections of this equilibrium position from the true vertical the deviations of the gyro-pendulum.

We shall determine them for an undamped gyro-pendulum, neglecting the friction

STAT

in the gimbals, since it would considerably complicate the analysis to allow for these factors, without adding anything new in principle.

The Equations of Motion of the Gyropendulum on a Moving Base

If, however, we take into consideration the moments of friction in the gimbals and the moments due to the hydraulic arrester, then for the moments L_x and L_y , allowing for the forces of inertia caused by the longitudinal acceleration of the aircraft, we get (Fig.4.6):

$$L_x = mgl\beta - ml\dot{V}$$

$$L_y = mgl\alpha$$

On substituting these expressions in (4.1) and (4.2), in which we also substitute \dot{p} and \dot{q} according to (2.34) and (2.35), and neglecting the expression

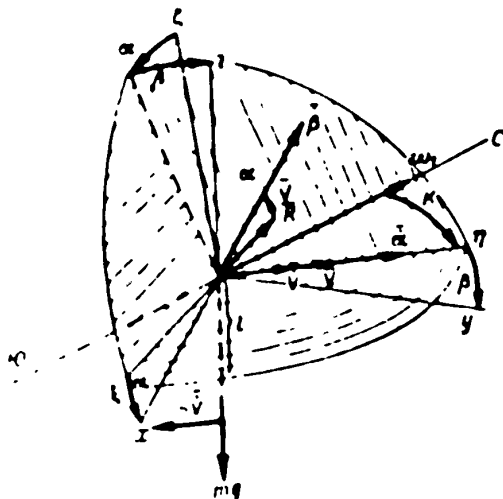


Fig.4.6 - Gyropendulum on Moving Base

$$\omega_1 + \frac{V}{R} \sin K \cos K$$

by comparison with

$$\frac{mgl}{H}$$

as a small quantity (which is true, even for high speeds and high latitudes), we get the equation of motion of the gyropendulum on a moving base in the following form:

$$H(\ddot{\alpha} + \omega_1 \cos K) = mgl\beta - ml\dot{V}$$

$$H(\ddot{\beta} + \omega_1 \sin K + \frac{V}{R}) = -mgl\alpha$$

or

$$\alpha - \beta = -\omega_1 \cos K - \lambda \frac{V}{R} \quad (4.21)$$

STAT

$$\dot{\beta} + \lambda \beta = -\omega_1 \sin K - \frac{V}{R} \quad (4.22)$$

Assume that $V = \text{const}$ and $k = \text{const}$, then the equations of motion of the gyro-
pendulum will take the form:

$$\ddot{\alpha} + \lambda \alpha = \omega_1 \cos K \quad (4.23)$$

$$\ddot{\beta} + \lambda \beta = -\omega_1 \sin K - \frac{V}{R} \quad (4.24)$$

which differ from the form of the equations of motion with a fixed base only in
their constant right sides. It is commonly known that the equilibrium position of
any system whose motion is described by linear differential equations with constant
coefficients and with a constant right side is determined by the partial solution of
these equations. In this connection the deviations are determined by the partial
solutions of eq.(4.23) and (4.24), which partial solutions are of the form

$$\beta_0 = \frac{\omega_1}{\lambda} \cos K \quad (4.25)$$

$$\alpha_0 = -\frac{\omega_1}{\lambda} \sin K - \frac{V}{\lambda R} \quad (4.26)$$

Thus the deviations of the gyro-pendulum consist of the deviations due to the
horizontal components of the earth rotation, which we shall denote by δ_e and the de-
viation due to the speed of flight, which we shall denote by δ_v .

It follows from (3.25) and (3.26) that numerically

$$\delta_1 = \sqrt{\left(\frac{\omega_1}{\lambda} \cos K\right)^2 + \left(\frac{\omega_1}{\lambda} \sin K\right)^2} = \frac{\omega_1}{\lambda} \quad (4.27)$$

$$\delta_2 = \frac{V}{\lambda R} \quad (4.28)$$

Deviation Due to Earth Rotation

The deviation δ_e represents the deflection of the spin axis from the true

STAT

vertical in the plane of the true meridian (Fig.4.7), since $\frac{\alpha_c}{\beta_c} = -\tan K$.

Under the influence of this deviation a moment due to the displacement of the

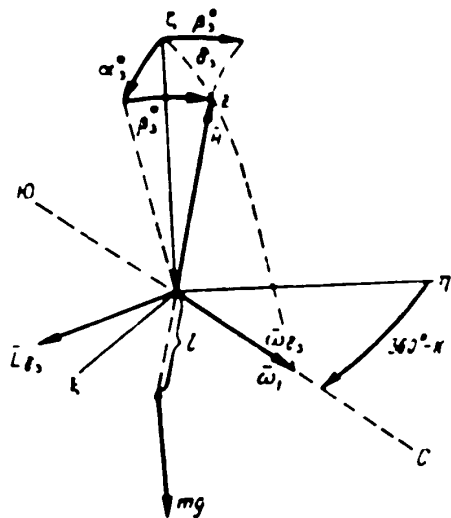


Fig.4.7 - Deviation Due to Earth Rotation

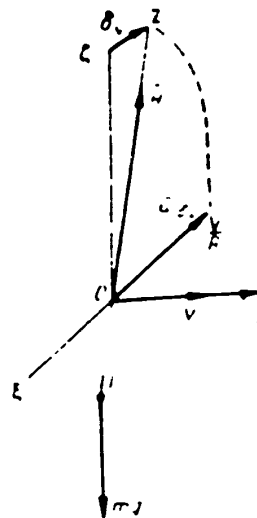


Fig.4.8 - Velocity Deviation

center of gravity L_{δ_e} , is produced, equal in magnitude to

$$mgl \sin \delta_e \approx mgl \beta_e$$

and directed perpendicular to the plane of the meridian, as shown in Fig.4.7.

This moment produces the precession ω_{δ_e} , which coincides in direction with the horizontal component of the earth's rotation ω_1 and equals it in magnitude, since from (4.27) it follows that:

$$\omega_{\delta_e} = \frac{L_{\delta_e}}{H} = \beta_e \omega_1 = \omega_1$$

Velocity Deviation

The deviation δ_v represents the deviation of the spin axis in the plane perpendicular to the direction of flight (Fig.4.8).

STAT

Under the influence of this deflection the moment L_{δ_V} is formed, which is directed as indicated in Fig. 4.8 and is equal in magnitude to

$$mgl \sin \delta_V \approx mgl \delta_V.$$

This moment produces the precession $\omega \delta_V$, coinciding in direction with the angular velocity of rotation of the system of coordinates $O\alpha n'$ owing to the velocity of flight of the aircraft with respect to the earth, and equal to it in magnitude, for, by (4.20)

$$\omega = \frac{L_{\delta_V}}{H} = \delta_V = \frac{V}{R}.$$

Condition of Non-disturbance

Let us find the condition under which (4.25) and (4.26) will be partial solutions of eqs. (4.21) and (4.22) for $V \neq \text{const.}$

Considering that $V \neq \text{const.}$ in the expressions for α_* and β_* we get

$$\begin{aligned} \dot{\alpha}_* &= -\frac{V}{R}, \\ \dot{\beta}_* &= 0. \end{aligned}$$

On substituting these expressions and also α_* and β_* , in eqs. (4.21) and (4.22), we get

$$\begin{aligned} -\frac{V}{R} - \omega_1 \cos K' &= -\omega_1 \cos K' - \lambda \frac{V}{R}, \\ \omega_1 \sin K' - \frac{V}{R} &= -\omega_1 \sin K' - \frac{V}{R}, \end{aligned}$$

Hence the required condition is written in the following form:

$$\lambda = \frac{R}{R}$$

or, for the period of the precessional oscillations of the gyropendulum (the precession arising under the action of the moment of the force of gravity along the cone):

STAT

$$T = 2\pi \sqrt{\frac{R}{\kappa}} = 84.4 \text{ ммм.}$$

This condition is called the condition of nondisturbance (Schuler). When it is satisfied, the behavior of the gyropendulum at $V \neq \text{const}$ will not in any way differ from its behavior for $V = \text{const}$.

It follows from this that by an appropriate choice of the design characteristics of the gyropendulum, the influence of the longitudinal accelerations on its deviation may be eliminated.

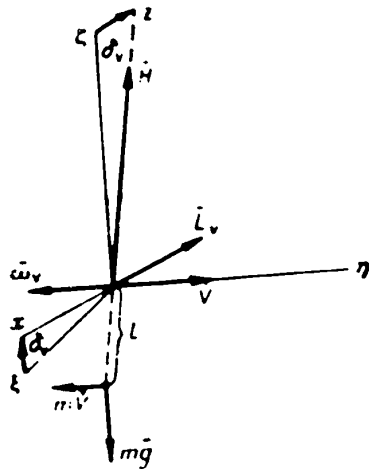


Fig.4.9 - Influence of Accelerations on the Gyropendulum

The physical meaning of this condition is that when it is satisfied, the precession of the gyropendulum under the action of the moment of the force of inertia, due to the longitudinal acceleration, brings the spin axis of the gyropendulum precisely into the position corresponding to the new value of the velocity deviation.

In fact, the moment due to the force of the inertia produced by the translational acceleration \vec{L}_v , is directed,

as indicated in Fig.4.9, and is equal to

$$L_v = m\dot{V}.$$

The precession ω_v , if the condition of nondisturbance is satisfied, is determined from the expression

$$\omega_v = \frac{m\dot{V}}{H} = \frac{\dot{V}}{\kappa} = \frac{\dot{V}}{\dot{R}}$$

directed as indicated in Fig.4.9.

STAT

It produces the increment of angle $\Delta\delta_v$, equal to

$$\Delta\delta_v = \int_0^t \dot{\delta}_v dt = \frac{1}{R} \int_0^t \dot{V} dt = \frac{1}{R} \Delta V.$$

As a result, the velocity deviation for each instant of time is determined by the expression

$$\delta_v = \delta_{v0} + \Delta\delta_v = \frac{1}{R} (V_0 + \Delta V) = \frac{V}{R},$$

where δ_{v0} and V_0 are the values of the velocity deviation and the flight speed for the beginning of the acceleration \dot{V} .

Section 4.4. Effect of a Turn on the Gyropendulum

Consider the behavior of the gyropendulum on a turn with respect to a system of coordinates rotating about the vertical together with the aircraft, i.e., let us determine the behavior of the gyropendulum with respect to an aircraft making a turn.

If we do not consider the moments of friction in the gimbals nor the damping moments, and if we neglect the earth rotation, then, considering the velocity vector of the aircraft to be parallel to the axis of rotation of the inner frame, we find the following expressions (Fig.4.10) for the moments L_x and L_y with respect to a left turn:

$$\begin{aligned} L_z &= mgl_z, \\ L_x &= -mgla - mlV\omega. \end{aligned}$$

Using, further, the expressions for p and q with respect to the left turn, (2.38) and (2.39) (cf. Chapter 2, Section 2.9), and substituting L_x , L_y , p and q in eq.(4.1) and (4.2), we get the equations of motion of the gyropendulum for the case we are studying, in the following form:

STAT

$$\begin{aligned} H(\dot{\alpha} - \omega_0 \beta) &= mg\beta, \\ H(\dot{\beta} + \omega_0 \alpha) &= -mg\alpha - ml\dot{\omega}_0. \end{aligned}$$

or

$$\frac{d\alpha}{dt} = \nu_{\text{res}}^* \beta, \quad (4.29)$$

$$\frac{d\beta}{dt} = -\nu_{\text{res}}^* (\alpha + \gamma_{\text{res}}^*). \quad (4.30)$$

where

$$\nu_{\text{res}}^* = \omega_0 + \lambda, \quad (4.31)$$

$$\gamma_{\text{res}}^* = \frac{\lambda}{\omega_0 + \lambda} \frac{V_{\omega_0}}{g}. \quad (4.32)$$

For a right turn the sign of ω_0 in (4.31) and (4.32) must be changed from positive to negative.

We shall consider the case when $\lambda = \frac{mg l}{H} < \omega_0$. Then, for a right turn, we have

$$\nu_{\text{res}}^* = -(\omega_0 - \lambda), \quad (4.33)$$

$$\gamma_{\text{res}}^* = \frac{\lambda}{\omega_0 - \lambda} \frac{V_{\omega_0}}{g}, \quad (4.34)$$

that is, the signs of u_{left}^* and u_{right}^* are different, while those of X_{left}^* and X_{right}^* are the same.

On dividing (4.29) by (4.30), we obtain, omitting the indices for the X^* :

$$\frac{d\alpha}{d\beta} = - \frac{\beta}{\alpha + \gamma^*}.$$

whence, separating the variables and integrating, we have the following equation of the path of the vertex of the spin axis:

$$\alpha^2 + \beta^2 + 2\gamma^* \alpha = A,$$

where A is the constant of integration

or

$$(\alpha + \gamma^*)^2 + \beta^2 = \theta^2.$$

STAT

Thus, during a turn, the end of the spin axis describes the circle about a point displaced from the origin of coordinates along the axis $O\alpha$, by the angle $\alpha = -X_{left}^*$, and during a right turn by the angle $\alpha = -X_{right}^*$ (Fig.4.11).

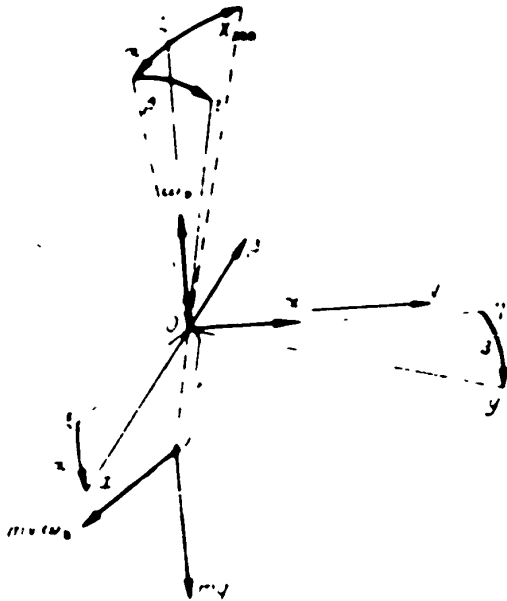


Fig.4.10 - Gyro pendulum in a Turn

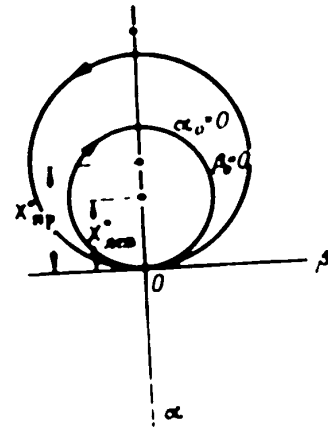


Fig.4.11 - Path of End of Spin Axis of Gyro pendulum in a Turn

We note that the apparent vertical, that is, the direction of the resultant of the force of gravity and the centrifugal force of inertia, during a left turn, is displaced in the coordinates of the plane $O\alpha\beta$ along the axis $O\alpha$ by the angle $\alpha = X_{left}^* = -\tan^{-1} \frac{V_{\omega B}}{g}$, that is, in the same sense in which the center of the circle representing the path of the end of the spin axis is displaced. With a right turn, the apparent vertical is displaced along the same axis $O\alpha$ by the angle $\alpha = X_{right}^* = \tan^{-1} \frac{V_{\omega B}}{g}$, that is in the sense opposite the displacement of the center of the circle representing the path of the end of the spin axis.

The motion of the end of the spin axis along its path is clockwise during a left turn and counterclockwise during a right turn.

This results directly from eq.(4.29) and (4.30), as well as from eq.(4.31) and (4.32). In a left turn, when $p_{left}^* > 0$, for positive β , the angle α increases,

STAT

while for negative β the angle α decreases; with a right turn, when $\mu_{\text{right}}^* < 0$ for positive values of β , the angle α decreases, and for negative values, it increases. From eq.(4.29), (4.30), (4.31), and (4.33), it results that the angular velocity of the motion of the gyrocompass axis along its path with respect to the aircraft takes place at various angular velocities: on a left turn at angular velocity $\omega_{\beta} + \lambda$, on a right turn at angular velocity $\omega_{\beta} - \lambda$.

If λ is selected with a magnitude such that it will satisfy the condition of nondisturbance, then for all practically conceivable values of ω_{turn} , the value of λ may be neglected by comparison with ω_{turn} . Doing this, we get

$$\begin{aligned}\dot{\gamma}_{\text{left}}^* &= \omega_{\text{turn}} \\ \dot{\gamma}_{\text{right}}^* &= \omega_{\text{turn}} \\ \dot{\gamma}_{\text{left}}^* = \dot{\gamma}_{\text{right}}^* &= \frac{V}{gR}\end{aligned}$$

Moreover, it should not be forgotten that the motion of the gyropendulum with respect to the earth will be performed in a manner completely different, since we must set up the system of coordinates $O\xi\eta^*$ and must set up the conditions of motion of the gyropendulum with respect to this fixed system of coordinates.

Examples. The gyropendulum gyro horizons designed with a weight of the order of 6 kg, have the following characteristics:

$$\begin{aligned}H &= 1.7 \cdot 10^8 \text{ g cm sec.} \\ mgl &= 1250 \text{ g cm.} \\ \frac{mgl}{H} &= 7.4 \cdot 10^{-3} \frac{1}{\text{sec.}}\end{aligned}$$

If we take for the moments of friction in the gimbals L_{ρ} , a quantity of the order of 5 g-cm, then for the angles of repose $\rho_{\alpha}^* \approx \rho_{\beta}^* = \rho$ we obtain

$$\rho = \frac{L_{\rho}}{mgl} = 0.23$$

For the deviation due to the earth rotation, δ_3 , taking for ω_1 its maximum

STAT

value $\omega_1 = \omega_e$, corresponding to a position on the equator, we get

$$\epsilon_3 = 0.56^\circ.$$

Let the aircraft be in flight at a speed of 540 km/hr = 150 m/sec. Then, for the velocity deviation, we shall have

$$\epsilon_V = \frac{V}{R} = 0.16^\circ.$$

When the conditions of nondisturbance are satisfied, the deviations will take the following values for the same values of ω_1 in V:

$$\epsilon_1 = 3.3 .$$

$$\epsilon_V = 1.1 .$$

Let the aircraft perform a right turn with a 30° bank at a speed $V = 540$ km/hr which corresponds to $\omega_{\text{turn}} = 37.8 \times 10^{-3}$ 1/sec. The center of the path is displaced in this case from the true vertical, with the characteristics given, by the angle

$$\begin{aligned} \epsilon_{\text{left}} &= \frac{V \omega_{\text{turn}}}{g} = 5.4^\circ \\ \epsilon_{\text{right}} &= \lambda \frac{V \omega_{\text{turn}}}{g} = 8.1 \end{aligned}$$

If the conditions of nondisturbance are satisfied, for the same characteristics of the turn, we have

$$\epsilon_{\text{left}}^* = 1.07 .$$

$$\epsilon_{\text{right}}^* = 1.14$$

The maximum deflection of the gyrohorizon from the true vertical during the turn may be taken as a quantity equal to double the value of ϵ^* .

Let us assume that during a period of 30 sec, the aircraft varies its speed by 75 m/sec, that is, that it moves with a translational acceleration $V = 0.25$ g.

When the condition of nondisturbance is satisfied, the spin axis of the gyro-

STAT

horizon, under the influence of this acceleration, will be deflected from the true vertical in the plane perpendicular to the direction of flight by the angle $\Delta\delta_v = 0.53^\circ$, with an accuracy equal to the increment of velocity deviation $\Delta\delta_v = 0.53^\circ$ for the velocity increment taken.

In the gyrohorizon under consideration, under the same conditions, the spin axis will be deflected by an angle $\Delta\delta_v$, equal to

$$\Delta\delta_v = \frac{\Delta V}{R} = 3.21$$

At the same time the increment of velocity deviation $\Delta\delta_v$ will be

$$\Delta\delta_v = \frac{\Delta V}{R} = 0.18^\circ$$

i.e., the deflection of the spin axis under the influence of the acceleration considerably exceeds the quantity corresponding to the increment of velocity deviation.

It follows from these data that a gyropendulum gyro horizon in which the condition of nondisturbance is completely satisfied, will have no error at all from the longitudinal accelerations, and will have a small error due to turns; as for the deviations due to the rotation of the earth and the velocity deviation, these can easily be taken into account.

The gyropendulum above considered has a considerable turning error. The longitudinal acceleration also has a substantial influence on it.

In other words, the deviation from the satisfaction of the condition of nondisturbance in a gyropendulum gyro horizon increases the most unpleasant feature, in the sense of the difficulties of estimating the error.

But, in order to satisfy the condition of nondisturbance, to decrease the value of $\lambda = \frac{mgL}{H}$, the kinetic moment of the gyroscope together with the kinetic moment of the entire installation, would have to be increased to several times the kinetic moment of the gyro horizon under consideration. The weight would also have to be

STAT

POOR ORIGINAL

increased several times. But the weight of this instrument is already rather great, it is 4-5 times as great as the weight of a gyrohorizon with a pendulum correction system.

In this connection, gyrohorizons with a pendulum correction system have proved more convenient with respect to satisfying the demands made on aviation instruments.

STAT

POOR ORIGINAL

CHAPTER V .

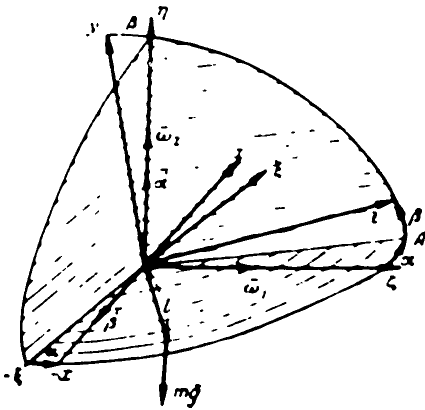
BASIC INFORMATION ABOUT THE THEORY OF THE GYROCOMPASS

Section 5.1. Behavior of the Undamped Gyrocompass on a Base

Fixed with Respect to the Earth

A gyroscope with three degrees of freedom whose center of gravity is displaced downward with respect to the center of the support in the equatorial plane, along

the negative semiaxis Oy , is called an undamped gyrocompass (Fig.5.1).



The influence of dry friction in the gimbals will not be taken into account, since it is very small in actual gyrocompasses.

Then, for the moments L_x, L_y the expressions

$$L_x = mg l \cos(\alpha) \quad mg l \beta$$

$$L_y = 0$$

Fig.5.1 - Gyrocompass on Base Fixed with Respect to the Earth

will hold (according to Fig.5.1).

On the basis of (2.36) and (2.37), in which we must put $V = 0$, or directly on the basis of Fig.5.1, we have the following formulas for p and q:

POOR ORIGINAL

$$p = -\dot{\beta} - \omega_1 \alpha,$$

$$q = \dot{\alpha} + \omega_1 \beta - \omega_1 \beta.$$

On substituting these expressions in the general equations of motion of the gyroscope, (3.1) and (3.2), we get

$$H(\dot{\alpha} + \omega_1 \beta - \omega_1 \beta) = mg l \beta,$$

$$H(\dot{\beta} - \omega_1 \alpha) = 0$$

or

$$\frac{d\alpha}{dt} = (\lambda + \omega_1) \beta - \omega_1 \alpha, \tag{5.1}$$

$$\frac{d\beta}{dt} = -\omega_1 \alpha, \tag{5.2}$$

where

$$\lambda = \frac{mg l}{H}.$$

We shall seek the path of the end of the spin axis of the gyrocompass, which is described by it on the coordinate plane $O\alpha\beta$, perpendicular to the meridian, i.e., the axis $O\zeta$, with origin at the point of intersection between this coordinate plane and the axis $O\zeta$.

On dividing, for this purpose, eq.(4.1) by eq.(4.2), we obtain

$$\frac{d\alpha}{d\beta} = \frac{(\lambda + \omega_1) \beta - \omega_1 \alpha}{-\omega_1 \alpha}.$$

Separating the variables in the differential equation so obtained, and integrating, we have the solution

$$\alpha^2 + \frac{\omega_1}{\lambda + \omega_1} \left(\beta - \frac{\omega_1}{\lambda + \omega_1} \alpha \right)^2 = \frac{H^2}{mg l}. \tag{5.2} \text{STAT}$$

or, dividing the right and left sides by $\frac{H^2}{mg l}$, we have

$$\alpha^2 + \frac{\left(\beta - \frac{\omega_1}{\lambda + \omega_1} \alpha \right)^2}{\frac{H^2}{mg l} \left(\frac{\lambda + \omega_1}{\omega_1} \right)^2} = 1.$$

the path sought is an ellipse with the center displaced from the origin of

POOR ORIGINAL

coordinates along the positive semiaxis $O\beta$ by the angle $\beta_* = \frac{\omega_2}{\lambda + \omega_1}$ with a major semiaxis equal to θ_0 and a minor semiaxis that is $\sqrt{\frac{\omega_1}{\lambda + \omega_1}}$ times smaller than θ_0 , where θ_0 depends on the initial conditions.

At $t = 0$, let $\alpha = 0$, $\beta = \beta_* = \frac{\omega_2}{\lambda + \omega_1}$. Then, on the basis of (5.3), we have

$$\dot{\theta}_0 = 0,$$

i.e., if, at the initial instant, the rotor of the gyrocompass was in the plane of the meridian, being raised above the plane of the horizon by the angle $\beta = \beta_*$, then it will remain in this position, thereby determining the position of the geographic meridian.

If, at $t = 0$, $\alpha = \alpha_0$, $\beta = \beta_0$, then, on the basis of eq.(4.3), we have

$$\theta_0 = \sqrt{\alpha_0^2 + \frac{(\beta_0 - \frac{\omega_2}{\lambda + \omega_1})^2}{\frac{\omega_1}{\lambda + \omega_1}}}$$

that is, if at the initial instant, the axis of the gyrocompass rotor occupies an arbitrary position, then it will rotate about the direction corresponding to the stable state $\beta = \beta_*$. In this case (Fig.5.2), the end of the axis describes, on the

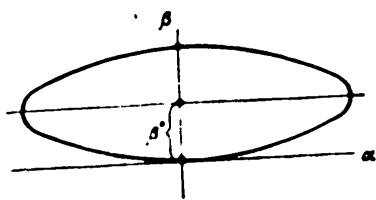


Fig.5.2 - Path of End of Axis of Gyrocompass

coordinate plane $O\alpha\beta$, an ellipse with the center displaced from the origin of coordinates by the angle $\beta = \beta_*$, with the major semiaxis $a = \theta_0$, by eq.(5.4), and a minor semiaxis $b = \sqrt{\frac{\omega_1}{\lambda + \omega_1}} \theta_0$, that is, equal to

$$b = \sqrt{\frac{\omega_1}{\lambda + \omega_1} \alpha_0^2 + \frac{(\beta_0 - \frac{\omega_2}{\lambda + \omega_1})^2}{\frac{\omega_1}{\lambda + \omega_1}}}$$

STAT

Thus, if an undamped gyropendulum performs a precessional motion about the true vertical with a deflection from it depending on the initial conditions, then the undamped gyrocompass will perform a precessional motion about the axis lying in

the plane of the meridian, with a deviation from it which likewise depends on the initial conditions.

By using damping of the oscillations in a gyro-compass, the character of its motion can be modified in such a way as to force the axis of its rotor to approach the true vertical, in an involutorial spiral.

By analogy, using damping of the oscillations of the gyrocompass (by the same method as in the gyro-compass or otherwise), the character of the motion in the gyrocompass may likewise be modified in the direction of forcing its rotor axis to approach, in an involutorial spiral, to the direction above described in the plane of the meridian.

Section 5.2. Influence of Velocity and Acceleration on the Behavior of the Gyrocompass

If we allow for the influence of acceleration on the displaced center of gravity, then we get, for the moments L_x and L_y , on the basis of Fig. 5.3, the following equations

$$\left. \begin{aligned} L_x &= mgl \cos(\theta, z) + mlV \cos K; \\ L_y &= 0. \end{aligned} \right\} \quad (5.4)$$

On substituting the values of L_x , L_y , p , and q (from eqs. 2.36 and 2.37) in the general equations of motion of the gyroscope, eqs. (4.1) and (4.2), and neglecting $\frac{1}{R} \sin K$ in comparison to ω_1 , and $\frac{r \sin K}{r \cos K}$ by comparison with ω_2 , we get:

$$H(\ddot{\alpha} - \omega_1 \dot{\beta} + \omega_2) = mgl \dot{\beta} + mlV \dot{\alpha} \cos K;$$

$$H(\ddot{\beta} + \omega_1 \dot{\alpha} - \frac{V}{R} \cos K) = 0.$$

or

$$\frac{d\alpha}{dt} = (\omega_1 + \omega_2) \beta - \omega_2 + \lambda \frac{V}{R} \cos K; \quad (5.5)$$

$$\frac{d\beta}{dt} = -\omega_1 \alpha + \frac{V}{R} \cos K. \quad (5.6)$$

STAT

Assume $V = \text{const}$, i.e., $\dot{V} = 0$.

Then the equations of motion of the gyrocompass, eqs.(5.5) and (5.6), in which the influence of the constant velocity of displacement with respect to the earth is taken into account, will differ from eqs.(5.1) and (5.2), which were investigated in the preceding section, only in the presence of an additional constant term in the right side of the second equation. It follows from this that the solution of eqs. (5.5) and (5.6) will differ from the preceding solution only in the displacement of the center of the ellipse representing the path. This displacement is defined by the partial solutions of eq.(4.5), (4.6), which are of the form:

$$\left. \begin{aligned} \alpha_0 &= \frac{V}{R\omega_1} \cos \lambda. \\ \beta_0 &= \frac{\omega_2}{\lambda + \omega_1}. \end{aligned} \right\} \quad (5.7)$$

It is clear that this displacement of the center of the ellipse from the meridian, which means the displacement of the stable state of the gyrocompass from the

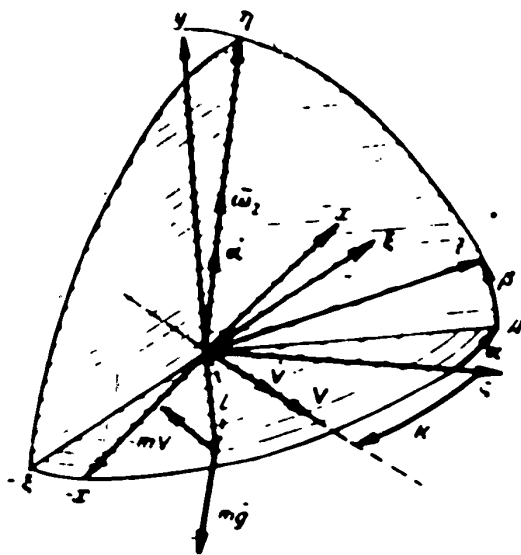


Fig.5.3 - Gyrocompass on Moving Base

meridian, did not vary by angle β , but did vary by angle α : when the gyrocompass was fixed with respect to the earth, this displacement was equal to zero, and, consequently, to the stable state there corresponded the position of the rotor axis of the gyrocompass in the plane of the meridian. On allowing for the rate of displacement with respect to the earth, it is not equal to zero, and consequently a deviation from the plane of the meridian corresponds to the stable state.

This deviation is called the deviation of the gyrocompass.

As follows from eq.(5.7), it depends on the rate of displacement, the course, and the latitude of the place.

Let the speed of displacement $V = 540$ km/hour, the latitude of the place $\varphi = 60^\circ$, the course $K = 0$ or 180° .

For these data the deviation α_* will be equal to

$$\alpha_* = 37.0^\circ.$$

At the same time, for a course $K = 90^\circ$ or 270° , it will be equal to zero, i.e., when applied to the speeds of modern aircraft, this variation has so wide a range that it would hardly be possible to estimate it in practice with sufficient accuracy.

Let us find the condition under which the functions α_* , β_* would be partial solutions of eqs.(5.5) and (5.6), even for $V \neq \text{const.}$

On substituting α^* and β^* in eqs.(5.5) and (5.6), we get

$$\begin{aligned} \frac{V}{R\omega_1} \cos K &= (\lambda + \omega_1) \frac{-\omega_2}{\lambda + \omega_1} - \omega_2 + \lambda \frac{V}{g} \cos K, \\ 0 &= -\frac{V}{R\omega_1} \cos K \omega_1 + \frac{V}{R} \cos K, \end{aligned}$$

whence it follows that the required condition will be written in the following form:

$$\lambda \omega_1 = \frac{g}{R}.$$

The condition so found also bears the name of the condition of nondisturbance (Schuler). If it is satisfied, then the gyrocompass will have no other deviations besides the velocity deviation.

It is easy to show that the period of free oscillations of the gyrocompass can be expressed with sufficient accuracy by the expression

$$T = \frac{2\pi}{\sqrt{\lambda \omega_1}},$$

from which it follows that, on satisfaction of the conditions of nondisturbance, the

STAT

period of free oscillations of a gyrocompass will equal:

$$T = 2\pi \sqrt{\frac{R}{k}} = 84,4 \text{ min}$$

The period of damping of the oscillations will be correspondingly great. In connection with this it takes a considerable time until the gyrocompass after starting occupies the position of the stable state.

This circumstance is an additional and fundamental obstacle to the use of the gyrocompass in aviation.

It is not hard to see that for ocean vessels, whose speed is relatively small, and whose voyages are prolonged, these circumstances do not play so substantial a role, and therefore the gyrocompass, as a compass whose readings do not depend on the surrounding ferromagnetic masses, finds wide application there.

STAT -

CHAPTER VI

SCHEMES AND CHARACTERISTICS OF CORRECTION SYSTEMS

Section 6.1. Structural Scheme of Correction Systems

The correction of a positional gyroscope as a whole is most often accomplished by means of two mutually independent systems, each of which is intended for one specific degree of freedom of the gyroscope suspension, i.e., for one definite frame of this suspension. There are very few exceptions to this rule, and even these are not of fundamental importance.

A structural diagram of the correction system can be drawn according to Fig.6.1, where D_{c1} and D_{c2} are signal transmitters, D_{L1} and D_{L2} are moment transmitters (moment devices) of the correction systems respectively of the first (inner) and the second (outer) frames of the gimbals, while the linkage between the signal transmitter and the moment transmitter in each correction system is accomplished by the crossover method, in which each frame is corrected by the application of a moment to the other frame. We note that, in certain cases, the signal transmitter and the moment transmitter of the correction system are merged in a single design unit.

As the signal transmitter, a certain distributing device is ordinarily used, consisting of two elements, one of which is connected to the sensitive element of the correction system, the other with the gyroscope frame to be corrected. When these elements are mismatched, energy of one form or another is transmitted to the

connected to the given signal transmitter.

STAT

By a moment transmitter we mean a certain actuating device which, under the influence of the energy received from the signal transmitter, develops a moment about the axis of rotation of that gyroscope frame which is diagonal with respect to the frame being corrected. The magnitude and sign of this moment depend on the magnitude and sign of the mismatch or discrepancy between the elements of the signal transmitter.

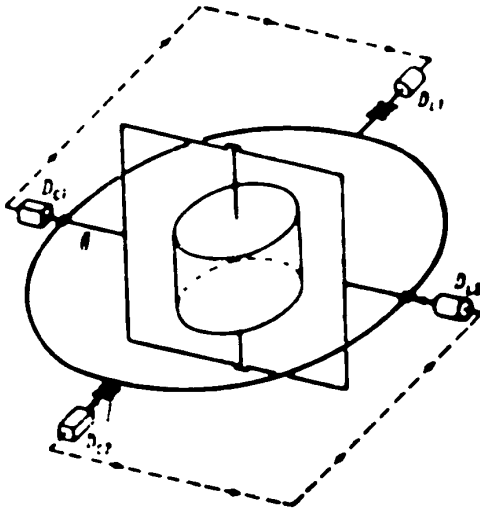


Fig.6.1 - System of Radial Correction

I, II - Axis of suspension; D_{c1} - Transmitter of signal; D_{L2} - Transmitter of correction moment to inner frame; D_{c2} - Signal transmitter; D_{L1} - Transmitter of correction moment to outer frame

We shall term the relation between the moment developed by the transmitter and the discrepancy in the signal transmitter the correction characteristic. Other devices can be used as the sensing members of the correction system, besides such instruments as the pendulum and the magnetic needle, for example the radio gyrocompass, air speed indicator, etc. The case of the so-called correction for perpendicularity of the gyroscope axis to the axis of the outer frame must be mentioned. In this case, the correcting signal appears on deflection of the spin axis from the position perpendicular to the axis of the outer frame.

Depending on the kind of connection between the signal transmitter and the gyroscope, we shall distinguish internal and external correction systems. By an internal correction system we shall mean a correction system in which there is a direct connection between the signal transmitter and the gyroscope, and by an external system, a system in which this connection is indirect. This type of connection

is often used in the gyroscopes of autopilots. It reduces down essentially to having the signal transmitter connected with the aircraft instead of being connected with the gyroscope. In this case it must be borne in mind that the aircraft is under the control of the gyroscope, which in this case is the sensing member of the autopilot. As a result, any departure of the gyroscope from the required direction results in the departure of the aircraft as well, and, consequently, in the displacement of the member of the signal transmitter that is connected with the aircraft, with respect to the member of this transmitter that is connected with the sensing member of the correcting system. This will mean that the corresponding moment transmitter is put into operation.

The use of the external correction system is explained, first, by the fact that in this case it is sometimes possible to obtain a more satisfactory design scheme of correction, and secondly, and this is of more substantial importance, that an external system of correction assures the liquidation of irregularities in the regulation, or, in other words, provides automatic compensation of the action of a constant disturbing moment on the aircraft. This latter is obtained as a result of the fact that the correction of the gyroscope, and with it the variation in the position of the aircraft, will continue until the aircraft occupies the only position in which the discrepancy in the transmitter of the correction signal disappears. But this means that any irregularity in the regulation will always be eliminated. The position of the gyroscope, when an external system of correction is used, is so selected that the signal fed from the gyroscope to the automatic pilot shall assure the compensation of the constant disturbing moment.

Section 6.2. Schemes and Characteristics of Pneumatic Type Correction Systems

According to the form of energy used to excite the positioning moment, radial correction systems are divided into pneumatic, electric, and mechanical.

Figure 6.2 gives one of the schemes of a pneumatic type of external correction system produced in the USSR, developed at the end of the 1930 for the lateral

STAT

stabilization gyroscope of an autopilot. The signal transmitter here is the air collector (1), connected with the aircraft. Two jets of the collector are covered by slide valves, connected with the pendulum (2), whose axis coincides with the axis of the frame being corrected.

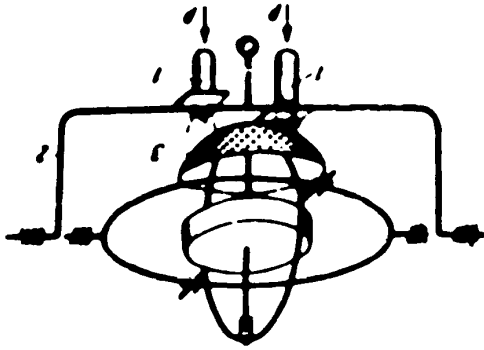


Fig.6.2 - Diagram of Air Correction:

P - Air Pressure;

1 - Air collector; 2 - Pendulum with shutters; 3 - Hemisphere with notches

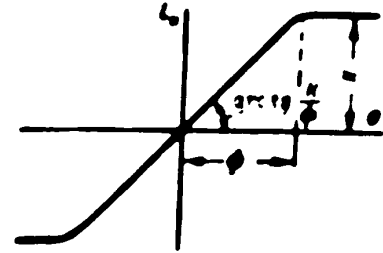


Fig.6.3 - Mixed Characteristic of Correction System

ϕ - Segment of proportional part;

k/ϕ - Steepness of proportional part of characteristic; k - Moment of correction of constant part of characteristic

The slides are so oriented with respect to the jets of the air collector that, on the deflection of the pendulum with respect to the air collector, the opening of one air jet will increase and that of the other will decrease.

The moment transmitter is a hemisphere connected with the gyroscope and having a grooved surface, against which the above described air jets impinge. If the aircraft occupies a position in which there is no disagreement between the elements of the signal transmitter (the air collector and the slide), that is, a position in which the slides equally cover both of the collector jets, then no moment will act on the gyroscope, since the pressures produced on the hemisphere by the air jets will be the same, by virtue of the identical covering of these jets. If the aircraft departs from the required position, then a discrepancy will arise between the

STAT

elements of the signal transmitter, and as a result the slides will cover the two collector jets differently. The pressures produced by the jets on the hemisphere will be different, and a resultant moment will appear in connection with that difference.

Under the action of the moment, the gyro will precess. In this case a signal will be fed from the transmitter connected with the gyro to the autopilot, which will then turn the aircraft into the necessary position.

It may be considered with a sufficient degree of accuracy that the correction moment is proportional to the discrepancy in the signal transmitter, until one of the air jet in the jets in the collector is completely covered and the other is completely open. After this happens, the moment will remain constant. Thus, if we denote the moment by L_k and the discrepancy in the signal transmitter by θ , we get the characteristic of the correction for the given case, as shown in Fig.6.3.

This external correction system using a pendulum is used in this gyro only with respect to the outer frame. The inner frame, however, is corrected by perpendicularity of the spin axis to the axis of the outer frame. For this purpose (Fig.6.4) two shutters are rigidly attached to the inner frame, and on the outer frame, two nozzles from the air collector. The reactive forces of the jets leaving the nozzles act on the outer frame. When the gyroscope axis is perpendicular to the axis of the outer frame, the reactive forces of the jets will be the same, since the jets themselves will be the same, and the moment produced by these forces will be equal to zero. When the perpendicular position is disturbed, the jet impinging on one shutter will increase, and that on the other shutter will decrease, the equality of the reactive forces of the jets will be impaired, and a resultant moment will appear about the axis of the outer frame. On account of this resultant moment, the inner frame will begin to precess in the sense necessary to restore the perpendicular position between the spin axis and the axis of the outer frame.

In this way, in the case we have described, the signal transmitter is used

STAT

directly as the moment transmitter, the elements of this transmitter being connected with the gyroscope, and, consequently, this system of correction is an internal one.

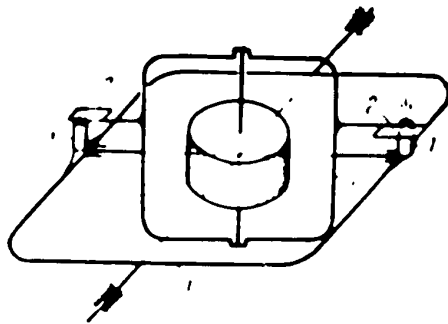


Fig. 6.4 - Pneumatic Correction System for Inner Frame, Holding Spin Axis Perpendicular to Axis of Outer Frame

I - Outer frame; II - Inner frame;
l - Air nozzles; 2 - Shutters

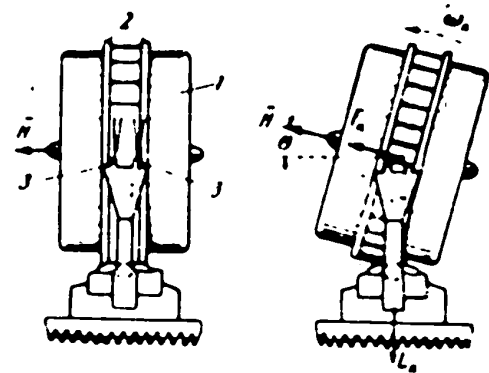


Fig. 6.5 - System of Pneumatic Correction for Inner Frame in Directional Gyro

1 - Rotor; 2 - Flanges; 3 - Air nozzles; F_k - Corrective force; L_k - Correction moment; ω_k - Angular velocity of corrective precession

The characteristic of this correction system will be the same in the working range of angles of mismatch, as in the preceding case (Fig. 6.3).

Figure 6.5 gives still another version of a correction system for the inner frame with respect to the position of the rotor axis relative to the axis of the outer frame, which is used in pneumatic directional gyrocompasses.

The moment of correction here is produced by means of fins on the rotor, and of the air jet used to maintain the rotation of the rotor. If the spin axis of the gyroscope occupies a position perpendicular to the axis of the outer frame, then this jet will impinge only on slits in the rim of the rotor and will only produce a

STAT

moment relative to the spin axis. If, however, this perpendicular position is disturbed, then the jet will also impinge in part on one flange or the other, as a result of which a certain moment about the axis of the outer frame will occur, thus producing a correction of the inner frame. Instead of the flanges today, scythe-shaped grooves are used, which produce an analogous effect.

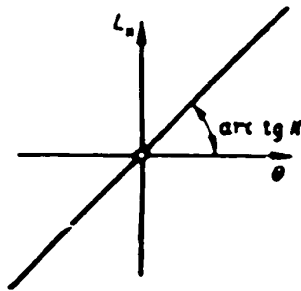


Fig.6.6 - Proportional Characteristics
of Correction

The characteristic of this correction over the working area may, with a sufficient degree of accuracy, be taken as proportional, that is, having the form indicated in Fig.6.6.

Figure 6.7a shows still another type of the system of pneumatic correction by maintaining a perpendicular position of the spin axis and axis of

outer frame. This system of correction is used in directional gyroscopic instruments having electric gyromotors.

On the periphery of the rotor casing of the gyromotor, a series of slits (1) has been cut.

When the rotor rotates, an increased air pressure is produced near its rim, and the air passes through the slits (1) in the jets tangent to the surface of the shell. The moment of the reactive forces of these air jets is balanced by the moment of the forces of reaction in the supports of the outer frame, when the rotor axis is perpendicular to the axis of the outer frame.

When the rotor deviates from the position perpendicular to the axis of the outer frame, then the moment of the reactive forces produces the pair of forces F_K and the moment of correction L_K . The moment of correction L_K causes the gyroscope to precess to the neutral position indicated.

Figure 6.7b shows a modification of this correction system. Instead of slits,

STAT

in this case the two nozzles (1), attached to the inner frame, are used. Jets of nitrogen emerge from the nozzles on opposite sides. When the rotor axis is perpendicular to the axis of the inner frame, the reactive force of the jets lies in the

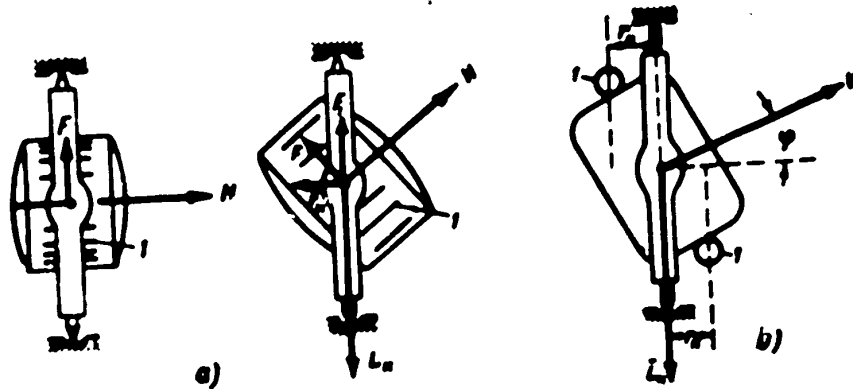


Fig.6.7 - System of Pneumatic Correction of Inner Frame of Directional Gyroscope with Electric Gyromotor

I - Slits in gyromotor casing; F_K - Force of correction; L_K - Moment of correction

plane of the axis of the outer frame. In this case there will be no moment relative to the outer frame. When the axis of the rotor deviates from this position, the force of the jets leaves the axis of the outer frame, and deviates by the quantity r_K , proportional to the sine to the angle of deflection of the spin axis. This produces the correction moment L_K , which returns the spin axis to its previous position.

The system of correction shown in Fig.6.7b is used in the gyro of the remote-reading electric gyromagnetic compass DGMK-3. In order to prevent the correcting moment from varying with the altitude of flight, the gyroscope of the DGMK-3 is placed in an air-tight casing, so that the reactive force of the jets remains constant.

Figure 6.8 gives a version of the pneumatic correction system where the signal

STAT

transmitter likewise directly plays the role of the moment transmitter.

The principle of its design is as follows. To the inner frame of the gyro, whose role in this particular case is played by the rotor casing (1), the air chamber (2) is rigidly attached. For each frame, this chamber has two ports (3) to discharge air from the chamber, which ports are arranged symmetrically with respect to the axes of rotation of the frames.

This chamber is an element of the signal transmitter connected with the gyro. But it is at the same time also the moment transmitter, since the reactive forces of the release of the air jets flowing from the ports produce a moment about the axis of rotation of the frame located diagonally to the frame being corrected. The second element of the signal transmitter is provided by the pendulum shutters, suspended on an axis parallel to the axis of rotation of the corrected frame. The shutter covers the ports of the air chamber in such a way that if the axis of symmetry of the ports coincides with the line of the edge of the shutters, then the air jets issuing from the ports will be the same. If this coincidence is disturbed, however, i.e., if a mismatch arises between the position of the corrected frame and the position of the shutters, then the equality between these air jets is destroyed. When the equality of the reactive forces is destroyed, a resultant moment of one sign or the other appears.

As already stated, this moment will be diagonal with respect to the corrected frame, that is, with respect to the plane in which the position of the gyro was disturbed.

This system of pneumatic correction is very widely used. It is used both to correct gyro verticals and for horizontal correction of directional gyros.

Its characteristic is of the form shown in Fig.6.3, the width of the area of proportional correction ϕ being determined by the width of the port and the length of the pendulum shutters.

Figure 6.9 gives the arrangement of the pneumatic corrector used in the

STAT

USSR-produced GMK-2 directional gyro for correcting the outer frame. The signal transmitter here is the air collector (5) with its two nozzles placed on the rotor casing and covered by the eccentric slide (7). The slide is connected with the magnetic system (6), whose axis of rotation is likewise attached to the rotor casing.

To the matched state of the transmitter corresponds the equal covering by this slide of the collector nozzles, while to the mismatched state of the transmitter corresponds unequal covering of the two nozzles. In the matched

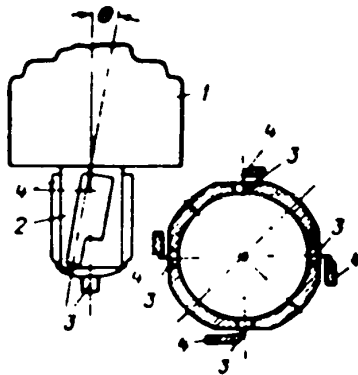


Fig. 6.8 - Arrangement of Pneumatic Corrector with Pendulum Slides

1 - Rotor casing; 2 - Air chamber;
3 - Air ports; 4 - Pendulum shutters;
 ϕ - Mismatch between rotor axis and shutter axis

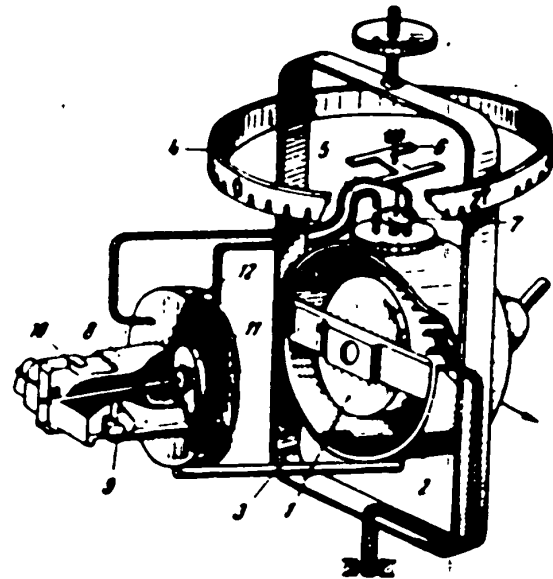


Fig. 6.9 - Arrangement of GMK-2
Pneumatic Corrector

1 - Rotor; 2 - Rotor casing (inner frame); 3 - Outer frame; 4 - Scale;
5 - Air collector; 6 - Magnet;
7 - Eccentric slide; 8 - Air chamber;
9 - Pendulum shutters; 10 - Shutter of outer-frame corrector; 11 - Membrane of pneumatic relay with plunger;
12 - Pneumatic relay

state, the same pressure reaches both the receiving nozzles, while in the mismatched state, there is a different pressure in each.

STAT

An air chamber with two pairs of ports, attached to the inner frame (casing) of the gyro, serves as the moment transmitter. One pair of the ports, the horizontal pair, is covered by pendulum slides and serves to correct the inner frame of the gyroscope, since the moment produced by the reactive forces of the discharge of the air jets issuing from these ports acts about the axis of the inner frame. The second pair of ports, the vertical ones, serves to correct the outer frame, since

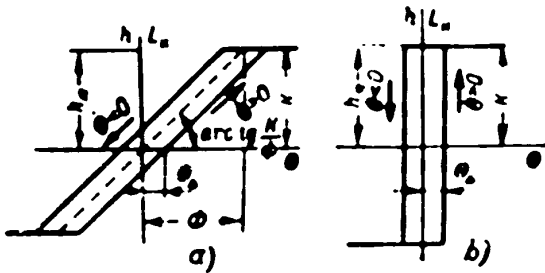


Fig.6.10 - Characteristics of Correction of Outer Frame of GMK-2

a - Characteristics of correction using elastic membrane; b - Characteristic of correction with inelastic membrane;

h - Path of membrane; h_m - Maximum path of membrane; Φ_{Δ} - Hysteresis zone

the moment produced by the reactive forces of the discharge of the air jets from these ports acts about the axis of the inner frame. The second pair of ports is covered by shutters connected by a plunger with the membrane of an air relay, the chambers of which communicate with the receiving nozzles of the above described signal transmitter. In the matched state of this transmitter, the pressures in the chambers are the same, the membrane is in a neutral position, and the shutters connected with the membrane equally cover their ports. With a mismatch in the signal transmitter, the equality in the relay chambers is impaired and the membrane is flexed toward one side or the other. This displaces the slide, and the covering of the ports becomes unequal, thus producing a moment of the corresponding sign.

Thus, for the correction of the inner frame, the air chamber in this case is at the same time a signal transmitter and a moment transmitter. The characteristic of the correction for this frame will be of the form shown in Fig.6.3. But for the correction of the outer frame, it will only be a moment transmitter, connected with

the signal transmitter by means of a special pneumatic relay. The characteristic of the correction will therefore depend, here as well, on the characteristics of the relay. If the relay has an elastic membrane, then the relation between the path of this membrane h and the mismatch θ will be of the form given in Fig.6.10a, where θ_{Δ} is the value of the error necessary to produce a pressure difference capable of overcoming the force of dry friction of the relay plunger; here the right part of the characteristic corresponds to the condition $\theta > 0$, while the left part corresponds to the condition $\theta < 0$; h_m is the maximum possible movement of the membrane.

Assuming further that the relations between the moment L_K and the displacement of the shutter is of a proportional nature up to full opening of the ports, and considering that the motion of the membrane does provide this full opening of the ports, we get the result that the diagram of Fig.6.10a on a different scale represents the characteristic of correction in the case here being considered.

If the relay has an inelastic membrane, then the relation between the motion of the membrane and the error will be different.

Until an error or mismatch equal to θ_{Δ} has accumulated, the membrane will be motionless, and will then be displaced as far as the stop; the backward motion, likewise as far as the stop, will be performed after an error of the opposite sign equal to θ_{Δ} has accumulated. If we retain the same assumption with respect to the dependence of the moment L_K on the motion of the membrane, then we get a characteristic of correction that in this case, as well, is of the hysteresis form given in Fig.6.10b.

The methods and characteristics of a pneumatic corrector that have been here considered are the most typical. Their principle merit resides in the simplicity of their design, which is a point particularly applicable to arrangements using a pendulum as the sensing member of the correction mechanism. It must be noted that in those cases where the rotation of the gyro rotor is likewise maintained by the energy of an air jet, it is most advisable to use a pneumatic type corrector as

STAT

well, and, in fact, this is usually done. However, the design simplicity of the pneumatic corrector impelled the search for means of applying it to gyroscopes with electrically driven rotors. Such designs for gyro verticals were particularly favored in Germany. But such a solution is not correct for nonhermetic instruments. The reason is that a pneumatic correction system for nonhermetic instruments has the disadvantage of having its efficiency depend substantially on the flight altitude. With a pneumatically driven rotor, this shortcoming will have less of an effect, since in this case the rotor speed also decreases with increasing altitude, although to a lesser extent, and the decreasing efficiency of the corrector is accompanied by some reduction of the kinetic moment as well. But, with an electric drive, the rotor speed will be practically independent of the altitude, and thus the reduced efficiency of the corrector will make it impermissibly sluggish at high altitudes, or, if it is selected for use under altitude conditions, it will become impermissibly sharp near the ground.

The transition to electrically driven gyro rotors has been due to such advantages of electric gyromotor as higher speed, and, consequently, smaller dimensions for equal kinetic moment, elevated starting torque, facilitating the starting of gyromotors at a low temperature, convenience of installation (no air line), weak altitude-dependence of the rotor speed, absence of the increased corrosion of parts that is characteristic of gyro instruments with pneumatic drive, absence of the heating owing to the heat given off by the gyromotors, etc.

Thus the transition to the electric drive in gyro instruments, with its substantial design and operating advantages, has made it necessary to develop electric forms of radial correction as well.

Section 6.3. Circuits and Characteristics of Electric Systems of Radial Correction

Figure 6.11 gives the circuit of one of the versions developed in the USSR of the electrical corrector of the induction type, as applied to one of the frames of

STAT

The signal transmitter (cf. Fig.6.11a), consists of a contact roller connected with the gyro frame being corrected, and a contact strip, connected with the sensor of the corrector and divided into two parts by an insulating gap.

In the matched state of this transmitter, the contact roller is at the center of the insulating strip; when it is mismatched, the roller is displaced from that center. The moment transmitter consists of a system of two inductance coils, in the slots of which there moves a current-conducting disc, connected with the axis of rotation of the corresponding frame (i.e., located diagonally to the corrected frame). As will be seen from the electrical circuit (Fig.6.11b), one of the coils is always energized by one of the phases of a triphase alternating current line. The second coil, however, which we shall term the control coil, is connected to one of the remaining two phases of the line through the signal transmitter, depending on which half of the contact blade of this transmitter is contacted by its contact roller. Thus, so long as the contact roller remains on the insulated strip, that is, so long as the signal transmitter is in the matched state, only one coil will be energized, and, consequently, no moment will be developed on the driving disc. When the signal transmitter is mismatched sufficiently to bring the contact roller onto either of the conducting halves of the blade, both coils will be energized, and the alternating magnetic fluxes produced by these coils will be phase-shifted by 120° , in one sense or the other, with respect to each other. Consequently a moment of one sign or the other, and of constant magnitude, that is, not depending on the degree of mismatching, will arise on the current-carrying disc on account of the interaction of the eddy currents and fluxes, which are phase-shifted with respect to each other.

Since the insulating strip has certain finite dimensions, a certain value of the mismatching is always required to cover this strip, and this value determines the zone of insensitivity of the given correction system. Taking this circumstance into account, and bearing in mind that after the roller passes onto the conducting part of the blade, the moment transmitter will develop a moment of constant value,

STAT

we obtain the correction characteristic for the given case presented in Fig.6.12.

Figure 6.13 shows the arrangement for a considerably later version of the electrical induction-type corrector, representing a different design solution of the same ideas used in the version described above.

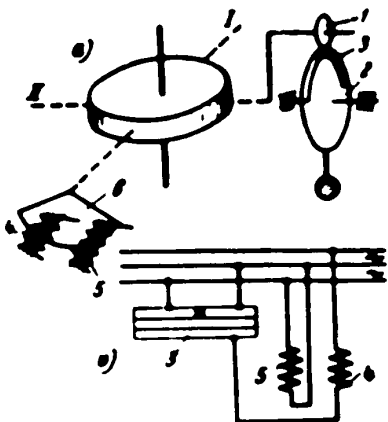


Fig.6.11 - Circuit of Induction
Electrical Corrector

I and II - Axes of suspension;
1 - Contact roller; 2 - Pendulum;
3 - Contact blade; 4 and 5 - Induction
coils; 6 - Current-carrying sector

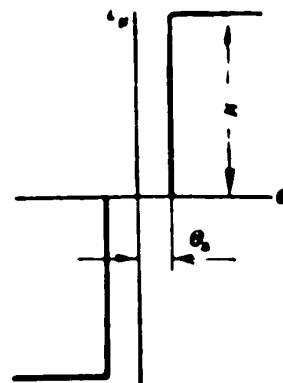


Fig.6.12 - Constant Characteristic of
Electrical Corrector

θ_{Δ} - Neutral zone of signal
transmitter of corrector

The signal transmitter here (Fig.6.13) is a bulb with a drop of mercury and three contacts so arranged that the plane of displacement of the mercury drop shall coincide with the plane of rocking of the corrected frame.

One of the contacts of the bulb is at its center, the other two at the edges.

In the matched state of this transmitter, the mercury drop is at the center of the bulb and covers only the central contact; in the unmatched state, the drop moves away from the center; and on operation, the mercury connects the central contact with one of the edge contacts. We note that by mismatching of the signal transmitter in this case we mean its inclination with respect to the vertical.

STAT

The moment transmitter here is a miniature induction motor with a short-circuited rotor, seated on the axis of rotation of the corresponding frame (that is, of the frame located diagonally across from the corrected frame). Exactly as in the preceding case (cf. diagram of Fig. 6.11b) one of the exciting windings of the miniature induction motor is always energized by one of the phases of a triphase supply line.

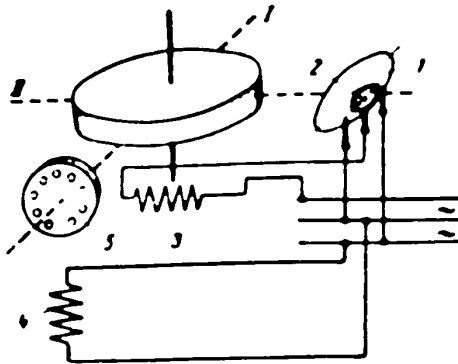


Fig. 6.13 - Diagram of Electric Corrector with Mercury Switch

I, II - Axis of suspension

1 - Bulb; 2 - Mercury; 3 and 4 - Windings of induction motor; 5 - Short circuited rotor of induction motor

will not depend on the value of the error in the signal transmitter).

When the mercury connects the central contact of the signal transmitter with one of the extreme contacts, the second phase of the miniature motor is connected with one of the other two phases of the supply line. As a result, a rotary field is produced in the miniature motor. The sense in which this field is directed will depend on what phase has been connected to the phase of the miniature motor. On this account, a moment of one sign or the other is developed on the rotor. It will be of constant magnitude (i.e., it

In order for the mercury drop to be able to roll from the central position and to close the contacts, a certain inclination of the bulb is necessary. The mercury drop obviously rolls in the opposite direction after the opposite inclination of the bulb has accumulated. When it rolls in this way, the mercury drop will naturally not remain in the central position, but will pass to the opposite extreme position.

On this basis, the characteristic of the correction for the given case will have the hysteresis form according to Fig. 6.10, b.

STAT

This system of correction can obviously be applied, and is, in fact, applied to correct the outer and inner frame of a gyro vertical, and to correct the inner frame of a directional gyro.

Figure 6.14 gives a diagram of the electrical connection of an induction-type gyro vertical. The signal transmitter here is a cup (Fig.6.14,a) with a current-conducting liquid, an electrolyte, and four electrodes. The cup is rigidly attached to the gyromotor casing. The electrodes are placed diagonally on the periphery of the cup. In this case, each diagonal pair of peripheral electrodes is intended for the correction of that frame of the gyro vertical whose axis of rotation is perpendicular to the axis joining the given pair of peripheral electrodes.

The cup of the electrolytic transmitter is not completely filled with liquid so that there is an air bubble. The electrolytic transmitter consists, as it were, of a bubble level producing electric signals.

If the axis of the gyro rotor occupies the vertical position (Fig.6.14,a), then this bubble will be in the center of the cup, and the resistance will be the same between the central electrode, that is, the cup itself, and either of the peripheral electrodes. When the gyro axis (Fig.6.14,b) deflects from the vertical, the air bubble will be displaced accordingly, and the resistances between the central electrode and the two peripheral electrodes become unequal. The appearance of a difference between the resistances is expressed as the error signal in this transmitter. Accordingly, on the circuit diagram of Fig.6.14,b, this transmitter is conventionally represented in the form of variable resistances between the central electrodes and the corresponding peripheral electrodes.

A basic feature of the electrolytic transmitter is the practical absence of any neutral zone; the smallest deflection from the vertical will produce a change of resistances of the bulk conductor electrolyte. This feature of this signal transmitter of the corrector, and its design simplicity, are responsible for the wide use of this type of correcting signal transmitter.

Two-phase miniature induction motors are used in this correction system. One of the phases of each of these miniature motors is always connected to a definite

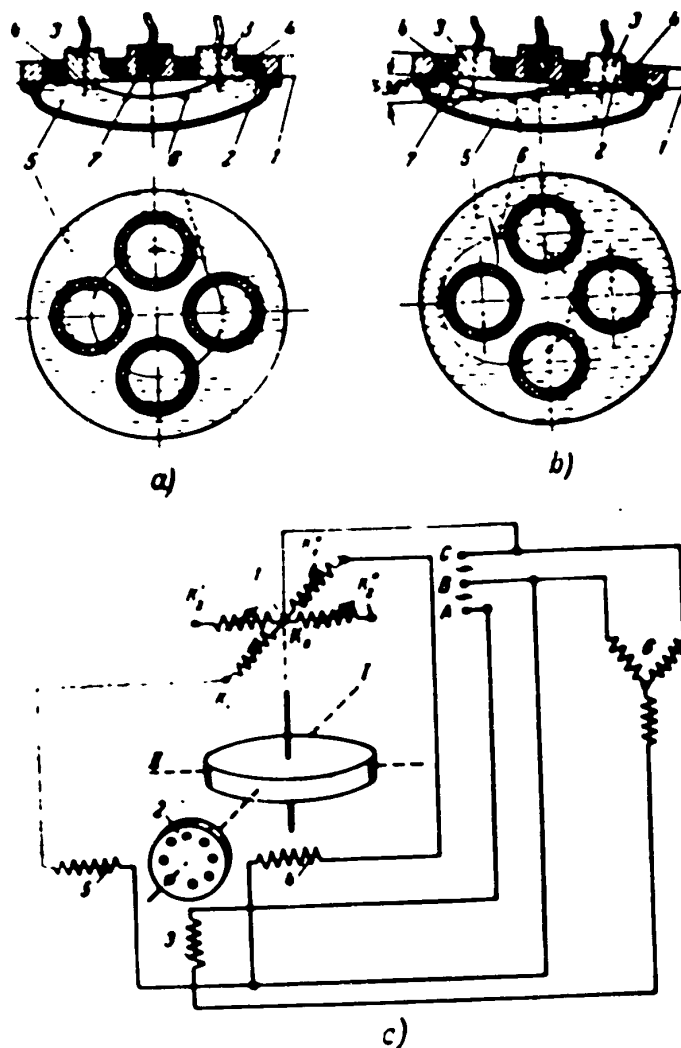


Fig.6.14 - Corrector with Electrolytic Transmitter
and Induction Motor

phase of the supply line (cf. diagram in Fig.6.17,c), the other phase consists of two windings connected in opposite directions and joined to the corresponding pair of electrodes of the signal transmitter. The second phase of the supply line is connected to the case. Thus, when the resistances between the upper electrode and the lower electrodes are equal, the resultant ampere-turns of the second

STAT

phase, and therefore also the moments at the shaft of the miniature motor, will be zero; when these resistances, differ, however, resultant ampere turns in a definite

sense appear, thus leading to the appearance of a moment in a definite sense, proportional to these resultant ampere-turns.

On the basis of the above, the characteristic of this corrector may be taken as analogous in form to the characteristic of the pneumatic corrector of the gyro vertical with pendulum slides given in Fig.6.3.

The zone of proportionality in the

transmitter amounts to 0.5° . For slopes over 0.5° , one of the electrodes is completely covered with air, and the other with liquid. The resistance from the first electrode will reach 5000 ohms, and that of the second 150 ohms. With greater slopes, the value of these resistances will no longer vary.

The moment transmitters in the form of induction motors have the advantage of allowing the correction system to operate when the axis of the suspension shifts through all of 360° . The latter will be unavoidable, for instance, in correcting directional gyroscopic instruments in azimuth.

The entire correction system is fed by a triphase alternating current source in which the voltage phases are shifted by 120° . For the operation of the biphasic motors, the phase shift between the voltages of the excitation winding must be 90° . To provide such a phase shift, part of the phase voltage of the phase A is fed to the winding (3) (cf. Fig.6.14,c) while the line voltage between the phases B and C is fed to the winding (4) and (5). These voltages, as follows from the voltage diagram of the triphase system given in Fig.6.15, are shifted in phase by 90° . The

STAT

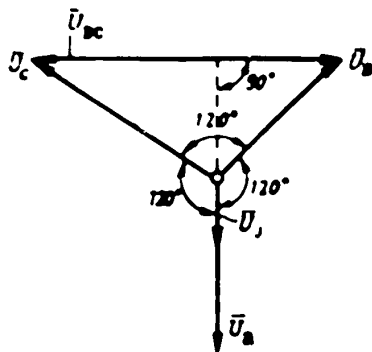


Fig.6.15 - Diagram of Voltages
of Triphase System

winding (3) is connected in the circuit of one of the phases of the stator winding of the motor for the gyro rotor. When the gyroscope is started up, starting

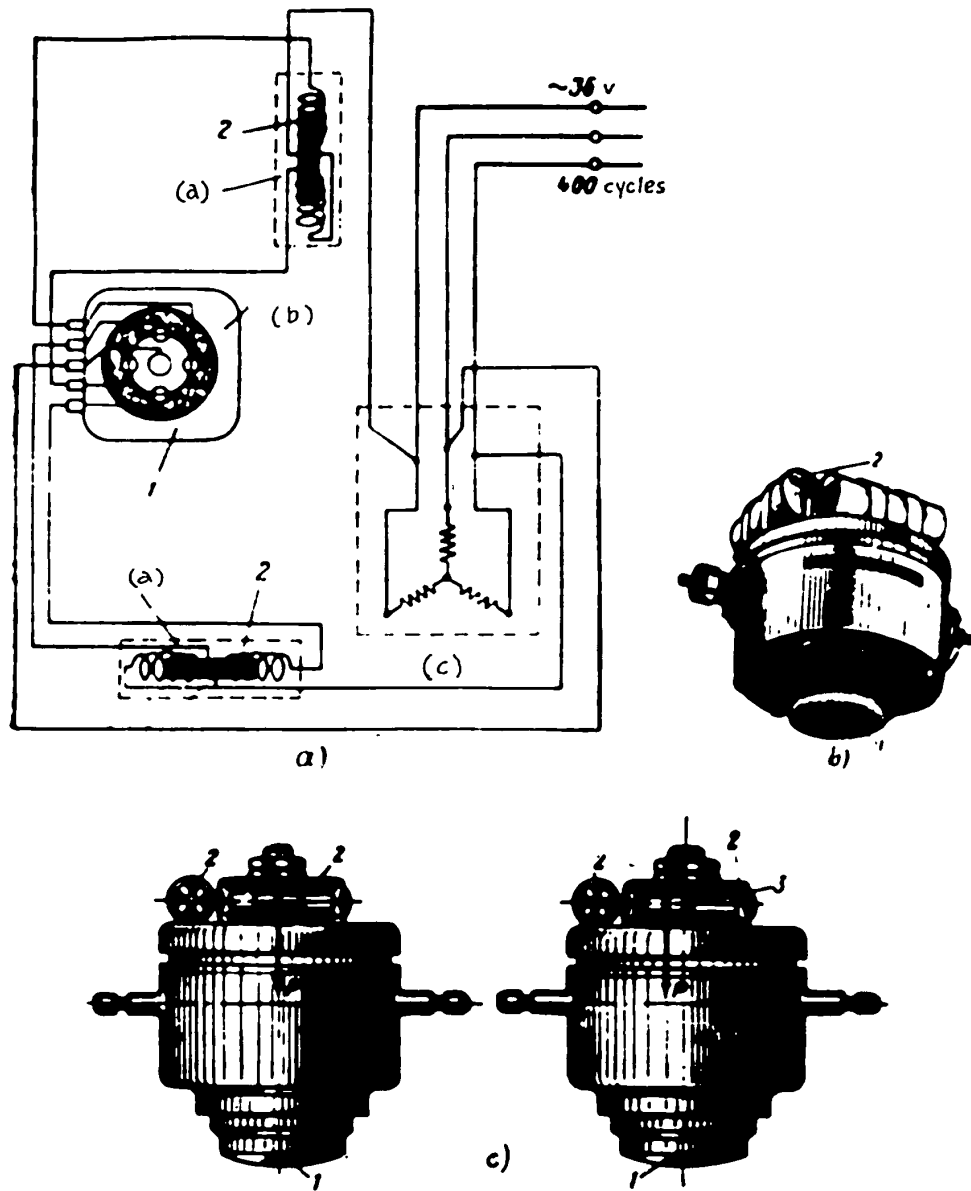


Fig.6.16 - Corrector for Electric Gyrohorizon

- 1 - Electrolytic pickup; 2 - Solenoids; 3 - Movable cores of solenoids
- (a) Solenoid; (b) Corrector switch; (c) Gyrohorizon gyromotor

currents of voltage higher than nominal flow in the stator winding, thus causing an STAT

increased rate of correction when the gyro starts. This shortens the time required for the gyro to move to its normal position.

A certain complexity in the design of induction motors has led to the use of moment transmitters of simpler design.

The correction system on one of the USSR electric gyro horizons consists of the electrolytic pickup (1) (Fig.6.16) and the two solenoids (2) with shiftable cores, connected according to the diagram of Fig.16,a. The solenoids are attached (Fig.6.16,b) to the casing of the gyro rotor, and a displacement of their cores with respect to the mean position (Fig.6.16,c) produces moments of unbalance, under the action of which, the gyroscope precesses toward the vertical. The displacement of the core of the solenoids takes place when the difference of current in the halves of the winding connected with opposite electrodes of the pickup, reaches a certain value. The characteristics of this correction system is close to that shown in Fig.6.10,a, and ordinarily $\phi = 0.5^\circ$.

Figure 6.17 gives a diagram of the electrical correction of the outer frame of a directional gyro accomplished by a remote-reading magnetic compass. The signal transmitter here is a disc connected with the axis of the outer frame and a brush connected with the repeater of the remote-reading compass. On the diagram of Fig.6.17, this is shown conventionally by the direct connection between the brush and the magnetic needle. One side of the disc is made of conducting material, the other side of insulating material. The positive pole of a direct current source is applied to the conducting part.

The moment transmitter used is a magnetoelectric device with its magnetic system attached to the outer frame of the gyroscope while the coil is connected to the axis of the inner frame. The coil is fed from the potentiometer of a two-coil magnetoelectric relay. One of the coils of this relay is energized during the entire time of operation of the correction system. The moment produced by the ampere-turns of this coil holds the brushes against the potentiometer in a position

STAT

such that the ampere-turns of the moment transmitter coil produce a moment causing precession of the gyro, and with it, also a shift of the signal transmitter disc in

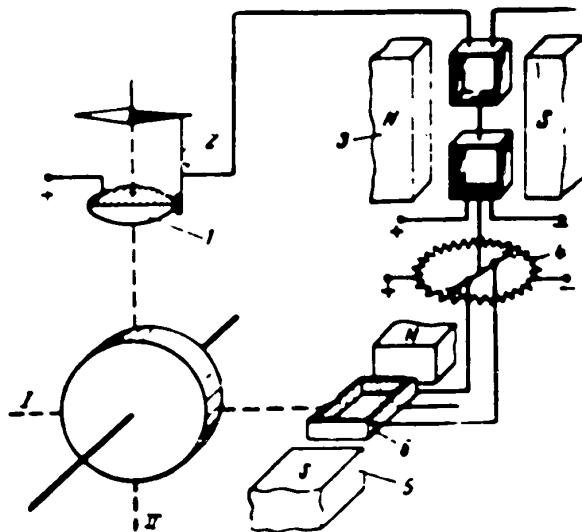


Fig.6.17 - Diagram of Magnetolectric Corrector of Outer Frame of Directional

1 - Disc of gyro signal transmitter;
 2 - Brush of signal transmitter connected with repeater of remote magnetic compass; 3 - Corrector relay; 4 - Potentiometer of relay; 5 - Magnetic system of moment transmitter of corrector; 6 - Coil of moment transmitter of corrector

the sense directed toward matching between the brush and the conducting part of the disc. The second coil of the relay is fed from the brush of the signal transmitter. In other words, this coil will be energized only when the above mentioned brush is in contact with the conducting part of the disc. In this case the ampere turns of this second coil will create a moment exceeding the moment produced by the ampere-turns of the first coil. Thus, as soon as the second coil is energized, the brushes of the relay potentiometer pass over into the extreme opposite position. The reverse direction of the correction moment and the sense of precession of the gyroscope change in accordance with this: now the motion of the gyroscope will be

in the sense of matching the brush of the signal transmitter with the insulated part of the disc.

Thus this system of correction in principle has no position of repose and has no neutral zones.

For this reason the gyroscope will not be damped in a definite position here,

STAT

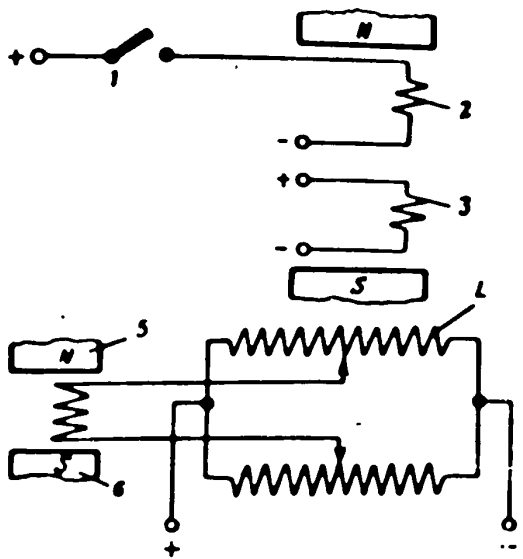


Fig. 6.18 - Electrical Circuit of Magneto-electric Corrector of Outer Frame of Directional Gyro

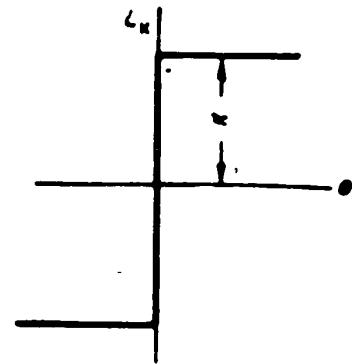


Fig. 6.19 - Constant Characteristic of Corrector of Hysteresis-Free Form with neutral zone Equal to 0

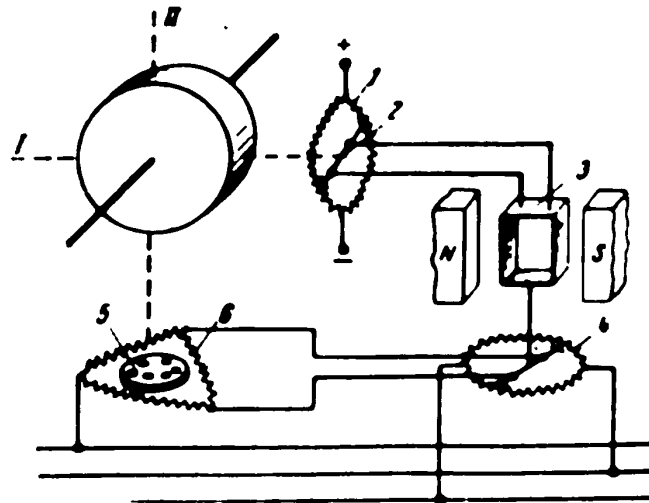


Fig. 6.20 - Diagram of Magnetolectric Corrector of Inner Frame of Directional Gyro

I, II - Axis of inner and outer gyro frames

- 1 - Signal transmitter potentiometer connected with outer frame; 2 - Brushes of signal transmitter connected with axis of inner frame; 3 - Relay of corrector;
- 4 - Potentiometer of relay of corrector; 5 - Short-circuited rotor of induction motor; 6 - Winding of induction motor

but instead it will oscillate about a certain position, in this case, about the position of the brush, that is, about the magnetic meridian. Owing to the low rate of correction, the amplitude of these self oscillations will be very small. Figure 6.18,a gives the electrical circuit of this corrector, and Fig.6.19 gives its characteristic.

Figure 6.20 shows a diagram of the electrical corrector of the inner frame of the same directional gyro. The signal transmitter here consists of a potentiometer placed on the outer frame, and a pair of brushes connected with the axis of the inner frame. Thus the correction of this frame is accomplished according to the position of the rotor axis with respect to the axis of the outer frame. The

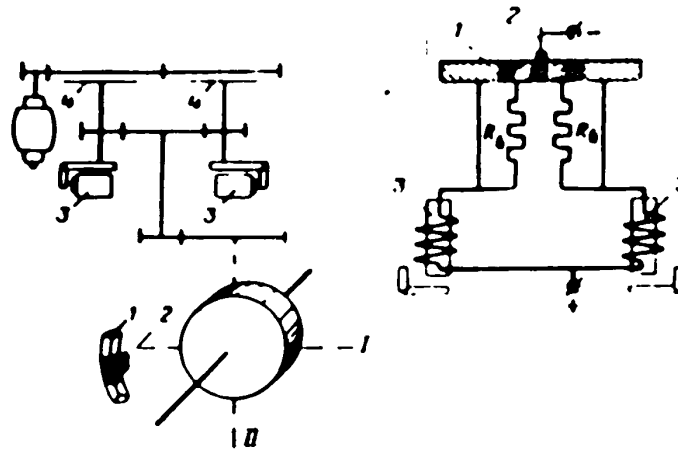


Fig.6.21 - Diagram of Electromechanical Corrector of Inner
Frame of Directional Gyro

I, II - Axes of inner and outer frames

- 1 - Contact strip of signal transmitter, connected with outer frame;
- 2 - Brush of signal transmitter connected with inner frame; 3 - Electro-
- magnet; 4 - Discs of friction coupling; 5 - Electric motor; R_b - Ballast
- resistors

mutually perpendicular position of these axes corresponds to the matched state of

• STAT

the signal transmitter.

The moment transmitter is a three-phase miniature induction motor with short-circuited rotor. One of the vertices of the triangle formed by the stator winding is connected to one of the phases of the supply line during the entire time of operation of the correction system.

The other two vertices are connected to two brushes mechanically connected to the axis of a magnetoelectric relay which is fed by the potentiometer of the signal transmitter. These brushes take off voltage from the potentiometer, connected on a bridge circuit to the other two phases of the supply line.

When no current flows through the relay the voltage taken off by these brushes is zero. When current appears in the relay winding, the brushes are displaced from the electrical neutral, and will transmit the voltage to the stator windings of the miniature induction motor. As a result, a moment in a definite sense appears, which is proportional by modulus to the displacement of these brushes from the electrical neutral, i.e., in the last analysis it is proportional to the deflection of the rotor axis from a right angle with the axis of the outer frame.

In accordance with the above, the characteristic of the corrector described will be of the form given in Fig.6.3.

Figure 6.21 gives a diagram of still another version of an inner frame corrector.

The signal transmitter here is a contact blade with an insulating strip placed on the outer frame, and a brush, connected with the axis of the inner frame. The moment transmitter is an electric motor rotating two gearwheels, which may be engaged by means of electromagnetic friction clutches, and systems of gears from the axis of the outer frame.

These electromagnets are controlled from the signal transmitter by means of the electric circuit of Fig.6.21. So long as the brushes remain on the insulated strip of the signal transmitter, both electromagnets are deenergized and the outer frame

STAT

is not coupled to the electric motor. As soon as the brush is displaced onto either conducting part of the blade, one electromagnet or the other is actuated. When this

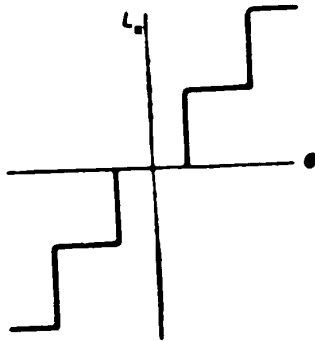


Fig.6.22 - Characteristic of Electromechanical Corrector

happens, the electric motor is coupled to the outer frame through two gears rotating in opposite senses. This will indicate that a moment of a definite sense has been applied to the outer frame. The magnitude of this moment will be determined by the force of the friction coupling, which in turn will be determined by the force developed by the electromagnets, i.e., by the number

of its ampere-turns. As follows from the electrical circuit, the electromagnets are fed at first through a ballast resistor, but then, with increasing mismatch, they are fed directly, bypassing this ballast resistor.

Thus the corrector characteristic in this case will have a stepped form, according to Fig.6.22.

Section 6.4. Mechanical Correction Systems

Of the mechanical systems we shall discuss only one friction correction system, designed for correcting a gyrovertical. Figure 6.23 gives a diagram of this system of correction. The correction sensor in it is a half-ring with an axis of rotation coinciding with the axis of rotation of the frame to be corrected. The semicircle has a slit with cork walls, through which passes a rotating roller connected by a reducer with the rotor axis.

It is this roller that forms the second element of the correction system.

These elements of the correction system here act simultaneously as signal transmitters and moment transmitters.

state of this correction system, the half ring is not pressed
STAT

against the roller by any side of the slit.

To mismatch, there corresponds a position in which the half ring is pressed against the roller by one side of the slit or the other, and therefore the force of

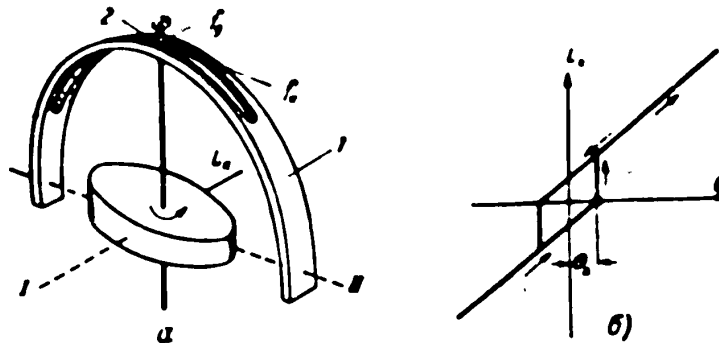


Fig.6.23 - Diagram of Friction Corrector of Gyrohorizon

I, II - Axes of gimbals

1 - Half-ring with friction slot; 2 - Rotating roller; f_g - Component of force of gravity pressing the wall of the slot of the half-ring against the rotating roller; f_k - Force of frictional adhesion, directed along slot; L_k - Element of force f_k

frictional adhesion f_k arises between them, which is proportional for the force of this compression of the half ring against the roller, and which is directed along the slot of the half ring.

Being applied to the axis of the rotor, this force exactly produces a precession of the gyro about the axis of rotation of the frame to be corrected and accordingly, also about the axis of rotation of the correcting half ring.

The force that presses the half ring against the roller will be the projection of the force of gravity of the half ring onto the normal to the rim of the roller. Within the limits of small deflections of the half ring from the vertical, it may be taken as proportional to these deflections. If we further consider the coefficient the roller and the walls of the slot as constant, we get t^{STAT}

result that the characteristic of this correction system will be proportional.

If the clearance between the roller and the half ring is taken into account, then the characteristic of the corrector takes the form shown in Fig.6.23,b. At angles of deflection of the gyrorotor axis θ_{Δ} and $-\theta_{\Delta}$, the half ring will be displaced from one side of the roller to the other, and as a result the correction moment will change its value with a jump.

As a whole, the gyrovertical has two correction systems of this type, one for each of its frames.

To eliminate the influence of the moment due to the force of gravity, owing to the force of the pressure of the half rings against the roller, counterweights are provided, which impose on the gyro a moment equal and opposite to the moment due to the force of gravity of the half rings.

We remark that if the roller does not rotate, then, in spite of the pressure of the slot of the half ring against the roller, this will not lead to the appearance of a force of frictional adhesion. In other words, when the rotation of the roller stops, the correction system will be turned off.

Section 6.5. Analytic Expressions of the Correction Characteristics

As follows from the above exposition, the characteristics of correctors may be divided into the following three groups, according to their form:

1. Proportional characteristics of hysteresis-free form (cf.Fig.6.6).
2. Constant characteristic of hysteresis-free form with zone of insensitivity not equal to zero (Fig.6.12), and equal to zero (Fig.6.19), and constant characteristics of hysteresis form (Fig.6.10,b).
3. Mixed characteristics of hysteresis-free (Fig.6.3) and hysteresis (Fig.6.10,a) forms.

We might introduce the notion of the generalized characteristic of a corrector of such a form that the above enumerated characteristics shall correspond to certain special cases for it. The form of the characteristic according to Fig.6.24,c $STAT^1$

satisfy such a condition.

The use of such a generalized characteristic in a theoretical analysis would involve no difficulties of principle. By dividing such a characteristic into a number of sections within which only some one law would operate, the behavior of the gyro in these sections could easily be obtained.

It would then remain for us to adjust the results obtained for the individual sections, and to obtain a general picture of the behavior. With the large number of such adjustments, however, this method would be inconvenient in practice. Since not

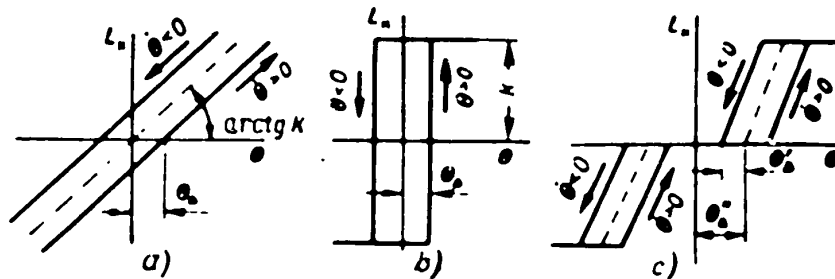


Fig.6.24 - Generalized Corrector Characteristics

a single one of the actual correction systems has a characteristic of such a generalized form, it is advisable to conduct our investigation with respect to simpler generalizations.

As such basic generalizations, we shall take the following:

- a) proportional characteristic of the hysteresis form (Fig.6.24,a);
- b) constant characteristic of the hysteresis form (Fig.6.24,b).

Using these generalizations, it will be easy to obtain the law of gyroscope behavior for other cases as well.

The analytic expressions of the corrector characteristics for the generalizations may be represented in the following form, distinguishing them by the literal subscripts a and b respectively:

STAT

$$L_{\Delta} = k(\theta - \theta_{\Delta} \text{sign } \theta), \quad (6.1)$$

$$L_{\Delta} = \begin{cases} k_{\Delta} \text{sign } \theta & \text{at } |\theta| \leq \theta_{\Delta}, \\ k \text{sign } \theta & \text{at } \theta > \theta_{\Delta}, \end{cases} \quad (6.2)$$

where θ - mismatch in signal transmitter of correction system;

k - slope of proportional characteristic of correction;

θ_{Δ} - zone of hysteresis;

k - value of constant correcting moment beyond zone of hysteresis;

k_{Δ} - value of constant correcting moment in zone of hysteresis;

$$\text{sign } \theta = \begin{cases} -1 & \text{at } \theta < 0, \\ +1 & \text{at } \theta > 0, \end{cases} \quad (6.3)$$

$$\text{sign } \theta = \begin{cases} -1 & \text{at } \theta < 0, \\ +1 & \text{at } \theta > 0. \end{cases} \quad (6.4)$$

We shall consider that the absence of the allowance for hysteresis corresponds, with a proportional characteristic, to the condition

$$\theta_{\Delta} = 0, \quad (6.5)$$

and with a constant characteristic, to the condition

$$k_{\Delta} = 0. \quad (6.6)$$

In allowing for hysteresis in the latter case, however, the equality

$$k_{\Delta} = k. \quad (6.7)$$

will hold.

To denote the angles of deflection of the gyro frames from the positions they should occupy, we shall, as before, use the letters α (for the angle of deviation of the outer frame), and β (for the angle of deviation of the inner frame).

All the remaining notations will be taken as the same for both systems of correction, that is, for the correction of both the outer and the inner frame, which are distinguished from each other by the subscripts 2 and 1 respectively.

The sensors of a correction system usually have certain static errors. Denot-
STAT

ing these errors, expressed in angular units, by γ , we obtain the following expressions for the mismatches θ_1, θ_2 :

$$\theta_1 = \beta - \gamma_1; \quad \theta_2 = \alpha - \gamma_2.$$

It is clear that γ_1 and γ_2 , the errors of the sensors of the corrector, are equal to their errors in the direction of the gyroscope.

STAT

CHAPTER VII

THE SETTING STATE WITH FIXED GIMBAL BASE AND UNDISTURBED
STATE OF THE CORRECTION SYSTEMSection 7.1. General Remarks

The consideration of the setting state is of great importance, since the quality of positional gyro instruments depends to a considerable extent on how accurately the gyro is set during flight and how long it takes to reach its operating position.

The setting state of the gyrohorizon and gyromagnetic compasses in the most complete form occurs on starting. The detailed consideration of the setting state on starting involves considerable difficulty owing to the presence of moments of forces of inertia, which manifest themselves on variation of the rotor speed. The starting state is therefore not discussed separately, but we shall consider the setting state of the gyroscope with constant kinetic moment.

In the following exposition of the theory of positional gyros, we shall investigate the setting states with the object of elucidating:

- a) the paths of motion of the spin axis toward the steady position;
- b) the duration of the setting state or of the setting time;
- c) the final position of the spin axis and the corresponding errors of the steady position of the spin axis.

Of the methodological considerations, following B.V.Bulgakov, we shall distinguish.

STAT

- 1) the setting state with fixed base of the suspension and undisturbed state of the correction system;
- 2) the setting state in presence of oscillatory motions of the base at fairly high frequency;
- 3) the setting state allowing for the motion of the base of the suspension in connection with the earth rotation, the displacements of the aircraft with respect to the earth, and the aircraft maneuvers.

The first of these states is the most favorable with respect to the possibility of shortening the duration of the build-up time and reducing the values of the errors of the steady state, but it is never observed under actual conditions. Nevertheless, the characteristics of this state are of substantial importance in that they establish the limiting relations which it is desirable, under actual conditions, to approach as much as possible.

The second state is less favorable from this point of view, but it is closer to actual operating conditions, since it allows for the disturbances in the correction system which always occur. A comparison of this state with the characteristics of the first state allows us to establish the specific influence of these disturbances on the gyro.

An investigation of the third state allows us to elucidate the influence of other factors under operating conditions.

The characteristics of the first and second states do not depend on the final position of the spin axis, i.e., they do not depend on what direction with respect to the earth should be indicated by the given gyro. The direction indicated by the gyro is determined only by the position with respect to the earth of the respective paths of motion of the gyro and the position of the end points of these paths, which will characterize the errors of the steady state. Allowance can easily be made for this by an appropriate specification with respect to the plane on which these paths are to be represented.

STAT

In contrast to this, the characteristics of the third state will depend on the final position of the spin axis, since the action of all the factors distinguishing the third state is related to definite earthbound axes.

We remark that this action is manifested, in the last analysis, in the displacement of the equilibrium position of the system, and thereby in the displacement of the end positions of the spin axis. We shall therefore distinguish the errors of the steady condition in the third setting state from the errors of the steady condition in the first setting state. And it will be in the elucidation of this very difference that the principal interest of our investigation of the third state will reside.

Section 7.2. Equations of Motion

As before, we shall use the system of coordinates $O\xi\eta\zeta$ bound to the earth and the system of coordinates $Oxyz$, bound to the gyro. Of the earthbound axes, we shall consider the axis $O\xi$ to be matched with the direction which the gyro must indicate in the given case, and we shall call it the principal axis; while the axis $O\eta$ will be considered matched with the direction of the axis of the outer frame. Of the gyroscopic axes, we shall consider the axis Oz as matched with the rotor axis, and the axis Ox as matched with the axis of the inner frame.

The position of the system of coordinates axes bound to the gyro with respect to the earthbound system of coordinates will be determined by the angles α and β (Fig.7.1), of which the angle α represents the shift of the gyroscope about the axis of the inner frame of the gyro, i.e., about the axis $O\eta$ in the plane $O\xi\xi$, while the angle β represents the shift of the gyroscope about the axis of the inner frame, i.e., about the axis Ox in the plane $Oz\eta$. We remark that, together with this, the angle α represents the shift of the outer frame of the gyroscope together with the inner frame, the angle β the shift of the inner frame alone with respect to the position at which the rotor axis is perpendicular to the axis of the outer frame.

The axes on Figs.7.1 are oriented with respect to the case of the gyro verti-

cal. This is the orientation that we shall use. For other cases, for example, for directional gyros, this orientation as a whole must be rotated in thought by the 90° .

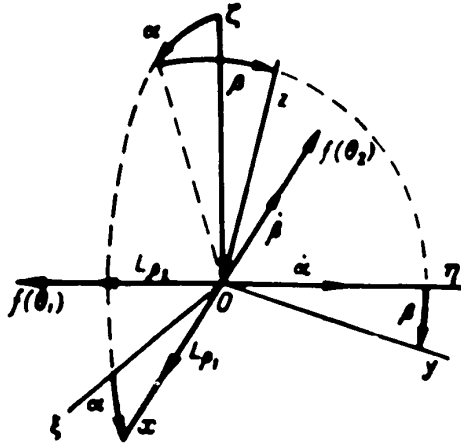


Fig.7.1 - Position of Axes of Gyroscope with Fixed Base of Suspension (with Fixed Earthbound Axes)

To judge the behavior of the gyro, we shall use the paths that will be described on a sphere of unit radius by the corresponding point on the rotor axis, we shall call this point the vertex of the gyro.

It is obvious that arcs of these paths will be respectively equal to the angles α and β (if we take as the origin of measurement the point of intersection of this sphere by the earth axis $O\xi$).

For small angles α and β , that is, in the immediate neighborhood of the point of origin of measurement, we may treat a portion of the sphere as a plane, and, accordingly, consider the paths of motion of the vertex of the gyroscope as being plane and analytically assignable in the system of rectangular coordinate axes $O\alpha\beta$ in the form of the equation

$$F(\alpha, \beta) = 0 \tag{7.1}$$

As our starting equations of motion we shall take, as usual, the approximate equations of motion of the gyro, that is, the equations of its precession. These equations are of the form:

$$\left. \begin{aligned} Hq &= L_r \\ -Hp &= L_r \end{aligned} \right\} \tag{7.2}$$

where both p and q are the projections of all the angular velocities of motion of

STAT

the gyro onto its equatorial axes, Ox and Oy respectively; while L_x and L_y are the projections on these same axes of the external moments acting on the gyroscope.

In the fixed position of the gyroscope, and under the condition that the angles shall be small (cf. Fig. 7.1), we get

$$\left. \begin{aligned} p &= -\dot{\beta}. \\ q &= \dot{\alpha}. \end{aligned} \right\} \quad (7.3)$$

For the moments L_x and L_y , taking into consideration only the action of the moments of correction moments and of the moments of friction about the axes of the suspension (cf. Fig. 7.1), we have

$$\left. \begin{aligned} L_x &= -f(\theta_2) + L_{\rho 1} \text{sign } \dot{\beta}. \\ L_y &= -f(\theta_1) - L_{\rho 2} \text{sign } \dot{\alpha}. \end{aligned} \right\} \quad (7.4)$$

where $f(\theta_2)$ and $f(\theta_1)$ are the characteristics of the correction of the outer and inner frames respectively;

θ_2 and θ_1 - the mismatches in the signal transmitters of the correction systems;

$L_{\rho 2}$ and $L_{\rho 1}$ - moments of friction about the axes of the same frames respectively;

$$\text{sign } \dot{\alpha} = \begin{cases} 1 & \text{at } \dot{\alpha} > 0. \\ -1 & \text{at } \dot{\alpha} < 0. \end{cases}$$

$$\text{sign } \dot{\beta} = \begin{cases} 1 & \text{at } \dot{\beta} > 0. \\ -1 & \text{at } \dot{\beta} < 0. \end{cases}$$

Since we shall not take account in this chapter of the disturbances in the correction system, we may consequently put

$$\left. \begin{aligned} \theta_1 &= \beta. \\ \theta_2 &= \alpha. \end{aligned} \right\} \quad (7.5)$$

Making use of eqs. (7.5), (7.4) and (7.3), we obtain the following equations of motion of the gyroscope axis:

STAT

$$\left. \begin{aligned} H\dot{\alpha} &= -f(\alpha) + L_{p1} \text{sign } \dot{\beta} \\ H\dot{\beta} &= -f(\beta) - L_{p2} \text{sign } \dot{\alpha} \end{aligned} \right\} \quad (7.6)$$

Section 7.3. The Setting State with Proportional Correction

Characteristics Equations of Motion

On substituting $f(\alpha)$ and $f(\beta)$ in eq. (7.6) according to the expression for the proportional characteristic, eq.(6.1), and replacing α in it by α and β respectively, and indicating by the subscripts 1 and 2 the frame to whose corrector the given slope belongs, we get

$$\left. \begin{aligned} H\dot{\alpha} + k_2\alpha &= L_{p1} \text{sign } \dot{\beta} + k_2\theta_{22} \text{sign } \dot{\alpha} \\ H\dot{\beta} + k_1\beta &= L_{p2} \text{sign } \dot{\alpha} + k_1\theta_{11} \text{sign } \dot{\beta} \end{aligned} \right\} \quad (7.7)$$

or, dividing the right and left sides of eq.(7.7) by H:

$$\left. \begin{aligned} \dot{\alpha} + \epsilon_2\alpha &= \epsilon_2\theta_{22} \text{sign } \dot{\beta} + \epsilon_2\theta_{22} \text{sign } \dot{\alpha} \\ \dot{\beta} + \epsilon_1\beta &= -\epsilon_1\theta_{11} \text{sign } \dot{\alpha} + \epsilon_1\theta_{11} \text{sign } \dot{\beta} \end{aligned} \right\} \quad (7.8)$$

where

$$\epsilon_1 = \frac{k_1}{H}; \quad (7.9)$$

$$\epsilon_2 = \frac{k_2}{H}; \quad (7.10)$$

$$\rho_1 = \frac{L_{p2}}{k_1}; \quad (7.11)$$

$$\rho_2 = \frac{L_{p1}}{k_2}. \quad (7.12)$$

To elucidate the physical meaning of the quantities ϵ_1 and ϵ_2 , let us substitute in eq.(7.8):

$$\begin{aligned} \rho_1 = \rho_2 = \theta_{11} = \theta_{22} &= 0, \\ \alpha = \beta &= 1. \end{aligned}$$

In this case we get:

STAT

$$\dot{\alpha} = -\epsilon_2,$$

$$\dot{\beta} = -\epsilon_1.$$

It follows from this that ϵ_2 and ϵ_1 are the relative rates of precession of the outer and inner frames respectively, i.e., the rates of precession that these frames will have when they deflect from the assigned position by an angle equal to one radian, on to the conditions that hysteresis of the characteristic and friction in the suspension shall be absent, and the corresponding position of the sensor of the correction system shall be undisturbed.

The actual values of the correcting rates of precession will be considerably less than their relative values, since the actual range of deflections of the gyro from its assigned position will be considerably less than an angle of one radian. The value of the relative rate of precession will therefore be of interest to us mainly as a characteristic of the efficiency of precession.

To elucidate the physical meaning of the quantity ρ_2 , put $\theta_{\Delta 1} = \theta_{\Delta 2} = 0$ and substitute, in the first of eq.(7.8)

$$\dot{\alpha} = 0.$$

In this case we get

$$\alpha = \rho_2 \text{ sign } \dot{\beta}. \quad (7.13)$$

It follows that ρ_2 indicates the deflection of the outer frame in its steady state ($\dot{\alpha} = 0$), due, according to eq.(7.12), to friction in the axis of the inner frame. The magnitude of ρ_2 is determined by the moment of friction in the inner frame and by the slope of the characteristic of correction of the inner frame.

By analogy, on substituting $\dot{\beta} = 0$, in the second of eqs.(7.8), we get

$$\beta = \rho_1 \text{ sign } \dot{\alpha}, \quad (7.14)$$

from which it follows that ρ_1 indicates the deviation of the inner frame in its steady state ($\dot{\beta} = 0$) due to friction in the axis of the inner frame. The magnitude ρ_1 is determined by the moment of friction of the inner frame and by the slope of the characteristic of correction of the inner frame. Thus ρ_1 and ρ_2 are of the

STAT

nature of angles of rest, but with certain peculiarities.

We shall elucidate the essential nature of these peculiarities below.

Geometrical Construction of the Build-Up Paths

In addition to the analytic method of determining the build-up paths of the gyroscope, which consists in the integration of the equations of motion, these paths may also be determined by graphical constructions.

Let us represent the components of the vector of the moment of correction and the vector of the moment of friction on the above mentioned α , β coordinate plane. By virtue of the smallness of the angles, the components of these vectors are practically equal to the vectors themselves. It follows from the theorem on the velocity of the end of the vector of kinetic moment that the vertex of the gyroscope will move in the direction of the resultant of the component vectors of moments.

For a proportional hysteresis-free characteristic of correction of the same efficiency:

$$L_{\alpha} = k\alpha,$$

$$L_{\beta} = k\beta.$$

The vector of the correction moment is therefore directed toward the origin of coordinates, and in the absence of friction in the bearing, the vertex of the gyro will move toward the point O along a straight line passing through the point O (Fig.7.2). The magnitude of the correction moment, however, is proportional to the distance of the gyroscope vertex from the origin of coordinates.

For a proportional correction of unequal efficiency:

$$L_{\alpha} = k_1\alpha,$$

$$L_{\beta} = k_2\beta; \quad k_1 \neq k_2$$

The vector of the correction moment is not directed toward the origin of coordinates (for all points except the points of the coordinate axes), and forms with a ray passing through the point O, an angle that is equal for any point of that ray,

STAT

since the tangent of the angle of inclination of the vector of moment $\frac{L_{k2}}{L_{k1}}$ is defined by the tangent of the angle of inclination of the ray, $\frac{\alpha}{\beta}$, according to the relation:

$$\frac{L_{k2}}{L_{k1}} = \frac{k_2}{k_1} \frac{\alpha}{\beta}$$

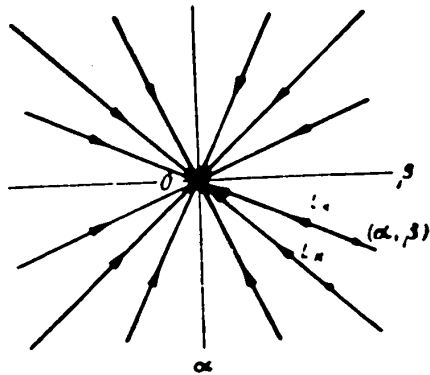


Fig.7.2 - Path of Vertex of Gyroscope with Proportional Hysteresis-Free Characteristics of Correction of equal Efficiencies. The Friction in the Gimbals is not Taken Into Account

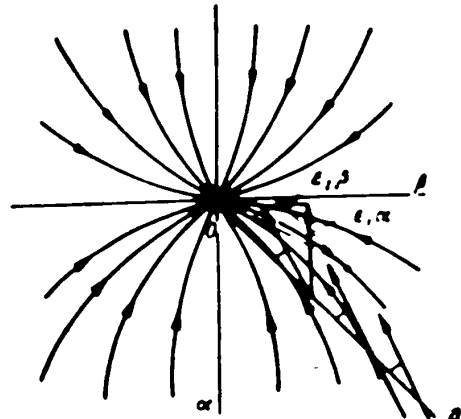


Fig.7.3 - Paths of the Vertex of the Gyroscope with Proportional Hysteresis-Free Correction Characteristics of Unequal Efficiencies. Friction in the Gimbals is not Taken Into Account.

The family of curves, the tangents to which form equal angles with a ray drawn from the origin of coordinates, is shown in Fig.7.3.

Build-Up Characteristics in the Absence of Friction in the Gimbals, without Allowing for Hysteresis

Putting $\rho_1 = \rho_2 = \theta_{\Delta 1} = \theta_{\Delta 2} = 0$, in eq.(7.8), in accordance with the conditions adopted, we rewrite them in the following form:

STAT

$$\left. \begin{aligned} \frac{d\alpha}{dt} &= -\epsilon_2 \alpha, \\ \frac{d\beta}{dt} &= -\epsilon_1 \beta. \end{aligned} \right\} \quad (7.15)$$

Or, dividing the right side by the left, we get

$$\frac{d\alpha}{d\beta} = v_1 \frac{\alpha}{\beta} \quad (7.16)$$

where

$$v_1 = \frac{\epsilon_2}{\epsilon_1} = \frac{k_2}{k_1} \quad (7.17)$$

Equation (7.16) is easily integrated. Separating the variables, we get

$$\frac{d\alpha}{\alpha} = v_1 \frac{d\beta}{\beta}$$

whence we have

$$\ln \alpha = v_1 \ln \beta + \ln c \quad (7.18)$$

where c = constant of integration.

Let, for $t = 0$; $\alpha = \alpha_0$; $\beta = \beta_0$.

Whence we get

$$\ln c = \ln \alpha_0 - v_1 \ln \beta_0$$

On substituting in eq.(7.18) the value for the integration constant so found, we get the following equation of path:

$$\ln \frac{\alpha}{\alpha_0} = v_1 \ln \frac{\beta}{\beta_0} \quad (7.19)$$

Let us take the special case where $k_1 = k_2$, and, consequently, $v_1 = 1$, as is most frequently the case. For this case, eq.(7.19) may be rewritten in the following form:

$$\frac{\alpha}{\alpha_0} = \frac{\beta}{\beta_0} \quad (7.20)$$

STAT

The equation of paths there obtained is the equation of the straight lines passing through the point with the initial coordinates (α_0, β_0) and the origin of coordinates (Fig.7.2). In other words, in this special case, the vertex of the gyro runs from the point of the initial disturbance to the origin of coordinates, that is, to the assigned position, in the direction of the shortest path. The fact that the vertex of the gyroscope follows the path found precisely toward the origin of coordinates, but not in the reverse sense, results from eq.(7.15), according to which

$$\text{at } \alpha > 0, \dot{\alpha} < 0 \text{ and at } \beta > 0, \dot{\beta} < 0$$

The numerical value of the velocity of the vertex on the path, u , is determined from the expression

$$u = \sqrt{\dot{\alpha}^2 + \dot{\beta}^2}. \quad (7.21)$$

On substituting the values of $\dot{\alpha}$ and $\dot{\beta}$ by eq.(7.15) in this expression, and bearing in mind that we are considering the case when

$$\epsilon_1 = \epsilon_2 = \epsilon.$$

we get

$$u = \epsilon r, \quad (7.22)$$

where $r = \sqrt{\alpha^2 + \beta^2}$ is the length of the radius-vector of the vertex.

But the direction of the path in this case is opposite to the direction of the radius-vector r . It follows from this that the velocity u will at the same time be equal to the derivative of the radius vector $\frac{dr}{dt}$ with reversed sign. Equation (7.22) may therefore be rewritten in the following form:

$$\dot{r} + \epsilon r = 0. \quad (7.23)$$

The integral of eq.(7.23) will be the function

$$r = R e^{-\epsilon t}. \quad (7.24)$$

where R is a constant of integration that is easy to determine.

It follows from eq.(7.24) that, in time, the setting state of the gyro in the

STAT

case we are considering will proceed according to an exponential law with the time constant $\tau = \frac{1}{\varepsilon}$. Consequently, T_y the practical duration of the setting state, may be determined from the expression

$$T_y = (3 \div 4) \frac{1}{\varepsilon}. \quad (7.25)$$

In the general case, eq.(7.19) may be rewritten in the following form:

$$\frac{d\alpha}{d\beta} = \left(\frac{\beta}{\beta_0} \right)^{v_1},$$

which, at $v_1 \leq 1$, that is, with different efficiencies of the correction in the two frames, will already denote the corresponding curvature of the paths (cf.Fig.7.3).

We note that the pictures of the paths so found may also be obtained directly by eq.(7.16), if we use it as the equation of the tangents to the paths $F(\alpha, \beta) = 0$.

Let us find the locus of points which these tangents have the same angular coefficient, i.e., the locus of points where

$$\frac{d\alpha}{d\beta} = k = \text{const.} \quad (7.26)$$

Such loci of points are called isoclinic.

On substituting $\frac{d\alpha}{d\beta}$ in eq.(7.16) according to eq.(7.26), we get

$$\alpha = \frac{k}{v_1} \beta. \quad (7.27)$$

Thus, as already stated, the isoclines are straight lines passing through the origin of coordinates and having an angular coefficient differing by a factor of $\frac{1}{v_1}$ from the angular coefficient of the tangents.

For $v_1 = 1$, that is, at the same efficiency of correction on both frames, the angular coefficients of the isoclines and those of the tangents coincide; this denotes coincidence with the isoclines of the paths themselves.

Assume $v_1 > 1$, that is, that the correction of the outer frame is more efficient than that of the inner frame.

In this case

STAT

$$\frac{\mu}{\eta} < \mu,$$

that is the angular coefficient of the tangent at each given point will be greater than the angular coefficient of the isocline, which is determined, according to (7.27), by joining a given point to the origin of coordinates. Thus the direction of the tangent at each point is easily determined. But, by constructing the field of tangents, it is easy to determine the approximate form of the paths (cf. Fig. 7.3). It will be clear that in this case they will have a curvature toward the axis $O\beta$. Physically, this curvature is a consequence of the higher efficiency of the correction of the outer frame.

For $v_1 = 1$, that is, in the case where the correction of the inner frame is more efficient, the position will be the opposite, that is, in this case the angular coefficient of the tangent at each given point will be less than the angular coefficient of the isocline. Accordingly, the paths will now be curved toward the axis $O\alpha$.

As for the duration of the build-up state, for $v_1 \leq 1$, it may be determined by the same formula (7.25), by substituting ϵ_1 in it if $\epsilon_1 < \epsilon_2$, or ϵ_2 , if $\epsilon_2 < \epsilon_1$. This follows directly from the exponential law of build-up, under which the duration of the build-up does not depend on the initial disturbance, but depends only on the time constant of the process. Since the build-up may be considered completed only after it has taken place with respect to both frames, it is natural to take as the total duration the duration of the build-up of the frame with the greater time constant, that is, with a smaller relative rate of correction.

This method will be unsuitable only in the special case when there is a deviation only of the frame whose build-up process is connected with the smaller time constant.

In this case, this small time constant must now be substituted in eq. (7.25).

Effect of Friction in the Gimbals on the Build-up State with
Hysteresis-Free Characteristics of Correction

Let us rewrite eq.(7.8) in the following form:

$$\left. \begin{aligned} \frac{d\alpha}{dt} &= -\epsilon_2 (\alpha - \rho_2 \operatorname{sign} \beta) \\ \frac{d\beta}{dt} &= -\epsilon_1 (\beta + \rho_1 \operatorname{sign} \alpha) \end{aligned} \right\} \quad (7.28)$$

We now introduce the notation

$$\alpha_{1,2} = \alpha - \rho_2 \operatorname{sign} \beta, \quad (7.29)$$

$$\beta_{1,2} = \beta + \rho_1 \operatorname{sign} \alpha. \quad (7.30)$$

where the first subscripts correspond to the values

$$\operatorname{sign} \alpha = \operatorname{sign} \beta = 1,$$

and the second subscripts to the values

$$\operatorname{sign} \alpha = \operatorname{sign} \beta = -1.$$

On excluding from the operations the instants of time when $\alpha_{1,2}$ and $\beta_{1,2}$ undergo a break in continuity in connected with the change of signs of α and β , we get

$$\begin{aligned} d\alpha_{1,2} &= d\alpha \\ d\beta_{1,2} &= d\beta \end{aligned}$$

On this basis, eq.(7.28) may now be rewritten in the following form

$$\begin{aligned} \frac{d\alpha_{1,2}}{dt} &= -\epsilon_2 \alpha_{1,2} \\ \frac{d\beta_{1,2}}{dt} &= -\epsilon_1 \beta_{1,2} \end{aligned} \quad (7.31)$$

And, accordingly, we get for the paths

$$\frac{d\alpha_{1,2}}{d\beta_{1,2}} = \nu_1 \frac{\alpha_{1,2}}{\beta_{1,2}}. \quad (7.32)$$

STAT

Thus the operation reduces down to the replacement of the system of coordinates $O\alpha\beta$ by the system of coordinates $O\alpha_{1,2}\beta_{1,2}$, connected with the former system by the corresponding displacement of the origin of coordinates.

Let us take the former system of coordinates $O\alpha\beta$. Draw in it the straight lines on which $\dot{\alpha}$ and $\dot{\beta}$ can change their signs, and, accordingly, the transition from β_1 to β_2 and from α_1 to α_2 , or the reverse transitions, can occur.

The equations of these straight lines will be

$$\alpha = \pm \rho_2.$$

$$\beta = \pm \rho_1.$$

These straight lines divide the coordinate plane into nine regions. In four of them, denoted by Roman numerals, the angles α and β are greater in modulus than ρ_2 and ρ_1 . In the four following cases, denoted by Arabic numerals, one of the angles, either α or β , is less in modulus than ρ_2 or ρ_1 respectively. And in the last, central region, C, both the angles, α and β , are less in modulus than ρ_2 and ρ_1 , respectively.

It follows from eq.(7.28) that in region I the conditions $\dot{\alpha} < 0$; $\dot{\beta} < 0$ are satisfied. In region 1, we know that the condition $\dot{\beta} < 0$ is satisfied, and accordingly also sign $\dot{\beta} = -1$, but in that case, for region I as well, $\dot{\alpha} < 0$. In region II, $\dot{\beta} < 0$; $\dot{\alpha} > 0$. In region 2 we know that $\dot{\alpha} > 0$ and, accordingly, sign $\dot{\alpha} = 1$, but then $\dot{\beta} < 0$. In region III, $\dot{\alpha} > 0$; $\dot{\beta} > 0$. In region 3 we know that $\dot{\beta} > 0$, and accordingly sign $\dot{\beta} = 1$, but then $\dot{\alpha} > 0$. In region IV, $\dot{\alpha} < 0$; $\dot{\beta} > 0$. In region 4 we know that $\dot{\alpha} < 0$, and accordingly sign $\dot{\alpha} = -1$, but then $\dot{\beta} > 0$.

Thus the regions of the same number in Roman and Arabic numerals are combined. In this case, in the region I, (1) the conditions of motion are such that the corresponding paths are defined by the equations

$$F(\alpha_2, \beta_2) = 0,$$

which means the transfer of the origin of coordinates to the point O_1 (Fig.7.4). In the region II, (2) the paths are defined for the equation

STAT

$$F(\alpha_2, \beta_1) = 0,$$

which means the transfer of the origin of coordinates to the point O_2 ; in the region III, (3) by the equation $F(\alpha_1, \beta_1) = 0$, which means the transfer of the origin of coordinates to the point O_3 ; in the region IV, (4) by the equation $F(\alpha_1, \beta_2) = 0$, which means the transfer of the origin of coordinates to the point O_4 .

These transfers of the origin of coordinates will be the only changes in the procedure of determining the paths, when the friction in the gimbals is taken into account, by comparison with the determination of these paths without taking this friction into account.

The equations of the paths, however, remain completely unchanged, as follows from a comparison of eq.(7.32) and eq.(7.16).

Thus, for the special case $v_1 = 1$, the spectrum of the paths is represented by Fig.7.4, while for the case $v_1 > 0$, by Fig.7.5.

These paths do not enter the central region, since the correction system is unable to assure motion in this region. Indeed, let us assume the contrary case, that such motion is possible. Let us take any combination of angular velocities of this motion, and let us assume $\dot{\alpha} > 0$, $\dot{\beta} < 0$, which will mean that

$$\text{sign } \alpha = 1; \quad \text{sign } \dot{\beta} = -1.$$

will hold.

But, by eq.(7.28), only $\dot{\alpha} < 0$; $\dot{\beta} < 0$ can hold in this case, which contradicts our hypothesis. If we take the latter combination, then by eq.(7.28) we get, for this case, $\dot{\alpha} < 0$, $\dot{\beta} > 0$. This combination in turn leads to the combination $\dot{\alpha} > 0$; $\dot{\beta} > 0$, etc. In other words, any assumption that motion is possible in the central region leads to a contradiction, from which it follows that such an assumption is untrue. Thus, the central region is a region of repose, and, to the stable state of equilibrium of the gyroscope vertex, there correspond four points on the boundary of this region, the vertices of the angles formed by the boundary lines.

the departure of the boundary of the region of repose from the
STAT

origin of coordinates 0 along the axis $O\beta$, which characterizes the repose of the inner frame, depends on the moment of friction about the axis of the outer frame, while the displacement of the boundary of the region of repose along the axis $O\alpha$,

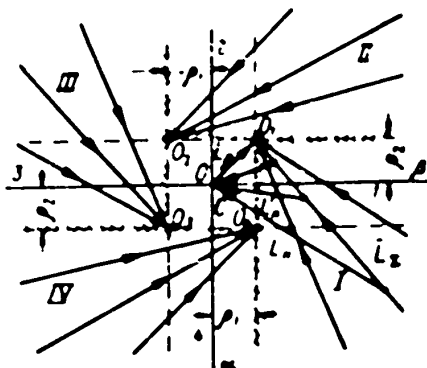


Fig. 7.4 - Paths of Vertex of Gyroscope with Proportional Hysteresis-Free Characteristics of Correction of Equal Efficiency, Allowing for the Friction in the Gimbals

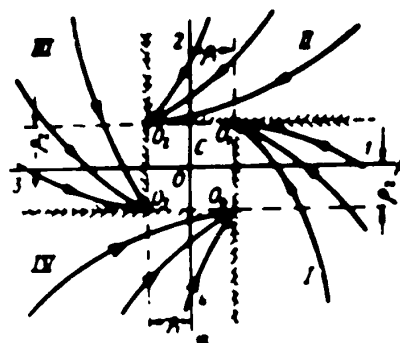


Fig. 7.5 - Influence of Hysteresis in Proportional Characteristics of Correction of Equal Efficiency for Both Frames. The Friction in the Gimbals is not Taken into Account

characterizing the stagnation of the outer frame, depends on the friction about the axis of the inner frame. Physically, this circumstance is a consequence of the diagonal position of the positional moments, or in other words, is a consequence of the fact that to obtain the precession, let us say, of the inner frame, a moment must be applied to the axis of the outer frame, with a magnitude which in any case exceeds the moment of friction about this axis, and conversely.

To maintain the structural form of the equations of motions means to maintain the time-laws of build-up of the gyroscope motion as well. In other words, this law remains exponential as before, with the previous value of the time constant

$$\tau = \frac{1}{\epsilon} \quad \text{at} \quad \epsilon_1 = \epsilon_2 = \epsilon.$$

STAT

$$\tau = \frac{1}{\epsilon_1} \quad \text{at} \quad \epsilon_1 < \epsilon_2 \quad \text{and} \quad \tau = \frac{1}{\epsilon_2} \quad \text{at} \quad \epsilon_2 < \epsilon_1.$$

or in other words, during the setting period, the friction in the gimbals has no effect in the case here under consideration.

In Fig. 7.4 we show a geometrical method of constructing the paths coinciding with the vector of the resultant moment ϵ , acting on the gyroscope. The vector of the resultant moment equals the sum of the vector of the correction moment \bar{L}_K and the vector of the total moment of friction \bar{L}_ρ . The magnitude of L_K is proportional to the modulus of the radius-vector of the vertex of the gyroscope (cf. Section 7.3, Paragraph (b)) with the same efficiency for the correction of both turns.

The magnitude of \bar{L}_ρ is proportional to the modulus to the radius vector of the vertex of the quadrangle of repose, since the magnitude of the angle of repose is determined by the moment of friction. The vector \bar{L}_C is directed toward the origin of coordinates, the vector \bar{L}_ρ toward one of the vertices of the quadrangle of repose, depending on the direction of motion of the gyroscope vertex. The total vector \bar{L}_Z in this case is directed toward the same vertex of the quadrangle of repose.

Effect of Hysteresis on the Build-up State

We shall not at first consider the influence of friction in the gimbals.

Accordingly, putting in eq. (7.8):

$$\rho_1 = \rho_2 = 0.$$

we rewrite them in the following form:

$$\left. \begin{aligned} \dot{\alpha} &= -\epsilon_2 (\alpha - \theta_{A2} \text{sign } \dot{\alpha}). \\ \dot{\beta} &= -\epsilon_1 (\beta - \theta_{A1} \text{sign } \dot{\beta}). \end{aligned} \right\} \quad (7.33)$$

We now introduce the notation:

$$\left. \begin{aligned} \tilde{\alpha}_{1,2} &= \alpha - \theta_{A1} \text{sign } \dot{\alpha}. \\ \tilde{\beta}_{1,2} &= \beta - \theta_{A2} \text{sign } \dot{\beta}. \end{aligned} \right\} \quad (7.34)$$

STAT

where, as in the preceding case, the first subscripts correspond to the case when $\dot{\alpha} > 0$, $\dot{\beta} > 0$; the second subscripts to the case when $\dot{\alpha} < 0$; $\dot{\beta} < 0$.

On excluding from the operations, the instants of time at which $\dot{\alpha}$ and $\dot{\beta}$ change their signs, i.e., when sign $\dot{\alpha}$ and sign $\dot{\beta}$ undergo a break in continuity, we get

$$\left. \begin{aligned} d\tilde{\alpha}_{1,2} &= d\alpha, \\ d\tilde{\beta}_{1,2} &= d\beta. \end{aligned} \right\} \quad (7.35)$$

As a result, we get, from the equations of motion, eqs.(7.33), the following equations for determining the paths of the vertex of the gyroscope (for the case $\varepsilon_1 = \varepsilon_2$):

$$\frac{d\tilde{\alpha}_{1,2}}{d\tilde{\beta}_{1,2}} = \frac{\tilde{\alpha}_{1,2}}{\tilde{\beta}_{1,2}}. \quad (7.36)$$

Hence it follows that the paths of the vertex of the gyroscope will be straight lines, connecting the point of the initial position with the origin of the coordinate system $O_i \alpha_{1,2} \beta_{1,2}$, whose displacement from the origin of the coordinate system $O\alpha\beta$ may be determined by eq.(7.34).

Let us now take the system of coordinates $O\alpha\beta$, on which we shall plot the locus of points at which $\dot{\alpha}$ and $\dot{\beta}$ can change signs. These loci will be, on the basis of eq.(7.33), the following straight lines respectively:

$$\left. \begin{aligned} \alpha &= \mp \theta_{21}, \\ \beta &= \mp \theta_{12}. \end{aligned} \right\} \quad (7.37)$$

These straight lines divide the coordinate plane into nine regions, for which we shall retain the same numbering as in the preceding case.

The intersection of these straight lines will give the point of the possible displacements of the origin of coordinates $O_i \alpha_{1,2} \beta_{1,2}$ with respect to the origin of coordinates $O\alpha\beta$. The choice of one or another of these origins will be determined by the signs of $\dot{\alpha}$ and $\dot{\beta}$. In the regions I, II, III, and IV (Fig.7.6), these signs are completely determined. In the regions 1, 2, 3, and 4, only the signs of

STAT

any one angular velocity will be determined (in 1 and 3, the sign of β , in 2 and 4, the sign of $\dot{\alpha}$), while in the region C, the signs of both angular velocities will be indeterminate.

Let the initial point lie in region I. According to the above, the vertex of the gyroscope will follow the straight line connecting the initial point with the point $(-\theta_{\Delta 2}, -\theta_{\Delta 1})$ marked by the letter O_1 . In this case, the vertex of the gyroscope will move toward the boundary between regions I and (1), since it has a negative angular velocity $\dot{\alpha} < 0$. Consequently, on the boundary, according to the first of eq.

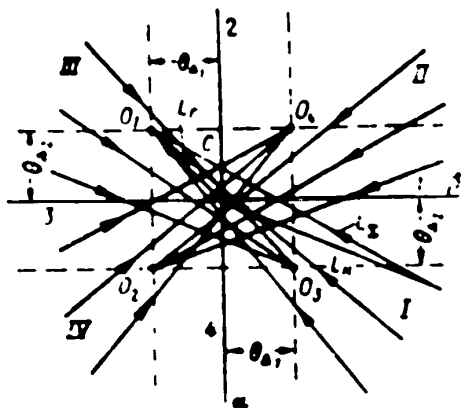


Fig.7.6 - Influence of Hysteresis with Proportional Characteristic of Correction, Allowing for Friction

a - Zone of hysteresis smaller than zone of repose; b - Zone of hysteresis larger than zone of repose

As a result, we get the spectrum of paths according to Fig.7.6. We note the peculiarity of this spectrum that in the regions with indeterminate signs these paths intersect, which means that motion is possible from the paths of this region not to only one position of repose, but to two (for points in the regions with

As a result, we get the spectrum of paths according to Fig.7.6. We note the peculiarity of this spectrum that in the regions with indeterminate signs these paths intersect, which means that motion is possible from the paths of this region not to only one position of repose, but to two (for points in the regions with

Arabic numbering) or even to four such positions, depending on what the preceding motion was.

In the geometrical construction of paths to obtain the resultant vector of the moment acting on the gyroscope, the vector of the moment of hysteresis \bar{L}_r , equal to the radius vector of the vertices of the quadrangle of hysteresis, must be added to the vector of the correction moment \bar{L}_K .

Let us now estimate the influence of friction in the gimbals. Rewrite the equation of motion eq.(7.8) in the following form:

$$\left. \begin{aligned} \dot{\alpha} &= -\varepsilon_2 (\alpha - \rho_2 \text{sign } \dot{\beta} - \theta_{22} \text{sign } \dot{\alpha}), \\ \dot{\beta} &= -\varepsilon_1 (\beta + \rho_1 \text{sign } \dot{\alpha} - \theta_{11} \text{sign } \dot{\beta}). \end{aligned} \right\} \quad (7.38)$$

Let us introduce the notation:

$$\left. \begin{aligned} \bar{\alpha}_i &= \alpha - \theta_{22} \text{sign } \dot{\alpha} - \rho_2 \text{sign } \dot{\beta}, \\ \bar{\beta}_i &= \beta - \theta_{11} \text{sign } \dot{\beta} + \rho_1 \text{sign } \dot{\alpha}. \end{aligned} \right\} \quad (7.39)$$

where $i = 1, 2, 3, 4$ the subscript showing which of the four possible combinations of signs of $\dot{\alpha}$ and $\dot{\beta}$:

$$(\dot{\alpha} > 0, \dot{\beta} > 0; \dot{\alpha} < 0, \dot{\beta} < 0; \dot{\alpha} < 0, \dot{\beta} > 0; \dot{\alpha} > 0, \dot{\beta} < 0)$$

holds in the given case.

Excluding from the operations, as before, the instants of time of change of sign of $\dot{\alpha}$ and $\dot{\beta}$ we have, for $\varepsilon_1 = \varepsilon_2$:

$$\left. \begin{aligned} d\bar{\alpha}_i &= d\alpha, \\ d\bar{\beta}_i &= d\beta. \end{aligned} \right\} \quad (7.40)$$

and on this basis, eq.(7.38) may be rewritten in the following form:

$$\frac{d\bar{\alpha}_i}{d\bar{\beta}_i} = \frac{\dot{\alpha}_i}{\dot{\beta}_i}. \quad (7.41)$$

Thus the form of the paths remains unchanged, while only the displacement of the origin of coordinates $\bar{\alpha}_i, \bar{\beta}_i$ with respect to the origin of coordinates α and β

STAT

is modified.

Let us take the system of coordinates $O\alpha\beta$, on which we shall plot the locus of points at which $\dot{\alpha}$ and $\dot{\beta}$ can change their signs. These loci of points will be the straight lines:

$$\begin{aligned} \alpha &= \cdot (\theta_{21} + \rho_2) \cdot | \\ \beta &= \cdot (\theta_{21} + \rho_1) \cdot | \end{aligned} \quad (7.42)$$

These straight lines, as in the preceding case, divide the coordinate plane $O\alpha\beta$ into regions with Roman numbering, in which the signs of the angular velocities of $\dot{\alpha}$ and $\dot{\beta}$ will be determinate, regions of Arabic numbering, in which only the sign of some one angular velocity will be determinate, and region C, in which the signs of both angular velocities will be indeterminate. As in the preceding case, this indeterminacy will be revealed by what the motion of the gyroscope was before the transition to these regions.

As a result, we obtain a spectrum of paths according to Fig. 7.7, a, for which the condition

$$\begin{aligned} \theta_{21} &< \rho_1 \cdot | \\ \theta_{22} &< \rho_2 \cdot | \end{aligned} \quad (7.43)$$

is satisfied, or, according to Fig. 7.6, b, for which the following condition is satisfied

$$\begin{aligned} \theta_{21} &> \rho_1 \cdot | \\ \theta_{22} &> \rho_2 \cdot | \end{aligned} \quad (7.44)$$

We remark that in the former case there exists, in region C, a region D, where the conditions of motion are not satisfied, but, in the latter case, this region disappears. In the geometrical construction the composition of the vectors of the correction moment \bar{L}_K , hysteresis moment \bar{L}_H , and moment of friction L_ρ must be accomplished.

Thus the effect of hysteresis, with proportional characteristics, reduces down

STAT

a) the maximum displacements of the equilibrium positions from the origin of coordinates $O\alpha\beta$ is determined by the sum of the angle of repose, due to friction in the gimbal ρ , and the angle of hysteresis of the characteristic θ_{Δ} ;

b) the paths of motion toward the equilibrium positions in certain areas of the coordinate plane $O\alpha\beta$ intersect, which indicates the possibility of motion from the points in these regions, not in only a single direction, but in several directions, and, in particular, indicates the possibility of the gyro moving from one equilibrium position to another, which, however, need not necessarily be the case;

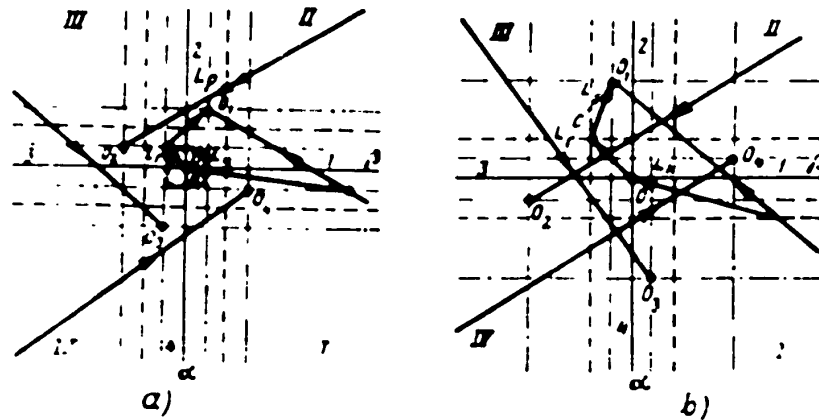


Fig.7.7 - Paths of Vertex of Gyroscope with Proportional Hysteresis-Free Characteristics of Different Efficiency, Allowing for Friction in the Gimbals

c) the region of repose, due to the presence of friction in the suspension, owing to hysteresis, is now evened out, while if the conditions of eq.(7.44) are satisfied, it disappears entirely. In other words, in this case, to which proceeds the setting of the gyroscope vertex (within the limits of the region defined by the total value of the corresponding angles, ρ and θ_{Δ}), this vertex may pass through any point in the coordinates of the plane $O\alpha\beta$.

It is easy to see that all the circumstances we have mentioned somewhat modify the picture of the behavior of the gyroscope close to the equilibrium position, and also modify this position itself. But the basic picture of the gyroscope motions

STAT

remains practically the same as when the hysteresis is not taken into account. Accordingly, the basic propositions with respect to the build-up time are also maintained.

Section 7.4. Build-up State for Constant Characteristics of
Correction Equations of Motion

On substituting $f(\alpha)$ and $f(\beta)$ in eq.(7.6), according to the expression for the constant characteristics eq.(6.2), with the same substitution of 0 in it, and with the same use of the subscripts 1, 2 as in the initial case, we get

$$\begin{aligned} //2 & \quad | \quad L_2 \text{ sign } \dot{\beta} + K_{22} \text{ sign } \dot{\alpha} \quad \text{for } \alpha = \theta_{21}, \\ & \quad | \quad K_{21} \text{ sign } \alpha + L_2 \text{ sign } \dot{\beta} \quad \text{for } \alpha = -\theta_{21}, \\ //3 & \quad | \quad L_1 \text{ sign } \alpha + K_{11} \text{ sign } \dot{\beta} \quad \text{for } \beta = \theta_{11}, \\ & \quad | \quad K_{12} \text{ sign } \beta + L_1 \text{ sign } \alpha \quad \text{for } \beta = -\theta_{11}. \end{aligned}$$

or, dividing the right and left sides by H, we get

$$\begin{aligned} \alpha & \quad \left| \begin{array}{ll} \omega_{k2} \text{ sign } \dot{\beta} + \omega_{k1} \text{ sign } \dot{\alpha} & \text{for } \alpha = \theta_{21}, \\ -\omega_{k2} \text{ sign } \alpha + \omega_{k1} \text{ sign } \dot{\beta} & \text{for } \alpha = -\theta_{21}, \end{array} \right. \\ \beta & \quad \left| \begin{array}{ll} \omega_{p1} \text{ sign } \alpha + \omega_{p2} \text{ sign } \dot{\beta} & \text{for } \beta = \theta_{11}, \\ -\omega_{p1} \text{ sign } \beta + \omega_{p2} \text{ sign } \alpha & \text{for } \beta = -\theta_{11}. \end{array} \right. \end{aligned} \quad (7.45)$$

where $\omega_{k2} = \frac{k_2}{H}$ - rate of correction about axis of outer frame of gyro;

$\omega_{k1} = \frac{K_1}{H}$ - rate of correction about axis of inner frame;

$\omega_{p2} = \frac{L_{p1}}{H}$ - rate of precession about axis of outer frame due to friction about axis of inner frame;

$\omega_{p1} = \frac{L_{p2}}{H}$ - rate of precession about axis of inner frame, due to friction about axis of outer frame.

ω_{k1}^{Δ} and ω_{k2}^{Δ} = rates of precession about the axes of the inner and outer frames

the zone of hysteresis of the characteristics, and are STAT

numerically equal, where such a zone exists, to ω_{K1} , ω_{K2} while, in the absence of a zone of hysteresis, they are equal to zero.

The physical meaning of all these quantities is obvious from their definition.

Build-up State in the Case of Hysteresis-Free Characteristics
without Allowing for Friction in the Gimbals

Putting in eq.(7.45)

$$\omega_1 = \omega_2 = \omega_{K1} = \omega_{K2} = 0,$$

we get:

$$\left. \begin{aligned} \frac{d\alpha}{dt} &= 0 & \text{for } \alpha & \in \theta_{\alpha 1} \\ &= -\omega_{K1} \text{ sign } \alpha & \text{for } \alpha & \in \theta_{\alpha 2} \\ \frac{d\beta}{dt} &= 0 & \text{for } \beta & \in \theta_{\beta 1} \\ &= \omega_{K1} \text{ sign } \beta & \text{for } \beta & \in \theta_{\beta 2} \end{aligned} \right\} \quad (7.46)$$

Let us produce in the coordinate plane $O \alpha\beta$, the straight lines

$$\alpha = \theta_{\alpha 1}$$

$$\beta = \theta_{\beta 1}$$

These straight lines will divide the coordinate plane into regions A, B and C (Fig.7.8), of which, in the regions of A, the lower expressions of the right sides of eq.(7.46) will be real, in the upper, in the region C, the upper, in the region B, in one equation the lower, and in the other the upper (in the regions B_1 and B_3 in the first equation, the upper in the second, the lower; in the regions B_2 and B_4 , conversely).

Bearing this in mind, and dividing one of eqs.(7.46) by the other, we get the following equation for determining the path in this case

$$\left. \begin{aligned} \frac{d\beta}{d\alpha} &= \frac{\text{sign } \alpha}{\text{sign } \beta} & - & \text{Region A,} \\ &= 0 & - & \text{regions } B_1 \text{ and } B_3 \end{aligned} \right\} \quad (7.47) \text{ STAT}$$

$$\left. \begin{matrix} d_1 \\ d_2 \end{matrix} \right\} \sim \begin{matrix} - & \text{regions } B_2 \text{ and } B_4, \\ 0 & - \text{region } C, \\ 0 & \end{matrix}$$

where

$$\beta = \frac{u_{22}}{u_{11}} = \frac{K_2}{K_1} \quad (7.48)$$

It follows from this equation that motion is possible in these regions, except for the region C, which is understandable enough, since this region is the zone of insensitivity of the correction system.

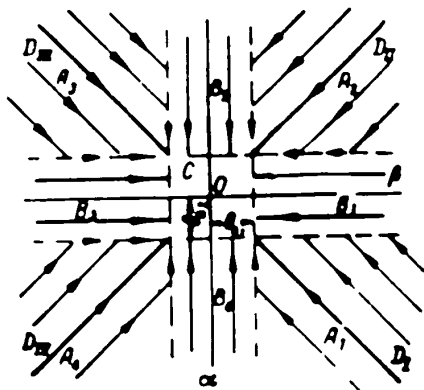


Fig. 7.4 - Paths of the Vertex of the Gyrocompass with Constant Hysteresis-Free Characteristics of Correction of the Same Efficiency. The Friction in the Gyrocompass is not Taken into Account.

$D_I, D_{II}, D_{III}, D_{IV}$ = Diagonal Paths

If the characteristics of the correction of both frames have a zero zone of insensitivity, then the region C contracts to the point O, and the regions B are narrowed to the corresponding coordinate axes.

For simplicity, let us integrate eq.(7.47), at first with respect to the conditions of the first quadrant, for which

$$\begin{matrix} \text{sign } \beta = 1 \\ \text{sign } \alpha = 1 \end{matrix}$$

and consequently,

$$\begin{matrix} \beta = \beta + D_1 & \text{region } A_1, \\ \beta = D_2 & \text{region } B_1, \\ \beta = -D_3 & \text{region } B_4, \end{matrix}$$

where $D_1, D_2,$ and D_3 are constants of integration.

On determining these constants under the initial conditions for $t = 0; \alpha = \alpha_0;$

$\beta = \beta_0,$ we get

STAT

$$\left. \begin{aligned} \dot{\alpha} - v_2 \alpha &= v_1 & \text{region } A_1, \\ \dot{\beta} &= v_2 & \text{region } B_1, \\ \dot{\beta} &= v_2 & \text{region } B_4, \end{aligned} \right\} \quad (7.49)$$

Thus all the paths will be straight lines: in the region A_1 , they will be inclined to the axis $O\alpha$, in the regions B_4 and B_1 , they will be respectively parallel to the axes $O\alpha$ and $O\beta$.

The motion along these paths is directed in the sense of reducing the current values of α and β , i.e., toward the boundaries of region C , as results directly from eq.(7.46). In this case it may terminate, depending on the initial conditions, at any point on these boundaries.

It is easy to see that for the third quadrant, the equations of the paths will be completely identical with those for the first quadrant, while for the second and fourth quadrants, the sign of v_2 is reversed.

In other words, the first of eq.(7.49) will relate to the region A_3 with no modification whatever, to the regions A_2 and A_4 with a reversed sign before v_2 ; the second of eq.(7.49) will also relate to the region B_3 , the third of eq.(7.49) will also relate to the region B_2 .

As a result we get the field of paths shown in Fig.7.8, where a special value equal to unity has been taken for v_2 .

From a comparison of this field of paths with the field of paths according to Fig.7.4, it will be seen that from the point of view of the end result, the zone of insensitivity of the correction system with constant characteristics of that system without the participation of the friction in the gimbals leads to about the same results as the friction in the gimbals with proportional characteristics: namely to the formation of a region in a neighborhood of the origin of coordinates to which the vertex of the gyroscope does not pass. The difference is only that with constant characteristics the motion may terminate at any point on the boundaries of

STAT

this region, while with proportional characteristics it can terminate only at the vertices of the quadrangle of repose.

Let us now dwell on questions of the determination of the setting time.

As will be easy to understand, the motion of the vertex of the gyroscope of the regions B is the result of the rotation of the gyro about the axis of only one of the frames: in the regions B_1 and B_3 , about the axis of the inner frame, in the regions B_2 and B_4 , about the axis of the outer frame.

It follows from this that on motion of the gyroscope vertex in these regions, the setting time T_y is determined by the following expressions

$$T_{yB} = \begin{cases} \int_0^{d_2} \frac{1}{\omega_{y2}} dt & \text{- on motion in the regions } B_2 \text{ and } B_4 \\ \int_0^{d_3} \frac{1}{\omega_{y1}} dt & \text{- on motion in the regions } B_1 \text{ and } B_3 \end{cases}$$

or

$$T_{yB} = \begin{cases} \frac{d_2}{\omega_{y2}} & \text{- on motion in the regions } B_2 \text{ and } B_4, \\ \frac{d_3}{\omega_{y1}} & \text{- on motion in the regions } B_1 \text{ and } B_3 \end{cases} \quad (7.50)$$

We note further that in each of the quadrants among the paths of the region A, one terminates at the corresponding vertex of the region C. We shall term these paths diagonal. They involve the peculiarity that the motion of the vertex of the gyroscope along them from beginning to end is the result of the simultaneous rotation of the gyroscope about the axes of both frames. In other words, on motion of the gyro vertex along these paths, the damping of both frames takes place simultaneously.

All the remaining paths of the regions A, however, are at first the result of the very same simultaneous rotation of the gyro about both frames, until the bounding region of B is reached; after this has taken place, $\bar{S}\bar{T}\bar{A}\bar{T}$

motion will be in accordance with the law for the region B that has been reached. In other words, on the motion of the gyroscope vertex along all nondiagonal paths of the region A, the damping of both frames is not simultaneous: on motion along paths resting on the boundaries of the region B_1 and B_3 , the inner frame is damped by it; on motion along paths resting on the boundaries of the regions B_2 and B_4 , the outer frame is damped by it.

Consequently, on motion of the gyro vertex in regions bounded by diagonal paths and adjoining the axis $O\beta$, the total setting time is determined by the setting time of the inner frame, that is, it is determined according to the lower expression of the right side of eq.(7.50); on motion of the gyroscope vertex in the regions adjoining the axis $O\alpha$, the total setting time is determined by the setting time of the outer frame, i.e., according to the upper expression of the right side of eq.(7.50).

On the basis of the above, eq.(7.50) may now be rewritten in the following form (the subscripts α and β indicate whether the formula relates to a region bounded by diagonal paths and the axis $O\beta$, or to a region bounded by diagonal paths and the axis $O\alpha$):

$$\left. \begin{aligned} T_{\alpha} &= \begin{cases} \omega_{\alpha} \theta_{\alpha 2} \\ \omega_{\alpha 2} \end{cases} \\ T_{\beta} &= \begin{cases} \omega_{\beta} \theta_{\beta 1} \\ \omega_{\beta 1} \end{cases} \end{aligned} \right\} \quad (7.51)$$

Influence of Friction in the Gimbals on the Setting State
with Hysteresis-Free Characteristics

Let us rewrite eq.(7.45) in the following form:

$$\left. \begin{aligned} \dot{\alpha} &= \begin{cases} \omega_{\alpha} \text{sign } \beta & \text{for } \alpha \leq \theta_{\alpha 2} \\ \omega_{\alpha 2} \text{sign } \alpha + \omega_{\beta} \text{sign } \beta & \text{for } \alpha > \theta_{\alpha 2} \end{cases} \\ \dot{\beta} &= \begin{cases} \omega \text{sign } \alpha & \text{for } \beta \leq \theta_{\beta 1} \\ \omega_{\beta 1} \text{sign } \beta + \omega_{\alpha} \text{sign } \alpha & \text{for } \beta > \theta_{\beta 1} \end{cases} \end{aligned} \right\} \quad (7.52)$$

STAT

Let us retain the former division of the coordinate plane into the regions A, B, and C. It will be clear from eq.(7.52) that in the regions A, the presence of friction in the axis of the suspension will increase the rate of motion of the gyroscope vertex toward that coordinate axis which is located to the right of the direction of motion of the gyroscope vertex, since the correcting moment responsible for this motion is compounded with the moment of friction (Fig.7.9). The rate of motion of the gyroscope vertex toward the coordinate axis located left of the direction of motion of the gyroscope vertex decreases on account of friction, since the moment of friction is directed opposite to the correcting moment. It follows from this that the motion of the gyroscope vertex in the regions A will take place along a straight line inclined to the coordinate axis lying right of the direction of motion of the gyroscope axis at the angle φ determined by the equation

$$\tan \varphi = \frac{\omega_{K1} + \omega_{\rho 1}}{\omega_{\rho 2}} \quad \text{for the regions } A_1 \text{ and } A_2. \quad (7.53)$$

or

$$\tan \varphi = \frac{\omega_{K1} + \omega_{\rho 1}}{\omega_{\rho 2}} \quad \text{for the regions } A_3 \text{ and } A_4. \quad (7.54)$$

In the regions B_1 and B_3 , the rate of motion of the gyroscope vertex along the axis of α , which is due only to the moment of friction, is equal to $\omega_{\rho 2}$. The rate of motion along the axis β , which is due to the difference between the moments of correction and the moment of friction is determined by the difference $\omega_{K1} - \omega_{\rho 1}$.

In the regions B_2 and B_4 , the rate of motion along the axis β due to the moment of friction, equals $\omega_{\rho 1}$, while the motion along the axis α is on account of the difference between the moments of correction and friction. Accordingly the motion of the gyro vertex in the regions of B will take place along a straight line making the angle φ with the coordinate axis passing through the center of the region, that angle φ being determined by the equation

STAT

$$\left. \begin{aligned} \operatorname{tg} \bar{\gamma} &= \frac{\omega_{p1}}{\omega_{k1} - \omega_{p1}} && \text{for the regions } B_1 \text{ and } B_3 \\ \operatorname{tg} \bar{\gamma} &= \frac{\omega_{p2}}{\omega_{k2} - \omega_{p2}} && \text{for the regions } B_2 \text{ and } B_4 \end{aligned} \right\} (7.55)$$

The motion of the gyroscope vertex will continue until it reaches the boundary of the region C.

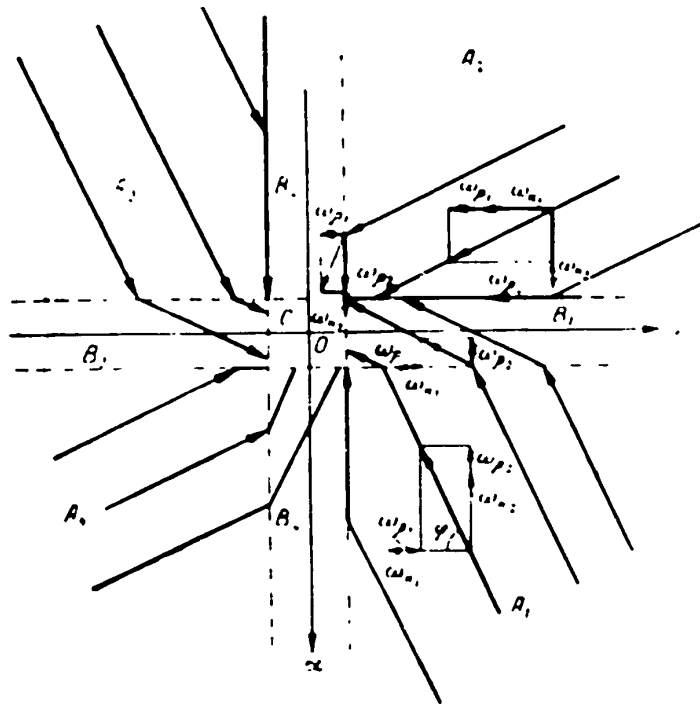


Fig.7.9 - Paths of Vertex of Gyroscope under Constant Hysteresis-Free Characteristics of Correction Allowing for the Friction in the Gimbals

$D_{Ip}, D_{IIp}, D_{IIIp}, D_{IVp}$ = diagonal paths; $D_{IO}, D_{IIO}, D_{III O}, D_{IVO}$ - diagonal paths corresponding to failure to take account of friction

The field of paths according to the equations so obtained will take the form indicated in Fig.7.9, for the same special case $\omega_{k1} = \omega_{k2}$ for $\omega_{p1} = \omega_{p2} = 0.3$, that is, under the condition that the moments of correction shall be 3.3 times as great

STAT

as the corresponding moments of friction in the gimbals.

Thus the role of friction in the suspension is manifested in the variation of the inclination of the paths. The zone of repose of the gyroscope, however, remains as before, determined by the zones of insensitivity of the correction signal transmitters. This is natural enough: as soon as the corresponding zone of insensitivity has been passed, the full moment of correction enters into action at once, and this correction in any case exceeds the moment of friction in the suspension and is therefore able to affect the motion of the gyroscope, from the very beginning. But nevertheless the moment of friction in the gimbals also exerts its influence in some cases as a moment of opposite direction to the moments of correction applied to the given frame, and in other cases as a moment coinciding with it in direction, thus explaining the different variation of the slope of the paths in different quadrants.

We shall define the setting time of the vertex of the gyroscope by the setting time of this frame, disturbances of which, if they exceed the zone of insensitivity of the respective corrector signal transmitter, will be liquidated by the corrector.

To determine the setting time of the gyroscope vertex, let us divide the entire coordinate plane into the regions C and D_1' , D_1'' , D_1''' ; D_2' and so on, as indicated in Fig.7.10. In the regions D_1' , D_1'' , this will eliminate the deviation along the axis α , while the motion along the segment A_1B_1 takes place during the course of the time

$$\Delta t_1 = \frac{\theta_0 - \theta_{\alpha 1}}{\omega_{\alpha 1} - \omega_{\beta 1}} \quad (7.56)$$

since the rate of correction along the axis of β is, by eq.(7.52), equal to $(\omega_{K1} - \omega_{\rho 1})$. The motion along the segment B_1C_1 requires the time

$$\Delta t_2 = \frac{B_1C_1}{\omega_{\beta 1}} \quad (7.57)$$

STAT

since the motion along B_1C_1 takes place only under the action of a correction moment with the velocity ω_{K2} .

Bearing in mind that $D_1C_1 = \alpha_0 - \alpha_0$, while $B_1D_1 = \Delta t_1 (\omega_{K2} + \omega_{\rho 2})$, since their motion toward the β axis along the segment A_1B_1 proceeds under the action of the sum of the moments of correction and friction with velocity $(\omega_{K2} + \omega_{\rho 2})$, we get

$$\Delta t_2 = \frac{\alpha_0 - \theta_{A2} - (\theta_0 - \theta_{A1}) \frac{\omega_{K2} + \omega_{\rho 2}}{\omega_{K1} - \omega_{\rho 1}}}{\omega_{K2}} \quad (7.58)$$

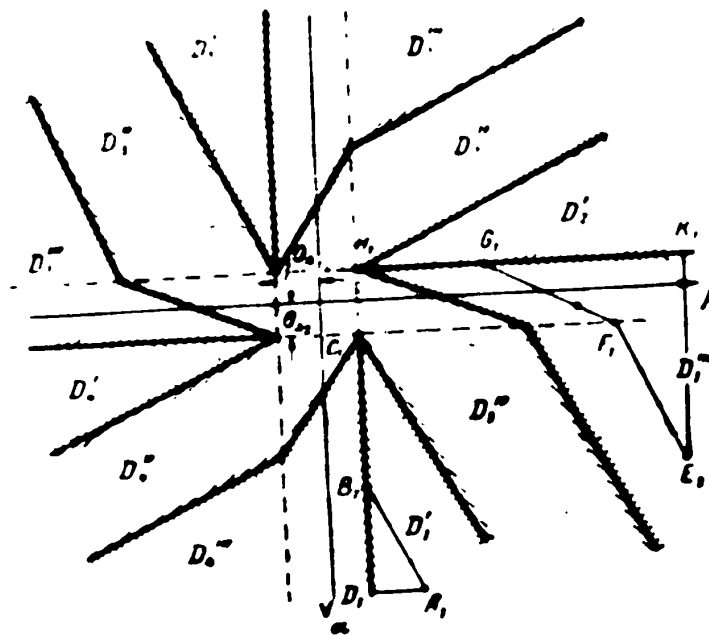


Fig.7.10 - Division of the Plane $O\alpha\beta$ into Regions for Determining the Setting Time of the Gyroscope Vertex

The total time of motion of the gyroscope vertex from the point $A(\alpha_0, \beta_0)$ of the region D_1' and D_3' is determined:

STAT

$$t_{11} = \Delta t_1 + \Delta t_2 = \frac{\omega_0 - \omega_{\beta 1}}{\omega_{\alpha 1} - \omega_{\beta 1}} + \frac{\omega_0 - \omega_{\beta 2} - (\omega_0 - \omega_{\beta 1})}{\omega_{\alpha 1} - \omega_{\beta 1}} \quad (7.59)$$

In the regions D_2' and D_4' , the latter eliminates the deviation along the β -axis. Similarly, for the regions D_2'' and D_4'' , the setting time of the gyro vertex is determined by the following formula:

$$t_{11} = \frac{\omega_0 - \omega_{\beta 1}}{\omega_{\alpha 1} - \omega_{\beta 1}} + \frac{\omega_0 - \omega_{\beta 2} - (\omega_0 - \omega_{\beta 1})}{\omega_{\alpha 1} - \omega_{\beta 1}} \quad (7.60)$$

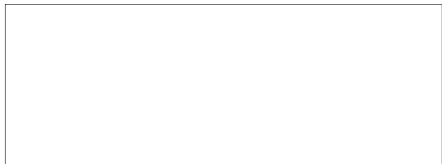
In the regions D''_1 , D''_2 , D''_3 and D''_4 , the motions along both the α axis and along the β axis are simultaneously interrupted. For the regions D''_1 and D''_3 , the setting time of the gyro vertex can be more advantageously determined from its motion toward the α axis; since the velocity of motion of the gyro vertex toward the α axis is maintained unchanged and equal, according to eq.(7.52), to $(\omega_{K1} - \omega_{\rho 1})$. Accordingly, the gyroscope setting time in the regions D''_1 and D''_3 is determined by the formula

$$t_{11} = \frac{\omega_0 - \omega_{\beta 1}}{\omega_{\alpha 1} - \omega_{\beta 1}} \quad (7.61)$$

For the regions D''_2 and D''_4 , the setting time of the gyroscope vertex can be more advantageously determined from its motion towards the β axis, since the velocity of this motion is maintained unchanged and equal to $(\omega_{K2} - \omega_{\rho 2})$. Accordingly the setting time of the gyroscope in the regions D''_2 and D''_4 is determined by the formula

$$t_{11} = \frac{\omega_0 - \omega_{\beta 2}}{\omega_{\alpha 1} - \omega_{\beta 1}} \quad (7.61')$$

In the regions D'''_1 and D'''_3 , the deviation of the gyroscope along the β -axis



is eliminated by this. The motion of the gyroscope vertex along the segment E_1F_1 will require the time

$$\Delta t_1 = \frac{\alpha_0 - \theta_{\Delta 1}}{\omega_{\alpha 1} + \omega_{\rho 1}} \quad (7.62)$$

since the rate of correction along the α axis is equal to $(\omega_{K2} + \omega_{\rho 2})$. Motion along the segment F_1G_1 will require the time

$$\Delta t_2 = \frac{2\theta_{\Delta 2}}{\omega_{\alpha 2}} \quad (7.63)$$

since in this case, the motion along the α axis takes place only under the action of the moment of friction, at velocity $\omega_{\rho 2}$.

Motion along the segment G_1H_1 takes place only under the action of the correction moment ω_{K1} .

Bearing in mind that

$$\begin{aligned} K_1 H_1 &= \beta_0 - \theta_{\Delta 1}, \\ K_1 G_1 &= (\omega_{\alpha 1} - \omega_{\rho 1})(\Delta t_1 + \Delta t_2), \\ G_1 H_1 &= K_1 H_1 - K_1 G_1, \end{aligned}$$

we obtain the following expression for the time of motion of the gyroscope along the segment G_1H_1 :

$$\Delta t_3 = \frac{\beta_0 - \theta_{\Delta 1} - (\omega_{\alpha 1} - \omega_{\rho 1})(\Delta t_1 + \Delta t_2)}{\omega_{K1}} \quad (7.64)$$

On the basis of what has been set forth above, we obtain the following expression for the setting time of the gyroscope vertex in the regions D''''_1 and D''''_3 :

$$t_{1,3} = \frac{\alpha_0 - \theta_{\Delta 1}}{\omega_{\alpha 1} + \omega_{\rho 1}} + \frac{2\theta_{\Delta 2}}{\omega_{\alpha 2}} + \frac{\beta_0 - \theta_{\Delta 1} - (\omega_{\alpha 1} - \omega_{\rho 1}) \left(\frac{\alpha_0 - \theta_{\Delta 1}}{\omega_{\alpha 1} + \omega_{\rho 1}} + \frac{2\theta_{\Delta 2}}{\omega_{\alpha 2}} \right)}{\omega_{K1}} \quad (7.65)$$

The following expression may be obtained, in an analogous way, for the setting time of the gyroscope vertex in the regions D''''_2 and D''''_4 : STAT

$$\dot{\alpha}_1 = \frac{M_{c1}}{J_{c1}} + \frac{M_{f1}}{J_{c1}} + \frac{M_{c2}}{J_{c2}} + \frac{M_{f2}}{J_{c2}} + \frac{M_{c3}}{J_{c3}} + \frac{M_{f3}}{J_{c3}} + \frac{M_{c4}}{J_{c4}} + \frac{M_{f4}}{J_{c4}} \quad (7.66)$$

We note that the formulas so derived are valid for the initial position of the vertex of the gyroscope in the regions of A (Fig.7.9), and that in these formulas the absolute values of the initial coordinates of the point α_0, β_0 must be taken. For its initial position in the regions of B, we must use formulas that can be derived by an analogous procedure.

Let us now compare the setting time of the gyroscope in the presence and absence of friction in the axes of the gimbals. In the regions $D'_{1,2,3}$ and $D'_{4,}$ the setting time is shorter in the presence of friction than in its absence. This is explained by the fact that the motion of one of the frames, determining the setting time, is accomplished, in the presence of friction, in these regions, on parts of the path, under the action of the sum of the moments of correction and friction, while in the absence of friction it is accomplished over the entire path under the action of the correction moment alone.

In the remaining regions, friction increases the setting time, since in the presence of friction the motion of the frame that determines the setting time is accomplished under the action of the difference between the moment of correction and the moment of friction; either on the entire path (for the regions $D''_{1,2,3,}$ and $D''_{4,}$), or on part of that path (for the regions $D'''_{1,2,3}$ and $D'''_{4,}$). In the absence of friction, however, this motion is accomplished under the action of the moment of correction alone.

The Role of the Hysteresis of the Correction Characteristics

It follows from a comparison of eq.(7.45) with eq.(7.52) that, when we allow for hysteresis, the motion of the gyroscope up to the boundaries of the zone of hysteresis will obey the same laws as the motion of the gyroscope with a STAT

hysteresis-free characteristic, up to the boundaries of the neutral zone.

The difference arises only with respect to the motions in the zones of hysteresis, that is, in the neighborhood of the axes $O\alpha$ and $O\beta$, as well as in the neighborhood of the origin of the coordinate system O .

In other words, when the former principle of dividing the coordinate plane into regions is retained, we find that the hysteresis of a constant correction characteristic changes the character of the motions of the gyro vertex only in the regions of B and C.

In the regions of A, the spectrum of the paths will be exactly the same as in the regions of the same designation with a hysteresis-free characteristic.

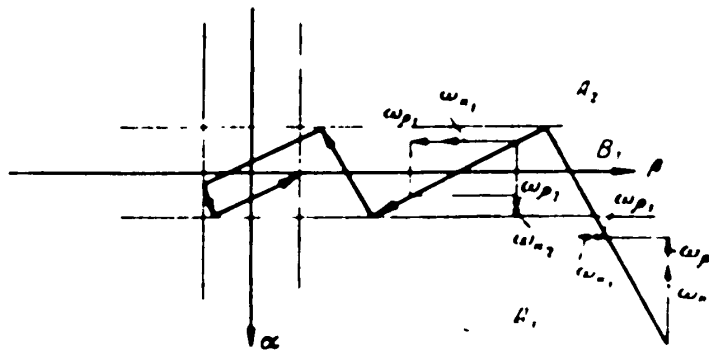


Fig.7.11 - Influence of Hysteresis with Constant Correction Characteristics, Allowing for Friction in the Axes of the Gimbals

Let us assume that as a result of motion along these paths, the gyro vertex has reached the boundary between regions A_1 and B_1 . It had the velocity $\dot{\alpha} < 0$. Consequently, according to the first of eq.(7.45), and according to the conditions of hysteresis, this velocity is maintained up to the boundary between the region B_1 and the region A_2 . At this boundary the direction of the correcting moment, as well as the magnitude and sign of the velocity $\dot{\alpha}$, all change.

The change of sign of the velocity $\dot{\alpha}$ causes, in turn, a change in the sign of the moment of friction about the β -axis, which leads to a jump-like increase in the ^{STAT}

velocity β . As a result, the angle of the path varies. With a new reading on the boundary of the regions, there is a new jump-like variation in $\dot{\alpha}$, etc. As a result, the motion in the region B_1 will be of oscillatory character, during which the gyro vertex will approach the boundary of region C. This latter consequence results from the fact that $\dot{\beta}$ maintains its negative sign during the entire course of this process.

For the region B_3 , the reasoning remains the same, but in connection with the change of sign of β , the angles of the paths vary in such a way that motion will be accomplished as before toward the region C. The motion of the gyro vertex in the regions B_4 and B_2 will be of similar nature. The only difference will be that the change of sign on the boundaries of these regions will be accomplished with respect to the angular velocity $\dot{\beta}$, while the angular velocity $\dot{\alpha}$ will maintain its sign without change, varying only its modulus.

In the region C, the signs of both angular velocities will already vary jump-wise: the signs of $\dot{\alpha}$ on those boundaries of this region, that are continuations of the boundaries of the region $B_1(B_3)$, and the signs of $\dot{\beta}$ on the boundaries which constitute a continuation of the boundaries of the region $B_2(B_4)$.

The oscillations will have the form indicated in Fig.7.11. The magnitude of the gyroscope velocity will oscillate within the region C. If this region is sufficiently limited, that is, with a sufficient limitation of the zones of hysteresis, and at a sufficiently slow rate of correction, their existence may be completely disregarded.

Section 7.5. The Setting State with Mixed Correction Characteristics

As remarked in Chapter VI, systems of correction with a characteristic of the mixed form shown in Fig.6.3 have enjoyed a relatively wide use. The zone proportionality in them usually does not exceed a quantity of the order of $2-3^\circ$. Let us denote the boundary of this zone for the outer frame by φ_2 , and for the inner frame

STAT

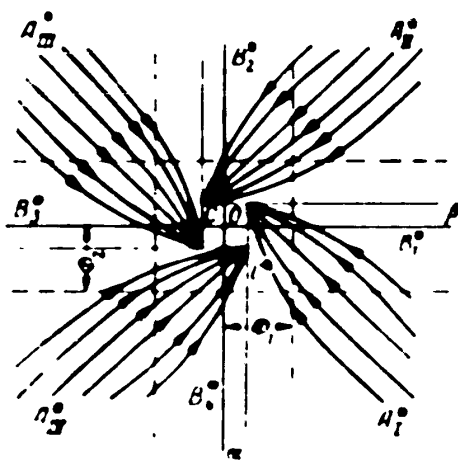
by ϕ_1 . Let us draw, in the plane of coordinates $O\alpha\beta$, the straight lines

$$\alpha = +\phi_1,$$

$$\beta = +\phi_1.$$

These straight lines divide the coordinate plane $O\alpha\beta$ into the regions A^* , B^* , and C^* (Fig.7.12). In the regions of A, the law of the constancy of the correction

characteristic will hold, and, consequently, the spectrum of the paths will be analogous here to the spectrum of the paths in the regions of A (cf. Fig. 7.9).



In the regions of C^* , the law of the proportional characteristic will likewise hold for both variables, and, consequently, the field of the paths will here be analogous to the field of the paths by Fig.7.4. In the regions of B^* , for one of the variables, the law of proportionality will hold, and for the other variable, the law of the constant characteristic.

Fig.7.12 - Paths of Gyro Vertex with Mixed Hysteresis-Free Correction Characteristics, Allowing for Friction in the Gimbals

Let us determine the path for this case with respect, let us say, to the conditions of the region B_1^* .

The equations of motion for this region are written in the following form:

$$\left. \begin{aligned} \dot{\alpha} &= \omega_1 \text{ sign } \alpha \\ \dot{\beta} &= \omega_2 \end{aligned} \right\} \quad (7.67)$$

In the right side of the first eq.(7.67), the variable $\alpha_2 = \alpha - \rho_2$, since, by the second eq.(7.63), the angular velocity $\dot{\alpha} < 0$ for all the region B_1^* . STAT

On dividing the right side by the left side, and bearing in mind that

$$d\alpha_2 = d\beta,$$

we get

$$\frac{d\alpha_2}{\alpha_2} = \frac{d\beta}{\alpha_2 \cdot \text{sign } \alpha_2} \alpha_2,$$

whence, after integration, we get the following equation of paths:

$$\ln \alpha_2 = \frac{\beta}{\alpha_2 \cdot \text{sign } \alpha_2} + D. \quad (7.68)$$

As the initial conditions, let us take as usual, for $t = 0$; $\alpha_2 = \alpha_{20}$, $\beta = \beta_0$. We remark that for α_{20} in this case, the following restriction will exist:

$$\alpha_{20} \cdot \Phi_2 = \beta_0.$$

Using the initial conditions taken, we get the result, after determining the integration constant D :

$$\alpha_2 = \alpha_{20} e^{\frac{\beta - \beta_0}{\alpha_{20} \cdot \text{sign } \alpha_{20}}}. \quad (7.69)$$

It follows from this solution so obtained that α_2 does not change its sign. Consequently, on the basis of the first equation of eq.(7.67), $\dot{\alpha}$ also does not change its sign, and therefore, sign $\dot{\alpha}$ in eq.(7.69) will have a completely determinate value.

Thus the paths sought will be curves of exponential form. The paths are determined by an analogous procedure for the other regions of B^* as well. As a result we get a field of paths in these regions according to Fig.7.11.

The setting time is determined in this case as the sum of the time of motion to the boundary of the C^* region and the time of motion in the C^* region.

The first of these times is determined according to the rules set up for determining the setting time with a constant correction characteristic, while the second of these times will be equal to three or four times the value of $\frac{1}{\varepsilon_1}$ or $\frac{1}{\varepsilon_2}$, according to which of the conditions, is satisfied, respectively: $\varepsilon_1 < \varepsilon_2$ or $\varepsilon_1 > \varepsilon_2$ STAT

CHAPTER VIII

INFLUENCE OF PERIODIC DISTURBANCES OF THE CORRECTION SYSTEM ON THE
SETTING OF THE GYROSCOPESection 8.1. General Remarks

As already mentioned, the basic idea of gyroscope correction is to utilize the selectivity of low-inertia correcting members (such as a pendulum or magnetic needle) to impart this selectivity to a gyro, and to utilize the gyroscopic rigidity to minimize the disturbances of the gyroscope connected with possible disturbances of the correcting members, this latter circumstance, the degree of pliability of the gyroscope, as B.V.Bulgakov expressed it, to the disturbances of the correcting members, being of decisive significance, since such disturbances always take place in aircraft flight.

We shall assume a sinusoidal law for these disturbances, as has been done, in particular, by Ye.B.Levental' (Bibl.10). The following arguments may be adduced in favor of this hypothesis.

On studying the motion of the gyroscope under sinusoidal disturbances, we determine the motion due to one of the components of the real disturbing forces. For linear systems, such as the gyroscope with proportional corrector, the principle of superposition holds. A consideration of the action of the sinusoidal forces will therefore allow us to obtain fairly general results.

It must be said that the frequency spectrum of aircraft acceleration that is of interest to us lies mainly in the frequency range between 0.02 and 3 cps, the slow

STAT

oscillations having the smaller amplitude. As for the frequency of the natural oscillations of the sensitive members of the correction system, it amounts to 1-2 cps for the pendulum usually employed, and to 0.1 - 0.5 cps for liquid magnetic compasses.

It follows from the above that the possible periods of the oscillations of the correcting members must be considered to lie in the range of 0.3 to 50 sec.

Mathematically, the disturbances of the correcting members mean the corresponding disturbances in the equilibrium position of the system, that is, the corresponding displacements of the origin of the $Ox\beta$ coordinates.

These displacements will also mean the corresponding modification in the directions of the path of the gyro vertex, and as a result these paths are subjected to certain deformations. The exact elucidation of these deformations is difficult, but it is also not of any substantial interest to us. It is more important, in the first place, to find what the steady oscillations of the gyroscope will be under the influence of the oscillations of the correcting members, and, in the second place, to elucidate how the oscillations of the correcting members will affect the build-up time of these oscillations of the gyro. But for this purpose it will be sufficient to investigate the motions about the axis of only one of the frames. Let us take the motions about the axis of the outer frame.

On substituting, in the first of eqs.(7.2), L_x , by eq.(7.4), and replacing θ_2 by eq.(6.8) and q by eq.(7.3), we get the equation of these motions in the following form:

$$H\ddot{\alpha} = f(\gamma, \gamma_2) L_{11} \text{ sign } \dot{\alpha}$$

or, expressing γ according to the condition

$$\gamma_2 = \gamma_{20} \sin \omega_2 t$$

and omitting, in what follows, the numerical subscripts of γ_2 , we get

$$H\ddot{\alpha} = f(\gamma, \gamma_{20} \sin \omega_2 t) L_{11} \text{ sign } \dot{\alpha} \quad (8.1)$$

STAT

Section 8.2. Influence of Disturbances of a Correction System with Proportional Characteristic on the Setting of the Gyroscope

Let us confine ourselves to the hysteresis-free form of the proportional characteristic. The equation of motion eq.(8.1) then takes the form:

$$\ddot{\alpha} + \rho_2 \dot{\alpha} + \gamma_m \sin \alpha = \rho_2 \text{sign } \dot{\alpha} \quad (8.2)$$

We shall not at first take into consideration the friction in the gimbals, i.e. we shall put $\rho_2 = 0$.

Then the integral of eq.(8.2) will be written in the following form

$$\dot{\alpha} = A e^{-\gamma_m t} + \alpha_m \sin(\omega t - \delta) \quad (8.3)$$

where A = an arbitrary constant,

$$\alpha_m = \gamma_m \frac{1}{\sqrt{1 - \frac{\gamma_m^2}{\omega^2}}} \quad (8.4)$$

$$\delta = \arctg \frac{\gamma_m}{\omega} \quad (8.5)$$

Let, for $t = 0$, $\alpha = \alpha_0$. Under these initial conditions, the arbitrary constant A is defined by the expression:

$$A = \alpha_0 - \alpha_m \sin \delta$$

Or, bearing in mind eq.(8.4) and eq.(8.5):

$$A = \alpha_0 + \gamma_m \frac{1}{\sqrt{1 - \frac{\gamma_m^2}{\omega^2}}} \quad (8.6)$$

Making use of eq.(8.6), let us rewrite eq.(8.3) in the following form

$$\dot{\alpha} = \alpha_0 e^{-\gamma_m t} + \gamma_m \frac{1}{\sqrt{1 - \frac{\gamma_m^2}{\omega^2}}} e^{-\gamma_m t} - \gamma_m \frac{1}{\sqrt{1 - \frac{\gamma_m^2}{\omega^2}}} \sin(\omega t - \delta) \quad (8.7)$$

The first term in the expression so obtained represents the law of setting in the absence of disturbances of the sensitive member of the corrector (for the case when friction in the gimbals is not taken into account). The second and third

terms characterize the influence of these disturbances. They reduce, as is clear, to the superposition, on the exponent which we shall call the principal exponent, expressing the law of setting in the absence of disturbances, of an additional exponent with the same time constant as the principal one, and, in the second place, that the curve of periodic oscillations shall have the period of oscillation of the sensitive member of the corrector, and an amplitude depending on the amplitude of the oscillations of the sensitive organ of the corrector, and on the ratio between ε and ω .

The time after which both these exponents (the principal and the additional) practically disappear, will be in this case the setting time. It will be exactly the same as the setting time in the absence of oscillations of the correcting members.

Thus the principal result of the oscillations of the correcting member with a proportional characteristic consists in the excitation of undamped oscillations. It follows from eq.(8.4) that if the value of the ε is sufficiently small by comparison with ω , then the amplitude of these oscillations may be likewise made rather small. In other words, the smaller the efficiency of the action of the corrector is taken, the less will be the influence of the disturbances of the sensor of the corrector. Physically this result is entirely natural: the value of $\varepsilon = \frac{k}{H}$, for a given value of k , which may be selected even from the consideration of reducing the angle of repose, will according to eq.(7.11) be the smaller, the greater the value of the kinetic moment characterizing the gyroscopic rigidity. In other words, a low value of ε for a given value of k signifies a high degree of gyroscopic rigidity, which is explained by the small influence, in this case, of the disturbances acting on the gyroscope, in connection with the disturbances of the sensor of the corrector. The possibilities of reducing ε , however, are limited by the requirement that the system of correction shall assure the setting of the gyroscope in the assigned direction under the action of the moments of friction and the imbalance, and also under the ^{STAT}

displacement of the assigned position (for example, due to the earth rotation, to the displacement of the gyroscope base, etc.).

As an illustration, we shall give an example of the calculation of the selection of the value of ε .

Let us assign the value of the recovery time T_y of the order of 100 sec, which is rather acceptable from the technical point of view. Putting $T_y = \frac{4}{\varepsilon}$, we get, starting out from this assignment,

$$\varepsilon = 0.04 \frac{1}{\text{sec.}}$$

Assume that the period of oscillation of the sensitive member of the corrector equals 1 sec.

For these data

$$\frac{\varepsilon}{\omega} \approx 0.64 \cdot 10^{-2}$$

and, consequently, on the basis of eq.(8.4), the amplitude of the undamped oscillations of the gyroscope α_m will amount to less than 1% of the amplitude of the amplitude of the oscillation of the correcting member.

Higher values for the periods of oscillations of the sensing element of the corrector are, generally speaking, more dangerous. Thus, if this period is taken as 30 sec, which corresponds to the order of the periods of the slow vibrations in the longitudinal position of an aircraft, then, with the same values of ε we get

$$\frac{\varepsilon}{\omega} \approx 0.19$$

and in this case α_m will already be a quantity amounting to 19% of γ_m .

But the slow oscillations of an aircraft also mean correspondingly smaller values for the accelerations, and consequently also correspondingly smaller values of the amplitudes of oscillations of the sensitive member of the corrector. It may therefore be expected that the amplitude of the oscillations of the gyro will ultimately remain, even in this case, within acceptable limits. STAT

In estimating the friction in the gimbals, the integral of eq.(8.2) takes the form

$$\alpha = Ae^{-\mu t} + \alpha_m \sin(\omega t - \delta) + \rho_2 \text{sign } \dot{\beta}. \tag{8.8}$$

where A - arbitrary constant;

α_m and δ are quantities to be determined, as when friction in the gimbals is neglected, according to eq.(8.4) and eq.(8.5).

Determining the arbitrary constant from the initial conditions for $t = 0$; $\alpha = \alpha_0$, and substituting it in eq.(8.8), we get

$$\alpha = (\alpha_0 - \rho_2 \text{sign } \dot{\beta}) e^{-\mu t} + \rho_2 \text{sign } \dot{\beta} + \gamma_m \frac{\epsilon}{1 + \frac{\epsilon^2}{\omega^2}} e^{-\mu t} + \gamma_m \frac{\epsilon}{\sqrt{1 + \frac{\epsilon^2}{\omega^2}}} \sin(\omega t - \delta). \tag{8.9}$$

The influence of the disturbances of the correcting member is represented by the last two terms, which is of form identical with the terms representing the in-

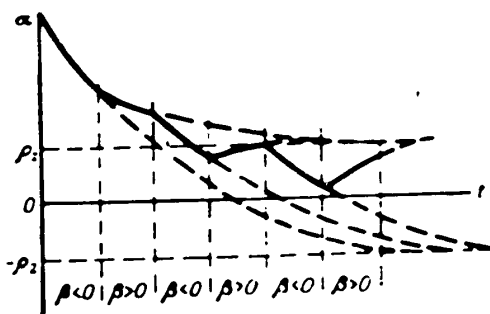


Fig.8.1 - Effect of Friction in Gimbals on the Setting State with Proportional Characteristic of Correction in the Case of Periodic Disturbances in the Correction System

fluence of the disturbances of the correcting member when friction is neglected. In other words, here the only thing that varies is the principal exponent expressing the law of variation of α in the undisturbed state of the correcting members.

The change consists in the variation, under the influence of the friction in the gimbals, of the limit to which the principal exponent approaches; while this limit was formerly the zero-th value of α , it will now

be $\alpha = \pm \rho_2$, while the sign of ρ_2 , upper or lower, will depend on the sign of the STAT

velocity of motion of the gyroscope about the axis of the other frame. That is, this means that if, in particular, this velocity changes its sign during the variation of α , then this limit for the principal exponent of eq.(8.9) will vary accordingly. As a result, the picture of variations of this exponent will take the form indicated in Fig.8.1. It follows from this picture that in the presence of oscillations of the gyro about the axis of the first (inner) frame, the motions of the gyroscope about the axis of the second (outer) frame which are characterized by the principal exponent, will not be damped during the lapse of the setting time, but will take the form of sawtooth oscillations in the limits of the zone of repose.

On these oscillations are also imposed the periodic oscillations characterized by the last term of eq.(8.9). Thus the boundaries of the limiting deviations in the process of total oscillations are determined by the sum of the angles of repose ρ_2 and the amplitude α_m .

All that has been said applies equally to the first (inner) frame, that is, also where in the case of the oscillations of the correcting member, on one hand, and of the oscillations of the gyroscope about the axis of the second frame, on the other, oscillations will occur arising as a result of the imposition of periodic oscillations on the sawtooth oscillations with the extreme deviations limited to the sum of the angle of repose ρ_1 with the amplitude of the periodic oscillations.

But this means that, if the correcting members for both frames oscillate, then these sawtooth oscillations will also occur with respect to the axes of both frames. Consequently, these total oscillations will also occur, in this case, with respect to both axes.

As for the build-up time, i.e., the time after which these oscillations will be established, it will practically not vary by comparison with the build-up time for the undisturbed state of the correction system, that is, with the period of time in which, in the absence of disturbances in the correction system, complete damping of the gyro occurs.

STAT

Section 8.3. Influence of Disturbances in Correction System with Constant Characteristic on the Setting of the Gyroscope

We shall confine ourselves here to the case of the hysteresis-free constant characteristic with zone of insensitivity equal to zero.

The equation of motion of the gyro, eq.(8.1), will be written in this case in the following form:

$$H\ddot{\alpha} = -k_2 \text{sign}(\alpha - \gamma_m \sin \omega t) + L_{p1} \dot{\alpha} \text{sign} \dot{\alpha}.$$

On dividing by it by H and omitting the numerical subscript in $\omega_{K2} = \frac{k_2}{H}$, we get

$$\ddot{\alpha} = -\omega_x \text{sign}(\alpha - \gamma_m \sin \omega t) + \omega_{p2} \dot{\alpha} \text{sign} \dot{\alpha}. \quad (8.10)$$

Let us first elucidate the picture of the phenomena without taking account of friction in the gimbals, that is, we shall consider, in eq.(8.10):

$$\omega_{p2} = 0.$$

Let us consider two cases.

The first case is of slow oscillations of small amplitude for which

$$\gamma_m \ll \omega_x. \quad (8.10a)$$

For the steady state, in which the mean value of the angle α equals zero, the amplitude of oscillation of the gyroscope equals the amplitude of oscillation of the sensitive element γ_m , and the gyroscope exactly repeats the motion of that element. Indeed, introducing the notation $\delta = \alpha - \gamma_m \sin \omega t$, eq.(8.10) may be transformed, for $\omega_{p2} = 0$, to the form:

$$\delta \dot{\delta} = \omega_x \text{sign} \delta = -\gamma_m \omega \cos \omega t. \quad (8.10b)$$

Under the conditions of eq.(8.10a), δ vanishes in the course of time. Indeed, if $\delta > 0$, then, by eqs.(8.10a) and (8.10b), $\dot{\delta} < 0$, and δ decreases to zero. If, however, $\delta < 0$, then according to this same relation $\dot{\delta} > 0$ and δ increases so long as it does not vanish.

Thus in the steady state

$$\delta = 0, \quad \alpha = \gamma_m \sin \omega t.$$

STAT

In this case the gyroscope does not perform its function of "averaging" the readings of the sensitive element; the errors in the direction of the gyro are equal to the errors of the sensitive element. But this is observed only at small amplitudes and small frequencies of oscillation of the sensitive element. Thus, if the angular velocity of the corrector amounts to $3^\circ/\text{min} = 0.05^\circ/\text{sec}$, then the frequency of the disturbances equals 0.02 cps, and then the relation of eq.(8.10a) is satisfied, if

$$\gamma_m \approx \frac{0.05}{2\pi \cdot 0.02} = 0.4 \text{ degree}$$

If the amplitude of the oscillations of the sensitive element is over 0.4° at the same frequency, then the follow-up will be disturbed and the gyroscope will oscillate at an amplitude smaller than the amplitude of the oscillations of the sensitive elements.

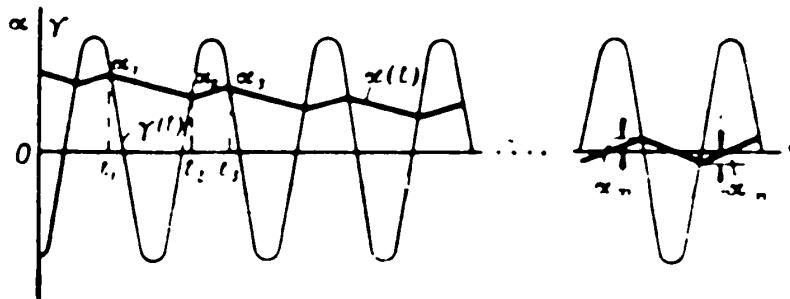


Fig.8.2 - Influence of Periodic Disturbances in the System of Correction with a Constant Correction Characteristic without Allowing for the Friction in the Base

The second case is more difficult, since the amplitude of the oscillations γ_m and the frequency ω in flight are usually such that $\gamma_m \omega > \omega_K$.

Let us now consider the second case.

Obviously, if the condition:

$$|\alpha| > \gamma_m,$$

STAT
(8.11)

is satisfied, then the oscillations of the correcting member will exert no influence whatever on the behavior of the gyroscope, since in this case, for any instant of time, the following condition will be valid:

$$\text{sign } \alpha = \text{sign}(\alpha - \gamma_m \sin \omega t). \quad (8.12)$$

For

$$|\alpha| < \gamma_m. \quad (8.13)$$

The condition of eq.(8.12) is now replaced by the following:

$$\text{sign}(\alpha - \gamma_m \sin \omega t) = \begin{cases} 1 & \text{for } \alpha > \gamma_m \sin \omega t \\ -1 & \text{for } \alpha < \gamma_m \sin \omega t \end{cases}$$

and the variation of α takes the form given in Fig.8.2.

Let us now take some cycle of oscillations γ (cf. Fig.8.2). Let α_1 be the value of α at the beginning of the cycle (time t_1), α_2 the value of α when $\dot{\alpha}$ changes its sign (time t_2) and α_3 , the value of α at the end of the cycle, or, what is the same thing, at the beginning of the following cycle (time t_3).

Let us write the obvious relations with respect to the reasoning for $\alpha_1 > 0$:

$$\alpha_2 = \alpha_1 - \omega_n(t_2 - t_1),$$

$$\alpha_3 = \alpha_2 + \omega_n(t_3 - t_2),$$

or

$$\alpha_3 = \alpha_1 - \omega_n[2(t_2 - t_1) - (t_3 - t_1)]. \quad (8.14)$$

Bearing in mind that

$$t_3 - t_1 = T + \tau_2,$$

$$t_2 - t_1 = \frac{T}{2} + \tau_1 + \tau_2,$$

$$T = \frac{2\pi}{\omega},$$

where

$$\tau_2 = \frac{1}{\omega} \left(\arcsin \frac{\alpha_1}{\gamma_m} - \arcsin \frac{\alpha_3}{\gamma_m} \right); \quad (8.15)$$

$$\tau_1 = \frac{1}{\omega} \arcsin \frac{\alpha_1}{\gamma_m}; \quad (8.15A)$$

$$\tau_2 = \frac{1}{\omega} \arcsin \frac{\alpha_2}{\gamma_m}; \quad (8.17)$$

we rewrite eq.(8.14) in the following form

$$\alpha_2 = \alpha_1 - 2\alpha_n \left(\tau_1 + \tau_2 - \frac{\pi}{2} \right). \quad (8.18)$$

It follows from eq.(8.18) that the increment of α for a single cycle, which we shall denote by $\Delta\alpha_1$, is determined by the expression

$$\Delta\alpha_1 = -2\alpha_n \left(\tau_1 + \tau_2 - \frac{\pi}{2} \right). \quad (8.19)$$

On the basis of eq.(8.19), as well as of eqs.(8.15), (8.16), and (8.17), the following expression can be obtained for $\omega_{K \text{ av}}$ for the mean value of the correction rate over the cycle:

$$\omega_{K \text{ av}} = \frac{\alpha_n}{\pi} \frac{\frac{1}{2} \arcsin \frac{\alpha_1}{\gamma_m} - \frac{1}{2} \arcsin \frac{\alpha_2}{\gamma_m} + \arcsin \frac{\alpha_2}{\gamma_m}}{1 + \zeta}, \quad (8.20)$$

where

$$\zeta = \frac{1}{2\pi} \left(\arcsin \frac{\alpha_1}{\gamma_m} - \arcsin \frac{\alpha_2}{\gamma_m} \right).$$

So long as the numerator of eq.(8.20) still retains the positive sign, $\omega_{K \text{ av}}$ will be negative, and, consequently, $\alpha_3 < \alpha_1$ will hold. From this, and from the condition of eq.(8.13), we get the chain of inequalities

$$\alpha_2 < \alpha_3 < \alpha_1 < \gamma_m. \quad (8.21)$$

and, consequently

$$|\omega_{K \text{ av}}| < \omega_n. \quad (8.22)$$

that is, the mean rate of correction in connection with the influence of the oscillation of the correcting element will be less in modulus than the normal rate of correction, that is, the rate of correction in the absence of such oscillations,

while, as α decreases from cycle to cycle, the inequality of eq.(8.22) is corrSTAT

spondingly intensified, since at small $\alpha \zeta \ll 1$ and a decrease in the denominator of the right side, eqs.(8.20) may be neglected, and, consequently, with declining α , the mean rate of correction decreases in modulus.

Thus, under the influence of the oscillations of the correcting element, the rate of correction with a constant characteristic is transformed from a constant to a variable, which decreases in modulus as the deviations of the gyroscope decrease, i.e., it becomes similar to the rate of correction with a proportional characteristic.

This phenomenon was first discovered and investigated by Ye.B.Levental'. It is a special case of the manifestation of what is called vibrational linearization (Bibl.7).

To the steady state will correspond, as is obvious, the zero-th value of $\alpha_{K av}$. The condition of this will be the vanishing of the numerator of eq.(8.20), i.e., the equation

$$\frac{1}{2} \arcsin \frac{\alpha_1}{\gamma_m} + \frac{1}{2} \arcsin \frac{\alpha_2}{\gamma_m} + \arcsin \frac{\alpha_3}{\gamma_m} = 0. \quad (8.23)$$

But for $\omega_{K av} = 0$; $\alpha_3 = \alpha_1$. Consequently the condition for eq.(8.23) to be satisfied will be that

$$\alpha_1 = -\alpha_2 \quad (8.24)$$

shall be satisfied.

The fact that the satisfaction of eq.(8.23) is assured by eq.(8.24) means that the steady state will in this case be a state of undamped oscillations.

The analytic expression for the amplitude of these oscillations may be found from the following reasoning.

For the half period of oscillation

$$\frac{T}{2} = \pi \quad (8.25)$$

The gyro under the action of the correction system will deflect by the angle $2\alpha_m$.
STAT

Consequently

$$2\alpha_m = \omega_r \frac{T}{2}. \quad (8.26)$$

It follows from eqs.(8.25) and (8.26) that the required amplitude α_m is determined by the expression

$$\alpha_m = \frac{\omega_r}{\omega} \frac{\pi}{2}. \quad (8.27)$$

We remark that the amplitude we have found for the undamped oscillations of the gyro in this case does not depend on the amplitude of the oscillations of the correcting member, in contrast to the situation in the case we considered earlier, where the characteristic was proportional. In particular this means that the low-frequency oscillations of the correcting member, having a small amplitude are here more dangerous than with a proportional characteristic, while the high frequency oscillations of great amplitude are, on the contrary, less dangerous.

The total setting time T_y , that is, the time in which the above undamped oscillations are established, is defined by the sum

$$T_y = T_{y1} + T_{y2}. \quad (8.28)$$

where:

T_{y1} = time in which α varies from the value $\alpha = \alpha_0$ to the value $\alpha = \gamma_m$;

T_{y2} = time in which, beginning at the value $\alpha = \gamma_m$, undamped oscillations with amplitude according to eq.(8.27) are established;

T_{y1} is determined according to the law of establishment for a constant characteristic in the absence of disturbances in the correction system, i.e., according to eq.(7.51), by the formula

$$T_{y1} = \frac{\alpha_0 - \gamma_m}{\omega_r}. \quad (8.29)$$

With respect to T_{y2} we confine ourselves to its approximate determination.

At a sufficiently high frequency of oscillation of the correcting member by comparison with their ω_K , the mean rate of correction $\omega_{K av}$, representing the ^{STAT}

rate of change of α_1 , may be treated as the first time derivative of α_1 , that is, we may put

$$\omega_{\alpha_1} \approx \frac{d\alpha_1}{dt} \quad (8.30)$$

Under the same condition, the difference between $\sin^{-1} \frac{\alpha_1}{\gamma_m}$ and $\sin^{-1} \frac{\alpha_3}{\gamma_m}$ in eq.(8.20) may be neglected, and we may put

$$\arcsin \frac{\alpha_1}{\gamma_m} \approx \arcsin \frac{\alpha_3}{\gamma_m} \quad (8.31)$$

We remark that, as we approach a state of undamped oscillations, the inaccuracy of eq.(8.31) will diminish.

Making use of eqs.(8.30) and (8.31), we obtain from eq.(8.20)

$$\frac{d\alpha_1}{dt} = \frac{\omega_{\alpha_1}}{\pi} \left(\arcsin \frac{\alpha_1}{\gamma_m} - \arcsin \frac{\alpha_3}{\gamma_m} \right)$$

or, expressing α_2 in terms of α_1 , and bearing in mind the approximation of eq.(8.31),

$$\frac{d\alpha_1}{dt} = - \frac{\omega_{\alpha_1}}{\pi} f(\alpha_1), \quad (8.32)$$

where

$$f(\alpha_1) = \arcsin \frac{\alpha_1}{\gamma_m} + \arcsin \frac{\alpha_1 - \omega_{\alpha_1} \left(\tau_1 + \tau_2 \cdot \frac{T}{2} \right)}{\gamma_m} \quad (8.33)$$

Since in the process of variation of α_1 from $\alpha_1 = \gamma_m$ to $\alpha_1 = \alpha_m$, $\tau_1 + \tau_2$ varies within the limits

$$\frac{T}{2} > \tau_1 + \tau_2 \geq 0,$$

and it therefore follows that, during this variation of α_1 , $f(\alpha_1)$ will vary within the limits

$$f_1(\alpha_1) \leq f(\alpha_1) \leq f_2(\alpha_1), \quad (8.34)$$

where

STAT

$$f_1(z_1) = \arcsin \frac{\alpha_1}{\gamma_m} + \arcsin \frac{\alpha_1 - \omega \pi T}{\gamma_m}, \quad (8.35)$$

$$f_2(z_1) = \arcsin \frac{\alpha_1}{\gamma_m} + \arcsin \frac{\alpha_1 - \frac{\omega \pi T}{2}}{\gamma_m}. \quad (8.36)$$

It follows from this that, with the accuracy of the assumptions adopted, the value of T_{y2} will lie within the following limits:

$$\frac{\pi}{\omega \pi} \int_{\alpha_1 - \gamma_m}^{\alpha_1 + \gamma_m} \frac{d\alpha_1}{f_1(\alpha_1)} \leq T_{y2} \leq \frac{\pi}{\omega \pi} \int_{\alpha_1 - \gamma_m}^{\alpha_1 + \gamma_m} \frac{d\alpha_1}{f_2(\alpha_1)}. \quad (8.37)$$

The integrals of the inequalities of eq.(8.37) may, speaking generally, be calculated, but they lack a sufficiently simple analytic expression. This circumstance hinders the use of the inequality of eq.(8.37) to determine the time T_{y2} . In order to obtain a simpler expression for this purpose, let us take recourse to a further simplification of eq.(8.33).

Let us approximate $f(\alpha_1)$ by the linear relation $f(\alpha_1)$, expressed by the straight line connecting the point $\left(\frac{\alpha_m}{\gamma_m}\right)$, $f_2\left(\frac{\alpha_m}{\gamma_m}\right) = 0$ with the point $\frac{\alpha_1}{\gamma_m} = 1$, $f_1\left(\frac{\alpha_1}{\gamma_m}\right) = \frac{\pi}{2} + \sin^{-1}\left(1 - 4 \frac{\alpha_m}{\gamma_m}\right)$ (Fig.8.3). One part of this straight line will lie between the curves $f_1(\alpha_1)$ and $f_2(\alpha_1)$, and, consequently, the points of this part of it will satisfy the condition for $f(\alpha_1)$ given by eq.(8.34). The other part will lie above the curve $f_2(\alpha_1)$, and, consequently, the points of this other part will satisfy the condition

$$f'(z_1) = f(\alpha_1). \quad (8.38)$$

On this basis we may expect the approximation $f'(\alpha_1)$ to yield, over a certain range of values of α_1 , an exaggerated value for the mean velocity, and, consequently, to yield an exaggerated value for T_{y2} .

On the other hand, let us approximate $f(\alpha_1)$ by the linear relation $f''(\alpha_1)$ STAT

representing the result of expanding $f_2(\alpha_1)$ into a series, retaining only the first term of that series. It is easy to see that the straight line expressing this

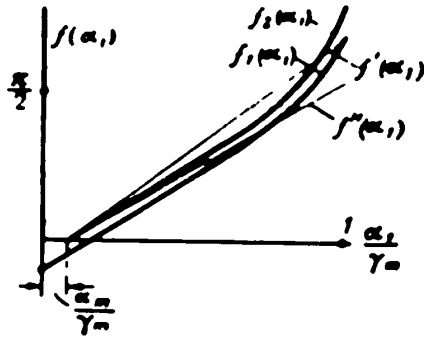


Fig. 8.3 - Approximation of Setting Time in the Case of Periodic Disturbances in Correction System with Constant Correction Characteristics

approximation will lie in part between the diagrams of $f_1(\alpha_1)$ and $f_2(\alpha_1)$ while in part it will lie below $f_1(\alpha_1)$. In other words, the points of one part of the straight line $f''(\alpha_1)$ will satisfy the condition for eq. (8.34), but the points of the other part will satisfy the condition

$$f''(\alpha_1) < f(\alpha_1). \quad (8.39)$$

The approximation $f''(\alpha_1)$ will therefore yield, over a certain section, too low a value for the mean rate

of correction, and consequently an exaggerated value of T_{y2} . For these approximations, eq. (8.32) may be rewritten in the following general form:

$$\frac{d\alpha_1}{dt} + \epsilon_{av}(\alpha_1 - \alpha_m) = 0, \quad (8.40)$$

while for the first approximation

$$\epsilon_{cp} = \epsilon'_{av} = \frac{\omega_n}{\gamma_m} \psi\left(\frac{\alpha_m}{\gamma_m}\right), \quad (8.41)$$

where

$$\psi\left(\frac{\alpha_m}{\gamma_m}\right) = \frac{1 - \frac{\alpha_m}{\gamma_m}}{\frac{1}{2} + \frac{1}{\pi} \arcsin\left(1 - 4 \frac{\alpha_m}{\gamma_m}\right)}, \quad (8.42)$$

and for the second approximation

$$\epsilon_{av} = \epsilon'_{av} = \frac{\omega_n}{\gamma_m} \frac{2}{\pi}. \quad (8.43) \text{ STAT}$$

Equations (8.41) and (8.42) may be obtained from the condition that the straight line $f'(\alpha_1)$ shall pass through the point $\frac{\alpha_1}{Y_m} = \alpha_m$, that $f_2(\alpha_m) = 0$ and that $\frac{\alpha_1}{Y_m} = 1$ $f_1(Y_m) = \frac{\pi}{2} - \arcsin(1 - 4\frac{\alpha_m}{Y_m})$. Equation (8.43) is obtained from the condition that the straight line $f''(\alpha_1)$ shall be tangent to the curve $f_2(\alpha_1)$ at the point $\frac{\alpha_1}{Y_m} = \frac{\alpha_m}{Y_m}$, $f_2(\alpha_m) = 0$, where $\frac{\alpha_m}{Y_m}$ is neglected by comparison with unity.

Considering the setting time T_{y2} equal to three times the value of the time constant of eq.(8.40), we get

$$3\psi\left(\frac{\alpha_m}{Y_m}\right) < T_{y2} < 3\frac{\pi}{2}\frac{Y_m}{\omega_k} \quad (8.44)$$

For $\frac{\alpha_m}{Y_m}$ so small by comparison with unity that we may put $\frac{\alpha_m}{Y_m} \approx 0$ in eq.(8.42), $\psi\left(\frac{\alpha_m}{Y_m}\right)$ will be correspondingly greater than unity. It follows from this that the upper limit of the values of T_{y2} exceeds the lower limit by about one and a half times.

Since on the basis of eq.(7.51), $\frac{Y_m}{\omega_k}$ is the setting time with a constant correction characteristic, which is necessary to eliminate the initial deviation $\alpha_0 = Y_m$ in the absence of any oscillations of the correcting number, it therefore follows from eq.(8.44) that on account of the oscillations of the correcting member this time will become 3 - 4 times as long.

Thus the oscillations of the correcting member with a constant characteristic lead, first, to the establishment of undamped oscillations and to the increase of the build-up time of these oscillations by comparison with the build-up time in the absence of disturbances in the correction system.

The amplitude of these oscillations, according to eq.(8.27), will be the greater, the greater the ratio $\frac{\omega_k}{\omega}$, that is, the greater the normal rate of correction ω_k is at a given value of the frequency of the oscillation of the correcting member. Consequently with this in mind it is desirable to select small values of ω_k .

Exactly like the value of ε for the proportional characteristic, the value of ω_k cannot be reduced below a certain limit determined by the value of the ^{STAT} moments

of friction, the imbalance, the rate of displacement of the direction indicated by the gyro, etc.

We shall now perform an illustrative calculation with the object of evaluating the possible amplitude of oscillation of the gyro.

We shall require that for a disturbance of 10° , the build-up time T_y in the absence of disturbances in the system of correction shall not exceed 100 sec, which is sufficiently acceptable from the operating standpoint.

On the basis of eq.(7.51), we get the result that in this case the rate of correction ω_K must equal

$$\omega_K = \frac{\gamma_y}{T_y} = 0.1 \frac{\text{degree}}{\text{sec}}.$$

Assume that the period of oscillation of the sensitive member of the corrector is

$$T = 1 \text{ sec} \quad \text{and} \quad \gamma_m = 1^\circ$$

Consequently

$$\omega_n = \frac{0.1}{30} \approx 3 \cdot 10^{-4},$$

and the amplitude of the self-oscillations α_m :

$$\alpha_m = 2.7^\circ \cdot 10^{-2},$$

that is, a value that is negligibly small.

For the period of oscillation of the correcting member $T = 30$ sec, corresponding to the order of the periods of slow oscillations of the aircraft, and for the same values of ω_K and γ_m , we get

$$\omega_n \approx 9 \cdot 10^{-3},$$

$$\alpha_m = 0.81^\circ.$$

that is, a quantity that is already rather large.

Results that are more favorable in this sense are given by the widely used mixed characteristic of correction according to Fig.6.3, that is, one which is STAT

proportional in the initial part (for $\theta \leq 2 - 3^\circ$), while it is constant in the remaining part. With this characteristic, the slow oscillations of the sensing member of the corrector remain within the zone of proportionality, while for a proportional characteristic, the unfavorable influence of a long period of oscillation of the sensing member of the corrector is adequately compensated, as already remarked, by the favorable influence of the small amplitude of these oscillations.

For rapid oscillations, on the other hand, the sensing member of the corrector, varying its position, will for the most part be in the zone of the constant characteristic, that is, in this case, the disturbances of the gyroscope will be determined primarily by a law corresponding to the constant characteristic.

But, as we have seen, for rapid oscillation, this law does not lead to significant disturbances of the gyro.

Let us now elucidate the role of friction in the gyroscope gimbals in the process under investigation.

As follows from eq.(8.10), if we allowed for friction in the gimbals, it would mean a change of the velocity $\dot{\alpha}$ by the quantity ω_ρ , meaning either a decrease or increase of $\dot{\alpha}$ in modulus, depending on whether the sign of the angular velocity of the diagonally opposite gyroscope frame agrees or not with the sign of $(\alpha - \gamma_m \sin \omega t)$.

Let us take the two limiting cases, the first one when the change of sign of ω_ρ is simultaneous with the change of sign of ω_K , while the second case is when the sign of ω_ρ remains unchanged during the entire setting state.

The former case will mean a process entirely analogous to the preceding process, with only the modulus of ω_K being increased or decreased by the quantity ω_ρ .

The second case will already mean a modification of the process in the sense that the resultant velocities in the process of reduction of α and in the process of its increase will differ from each other in modulus by $2\omega_\rho$ (Fig.8.4).

Let us write out the relations for one cycle with reference to this case,
STAT

taking $\alpha_1 > 0$ and sign $\beta = 1$:

$$\left. \begin{aligned} \alpha_2 &= \alpha_1 - (\omega_n - \omega_p)(t_2 - t_1), \\ \alpha_3 &= \alpha_2 + (\omega_n + \omega_p)(t_3 - t_2). \end{aligned} \right\} \quad (8.45)$$

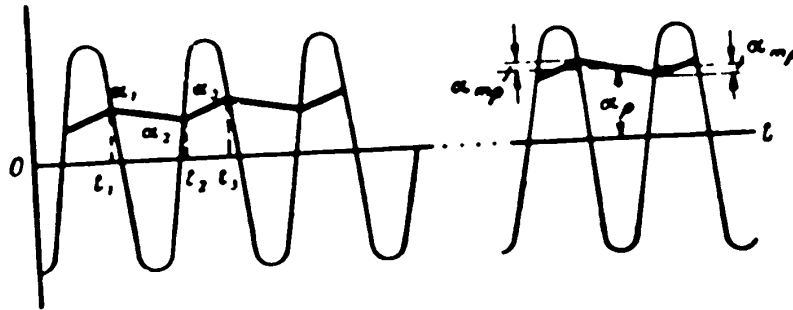


Fig.8.4 - Influence of Periodic Disturbances in the Correction System with a Constant Correction Characteristic, Allowing for Friction in the Gimbals

On the basis of eqs.(8.15); (8.16), (8.17) and (8.45), we may write

$$\alpha_3 = \alpha_1 - 2\omega_n \left(\tau_1 + \tau_2 - \frac{\tau_3}{2} \right) + \omega_p (T + \tau_2). \quad (8.46)$$

Let us neglect the quantity τ_3 by comparison with the value of the period T , which is entirely permissible. Then we get the following formula for the mean rate of correction in this case, which we shall denote by $\omega_{K_{av}}^{\dagger}$

$$\omega_{K_{av}}^{\dagger} \approx \omega_{K_{av}} + \omega_p$$

or, bearing in mind eq.(8.28) for $\omega_{K_{av}}^{\dagger}$, in which the quantity ζ is neglected by comparison with 1

$$\omega_{K_{av}}^{\dagger} = \frac{\omega_n}{\pi} \left[\frac{1}{2} \arcsin \frac{\alpha_1}{T_m} + \frac{1}{2} \arcsin \frac{\alpha_2}{T_m} + \arcsin \frac{\alpha_3}{T_m} - \pi \frac{\omega_p}{\omega_n} \right]. \quad (8.47)$$

The condition of the steady state $\omega_{K_{av}}^{\dagger} = 0$, as before, will mean that

$$\alpha_3 = \alpha_1.$$

STAT

Whence the condition of the steady state may be written as follows:

$$\arcsin \frac{\alpha_1}{\gamma_m} + \arcsin \frac{\alpha_2}{\gamma_m} = \pi \frac{\omega_p}{\omega_x}. \quad (8.48)$$

The left side of this condition is unchanged by comparison with the case when the role of friction in the gimbals was neglected, but in the right side, instead of zero, a quantity proportional to the ratio $\frac{\omega_p}{\omega_x}$ appears. It is easy to understand that this circumstance means a shift of the axis of the undamped oscillations of the gyro from the zero position by the quantity ω_p , determined by the equation.

$$\alpha_p = \frac{\alpha_1 + \alpha_2}{2}, \quad (8.49)$$

where α_1 and α_2 satisfy the condition of eq.(8.48).

The amplitude of the undamped oscillations about the value of α_p , which we shall denote by α_m , will be determined by the expression

$$\alpha_m = \frac{\alpha_1 - \alpha_2}{2}. \quad (8.50)$$

But, by eq.(8.45),

$$\alpha_2 = \alpha_1 - (\omega_x - \omega_p)(t_2 - t_1). \quad (8.51)$$

Since for the state of undamped oscillations, $\alpha_3 = \alpha_1$, we therefore obtain from eq.(8.45)

$$\frac{t_2 - t_1}{t_2 - t_1} = \frac{\omega_x - \omega_p}{\omega_x + \omega_p}. \quad (8.52)$$

On forming, from eq.(8.52), the derivative proportion, and neglecting α_3 by comparison with T, we get

$$\frac{T}{t_2 - t_1} = \frac{2\omega_x}{\omega_x + \omega_p}. \quad (8.53)$$

On substituting in eq.(8.51) $t_2 - t_1$ according to eq.(8.53), we get

$$\alpha_2 = \alpha_1 - \pi \frac{\omega_p}{\omega_x} \left(1 - \frac{\omega_p^2}{\omega_x^2}\right). \quad (8.54) \text{ STAT}$$

On substituting eq.(8.54) in eq.(8.50), we obtain

$$\alpha_m' = \frac{\pi}{2} \frac{\omega_p}{\omega_x} \left(1 - \frac{\omega_p^2}{\omega_x^2} \right). \quad (8.55)$$

It is clear from a comparison of eq.(8.55) with eq.(8.27) that, owing to the friction in the gimbals, the amplitude of the undamped oscillation of the gyro decreases.

Using now α_m' as a known quantity, and bearing in mind that

$$\begin{aligned} \alpha_1 &= \alpha_p + \alpha_m', \\ \alpha_2 &= \alpha_p - \alpha_m', \end{aligned}$$

let us rewrite eq.(8.48) in the following form

$$\arcsin \frac{\alpha_p + \alpha_m'}{\gamma_m} + \arcsin \frac{\alpha_p - \alpha_m'}{\gamma_m} = \pi \frac{\omega_p}{\omega_x}. \quad (8.56)$$

On expanding the left side of eq.(8.56) into a series and retaining the first two terms of this series, which is entirely sufficient in this case, we obtain, after elementary transformations, and neglecting $\frac{\alpha_m'^2}{\gamma_m^2}$ by comparison with unity:

$$\alpha_p \left(1 + \frac{\alpha_p^2 + 2\alpha_m'^2}{6\gamma_m^2} \right) = \frac{\pi}{2} \frac{\omega_p}{\omega_x} \gamma_m. \quad (8.57)$$

It follows from this that

$$\alpha_p < \frac{\pi}{2} \frac{\omega_p}{\omega_x} \gamma_m.$$

and for values of α_p sufficiently small by comparison with γ_m ,

$$\alpha_p \approx \frac{\pi}{2} \frac{\omega_p}{\omega_x} \gamma_m. \quad (8.58)$$

Let us assume that $\frac{\omega_p}{\omega_k} = 0.2$, which corresponds to a moment of correction five times as great as the moment of friction, a relation which is entirely realistic.

in, for these data:

STAT

$$\alpha \approx 0.314 \gamma_m.$$

that is, a quantity with which one must already reckon.

In this way we find that, with a single-valued rate of motion of the diagonal frame, the oscillation of the sensitive member of the corrector of the given frame leads to the displacement of its mean position from the zero value, and at that, by a rather perceptible quantity.

The limiting cases of the change of sign of ω_p are improbable in their true form. It is more probable to expect the mean position of the oscillations to be in the range up to the values of α_p determined by eq.(8.57), but to be the greater, the greater the value of $\frac{\omega_p}{\omega_k}$.

Thus, in the absence of oscillations of the correcting members, friction in the gimbals with a constant correction characteristic leads only to nonuniformity of the correction. But if such oscillations do occur, then this friction will be able to cause indeterminate slipping of the gyroscope axis from zero position, and this slipping will be the greater, the greater the moment of this friction by comparison with the moment of correction.

STAT

CHAPTER IX

DEVIATIONS OF THE GYRO HORIZON

Section 1. Deviations due to the Earth Rotation and to the Displacement of the Aircraft with Respect to the Earth

By the deviations of a gyro horizon we mean its errors due to the motion of the base of the gimbals.

The starting equations of motion of the gyro in investigating these errors will be, as before, the equations of precession:

$$\left. \begin{aligned} Hq &= L_x \\ -Hp &= L_y \end{aligned} \right\} \quad (9.1)$$

where the terms representing the rotations of constraint of the gyroscope must be taken into account in the expressions for p and q , and the terms taking account of the action of the corresponding accelerations on the sensitive elements of the corrector in the expressions for L_x and L_y .

In this Section we shall investigate the rotations of constraint in connection with the earth rotation and the displacements of the aircraft with respect to the earth.

The expressions for p and q corresponding to this case may be taken in the following form when the axis of the outer frame of the gyro horizon is oriented along the longitudinal axis of the aircraft (cf. (2.34) and (2.35) and Fig.2.11)

STAT

$$p = -\dot{\beta} - \omega_1 \sin K - \frac{v}{R} \quad (9.2)$$

$$q = \dot{\alpha} + \omega_1 \cos K,$$

where $\omega_1 = \omega_3 \cos \varphi$ - horizontal component of the earth rotation;

K - course of aircraft;

v - speed of aircraft;

R - radius of the earth.

The terms $(\omega_2 + \frac{v}{R} \sin k \tan \varphi) \alpha$ and $\omega_2 + \frac{v}{R} \sin k \tan \varphi \beta$ are omitted from eqs.(9.2) in comparison with eqs.(2.34) and (2.35), in view of the fact that they represent numbers of a higher order of smallness by comparison with the remaining summands.

As for the expression for the moments L_x and L_y , we shall take then for the conditions of the undisturbed state of the correcting members. In other words, we shall consider that the velocity entering into eqs.(9.2) is constant. The influence of inconstancy of velocity will be considered later.

Proportional Characteristic of Correction

On substituting in eqs.(9.1), p and q according to eqs.(9.2), and L_x and L_y according to the conditions of the proportional characteristic (considering it hysteresis-free), we obtain the equations of motions in the following form:

$$H(\dot{\alpha} + \omega_1 \cos K) = -k_2 \alpha + L_1 \text{sign } \dot{\beta},$$

$$H\left(\dot{\beta} + \omega_1 \sin K + \frac{v}{R}\right) = -k_1 \beta - L_2 \text{sign } \dot{\alpha}.$$

On dividing the right and left sides equations by H and, for simplicity, taking $k_1 = k_2$, we rewrite them in the following form:

$$\left. \begin{aligned} \dot{\alpha} &= -\epsilon \left(\alpha - p_2 \text{sign } \dot{\beta} + \frac{\omega_1 \cos K}{\epsilon} \right), \\ \dot{\beta} &= -\epsilon \left(\beta + p_1 \text{sign } \dot{\alpha} + \frac{\omega_1 \sin K}{\epsilon} + \frac{v}{\epsilon R} \right). \end{aligned} \right\} \quad (9.3)$$

STAT

The difference between the equations so obtained and the equations related to the behavior of the gyro on a fixed base, consists merely in the change of the equilibrium conditions with respect to the axis $O\beta$ by the quantity

$$\alpha_1 = - \frac{\omega_1 \cos K}{\epsilon} \quad (9.4)$$

and along the axis $O\beta$ by the quantity

$$\beta_1 = - \frac{\omega_1 \sin K}{\epsilon} - \frac{r}{\epsilon R} \quad (9.5)$$

It follows from this that the behavior of the gyro horizon, when the influence of the earth rotation and the displacements of the aircraft are taken into account, will be determined by the same formulas and diagrams that relate to its behavior when these factors are not taken into account, merely displacing the origin of the coordinate system along the axis $O\beta$ by the quantity α_1 and along the axis $O\zeta$ by the quantity β_1 . These displacements will be the total values of the deviation due to the earth rotation and to the displacements of the aircraft. These latter deviations are also called velocity deviations.

We remark that the influence of velocity is reflected only in the displacements of the origin of the coordinates on the $O\beta$ axis on account of the second term β_1 . In this way, the velocity deviation, which we shall denote by δ_v , will be determined by the expression

$$\delta_v = - \frac{r}{\epsilon R} \quad (9.6)$$

It determines the deviation of the gyroscope axis in the plane passing through the axes $O\zeta$ and $O\beta$, that is, in the plane $O\zeta\eta$ (Fig.9.1), coinciding with the longitudinal plane of the aircraft.

α_1 and the first term of β_1 , which depend only on the earth rotation, will be the components of the deviation due to the earth rotation, which we shall denote by δ_3 . Geometrical composition of these components gives us the following expres-

on

STAT

$$\delta_3 = \frac{v}{R} \tag{9.7}$$

The deviation due to the earth rotation determines the deflection of the gyro axis in the vertical plane perpendicular to the geographical meridian (Fig.9.2).

The deviation of the gyro axis from the axis $O\zeta$ (which in this case denotes the position of the sensing member of the corrector) assures the appearance of a correction moment which causes the gyro to precess in the plane of the given deflection of the gyro in the sense toward matching with the axis $O\zeta$. The vector of angular velocity of this precession will accordingly be perpendicular to the plane of deflection of the gyro axis.

Hence the presence of the deviations δ_v and δ_e will mean the presence of the corresponding precessions of the gyro, the vectors of whose angular velocities will be perpendicular to the planes of these deviations and will be directed as indicated in Figs.9.1 and 9.2.

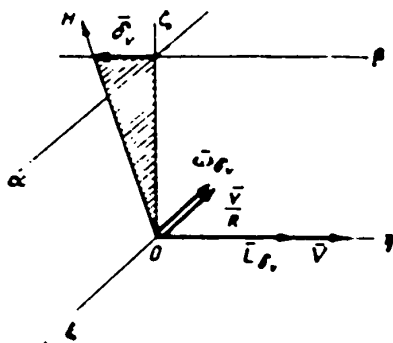


Fig.9.1 - Velocity Deviation of Gyrohorizons with Proportional Characteristics of Correction

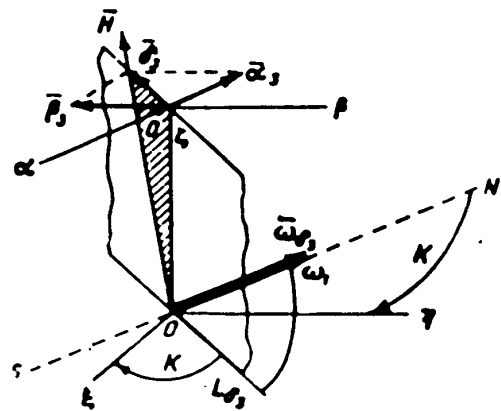


Fig.9.2 - Deviations, Due to Earth Rotations, of a Gyrohorizon with Proportional Characteristics of Correction

Bearing in mind that the theory here developed relates to the longitudinal situation of the gyro horizon, that is, to the case when the vector of the ground

STAT

speed is directed along the axis $O\eta$, we get the result that the vector of angular velocity of precession, ω_{δ_v} , due to the rate of deviation δ_v , will be directed perpendicular to the vector of flight velocity \vec{v} , and in the same sense as the vector of angular velocity of the additional rotation of the plane of the horizon which represents the effect of the displacements of the aircraft with respect to the earth. The vector of the angular velocity of precession ω_{δ_e} , however, which is caused by the deviations due to the earth rotation δ_e , will be found to be directed along the meridian, in the same sense as the vector of the horizontal component of the earth rotation, ω_1 .

According to the condition of the proportional characteristic of correction, we may write

$$\omega_{\delta_v} = \frac{A\delta_v}{H},$$

$$\omega_{\delta_e} = \frac{A\delta_e}{H}.$$

On substituting here the expressions for δ_v and δ_e according to eqs.(9.6) and (9.7), we get

$$\omega_{\delta_v} = \frac{r}{R},$$

$$\omega_{\delta_e} = \omega_1.$$

Thus the rate of precession of the gyro that is due to the velocity deviation coincides identically in magnitude and direction with the rate of rotation of the plane of the horizon due to the displacement of the aircraft, while the rate of precession of the gyroscope due to the deviation owing to the earth rotation coincides identically with the rate of rotation of the plane of the horizon under the influence of the horizontal component of the earth rotation. As a result, the axis of the gyroscope, deflected from the vertical by the values δ_v and δ_e , will then exactly follow the motion of the vertical.

what has been set forth above, the nature of the deviation due
STAT

to the earth rotation may be defined in the following way: by this deviation we mean that angle of deflection of the gyroscope axis from the local vertical, at which, owing to the action of the correction system, a rate of precession of the gyroscope is produced which is exactly equal in magnitude and direction to the rate of rotation of the local vertical due to the earth rotation.

By analogy to this, the velocity deviation may be defined as that angle of deflection of the gyro axis from the local vertical at which, owing to the moment of the correction system, a rate of precession of the gyroscope is produced which is exactly equal in magnitude and direction to the rate of rotation of the local vertical that is due to the displacement of the aircraft with respect to the earth.

Let us determine the possible order of the numerical value of the deviation due to the earth rotation. Taking the value $\varepsilon \times 10^{-2}$ 1/sec, and bearing in mind that the maximum value of the horizontal component of the earth rotation, which it acquires on the equator, is equal to

$$\omega_3 = 7.3 \cdot 10^{-5} \text{ 1 sec} :$$

we obtain, for the maximum value of δ_e (for a given ε):

$$\delta_3 = 0.07^\circ .$$

The velocity deviation will be still smaller.

Since the value of ε taken by us is entirely realistic, it may to that extent be considered that the order of the deviations of a gyrohorizon due to the earth rotation, and, a fortiori, the order of the velocity deviations, is in general, rather small. For this reason, these deviations with a mixed characteristic of correction will be determined by the same formulas as for the case of a proportional characteristic, now being discussed, since the deviations remain within the limits of the zone of proportionality of the mixed characteristic.

But, for a mixed characteristic, the absolute magnitude of the deviation is usually considerably smaller than for a proportional characteristic, since for a mixed characteristic the coefficient of the correcting moment in the zone of

STAT

proportionality is usually taken considerably larger than in the case of a purely proportional characteristic.

Constant Characteristic of Correction

With the constant characteristic of correction there will be neither deviations due to the earth rotation nor velocity deviations. This is explained by the fact that in this case, immediately after leaving the zone of insensitivity of the correction, a rate of precession that is many times the velocity of rotation of the local vertical due to the earth rotation and to the displacements of the aircraft will arise. It follows that the axis of the gyro will never be able to depart from the local vertical by a quantity greater than the zone of insensitivity of the correction. But within the limits of the zone of insensitivity of the correction, the gyro axis may fail to coincide with the local vertical even when the local vertical is not rotating at all.

Consequently the allowance for this rotation can yield nothing new.

Section 9.2. Turning Deviations of Gyrohorizon Equations of Motion of the Gyroscope during a Turn

In this case we need not take into account the role of the rotations of constraint due to the rotation of the earth and the longitudinal velocity of the aircraft, but may confine ourselves to allowing only for the rotations of constraint due to the rotation of the gyro together with the aircraft at the angular rate of turn ω_t . In accordance with this condition, the expressions for p and q will take the following form 9.2.3

$$p = -\dot{\beta} - \omega_t \alpha \quad (9.8)$$

$$q = \dot{\alpha} - \omega_t \beta \quad (9.9)$$

STAT

In the expression for L_x and L_y the influence of the centripetal accelerations on the pendulums of the correction system must be taken into account. This influence reduces down to the displacement of the equilibrium position for the pendulum from the true vertical to the apparent vertical, which will be deflected from the true vertical in a direction perpendicular to the vector of velocity of flight v , by the angle α , equal to the angle of bank of the aircraft in a regular turn, and defined by the expression

$$\gamma_0 = \text{arc tg } \frac{v^2}{g} \quad (9.10)$$

since all our reasoning will relate to a regular turn. With respect to the longitudinal position of the gyro horizon, this will mean deflection, by this angle, of the pendulum correcting the outer frame.

In the position of the pendulum correcting the inner frame, however, there will be no changes (cf. Fig. 9.3). It follows that the action of the corrector on the angle α will be determined by the value of the mismatch

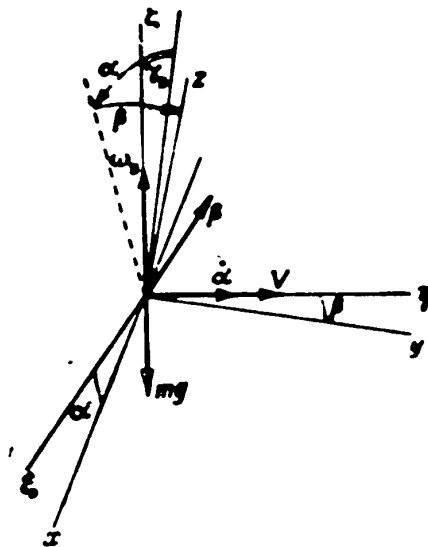


Fig.9.3 - Position of Axes of Gyrohorizon during a Turn

$$\theta_0 = \alpha + \gamma_0 \quad (9.11)$$

while in the angle β , the action of the correction system will be defined, as before, by the value of the

STAT

mismatch

$$\theta_1 = \beta. \quad (9.12)$$

Thus the correction system will tend to bring the gyro axis to the position of the apparent vertical. But this will not in fact take place, since, together with this action of the system of correction, the rotations of constraint of the turn will also take effect. The task of the present section will thus be to elucidate the behavior of the gyro under these circumstances.

Turning Deviations of Gyrohorizon with Proportional Characteristic of Correction

On substituting in eq.(9.1) the expressions for p and q given by eq.(9.8) and eq.(9.9) respectively, and the expressions for L_x and L_y according to the conditions of the proportional (hysteresis-free) characteristic, and likewise bearing in mind the conditions of eqs.(9.11) and (9.12), and, for simplicity, taking $k_1 = k_2 = k$, we obtain the equations of motions in the gyro in the following form:

$$\left. \begin{aligned} H(\ddot{\alpha} - \omega_s \dot{\beta}) &= -k(\alpha + \gamma_0) + L_1 \text{sign } \dot{\beta}. \\ H(\ddot{\beta} - \omega_s \dot{\alpha}) &= -k\beta - L_2 \text{sign } \dot{\alpha}. \end{aligned} \right\} \quad (9.13)$$

or

$$\left. \begin{aligned} \ddot{\alpha} &= -\omega_s \dot{\beta} + \gamma_0 - \rho_2 \text{sign } \dot{\beta}. \\ \ddot{\beta} &= -\omega_s \dot{\alpha} - \rho_1 \text{sign } \dot{\alpha}. \end{aligned} \right\} \quad (9.14)$$

where

$$\rho_i = \frac{k}{H}. \quad (9.15)$$

Let us reject at first the terms characterizing the influence of friction in the gimbals, and let us thus rewrite the equations so obtained in the following form:

STAT

$$\left. \begin{aligned} \dot{\alpha} + \epsilon \alpha - \epsilon \omega \dot{\beta} &= -\epsilon \gamma_B \\ \dot{\beta} + \epsilon \dot{\alpha} + \epsilon \omega \alpha &= 0. \end{aligned} \right\} \quad (9.16)$$

On eliminating the variable β from the first equation, with the half of the second one, we get

$$\alpha \cdot 2\epsilon \dot{\alpha} - \epsilon^2(1 + \omega^2)\alpha = -\epsilon^2 \gamma_B. \quad (9.17)$$

The integral of this equation will be

$$\alpha = A e^{-\epsilon t} \sin(\omega_0 t + \delta) + \alpha_{st}, \quad (9.18)$$

where

$$\alpha_{st} = -\frac{\gamma_B}{1 + \omega^2}. \quad (9.19)$$

A and δ are arbitrary constants.

On substituting the solution so found in the first equation of eqs.(9.16), we get

$$\omega_0 \dot{\beta} = A \omega_0 e^{-\epsilon t} \cos(\omega_0 t + \delta) + \epsilon(\alpha_{st} + \gamma_B)$$

or

$$\beta = A e^{-\epsilon t} \cos(\omega_0 t + \delta) + \beta_{st}, \quad (9.20)$$

where

$$\beta_{st} = \frac{\epsilon \gamma_B}{1 + \omega^2}. \quad (9.21)$$

After the lapse of a sufficient interval of time, the terms depending on time will vanish in the solution so found, after which there will remain

$$\begin{aligned} \alpha(t)_{t \rightarrow \infty} &= \alpha_{st}. \\ \beta(t)_{t \rightarrow \infty} &= \beta_{st}. \end{aligned}$$

Thus the values of α_{B1} and β_{B1} are the coordinates of the equilibrium position C_1 of the gyro vertex during a turn.

We remark that the coordinate of the equilibrium position along the $O\beta$ axis, β_{B1} , has a positive sign for both a left and a right turn, since the change of signs in γ_B and ω from positive to negative on transition from a left to a right turn are mutually compensated, while the coordinate of the equilibrium position along the $O\alpha$

STAT

axis, α_{E1} , has a negative sign for a left turn, while for a right turn, in connection with the change of sign of γ_B , it has a positive sign.

Let us find the locus of the points of the possible positions of this equilibrium position at different angular velocities of turn ω_B differing in magnitude and sign. On squaring the left and right sides of eqs.(9.19) and (9.21), and adding them, we get the following equation for this locus:

$$\alpha_{E1}^2 + \beta_{E1}^2 - B\beta_{E1} = 0, \tag{9.22}$$

where

$$B = \frac{v^2}{a} \approx \frac{v^2}{g}. \tag{9.23}$$

Equation (9.22) is the equation of the circle with center located on the positive semiaxis of β at the distance $\frac{B}{2}$ from the point 0.

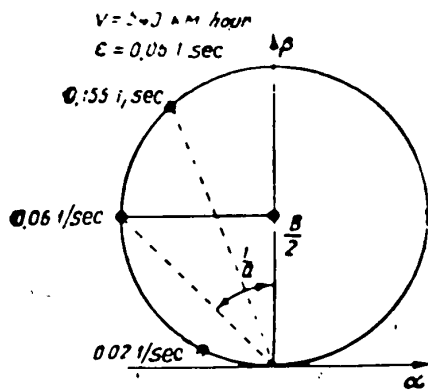


Fig.9.4 - Locus of Equilibrium Positions of Vertex of Gyrohorizon with Proportional Characteristics of Correction on Turns with Various Angular Velocities and Constant Speed of Aircraft

Figure 9.4 shows this circle for velocity $v = 540 \text{ km/hour}$ and $\epsilon = 0.06 \text{ sec}^{-1}$, with the values of the angular velocity ω_B relating to the given point of this circle indicated by figures.

If we assume that the full circle of turning is covered in the course of 1 min, that is, if we take a turning period $T_B = 1 \text{ min.}$ and take, as before, the value $\epsilon = 0.06 \text{ 1/sec}$, then we get for a:

$$a = 1.7,$$

i.e., a value exceeding unity.

For a higher rate of turn, the values of a will be correspondingly greater.

From this it follows, also on the basis of eqs.(1.19) and (9.21) that in

STAT

relatively deep turns and correspondingly great values of γ_B ,

$$|\beta_{B1}| > |\alpha_{B1}|.$$

will ordinarily hold good.

For the value $a = 1.7$ calculated by us, the values of α_{B1} and β_{B1} will be equal

$$\begin{aligned}\alpha_{B1} &= 0.258 \gamma_{B1} \\ \beta_{B1} &= 0.438 \gamma_{B1}.\end{aligned}$$

To a turn, at the angular velocity $\omega_B = \frac{2\pi}{60}$ 1/sec taken in calculating a , there will correspond, for instance, an angle of bank of the order of 57° at a flight speed of 540 km/hr.

It will be clear from this that for relatively deep turns, α_{B1} and β_{B1} may reach considerable values.

For turns at higher angular velocity and correspondingly steeper banks, the values of α_{B1} and β_{B1} will be smaller. Thus, for the case when a full turning circle is made in 20 sec, $a = 5$. In this case we shall have

$$\begin{aligned}\alpha_{B1} &= 0.04 \gamma_{B1} \\ \beta_{B1} &= 0.19 \gamma_{B1}.\end{aligned}$$

To this value of the angular velocity at the same flying speed of 540 km/hour, there corresponds a bank of the order of 78° . Thus we get $\alpha_{B1} = 3^\circ$ and $\beta_{B1} = 15^\circ$, as against $\alpha_{B1} = 14.7^\circ$ and $\beta_{B1} = 25^\circ$ of the preceding case.

As follows from eqs. (9.18) and (9.20), the vertex of the gyroscope reaches this equilibrium position after the lapse of the time

$$T_y = 3 : 4 \frac{1}{\epsilon}.$$

that is, if we take $\epsilon = 0.06$ 1/sec, that is, after 50-70 sec. This means that with a slower turn, for instance with a turn making a full circle in 1 min, the vertex of the gyro practically reaches the equilibrium position already at the end of the first turning circle. In slower turns, the vertex of the gyro may be set considerably before the first whole turning circle is completed. In a turn according to ^{the} STAT

second example, three turning circles must be made for this. Let us find the path of the gyro vertex to the equilibrium position.

For this purpose let us transfer in eqs.(9.18) and (9.20) respectively α_{B1} and β_{B1} to the left sides, square the right and left sides of the equation so obtained, and add them by parts. As a result we get

$$(\alpha - \alpha_{B1})^2 + (\beta - \beta_{B1})^2 = A^2 e^{-2\omega t}. \quad (9.24)$$

This equation is the equation of a spiral in the coordinates $\alpha\beta$ with its origin at the point $(\alpha_{B1}, \beta_{B1})$. The magnitude of the radius vector of the spiral decreases by an exponential law with the passage of time.

The angular velocity of rotation of the radius vector of the gyroscope vertex will be equal, as is obvious from eqs.(9.18) and (9.20), to the angular velocity of the turn ω_D . Making use of this fact, in the equations of the path, eq.(9.24), the time p may be expressed in terms of the angle of rotation of the radius vector of the vertex φ . Indeed, since this turn is accomplished at constant angular velocity ω_D , it follows that the time t required for rotation by the angle φ , will be determined by the formula

$$t = \frac{\varphi}{\omega_D}.$$

Making use of this relation and putting $\varphi = 0$ for $t = 0$, we may rewrite the equation of path, eq.(9.24), in the following form:

$$(\alpha - \alpha_{B1})^2 + (\beta - \beta_{B1})^2 = A^2 e^{-2\omega \frac{\varphi}{\omega_D}}.$$

Or, in polar coordinates, with origin at the equilibrium point α_{B1}, β_{B1} :

$$r = A e^{-\frac{\omega}{\omega_D} \varphi}. \quad (9.25)$$

where

$$r = \sqrt{(\alpha - \alpha_{B1})^2 + (\beta - \beta_{B1})^2}. \quad (9.26)$$

On determining the arbitrary constant A from the initial conditions for $\varphi = 0$,

STAT

$r = R_0$, we get

$$A = R_0$$

and, consequently, the equation of the path of the vertex will finally be written in the following form:

$$r = R_0 e^{-\alpha \theta} \quad (9.27)$$

Thus the path of the vertex will be an involutorial logarithmic spiral, ending in the equilibrium point.

Let us assume that at the initial instant the gyro axis was at the true vertical.

This means that

$$R_0 = \sqrt{\alpha_{B1}^2 + \beta_{B1}^2} = \frac{\gamma_0}{1 + \alpha^2}$$

Figure 9.5 gives the paths of the vertex for such initial conditions and the value $\alpha = 2.0$. It will be clear from them that during motion toward the equilibrium position, the vertex will pass points with coordinates exceeding in modulus α_{B1} and β_{B1} , but these latter deviations are in themselves so great that the use of a gyrohorizon under such conditions during a turn becomes practically impossible. In this connection, in those gyro horizons that use a system of correction with proportional characteristics, the action of the system of correction along the angle α during a turn is sometimes cut out. Since the duration of a turn usually does not exceed 1-2 min, a gyro with the correction system cut off for this time will maintain its position sufficiently well. Although this measure involves certain complications in the design of the correction system, it is nevertheless not only entirely rational, but also in this case entirely necessary. This behavior of the gyro may be treated as a direct consequence of the composition of the precession due to the resultant moment of the correction system and the rotation of the system of coordinates $O\alpha\beta$, due to the rotation of the aircraft.

Let us now determine the value of the maximum turning errors. For this it STAT

sufficient to find the coordinates of the first points of intersection of A and B with the path of the gyro vertex with the straight lines at which $\alpha = 0$ and $\beta = 0$, respectively. The equations of these straight lines will be obtained if we put $\alpha = 0$ and $\beta = 0$ in eq.(9.16).

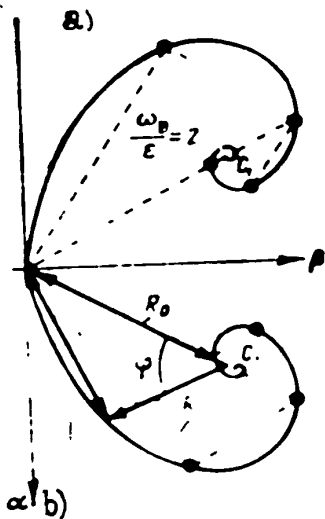


Fig.9.5 - Path of Vertex of Gyro Horizon during a Turn with Proportional Characteristics of Correction, without Allowing for Friction in the Gimbals

- a) $\omega_B > 0$ (Left Turn)
- b) $\omega_B < 0$ (Right Turn)

and the length of the radius vector R_2 by the formula

$$R_2 = R_0 e^{\frac{\pi}{a}}$$

From evident geometrical considerations we get

$$\alpha_{max} = a_{s1} \cdot R_1 \cos \dots$$

$$\beta_{max} = a_{s1} \cdot R_2 \cos \dots$$

Substituting the expressions for α_{B1} , β_{B1} , R_1 , R_2 and $\cos \varphi$, we obtain, as for

STAT

$\beta = 0$ on the straight line

$$\beta - a\gamma = 0,$$

and $\alpha = 0$ on the straight line

$$\beta = -\frac{1}{a} \alpha + \frac{1}{a} \gamma_s.$$

These straight lines are mutually perpendicular, the straight line $\alpha = 0$ forming the angle φ with the axis α (Fig.9.6), for which the following equation

$$\cos \varphi = \frac{1}{\sqrt{1+tg^2 \varphi}} = \frac{1}{1+\frac{1}{a^2}} = \frac{a}{1+a^2} \quad (9.28)$$

is true, while the straight line $\beta = 0$ passes through the origin of coordinates. Then the length of the radius vector R_1 will be determined, according to eq.(9.27), by the formula

$$R_1 = R_0 e^{-\frac{\pi}{a}}$$

By analogy, for β_{\max} ,

$$\lim_{a \rightarrow \infty} \beta = \lim_{a \rightarrow \infty} \gamma_B \left(\frac{1 + e^{-\frac{\pi}{a}}}{1 + a^2} \right) = 0.$$

Thus when $a = \frac{\omega_B}{\varepsilon}$ varies from 0 to ∞ , there are limiting values of β_{\max} .

Let us determine the value of a at which, for an assigned ε , the limiting value β_{\max} will obtain. For this purpose, let us solve the equation

$$\frac{d\beta_{\max}}{da} = 0,$$

i.e.,

$$\left(1 + e^{-\frac{\pi}{a}} + \frac{\pi}{a} e^{-\frac{\pi}{a}} \right) (1 + a^2) - 2a^2 \left(1 + e^{-\frac{\pi}{a}} \right) = 0.$$

The equation so obtained is now transformed in the following way:

$$e^{-\frac{\pi}{a}} = \frac{(a-1)\pi}{(a^2-1)a} - 1.$$

This equation is satisfied by the root $a \approx 1.05$.

Substituting $a = 1.05$ in eqs.(9.29) and (9.30), we get

$$(\beta_{\max})_{\lim} = 0.524 \gamma_B.$$

In this case α_{\max} takes the value defined by the expression

$$\alpha_{\max} = 0.598 \gamma_B.$$

When a varies from 0 to ∞ , α_{\max} varies from γ_B to 0, always remaining less in modulus than γ_B , since

$$\frac{d\alpha_{\max}}{da} = \gamma_B \frac{e^{-\frac{\pi}{2a}} \left(1 + \frac{\pi}{2a} + \frac{\pi a}{2} - a^2 \right) - 2a}{(1+a^2)^2} < 0 \text{ for } 0 < a < \infty.$$

On the basis of these calculations, let us construct the graphs of the variation of $\frac{\alpha_{\max}}{\gamma_B}$ and $\frac{\beta_{\max}}{\gamma_B}$ as a function of a , which are shown in Fig.9.7.

STAT

From a consideration of these graphs the following conclusion can be drawn: for a given bank, the turning errors are less at higher values of the angular velocities of turning.

Let us now elucidate the influence of friction in the gimbals. For this purpose let us rewrite the equations of motion, eq.(9.14), in the following form:

$$\left. \begin{aligned} \dot{\alpha} + a\alpha - a_1\beta &= -\tilde{\gamma}_0 \\ \dot{\beta} + a\beta + a_1\alpha &= -a\rho_1 \text{sign } \dot{\alpha} \end{aligned} \right\} \quad (9.31)$$

where

$$\tilde{\gamma}_0 = \gamma_0 - \rho_2 \text{sign } \dot{\beta}.$$

On eliminating the variable β from the first equation by means of the second equation, first considering that the instant of time at which $\text{sign } \dot{\alpha}$ and $\text{sign } \dot{\beta}$ undergo breaks in continuity are excluded from the operations, we obtain

$$\ddot{\alpha} + 2a\dot{\alpha} + a^2(1+a^2)\alpha = -a^2(\tilde{\gamma}_0 + a\rho_1 \text{sign } \dot{\alpha}). \quad (9.32)$$

The integral of this equation will be

$$\alpha = A e^{-at} \sin(\omega_0 t + \delta) + (\alpha_0)_t, \quad (9.33)$$

where

$$(\alpha_0)_t = -\frac{1}{1+a^2} (\tilde{\gamma}_0 + a\rho_1 \text{sign } \dot{\alpha}). \quad (9.34)$$

Substituting the solution eq.(9.30) in the first equation of eqs.(9.28), we get

$$\beta = A e^{-at} \cos(\omega_0 t + \delta) + (\beta_0)_t, \quad (9.35)$$

where

$$(\beta_0)_t = -\frac{a}{1+a^2} (\tilde{\gamma}_0 - \frac{\rho_1}{a} \text{sign } \dot{\alpha}). \quad (9.36)$$

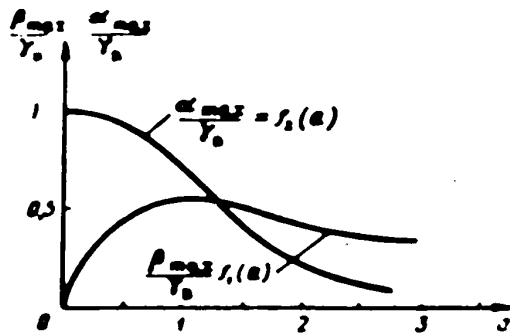


Fig.9.7 - Graphs of $\frac{\beta_{\max}}{\gamma_B} = f_1(a)$

and $\frac{\alpha_{\max}}{\gamma_B} = f_2(a)$

Thus the problem reduces to the change in the values of the coordinates of the

STAT

equilibrium position by quantities depending on the friction in the gimbals and on the values of $\dot{\alpha}$ and $\dot{\beta}$.

We remark that the relative value of these changes under actual conditions will be small, since they reduce to the algebraic addition to a quantity of the order of a few tens of degrees of the quantities p_1 and p_2 , which are of the order of a few tenths of a degree. In the interests of completeness of this study, however, let us carry it to the end.

Let us find the locus of the points in the coordinate system where $\dot{\alpha}$ and $\dot{\beta}$ change their signs.

To these loci of points there will correspond, by eq.(9.31), the straight lines

$$\alpha = a\beta - \gamma_1 + \rho_1 \text{ sign } \dot{\beta}. \quad (9.37)$$

$$\alpha = -\frac{1}{a} \beta - \frac{1}{a} \rho_1 \text{ sign } \dot{\alpha}. \quad (9.38)$$

The change of sign of $\dot{\alpha}$ takes place on the straight line of expression (9.37), while the change of sign of $\dot{\beta}$ takes place on the straight line of eq.(9.38) (left turn).

In Fig.9.8, the straight lines A_1 and A_2 (eq.(9.37) have been plotted for the case $\psi_3 > 0$. These lines are the loci of points at which $\dot{\alpha}$ changes its sign. On the same figure the straight lines B_1 and B_2 (eq.(9.38) have also been plotted, being the loci of points at which $\dot{\beta}$ changes its sign.

It is clear from eqs.(9.37) and (9.38) that the straight lines A_1 and A_2 are perpendicular to the straight line B_1 and B_2 . This follows from the fact that the product of the angular coefficients for the coordinates of β in the equations of these straight lines are equal to -1. In this case, the straight line A_1 corresponds to the conditions $\dot{\beta} > 0$ and $\text{sign } \dot{\beta} = 1$; the straight line A_2 , to the conditions $\dot{\beta} < 0$ and $\text{sign } \dot{\beta} = -1$; the straight line B_1 to $\dot{\alpha} > 0$ and $\text{sign } \dot{\alpha} = 1$; the straight line B_2 , to $\dot{\alpha} < 0$ and $\text{sign } \dot{\alpha} = -1$.

It follows from this that the change of sign of $\dot{\beta}$ means a change in the locus

STAT

of points at which the sign of $\dot{\alpha}$ can change, and conversely. We note further that the region of points for which the condition $\dot{\alpha} > 0, \dot{\beta} > 0$ will hold, lies below the

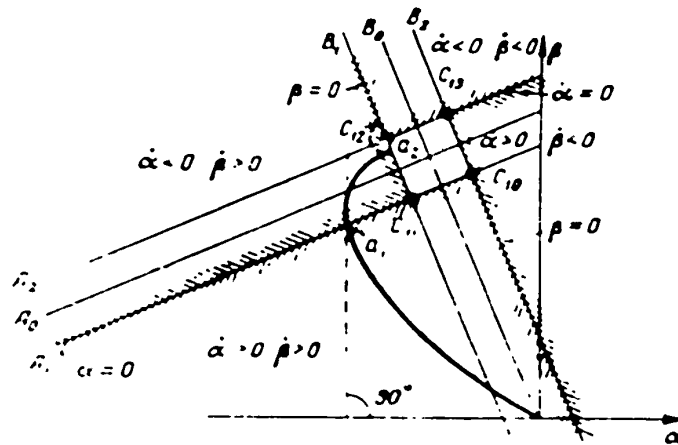


Fig.9.8 - Paths of Vertex of Gyro Horizon on Left Turn with Proportional Characteristics of Correction, Allowing for Friction in the Gimbals

A_1 and A_2 - Loci of points where $\dot{\beta}$ changes sign; B_1 and B_2 - Loci of points where $\dot{\alpha}$ changes sign; C_{10} - Initial focus of spiral; C_{11} - Eocus of spiral after intersection of vertex by straight line A at point a_1 ; C_{12} - Focus of spiral after intersection of vertex by straight line B at point a_2 , etc.

corresponding locus of points of A and B, and the region of points for which the condition $\dot{\alpha} < 0, \dot{\beta} < 0$ will be satisfied lies above these loci.

Let at the initial instant of the turn, the vertex of the gyro be at the point O, i.e., let the gyro axis coincide with the vertical. For this points, under all circumstances, $\alpha < 0$. Consequently the straight line B_2 must be taken as the locus of points where $\dot{\beta}$ can change its sign. But in that case, for $\dot{\beta}$, at the initial instant of time, the condition $\dot{\beta} > 0$ will be satisfied, and, consequently the straight line A_1 must be taken as the locus of points where $\dot{\alpha}$ changes its sign.

In connection with the signs of $\dot{\alpha}$ and $\dot{\beta}$ so established, the expressions for the coordinates of the equilibrium position at the initial instant of time may be found

STAT

by simultaneous solution of eqs.(9.37) and (9.38)

$$(\alpha_{01})_x = -\frac{1}{1+a^2} (\gamma_0 - \rho_2 - a\rho_1), \quad (9.39)$$

$$(\beta_{01})_x = \frac{a}{1+a^2} \left(\gamma_0 - \rho_2 + \frac{1}{a} \rho_1 \right). \quad (9.40)$$

Thus, at the initial instant, the spiral will be drawn from the point C_{10} , the point of intersection of the straight line A_1 and B_2 , having coordinates in accordance with eqs.(9.39) and (9.40). Let it be intersected in this case by the straight line A_1 at the point a_1 . This will mean a change of sign for $\dot{\alpha}$, and, in the first place, a corresponding change of the expressions for the coordinates of the point C_{11} of the equilibrium position, which now take the form:

$$(\alpha_{01})_x = -\frac{a}{1+a^2} (\gamma_0 - \rho_2 + a\rho_1), \quad (9.41)$$

$$(\beta_{01})_x = \frac{a}{1+a^2} \left(\gamma_0 - \rho_2 - \frac{1}{a} \rho_1 \right), \quad (9.42)$$

and secondly, the change in the locus of points of change of sign of $\dot{\beta}$ from the straight line B_2 to the straight line B_1 . It will be easily seen that as a result of these changes, the length of the radius-vector of the spiral decreases (cf.Fig.9.8).

During the further tracing of the spiral from the new center, let it intersect at the point a_2 , the straight line B_1 , which is now the locus of points of the change of sign of $\dot{\beta}$. As a result of this change, in the first place, the expressions for the coordinates of the point C_{12} of the equilibrium position will again change, and will now take the form

$$(\alpha_{01})_x = -\frac{1}{1+a^2} (\gamma_0 + \rho_2 + a\rho_1), \quad (9.43)$$

$$(\beta_{01})_x = \frac{a}{1+a^2} \left(\gamma_0 + \rho_2 - \frac{1}{a} \rho_1 \right) \quad (9.44)$$

and secondly, the locus of points of change of sign of $\dot{\alpha}$ will change from the

straight line A_1 to the straight line A_2 . As will be clear, the coordinates of the equilibrium position, that is, of the focus of the spiral, will already vary in this case to such an extent that $\dot{\beta}$ will become positive (cf. the dashed segment in Fig.9.8). But after the arrival at the straight line B_1 , the sign of $\dot{\beta}$ would have to change from positive to negative.

A contradiction thus arises, from which it follows that a further motion of the vertex (i.e., motion after it arrives at the point a_2) will no longer be possible. Consequently the point a_2 in this case will be the position of rest of the vertex.

Thus, in this case of a left turn, the friction in the gimbals favors the more rapid arrival of the gyro vertex at the equilibrium position, and also favors the deformation of its path in the direction of reducing the maximum values of the current deviations.

Let us now consider the case of a right turn. In connection with the change of sign of \dot{a} and $\dot{\gamma}_B$, the locus of points where \dot{a} and $\dot{\beta}$ change their signs are already located in the positive quadrant of $O\alpha\beta$, as indicated in Fig.9.9. In this case, the region of points for which the condition $\dot{a} > 0$ is satisfied, as in the preceding case, will lie above the corresponding straight lines A , while the region of points for which the condition $\dot{\beta} < 0$ will lie below those straight lines, the region of points for which the condition $\dot{\beta} < 0$ is satisfied will lie below the corresponding straight line B , and the region of points for which the condition $\dot{\beta} < 0$ is satisfied will lie above those lines.

For the same initial conditions as in the preceding case, we shall in this case have for the initial instant of time $\dot{a} > 0$, $\dot{\beta} < 0$, the straight lines A_2 and B_1 as the loci of points of change of sign, and the following expressions for the coordinates of the equilibrium position of the points C_{10}

$$(\alpha_{s1})_{i_0} = + \frac{1}{1+a^2} (-\gamma_s - \rho_s - a\rho_1), \quad (9.45)$$

$$(\beta_{s1})_{i_0} = - \frac{a}{1+a^2} (\gamma_s + \rho_s - \frac{\rho_1}{a}). \quad (9.46)$$

STAT

It will be seen from Fig.9.9 that the vertex of the gyro, after traveling the very short distance separating the straight line F_1 , which is the locus of points of

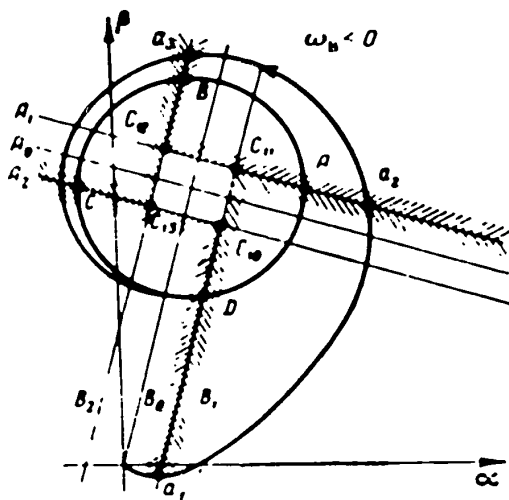


Fig.9.9 - Paths of Vertex of Gyro Horizon on Right Turn with Proportional Characteristics of Correction, Allowing for Friction in the Gimbals

A_1, A_2 - Locus of points of change of sign of $\dot{\alpha}$; B_1, B_2 - Locus of points of change of sign of $\dot{\beta}$; C_{10} - Initial focus of spiral; C_{11} - Focus of spiral beginning at point a_1 ; C - Focus of spiral beginning at point a_2 ; etc.

change of sign of $\dot{\beta}$, from its initial position as taken by us, will intersect this straight line, and in connection with this the sign of $\dot{\beta}$ will change from positive to negative, which will mean that the locus of points of change of sign of $\dot{\alpha}$ will change from the straight line A_2 to the straight line A_1 , and the expressions for the coordinates of the equilibrium of the point C_{11} will change to the following:

$$(\alpha_{e1})_{e1} = + \frac{1}{1+a^2} (-\gamma_2 + \rho_2 - a\rho_1) \tag{9.47}$$

$$(\beta_{e1})_{e1} = \frac{a}{1+a^2} \left(\gamma_2 - \rho_2 - \frac{1}{a}\rho_1 \right) \tag{9.48}$$

STAT

As a result of this change, the length of the radius vector of the vertex of the gyroscope will be increased.

On intersection with the straight line A_1 , a change of sign of $\dot{\alpha}$ takes place, in connection with which the locus of points of change of sign of $\dot{\beta}$ will change from the straight line B_1 to the straight line B_2 , and the expressions for the coordinates of the equilibrium position of the points C_{12} will change to the following

$$(\alpha_{e1})_n = + \frac{a}{1+a^2} (-\gamma_0 + \rho_2 + a\rho_1), \quad (9.49)$$

$$(\beta_{e1})_n = \frac{a}{1+a^2} \left(\gamma_0 - \rho_2 + \frac{1}{a} \rho_1 \right). \quad (9.50)$$

With this change, the length of the radius vector of the vertex will likewise increase. Let us assume that there is subsequently intersection with the straight line B_2 , which will mean the change of the locus of points of change of sign from the straight line A_1 to the straight line A_2 and the change of the expressions for the coordinates of the equilibrium position of the point C_{13} to the following:

$$(\alpha_{e1})_n = + \frac{1}{1+a^2} (-\gamma_0 - \rho_2 + a\rho_1), \quad (9.51)$$

$$(\beta_{e1})_n = \frac{a}{1+a^2} \left(\gamma_0 + \rho_2 + \frac{1}{a} \rho_1 \right), \quad (9.52)$$

as a result of which the length of the radius vector of the vertex is again increased, and so on.

The motion of the vertex of the gyro in the plane $O\alpha\beta$ leads to the establishment of a self-oscillatory closed cycle embracing the rectangle of repose. Let us derive the conditions that determine the parameter of the cycle. As the parameter of the cycle, let us take the distance from the point A of the intersection of the cycle with the straight line A_1 to the vertex C of the rectangle of repose. Let us denote this distance by r_{np} . Let us also denote the sides of the rectangle of repose as follows:

STAT

$$C_{11}C_{12} - C_{12}C_{10} = [(z_{01})_{11} - (z_{01})_{12}] \frac{1}{\cos \varphi} = \frac{2\rho_1}{1+a^2} \frac{a}{\cos \varphi} = \frac{2\rho_1}{\sqrt{1+a^2}} = b,$$

$$C_{12}C_{13} - C_{10}C_{11} = [(z_{01})_{11} - (z_{01})_{10}] \frac{1}{\cos \varphi} = \frac{2\rho_1}{(1-a^2)} \frac{a}{\cos \varphi} = \frac{2\rho_1}{\sqrt{1+a^2}} = c.$$

then, according to what has been set forth and eq.(9.27), we shall have the following system of equations describing the motion of the gyro vertex along the limit cycle:

$$\begin{aligned} BC_{12} &= AC_{12}e^{2a} = (AC_{11} + b)e^{2a}; \\ CC_{12} &= BC_{12}e^{2a} = (BC_{12} + C)e^{2a}; \\ DC_{10} &= CC_{10}e^{2a} = (CC_{12} + b)e^{2a}; \\ AC_{11} &= DC_{11}e^{2a} = (DC_{10} + C)e^{2a}. \end{aligned}$$

Since for a right turn $\gamma_B < 0$, it follows that $\omega_B < 0$, $\alpha < 0$ and the angles $\varphi < 0$.

From the equations so obtained, we find:

$$r_{np} = \left[\left[(r_{np} + b)e^{\frac{\pi}{2a}} + C \right] e^{\frac{\pi}{2a}} + b \right] e^{\frac{\pi}{2a}} + C \Big] e^{\frac{\pi}{2a}}.$$

Thus the parameter of the limit cycle is determined from the following condition

$$r_{np} = \frac{be^{\frac{\pi}{2a}} + ce^{\frac{\pi}{2a}}}{1 - e^{\frac{\pi}{2a}}}. \quad (9.53)$$

For the special case where the rectangle of repose is a square, and $b = c$, we get

$$r_{np} = \frac{be^{\frac{\pi}{2a}}}{1 - e^{\frac{\pi}{2a}}}$$

STAT

$$r_{np} = \frac{b}{\pi} \frac{1}{\omega} \quad (9.54)$$

We shall now show that this cycle is stable. Let the vertex of the gyro at the initial instant of time be on the straight line A_1 at the distance $\pm r$ from the point C, which is the point of intersection of the limit cycle with the straight line A_1 . Then, by analogy to the preceding, we may determine the position of the vertex of the gyro on the straight line A_1 after it has described one loop of the spiral:

$$r_1 = \left| \left| (r_{np} \pm \Delta r) e^{2\pi a} + c \right| e^{2\pi} + b \right| e^{2\pi} - c \left| e^{2\pi} \right.$$

Whence we obtain, taking eq.(9.53) into consideration:

$$r_1 = r_{np} + \Delta r e^{2\pi a}$$

After the second loop of the spiral, the distance from the gyro vertex to the limit cycle along the straight line A_1 will be equal to

$$r_2 = r_{np} + \Delta r e^{2 \cdot 2\pi a}$$

and, after the n-th loop it will be equal to

$$r_n = r_{np} + \Delta r e^{n \cdot 2\pi a}$$

Since the quantity $\Delta r e^{\frac{2\pi}{a} n} \rightarrow 0$ as $n \rightarrow \infty$, the vertex of the gyro will approach the limit cycles, moving along the spiral.

We remark that the vertex of the gyro will approach the limit cycle, both when it is inside the limit cycle at $-\Delta r$, and in the case when it is outside the limit cycle at Δr .

STAT

It follows from the presence of the limit cycle in a right turn that the gyro vertical will have a greater error on a right turn than on a left turn. The left turn is used more in aviation (in landing, in formation flying of aircraft). In this connection the gyro vertical should have a kinetic moment directed upward. If the kinetic moment is directed in the opposite way, the expression of error will be greater for the more usual left turn.

Let us now calculate the value of the maximum deflections of the vertex of the gyro on a right turn when moving along the limit cycle. The maximum deviation along the axis will be at the point A, the point of intersection between the straight line A_1 and the limit cycle. The coordinate $(\alpha_{\min})_{\max}$ of this point is determined from the formula

$$(\alpha_{\min})_{\max} = (\alpha_{\min})_{pl} + r_{np} \cos(\pi - \varphi),$$

where $(\alpha_{pl})_{pl}$ = coordinate along α axis of point C_{11} , is determined by eq.(9.47);

φ = angle between straight line A_1 and $O\alpha$ axis, determined from eq.

$$(9.28);$$

r_{np} = limiting radius of cycle, determined by eq.(9.53).

On substituting the value of $(\alpha_{pl})_{pl}$, r_{np} and $\cos \varphi$, we obtain the following formula:

$$(\alpha_{\min})_{\max} = \frac{1}{1 - a_2} \left[-\gamma_0 + \beta_2 - a_2 \alpha_1 - 2a_2 \frac{\beta_1 + \beta_2 - \frac{\pi}{2a}}{a - 1} \right]. \quad (9.55)$$

The maximum deviation along the β will be at point B, the point of intersection of the straight line B_2 with the limit cycle. The coordinate $(\beta_{np})_{\max}$ of this point is determined by the formula

$$(\beta_{np})_{\max} = (\beta_{pl})_{pl} - (r_{np} + b) e^{-\frac{\pi}{2a}} \cos \varphi.$$

where $(\beta_{pl})_{pl}$ = coordinate of point C_{12} , determined by eq.(9.50)

STAT

$$b = C_{11}C_{12} = \frac{2\gamma_0}{1+a^2}$$

After substituting the values of $(\beta_{Bl})_{p2}$, r_{np} , b and $\cos \varphi$, we get

$$(\gamma_0)_{max} = \frac{1}{1+a^2} \left[a\gamma_0 - a\gamma_2 \cdot \rho_1 - \frac{2 \left(\rho_2 + \frac{2a}{c} \right) \left(\frac{\pi}{2a} \right)}{c \frac{\pi}{2a} - 1} \right] \quad (9.56)$$

For $p_1 = p_2 = p$, eq.(9.55) and eq.(9.56) take the following form:

$$(\gamma_0)_{max} = \frac{1}{1+a^2} \left[-\gamma_0 + \rho(1-a) - \frac{2ap}{c \frac{\pi}{2a} - 1} \right] \quad (9.57)$$

$$(\gamma_{np})_{max} = \frac{1}{1+a^2} \left[a\gamma_0 + \rho(1-a) - \frac{2ap}{c \frac{\pi}{2a} - 1} \right] \quad (9.58)$$

The quantities $(\alpha_{np})_{max}$ and $(\beta_{np})_{max}$ may be represented as follows:

$$(\alpha_{np})_{max} = \alpha_{01} + R, \quad (9.59)$$

$$(\beta_{np})_{max} = \beta_{01} + R, \quad (9.60)$$

where α_{Bl} and β_{Bl} are the coordinates of the equilibrium position of the gyro vertex on a turn in the absence of friction, as determined by eqs.(9.19) and (9.21);

R = maximum deviation of gyro vertex along the α and β axes from the point of equilibrium position with coordinates $(\alpha_{Bl}, \beta_{Bl})$ on motion along the limit cycle

$$R = \frac{1-a}{1+a^2} \rho - \frac{2a}{(1+a^2) \left(c \frac{\pi}{2a} - 1 \right)} \rho$$

Let us determine how the value of R varies with variation of the angular velocity of a right turn ω_B from 0 to $-\infty$, that is, on variation of a from 0 to $-\infty$

$$\lim_{a \rightarrow 0} R = \lim_{a \rightarrow 0} \left[\frac{1-a}{1+a^2} \rho - \frac{2a}{(1+a^2) \left(c \frac{\pi}{2a} - 1 \right)} \rho \right] = \rho - \rho \lim_{a \rightarrow 0} \frac{2a}{c \frac{\pi}{2a} - 1}$$

STAT

We obtain finally

$$\lim R \rightarrow \rho.$$

But as $a \rightarrow 0$, $\alpha_{Bl} \rightarrow 0$ and $\beta_{Bl} \rightarrow 0$, while the sides of the rectangle of repose $b \rightarrow 2p$. In accordance with this, as $a \rightarrow 0$, the limit cycle approaches the rectangle of repose.

Let us now determine the value of R as $a \rightarrow -\infty$:

$$\lim_{a \rightarrow -\infty} R = \lim_{a \rightarrow -\infty} \left[\frac{1 + a^2 \rho - \frac{2a}{(1+a^2)} \left(e^{-\frac{\pi}{2a}} - 1 \right)}{1 + a^2} \right] = \lim_{a \rightarrow -\infty} \frac{2a}{e^{-\frac{\pi}{2a}} - 1}.$$

On expanding the indeterminate expression by L'Hospital rule, we get

$$\lim_{a \rightarrow -\infty} R = \frac{4}{\pi} \rho. \tag{9.61}$$

We may make sure that

$$\frac{dR}{da} = \frac{a^2 - 2a}{(1+a^2)^2} \rho + \frac{[(2\pi - 2) + (2\pi + 2)a^2] e^{-\frac{\pi}{2a}} + 2(1-a^2)}{(1+a^2)^2 \left(e^{-\frac{\pi}{2a}} - 1 \right)^2} > 0$$

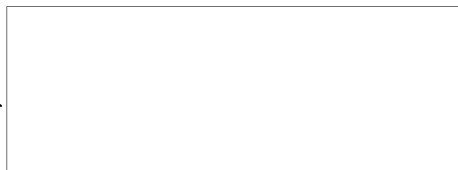
as a varies from 0 to $-\infty$. Accordingly, R increases monotone from ρ to $\frac{4}{\pi} \rho$ as a varies from 0 to $-\infty$. For $|a| > 1$, $R \approx \frac{4}{\pi} \rho$, $\beta_{Bl} > \alpha_{Bl}$, and the maximum deviation of the gyro vertex from the origin of coordinates, when moving along the limit cycle, is determined according to eq.(9.60) from the following formula:

$$(\beta_{np})_{max} = \frac{a \gamma_n}{1+a^2} + \frac{4}{\pi} \rho. \tag{9.62}$$

On replacing a by $\frac{\omega_{\beta}}{\varepsilon}$ and p by $\frac{i_{\rho}}{\varepsilon i}$, we get

$$(\beta_{np})_{max} \approx \frac{\varepsilon \omega_{\beta}}{\varepsilon^2 \cdot \omega_{\beta}^2} \gamma_n + \frac{4}{\pi} \frac{L_p}{\varepsilon i} \approx \frac{\gamma_n}{\omega_{\beta}} + \frac{4}{\pi} \frac{L_p}{\varepsilon i}. \tag{9.63}$$

Let us determine the value of ε_0 for which $(\beta_{np})_{max}$ takes the minimum value for a given ratio $\frac{\gamma_{\beta 0}}{\omega_{\beta 0}}$. For this purpose, let us set the derivative of $(\beta_{np})_{max}$ with respect to ε equal to 0:



STAT

$$\left. \begin{aligned} \frac{d(\beta_{np})_{max}}{dt} - \frac{\gamma_{\infty}}{\omega_{\infty}} - \frac{4L_p}{\pi \epsilon_0^2 H} &= 0, \\ \epsilon_0 &= \sqrt{\frac{4L_p \omega_{\infty}}{H \pi \gamma_{\infty}}} \end{aligned} \right\} \quad (9.64)$$

For ϵ_0 we shall have

$$\begin{aligned} \beta_{n1} = R_0 &= \frac{\omega_{\infty}}{\omega_{B0}} = \frac{4}{\pi} \frac{L_p}{\epsilon_0 H} = \frac{4}{\pi} \rho; \\ (\beta_{np})_{max} &= \frac{8}{\pi} \frac{L_p}{\epsilon_0 H} = \frac{8}{\pi} \rho. \end{aligned} \quad (9.65)$$

Let us now determine the value of the maximum deviation of the gyro vertex from the origin of coordinates on motion along the limit cycle on of $(\beta_{np})_{max}$ for the selected value of ϵ_0 and the other values of $\frac{\gamma_B}{\omega_B}$. For this purpose, let us substitute in eq.(9.63) for ϵ_0 its value as determined according from eq.(9.64):

$$(\beta_{np})_{max} = \sqrt{\frac{4L_p \omega_{\infty}}{\pi H \gamma_{\infty}} \gamma_{\infty} + \frac{4L_p}{\pi H} \sqrt{\frac{\pi H \gamma_{\infty}}{4L_p \omega_{\infty}}}}$$

After simple transformations we get

$$\beta_{np})_{max} = \sqrt{\frac{4L_p}{\pi H} \frac{\gamma_{\infty}}{\omega_{\infty}} + \frac{\gamma_{\infty}}{\omega_{\infty}}} \quad (9.66)$$

Figure 9.10 shows the variation of the value of $\frac{\gamma_B}{\omega_B}$ on variation of ω_B from 0 to $-\infty$. In fact, as $\omega_B \rightarrow 0$,

$$\lim_{\omega_B \rightarrow 0} \gamma_{\infty} = \lim_{\omega_B \rightarrow 0} \frac{\text{arctg} \frac{\omega_B V}{R}}{\omega_B} = \frac{V}{R},$$

as $|\omega_B| \rightarrow \infty$, $|\frac{\gamma_B}{\omega_B}|$ decreases monotone, and approaches 0 as $|\omega_B| \rightarrow \infty$.

If for $\frac{\gamma_{B0}}{\omega_{B0}}$ we take its maximum value A, obtained in the actual range of ω_B and aircraft speeds V, then $(\beta_{np})_{max}$ will vary with the variation of $\frac{\gamma_B}{\omega_B}$ within the STAT

limits

$$\frac{A+B}{2} \sqrt{\frac{H}{\pi H}} \cdot (\beta_{np})_{max} \cdot 2 \sqrt{\frac{4L_2}{\pi H}} \quad (9.67)$$

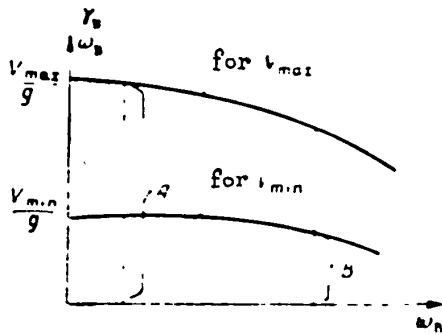
where B - minimum value of $\frac{Y_B}{\omega_B}$ for v_{max} . If, however, we take the value B for $\frac{Y_{B0}}{\omega_0}$, then

$$2 \sqrt{B} \sqrt{\frac{4L_2}{\pi H}} < (\beta_{np})_{max} \cdot \frac{A+B}{2} \sqrt{\frac{H}{\pi H}} \quad (9.68)$$

Taking the inequality $A > B$ into account, we have the following inequalities

$$\frac{A+B}{2} \geq A \quad (9.69)$$

$$\frac{A+B}{2} \geq B \quad (9.70)$$



since the arithmetic mean is greater than the geometric mean.

Further,

$$2 \sqrt{A} \geq \frac{A+B}{2} \quad (9.71)$$

Fig. 9.10 - Graphs of $\frac{Y_B}{\omega_B} = f(\omega_B)$ for v_{max} and v_{min}

From the inequalities (9.69), (9.70), and (9.71), we obtain

$$\frac{A+B}{2} \geq A > \frac{A+B}{2} \geq B \quad (9.72)$$

The conclusion may be drawn on the basis of eqs.(9.67), (9.68) and (9.72) that to reduce the turning errors, the value of ϵ_0 should be selected for the maximum value of the ratio $\frac{Y_B}{\omega_B}$, equal to about $\frac{v_{max}}{g}$.

Then from eqs.(9.64) and (9.65) we get

$$\epsilon_0 = \sqrt{\frac{4L_2}{\pi H} \frac{g}{v_{max}}} \quad (9.73)$$

STAT

$$(\beta_{np})_{max} = 4 \sqrt{\frac{L_p}{\pi l} \frac{V_{max}}{g}} \tag{9.74}$$

To illustrate these conclusions we present an example. Let $\frac{L_p}{\pi l} = 0.000314$ 1/sec, and let the speed vary from 100 m/sec to 300 m/sec.

In this case let us assume that $\left(\frac{Y_B}{\omega_B}\right)_{min} = 10$ sec, $\left(\frac{Y_B}{\omega_B}\right)_{max} = 30$ sec. Then, if we select ϵ_0 according to $\left(\frac{Y_B}{\omega_B}\right)_{min}$, we shall have, by eq.(9.66):

$$\epsilon_0 = 0.0063 \text{ 1/sec.}$$

for $\frac{Y_B}{\omega_B} = 10$ sec. $(\beta_{np})_{max} = 0.126 = 7.2$.

for $\frac{Y_B}{\omega_B} = 30$ sec. $(\beta_{np})_{max} = 0.253 = 14.5$.

If we select ϵ_0 according to $\left(\frac{Y_B}{\omega_B}\right)_{max}$, we shall obtain, analogously: $\epsilon = 0.0036$ 1/sec

for $\frac{Y_B}{\omega_B} = 10$ sec. $(\beta_{np})_{max} = 0.139 = 7.9^\circ$,

for $\frac{Y_B}{\omega_B} = 30$ sec. $(\beta_{np})_{max} = 0.219 = 12.5^\circ$.

Since for $\frac{Y_{B0}}{\omega_{B0}}$, by eq.(9.65), $\rho_{B1}^0 = R^0$, it follows that the limit cycle will practically pass through the origin of coordinates (Fig.9.11). If the ratio $\frac{Y_B}{\omega_B}$

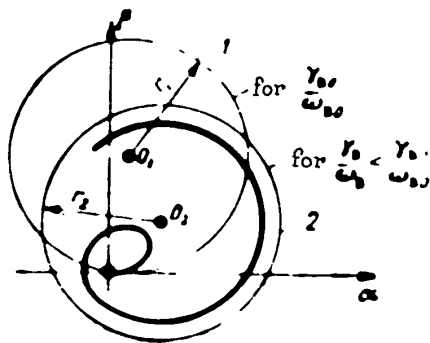


Fig.9.11 - Limit Cycles:

Curve 1, for $\frac{Y_{B0}}{\omega_{B0}}$;

Curve 2, for $\frac{Y_B}{\omega_B} < \frac{Y_{B0}}{\omega_{B0}}$.

for any duration of turn.

decreases on account of the decrease in the velocity v or the increase of ω_B , then this will lead to the decrease of β_{B1} with the radius of the limit cycle being maintained practically the same. In this case the origin of coordinates comes inside the limit cycle. The vertex of the gyro will approach the limit cycle from inside, while the value of the maximum error will not exceed the values given in eq.(9.74)

STAT

Turning Deviations of Gyro Horizon with Constant Characteristic of Correction

On substituting in eq.(9.1) the expressions for p and q according to eq.(9.10) and the expressions for L_x and L_y according to the conditions of the constant characteristic, taking it as being hysteresis-free and without a zone of insensitivity, and also bearing the conditions of eqs.(9.11) and (9.12) in mind, we obtain the equations of motion in the following form:

$$\begin{aligned} H(\dot{\alpha} - \omega_0 \beta) &= -k_2 \operatorname{sign}(\alpha + \gamma_0) + L_1 \operatorname{sign} \beta, \\ H(\dot{\beta} + \omega_0 \alpha) &= -k_1 \operatorname{sign} \beta - L_2 \operatorname{sign} \alpha. \end{aligned} \quad (9.75)$$

or

$$\left. \begin{aligned} \dot{\alpha} - \omega_0 \beta - \omega_{2j} [\operatorname{sign}(\alpha + \gamma_0) - \kappa_{21} \operatorname{sign} \beta], \\ \dot{\beta} + \omega_0 \alpha - \omega_{1j} [\operatorname{sign} \beta + \kappa_{12} \operatorname{sign} \alpha]. \end{aligned} \right\} \quad (9.75a)$$

where n_j , $j = \frac{1, 2}{1, 2}$, the second digit of the subscript indicating the number of the moment of friction L_j , the first digit the number of the moment of correction K .

Let us for the time being reject the terms characterizing the influence of friction, and let us rewrite the equations so obtained in the following form:

$$\left. \begin{aligned} \dot{\alpha} - \omega_0 \beta &= -\omega_{2j} \operatorname{sign}(\alpha + \gamma_0), \\ \dot{\beta} + \omega_0 \alpha &= -\omega_{1j} \operatorname{sign} \beta. \end{aligned} \right\} \quad (9.76)$$

Assuming, as usual, that the operation of differentiation does not include those moments of time when $\operatorname{sign}(\alpha + \gamma_0)$ and $\operatorname{sign} \beta$ undergo a break in continuity, that is, when $\alpha + \gamma_0$ and β change their signs, we find it possible to operate an eq.(9.76) as on linear equations.

Taking this into account, let us eliminate the variable β from the first equation by the aid of the second equation. As a result we obtain

$$\alpha + \omega_0^2 \alpha = -\omega_{2j}^2 b_1 \operatorname{sign} \beta, \quad (9.77)$$

where

$$b_1 = \frac{\omega_{2j}^2}{\omega_0}. \quad (9.78)$$

STAT

The integral of this equation will be the expression

$$\alpha = A \sin(\omega_p t + \delta) + \alpha_{s2}, \quad (9.79)$$

where

$$\alpha_{s2} = -b_1 \operatorname{sign} \dot{\alpha}. \quad (9.80)$$

A and δ are arbitrary constants.

On substituting the solution eq.(9.79) in the first of eqs.(9.76), we find

$$\beta = A \cos(\omega_p t + \delta) + \beta_{s2}, \quad (9.81)$$

where

$$\beta_{s2} = b_2 \operatorname{sign}(\alpha + \gamma_p). \quad (9.82)$$

$$b_2 = \frac{\omega_p^2}{\omega_n^2}. \quad (9.83)$$

Thus both α and β are periodic functions in this case.

In other words, in contrast to the preceding case of proportional correction characteristics, in this case, with constant correction characteristics, there exists no position of stable equilibrium for the gyro axis in the process of turning. We shall specially dwell on this circumstance somewhat later.

Let us transfer α_{B2} and β_{B2} to the left side of eq.(9.79) and eq.(9.81) respectively, square the equations so obtained, by parts, and add these parts, as a result of which we obtain

$$(\alpha - \alpha_{s2})^2 + (\beta - \beta_{s2})^2 = A^2 \quad (9.84)$$

The equation so obtained will be the equation of the path of the gyro vertex in $O\alpha\beta$ coordinates. As will be clear it is the equation of a circle with α_{B2}, β_{B2} as the coordinates of its center.

However, before making use of this equation to construct the path of the vertex, we must first determine the locus of points passage through which involves a break in the continuity of $\operatorname{sign}(\alpha + \gamma_p)$ and $\operatorname{sign} \dot{\beta}$.

Let the vertex of the gyro be located at the initial instant of time at the origin of coordinates $O\alpha\beta$ (that is, the gyro axis was in the local vertical). In this case, for the initial instant of time, for a left turn $\gamma > 0$, the condition STAT

$$\text{sign}(\alpha + \gamma_s) = 1$$

will obtain, and, consequently, on the basis of eq.(9.76), the condition

$$\alpha < 0$$

and the corresponding accumulation of the negative value of α .

The positive term $\omega_B \alpha$ will therefore accumulate in eq.(9.76) for β . But motion along the axis $O\beta$ cannot at first take place, since on appearance of a small positive value of β , on account of the positive $\dot{\beta}$, the negative term ω_{K1} will appear with a jump in the expression for $\dot{\beta}$, and this term will at first exceed in modulus the positive term $\omega_B \alpha$. Therefore β will vary with a jump from its positive value to some negative value, and on account of this, the positive value of β , which appears at first, and is as small as may be desired, will be eliminated.

Things will proceed in this way until the condition

$$\omega_B \alpha > \omega_{K1}$$

begins to be satisfied, that is, until α reaches in modulus a value satisfying the condition

$$|\alpha| > b_1$$

By satisfying this condition the existence of the already discontinuous function

$$\dot{\alpha} > 0$$

will be assured; which will mean the accumulation of the continuous function

$$\dot{\alpha} > 0$$

as well.

In this way, in the range of values

$$0 > \alpha > -b_1 \quad (9.85)$$

the vertex of the gyro will move along the axis $O\alpha$ toward the negative values of α .

Beginning with the value

$$\alpha = -b_1 \quad (9.86)$$

the path will already be determined by eq.(9.84) for

STAT

$$\text{sign}(a - \gamma_0) = 1 \quad \text{or} \quad \text{sign } \beta = -1.$$

Let us find the time that will elapse from the instant the turn begins until the condition

$$a = -b_1,$$

is satisfied.

The motion of the gyro vertex during this time will obey the law

$$a = -\int_0^t \omega_{K1} dt,$$

or, bearing in mind the fact that ω_{K1} is constant,

$$a = -\omega_{K1} t.$$

Whence, after replacing a according to eq.(9.86) and introducing the notation t_1 for the required time interval, we obtain

$$t_1 = \frac{1}{\omega_{K1}}.$$

i.e., the required time interval will be equal to the $\frac{1}{2\pi}$ part of the period of the turn.

The initial conditions for determining the arbitrary constant for the next part of the path will be

$$\begin{aligned} a &= b_1, \\ \beta &= 0, \end{aligned}$$

whence, bearing in mind eqs.(9.80) and (9.82), we get

$$A^2 = b_1^2. \quad (9.87)$$

If, in addition to the above, we take, as is usual, and occurs, $\omega_{K1} = \omega_{K2} = \omega_K$, which means $b_1 = b_2 = b$, and assume that during the motion of the vertex of the gyro around the circle, the coordinate of this vertex remains in modulus less than γ_B , then we get the result that the remaining part of the path will be a circle inscribed in the quadrant $\alpha\beta$ with the coordinates $(-b, b)$ for the center, where b is considered a positive quantity (Fig.9.12a). For a right turn, the center of the circle will have the coordinates $(+b, b)$.

STAT

If the condition

$$b_1 = b_2$$

obtains, considering that b_1 and b_2 are quantities essentially positive, then the path will likewise be a circle with $(\mp b_1, b_2)$ as the coordinates of the center, tangent to only one axis $O\alpha$ and either not reaching axis $O\beta$, for $b_1 > b_2$ or else intersecting it (for $b_1 < b_2$).

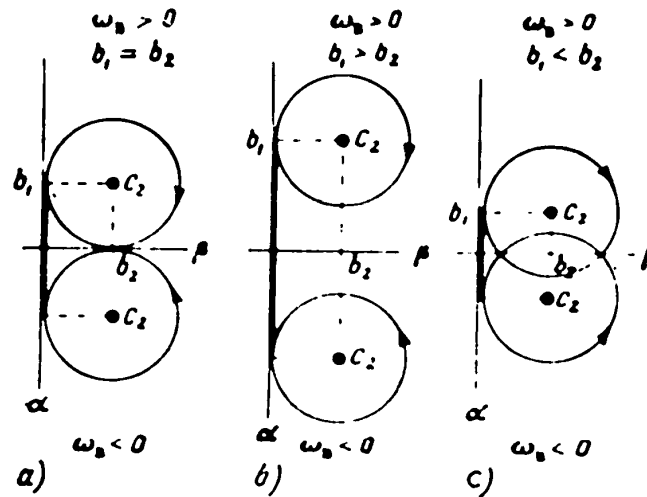


Fig. 9.12 - Paths of Motion of Vertex of Gyrohorizon with Constant Characteristics of Correction on Motion of the Vertex of the Gyroscope from the Origin of Coordinates

Let us find the locus of possible positions of the centers of the circle so found with varying ω_p , limited by the condition that

$$\omega_{s1} = \omega_{s2} = \omega_k$$

By eliminating ω_t from eqs. (9.80) and (9.82), for this purpose, we get

$$a_{s1} = \mp 3a_{s2}$$

where the upper sign corresponds to a left turn and the lower sign to a right turn.

Thus these loci will be straight lines with an angular coefficient equal in modulus to unity, with increasing distance of the points of the straight lines from the origin of coordinates corresponding to decrease of ω_p (Fig. 9.13).

STAT

As ω_B decreases, the radius of the circle increases, reaching, at $\omega_B = \omega_{B\text{kp}}$, its maximum value, equal to $\frac{\gamma_B}{2}$ (Fig.9.14). Taking account of eqs.(9.78) and (9.83), we shall have for $\omega_B = \omega_{B\text{kp}}$:

$$\omega_{\text{kp}} = \frac{\gamma_B}{2}$$

Since we may take $\omega_B \approx \frac{\omega_{13}V}{g}$ (for banks that are not very great), we shall have

$$\omega_{\text{kp}} = \sqrt{\frac{2\omega_{13}g}{v}}, \quad \gamma_B = \sqrt{\frac{2\omega_{13}V}{g}}$$

For $\omega_B > \omega_{B\text{kp}}$, the maximum turning errors are determined by the formula

$$\alpha_{\text{max}} = \beta_{\text{max}} = 2b. \tag{9.88a}$$

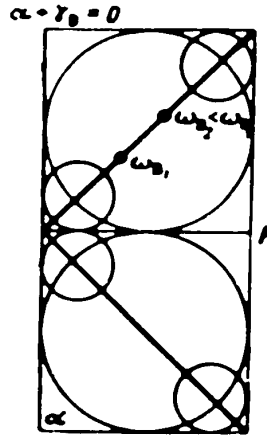


Fig.9.13 - Locus of Point of Centers of Circles Described by the Vertex of Gyro Horizon during a Turn, with Constant Characteristics of Correction, Allowing for Friction

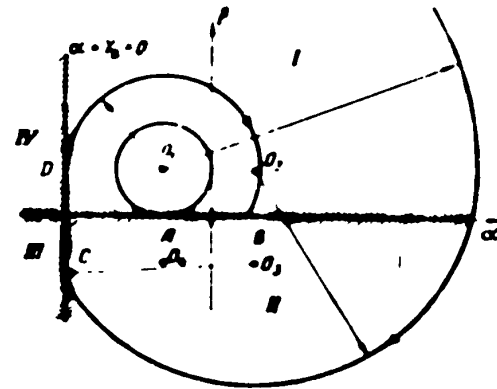


Fig.9.14 - Path of Motion of Vertex of Gyro Horizon with Constant Characteristics of Correction when the Gyro Vertex Moves from an Arbitrary Point

For $\omega_B < \omega_{B\text{kp}}$, the limit circles touch the straight line $\alpha + \gamma_B = 0$ and $\beta = \gamma_B$, and the maximum errors are determined by the formula

$$\alpha_{\text{max}} = \beta_{\text{max}} = \gamma_B. \tag{9.88b}$$

Usually $\omega_B > \omega_{B\text{kp}}$, and the maximum turning errors are determined by eqs. (9.88a).

All the... have enumerated are presented in Figs.9.12. It is easy to STAT

see that, beginning at the instant of time when the vertex of the gyro enters on the circle, the behavior of the gyro will be analogous to the behavior of an undamped gyro pendulum with its equilibrium point at the center of the circle C_2 . In this case a left turn will correspond to the lower position of the center of gravity in the gyro pendulum, and a right turn to the upper position.

We have discussed the motion of the gyro vertex during a turn in the case when it was at the origin of coordinates. It can be shown that at any initial position whatever it will move during a turn along the circle determined by us and having the radius b_2 . For this we remark that the straight lines $\alpha + \gamma_B = 0$ and $\beta = 0$ divide the entire plane into four quadrants (Fig. 9.13) in each of which the motion proceeds along the circles with centers at the points $O_1, O_2, O_3,$ and O_4 having the coordinates α_{B2} and β_{B2} according to eqs. (9.60) and (9.62):

in first quadrant: $\alpha + \gamma_B > 0, \beta > 0, \alpha_{B2} = -b_1, \beta_{B2} = -b_2,$

in second quadrant: $\alpha + \gamma_B > 0, \beta < 0, \alpha_{B2} = b_1, \beta_{B2} = b_2,$

in third quadrant: $\alpha + \gamma_B < 0, \beta < 0, \alpha_{B2} = b_1, \beta_{B2} = -b_2,$

in fourth quadrant: $\alpha + \gamma_B < 0, \beta > 0, \alpha_{B2} = -b_1, \beta_{B2} = -b_2.$

Figure (9.13) gives a construction for the motion of the gyro vertex from an arbitrary point. With this construction it was taken into account that when the gyro vertex reaches the points of the segments $AB = 2b_1$ or $CD = 2b_2$, it will move along these segments according to what has been said on page 148. As a result of this construction we may convince ourselves that the vertex of the gyroscope moves along a circle of radius b_2 .

Example. Taking $\omega_{K1} = \omega_{K2} = \omega_K = 6^\circ/\text{min}$, we get for $\omega_B = \frac{2\pi}{60} \text{ l/sec}$, i.e., for a turn the full circle of which is completed in 1 min,

$$\alpha_{\text{max}} - \beta_{\text{max}} \approx 2$$

For $\omega_{K1} = \omega_{K2} = 6^\circ/\text{min}$ and $v = 150 \text{ m/sec} = 540 \text{ km/hour}$. The maximum error is determined as:

STAT

$$\gamma = \sqrt{2 - \alpha} V = 0.23 \approx 13.$$

The values of ω_K taken by us correspond to the order of this quantity that is ordinarily used in actual practice. As will be clear, with this order of ω_K , the maximum values of the turning deviation with constant characteristics of correction have a considerable magnitude. For this reason, even with a constant characteristics of correction, it is necessary to shut off the corrector.

Let us elucidate the influence of friction in the gimbals on the behavior of a gyro horizon with constant characteristic of correction during a turn.

We remark first of all that, from the above noted analogy in the behavior of the gyro in the case we are considering to the behavior of a gyro pendulum, it may be expected that the influence of friction in the gimbals in this case will have the same effect as the influence of this friction on the gyro pendulum. More specifically, with a left turn, for which the analogy with the behavior of the lower gyro pendulum holds true, the friction in the gimbals will encourage the transformation of the motion of the vertex of the gyro along a circle into motion along an involutorial spiral; with a right turn, for which the analogy with the behavior of the upper gyro pendulum holds, the friction in the gimbals will encourage the transformation of the circular motion into motion along an evolutionary spiral. And this has been confirmed.

As follows from eq.(9.75), allowance for the friction in the gimbals modifies, in the first place, the value of the factors before ω_{K1} and ω_{K2} in modulus, and in the second place adds, as instants of time when these factors undergo a break in continuity, those instants when $\dot{\alpha}$ and $\dot{\beta}$ change their signs, in addition to the instants of time when $(\alpha + \gamma_B)$ and β change their signs.

On excluding from the operation, in addition to the former instants of time when $(\alpha + \gamma_B)$ and β change their signs, these new instants of time as well, we are

(9.75), as before, as linear equations. On doing this under STAT

same procedure as before, we obtain solutions in the following form:

$$\left. \begin{aligned} \alpha &= A \sin(\omega_0 t + \delta) + (\alpha_{02})_t, \\ \beta &= A \cos(\omega_0 t + \delta) + (\beta_{02})_t. \end{aligned} \right\} \quad (9.89)$$

where

$$\left. \begin{aligned} (\alpha_{02})_t &= -b_1 (\text{sign } \beta + n_{12} \text{sign } \dot{\alpha}), \\ (\beta_{02})_t &= b_2 [\text{sign}(\alpha + \gamma_0) - n_{21} \text{sign } \dot{\beta}]. \end{aligned} \right\} \quad (9.90)$$

or, eliminating the time,

$$[\alpha - (\alpha_{02})_t]^2 + [\beta - (\beta_{02})_t]^2 = A^2. \quad (9.91)$$

Let, for $t = 0$ $\alpha = 0$, $\beta = 0$. Then, by eq.(9.75), $\dot{\alpha} < 0$, and, consequently, $\dot{\beta} > 0$. Thus at the initial instant of time, the negative values of α and the positive values of β begin to accumulate. The first accumulation can take place without hindrance for a certain definite time, but a second accumulation cannot be accomplished, since at a negative value of β , no matter how small in modulus, the correction on angle β is already turned on, that is,

$$\text{sign } \dot{\beta} = -1$$

appears and $\dot{\beta}$ becomes negative, and, consequently, this positive value of β will be liquidated.

This will continue until

$$\alpha = -b_1(1 - n_{12}) \quad (9.92)$$

is satisfied. Since in this case, under all conditions, on account of γ_B , the value of $\dot{\alpha} < 0$ still persists, then, consequently, on account of the persisting accumulation of negative values of α , the appearance of $\dot{\beta} > 0$ can still be possible.

As a result, the accumulation of positive β begins, and, beginning at this instant, the equation of path of the vertex of the gyro according to eq.(9.91) already becomes applicable, however, taking into account the fact that when $\dot{\alpha}$ and $\dot{\beta}$ change their signs, the values of $(\alpha_{B2})_p$ and $(\beta_{B2})_p$, i.e., the coordinates of the center of the circle by eq.(9.90), will also vary accordingly.

Let us find the loci of points where $\dot{\alpha}$ and $\dot{\beta}$ will change signs. From eq.(9.75)

STAT

it follows that these loci will be respectively the straight lines A and B (Fig.9.15), defined by the equations

$$\beta = b_2 (\text{sign } \alpha + \gamma_0) - n_{21} \text{sign } \dot{\alpha}, \quad (9.93)$$

$$\alpha = -b_1 (\text{sign } \beta + n_{12} \text{sign } \dot{\beta}).$$

Since, directly after the instant that eq.(9.92) is satisfied, as has been shown, the values

$$\begin{aligned} \alpha < 0, \quad \dot{\alpha} < 0, \quad \alpha + \gamma_0 > 0, \\ \beta > 0, \quad \dot{\beta} > 0, \end{aligned}$$

will hold, then, consequently, the coordinates of the initial position of the center of the circle, being the point of intersection, C_{21} , of the straight lines A_1 and B_2 , are defined by the expressions

$$(\alpha_{C_{21}})_1 = -b_1 (1 - n_{12}), \quad (9.93a)$$

$$(\beta_{C_{21}})_1 = b_2 (1 - n_{21}), \quad (9.93b)$$

while the equation of the locus of points of change of sign of $\dot{\alpha}$, which will be the first to be intersected by the path of the gyro vertex, will take the form (cf. straight line A_1 on Fig.9.15)

$$\beta = b_2 (1 - n_{21}).$$

When this intersection takes place, then as a result of the change of sign of $\dot{\alpha}$, the expression for the coordinate of the center of the circle α_{B2} also changes to the following

$$(\alpha_{B2})_2 = -b_1 (1 + n_{12}). \quad (9.93c)$$

As will be easily seen (cf. Fig.9.14), as a result of this change of sign of $\dot{\alpha}$, the component of the radius of the circle along the axis $O\alpha$ decreases by the quantity

$$\Delta \alpha = 2b_1 n_{12}.$$

or, bearing in mind the expressions for b_1 and n_{12} :

$$\Delta \alpha = 2 \frac{L_n}{H_{\omega_0}}. \quad (9.94)$$

STAT

In the subsequent motion, the path of the gyro vertex intersects the locus of points of change of sign of $\dot{\beta}$, the equation of which is defined by the expression

$$\alpha = -b_1(1 + n_{12}).$$

When this intersection takes place, then, as a result of the change of sign of $\dot{\beta}$, the expression for the coordinate of the center of the circle $(\beta_{B2})_p$ changes to the following

$$(\beta_{B2})_p = b_2(1 + n_{21}). \quad (9.93d)$$

As a result of this change of sign of $\dot{\beta}$, the component of the radius of the circle along the axis $O\beta$ decreases by the quantity

$$\Delta\beta = 2b_2n_{21}.$$

or, bearing in mind the expressions for b_2 and n_{21} ,

$$\Delta\beta = 2 \frac{L}{H\omega_s}. \quad (9.95)$$

Fig.9.15 - Path of Motion of Vertex of Gyrohorizon during a Left Turn with Constant Characteristics of Correction, Allowing for Friction

C_{21} - Initial position of center of circle; C_{22} - Position after intersection of straight line A_1 , etc.

In the following motion, the path of the gyro vertex again intersects the locus of the points of change of sign of $\dot{\alpha}$. Since in this motion $\dot{\beta} < 0$, the equation of this locus will already have the form (cf. the straight line A_2):

$$\beta = b_2(1 + n_{21}).$$

In this case the expression for $(\alpha_{B2})_p$ again takes the form according to a_1 , but the position of the vertex of the gyro will be such in this case that the component of the radius of the circle along the axis $O\alpha$ again decreases by the quantity $\Delta\alpha$, etc.

In this way, beginning at the instant when eq.(9.92) is satisfied, after every quarter period of the turn, there will be a decrease in turn of one component of the

STAT

radius of the circle after the other, as a result of which an involutorial spiral is formed.

It follows from Fig.9.15 and eqs.(9.93a, 9.93b, 9.93c, and 9.93d) that the maximum turning errors on a left turn in the presence of friction are defined by the following formulas:

$$\alpha_{B \max} = (\alpha_{B2})_1 - (\beta_{B2})_1 = -b_1(1-n_{12}) - b_2(1-n_{21}), \quad (9.96)$$

$$\beta_{B \max} = (\beta_{B2})_1 - \alpha_{B \max} + (\alpha_{B2})_1 = 2b_2(1-n_{21}) + b_1(1-n_{12}) - b_1(1-n_{12}). \quad (9.97)$$

For $b_1 = b_2 = \frac{\omega_k}{\omega_B}$ and $n_{21} = n_{12} = \frac{L_p}{L_k}$, we shall have:

$$\alpha_{B \max} = -\frac{2\omega_k}{\omega_B} + 2\frac{L_p}{L_k} \frac{\omega_k}{\omega_B}. \quad (9.98)$$

$$\beta_{B \max} = 2\frac{\omega_k}{\omega_B} - 4\frac{L_p}{L_k} \frac{\omega_k}{\omega_B}. \quad (9.99)$$

If we decrease ω_B , then the values of $\alpha_{B \max}$ and $\beta_{B \max}$ will increase until the path of the gyro vertex makes contact with the straight line $\alpha + \gamma_B = 0$, the limiting values of $\alpha_{B \max}$ and $\beta_{B \max}$ being defined by the formulas:

$$\alpha_{B \max} = \gamma_B. \quad (9.100)$$

$$\beta_{B \max} = \gamma_B - \Delta\alpha = \gamma_B - 2\frac{L_p}{L_k} \frac{\omega_k}{\omega_B}. \quad (9.101)$$

Let us consider the case of a right turn for $b_1 = b_2 = b$ and $n_{21} = n_{12} = n$.

In the case for right turn, motion will begin under the same initial conditions at $\alpha > 0$.

Up to the values

$$\alpha = b(1-n) \quad (9.102)$$

motions will take place along the $O\alpha$ axis in the positive sense, and then along the circle. In this case, the initial expressions for the coordinates of the center of this circle will be of the form

$$(\alpha_{B2})_1 = -b(1+n), \quad (9.102a)$$

STAT

$$(\beta_{B2}) = -b(1+n). \quad (9.102b)$$

We remark that for a right turn, $\omega_B > 0$ and $\frac{\omega_K}{\omega_B} = b < 0$. The first to be intersected, as in the preceding case, will be the locus of points of change of sign of $\dot{\alpha}$, defined by an equation of the following form (cf. straight line A_1), (Fig.9.16).

$$\alpha = b(1+n). \quad (9.103)$$

As a result of this change of sign of $\dot{\alpha}$, the expression for the coordinate of the center of the circle $(\alpha_{B2})_{p2}$ will take the form

$$(\alpha_{B2})_{p2} = -b(1-n), \quad (9.102c)$$

which will mean the increase of the component of the radius of the circle along the axis $O\alpha$ by the quantity $\Delta\alpha$.

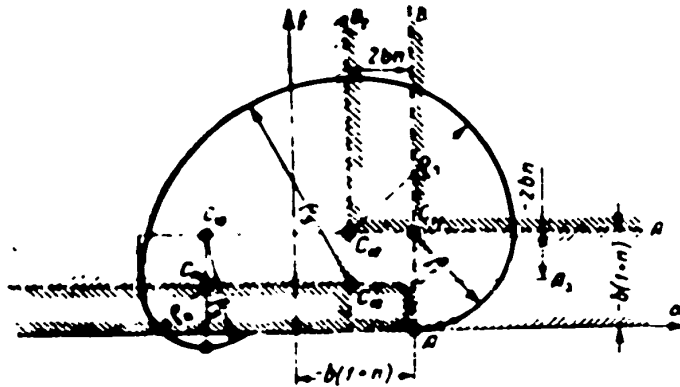


Fig.9.16 - Limit Cycle of Motion of Vertex of Gyro Horizon during Right Turn with Constant Characteristics of Correction and $\frac{L_p}{L_k} > 0.37$

When, during the following motion, the path of the vertex intersects the locus of points of change of sign of β , whose equation will be of the form (cf. straight line B_2):

$$\beta = -b(1-n) \quad (9.104)$$

the expression for the coordinate of the center of the circle $(\beta_{B2})_{p2}$ will now change to the following:

STAT

$$(\beta_{22})_n = b(1 - n), \tag{9.102d}$$

which will mean that the component of the radius of the circle along the axis $O\beta$ will increase by the quantity $\Delta\beta$, etc.

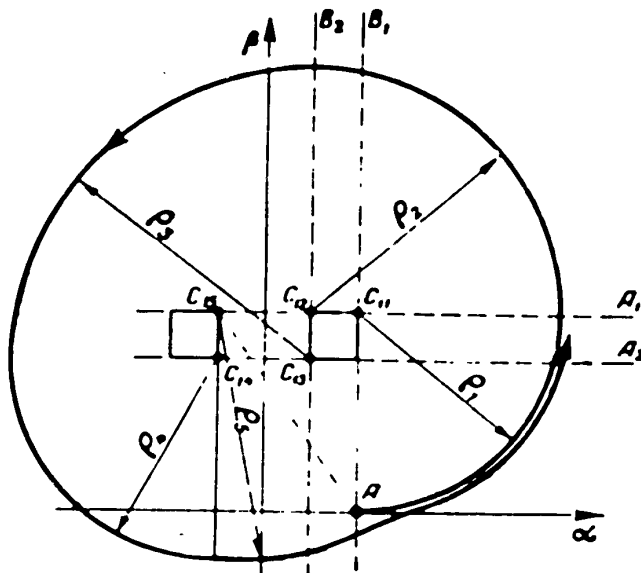


Fig.9.17 - Path of Motion of Vertex of Gyro Horizon during a Right Turn with Constant Characteristics of Friction

$$\text{and } \frac{L_\rho}{L_k} > 0.37.$$

On continuing this construction further, we may obtain the entire path of motion of the gyro vertex as has been done in Figs.9.16 and 9.17. Here, depending on the ratio $\frac{L_\rho}{L_k}$, we may obtain a closed stable cycle (Fig.(9.16), if $\frac{L_\rho}{L_k} < 0.37$, or a divergent path (Fig.9.17), if $\frac{L_\rho}{L_k} > 0.37$ (Bibl.5).

The value of the critical ratio $\frac{L_\rho}{L_k} = 0.37$, at which a stable cycle is still possible, may be determined by equating the segment AC_{15} and the radius p_5 , which may be expressed in terms of $b = \frac{\omega_k}{\omega_D}$ and n .

The values of the maximum errors in motion along the limit cycle during a right turn may be determined on Fig.9.16:

STAT

$$\alpha_{max} = 2b(1+n) \tag{9.105}$$

$$\beta_{max} = -2b(1+2n) \tag{9.106}$$

These formulas will hold until the limit cycle intersects the straight line $\alpha + \gamma_B = 0$. If this intersection takes place, then the maximum errors during a right turn may be determined from Fig.9.18:

$$\alpha_{max} = \gamma_B \tag{9.107}$$

$$\beta_{max} = \gamma_B \cdot 2bn \tag{9.108}$$

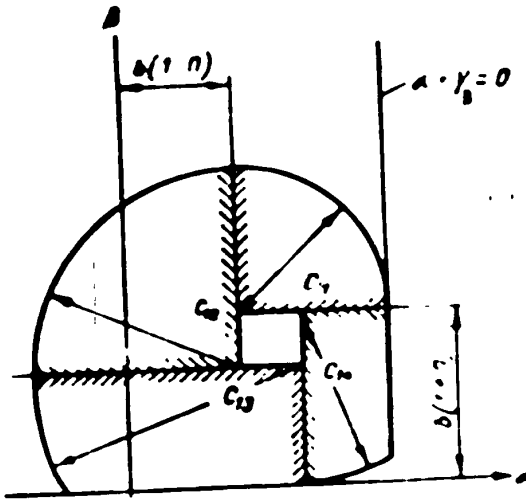


Fig.9.18 - Limit Cycle during a Right Turn as it Intersects the Straight Line $\alpha + \gamma_B = 0$

If $\frac{L_p}{L_k} > 0.37$, then, as has already been stated, the path of the gyro vertex will be divergent. Even this path, however, will still tend to its limit cycle after a few revolutions. The values of the maximum errors here will increase by more than in the case $\frac{L_p}{L_k} < 0.37$.

The case of $\frac{L_p}{L_k} > 0.37$ has not been considered in detail, since in practice $\frac{L_p}{L_k} < 0.37$ is usually the case.

Mixed Characteristic of Correction

Fundamental studies of the behavior of a gyro horizon with mixed correction characteristic during a turn have been made, and in particular, by S.S.Tikhmenev. It is on these studies that the theory given below is based.

According to the ratios between the deviations of the gyro axes α and β , the angle of bank in the turn γ_B , and the values of the zones of proportionality Φ_1 and Φ_2 of the mixed characteristic, the following four cases may hold:

$$\begin{aligned} 1. \gamma_B < \Phi_1; \quad \beta < \Phi_1, \\ 2. \gamma_B > \Phi_1; \quad \beta > \Phi_1, \end{aligned}$$

1st case

2nd case

STAT

$$\begin{array}{ll} \alpha + \gamma_0 < \Phi_0; & \beta > \Phi_1. & \text{3rd case} \\ \alpha + \gamma_0 > \Phi_0; & \beta < \Phi_1. & \text{4th case} \end{array}$$

The 1st and 2nd cases correspond to the cases already investigated for characteristics that are only proportional (1st case) and only constant (2nd case); the 3rd and 4th cases are now to be investigated.

We remarked that the 4th case must be considered the most real of all these cases, and we shall therefore initiate our investigation with that case. This means that during all the motions of the gyro vertex along the $O\alpha$ axis, the law of the constant characteristic will hold, and along the $O\beta$ axis, the law of the proportional characteristic.

The equations of motion for this case are written in the following form

$$\left. \begin{array}{l} H(\dot{\alpha} - \omega_0 \dot{\beta}) = -K_0 \text{sign}(\alpha + \gamma_0) + L_0 \text{sign} \dot{\beta}, \\ H(\dot{\beta} + \omega_0 \dot{\alpha}) = -K_1 \beta - L_1 \text{sign} \dot{\alpha}, \end{array} \right\} \quad (9.109)$$

or

$$\left. \begin{array}{l} \dot{\alpha} = \omega_0 \dot{\beta} - \omega_{02} [\text{sign}(\alpha + \gamma_0) - \pi_{21} \text{sign} \dot{\beta}], \\ \dot{\beta} = -\epsilon (\beta + a_1 \alpha + \rho_1 \text{sign} \dot{\alpha}), \end{array} \right\} \quad (9.110)$$

where

$$a_1 = \frac{\omega_{02}}{\epsilon_1}.$$

Let us reject, for simplicity, the terms allowing for friction in the gimbals. Equation (9.110) is then rewritten in the following form

$$\left. \begin{array}{l} \dot{\alpha} - \omega_0 \dot{\beta} = -\omega_{02} \text{sign}(\alpha + \gamma_0), \\ \dot{\beta} + \omega_0 \dot{\alpha} + \epsilon_1 \beta = 0. \end{array} \right\} \quad (9.111)$$

Assuming as usual that the operations will not include the instants of time at which $\text{sign}(\alpha + \gamma_0)$ changes its sign, and eliminating the variable β from the first equation by the aid of the second equation, we get

$$\alpha + \epsilon_1 \dot{\alpha} + \omega_0^2 \alpha = -\omega_0^2 \frac{h_2}{a_1} \text{sign}(\alpha + \gamma_0). \quad (9.112)$$

STAT

The integral of this equation will be

$$\alpha = Ae^{-\frac{1}{2}t} \sin(m\omega_0 t + \delta) + \alpha_{st}, \quad (9.113)$$

where A and δ are arbitrary constants,

$$m = \sqrt{1 - \frac{1}{4a_1^2}}, \quad (9.114)$$

$$\alpha_{st} = -\frac{b_1}{a_1} \operatorname{sign}(\alpha + \gamma_0). \quad (9.115)$$

On substituting eq.(9.113) in the first of eqs.(9.11), we obtain

$$\beta = Ae^{-\frac{1}{2}t} \left[m \cos(m\omega_0 t + \delta) - \frac{1}{2a_1} \sin(m\omega_0 t + \delta) \right] + \beta_{st}, \quad (9.116)$$

where

$$\beta_{st} = b_2 \operatorname{sign}(\alpha + \gamma_0). \quad (9.117)$$

It follows from eqs.(9.113) and (9.115) that in the fourth case which we are studying here there exists an equilibrium position for the gyro vertex, as for the case of the proportional characteristics, but with a time constant of the transient state twice as long as in the case of the proportional characteristics alone.

As will be seen from eqs.(9.115) and (9.117), the coordinate of this equilibrium position, β_{B4} coincides identically with the expression for the coordinate β_{B2} of the center of the circle described by the gyro vertex with constant characteristics of correction while the coordinate α_{B4} is less than the coordinate α_{B2} of this center by a factor of a_1 (here and hereafter we shall put $a_1 > 1$).

As before, the coordinate β_{B4} will be the same for a left and right turn; while the coordinate α_{B4} will be negative for a left turn and positive for a right turn.

Let us find the locus of points of this equilibrium position. For this purpose, after eliminating the angular velocity of the term for this purpose, from eqs.(9.115) and (9.117), and bearing in mind that $b_2 = \frac{\omega_{K2}}{\omega_B}$, $a_1 = \frac{\omega_B}{\varepsilon}$, we get:

$$\alpha = -\frac{a_1}{a_1} \beta_{st} \operatorname{sign}(\alpha + \gamma)$$

STAT

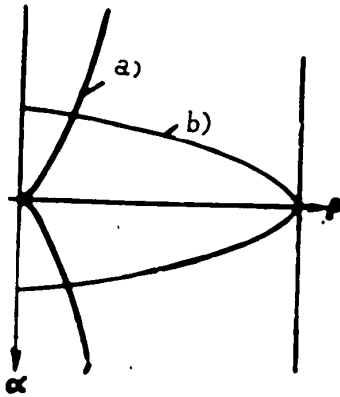
or, bearing in mind that $\omega_{K2} = \varepsilon_2 \phi_2$,

$$z = -\frac{\beta_1}{\beta_2} \beta' \operatorname{sign}(z + \gamma).$$

that is, this locus will be a parabola with its vertex at the point 0 (Fig.9.19).

In this case, to the points more remote from the vertex of the parabola, the smaller

values in modulus of the angular velocities of turn ω_B will correspond.



From the equation of the coordinates of the steady value of the turning deviations for the case under consideration, with coordinates of the center of the circle described by the vertex of the gyro for constant characteristics of correction (second case), and from the coordinates of the steady position of the vertex for proportional characteristics (first case) it follows that in this case the turning deviations will be minimum, since

Fig.9.19 - Locus of Equilibrium
Position of Vertex of Gyro during Turn
in the Case of Various Correction
Characteristics: Locus IV Corresponds
to Constant Characteristic with Respect
to Angle α and to Proportional Charac-
teristic with Respect to Angle β ;
Locus III Corresponds to the Opposite
Case

$$|z_{st}| < |z_{st}| < |z_{st}|, \\ \beta_{st} = \beta_{st} < \beta_{st}.$$

a) Case IV; b) Case III

As will be seen from the expres-
sions for α and β , eqs.(9.113) and
(9.115), the path of the gyro vertex
toward the steady position in this case

will be more complex than the path of the gyro vertex toward the steady state with
proportional characteristics. This complexity is due, first, to the fact that the
period of oscillation differs in this case from the period of the turn, being

STAT

longer, and in the second place by the fact that the variation of β differs from the variation of α by a phase angle less than $\frac{\pi}{2}$, since the expression for β , eq.(9.116), may easily be transformed to the following form:

$$\beta = Ae^{-\frac{1}{2} \epsilon t} \cos(m\omega_0 t + \gamma - \delta_1) + \beta_{st} \quad (9.118)$$

where

$$\operatorname{tg} \delta_1 = \frac{1}{2a_1 m} \quad (9.119)$$

For actual turning rates, the value of $\frac{1}{2a_1 m}$ may be neglected, with a sufficient degree of accuracy, by comparison with unity in eq.(9.114). Then we may take $m = 1$.

On then transferring α_{B4} and β_{B4} in eqs.(9.113) and (9.116) to the left side, squaring the equations so obtained, and adding them by parts, we get

$$(\alpha - \alpha_{st})^2 + (\beta - \beta_{st})^2 = A^2 e^{-\epsilon t} \left[1 + \frac{1}{4a_1^2} \sin^2(\omega_0 t + \delta) - \frac{1}{2a_1} \sin 2(\omega_0 t + \delta) \right]$$

On neglecting, on the same basis as above, the second term in the brackets on the right side of the expression so obtained, and going over to polar coordinates with origin at the point C_4 , we get

$$r = Ae^{-\frac{1}{2} \epsilon t} \sqrt{1 - \frac{1}{2a_1} \sin 2(\varphi + \gamma)} \quad (9.120)$$

where R and δ are arbitrary constants.

Thus, the required path is represented by a logarithmic spiral with a damping exponent half as great as with a proportional correction characteristic, with additional periodic variations of the radius vector superimposed on this spiral, ranging from the value $\sqrt{1 + \frac{1}{2a_1}}$ to the value $\sqrt{1 - \frac{1}{2a_1}}$ of its current length, at frequency double the frequency of rotation of the radius vector.

This path is presented in Fig.9.20 for the value $a = 2.0$, which corresponds, for $\epsilon = 0.05$ 1/sec, to a value of 1 min for T_B . The dashed curve corresponds to the logarithmic spiral. For shorter periods of turning, these additional variations of

STAT

the radius vector will have an even less marked effect.

Thus, with an accuracy sufficient for practice, it may be asserted that the

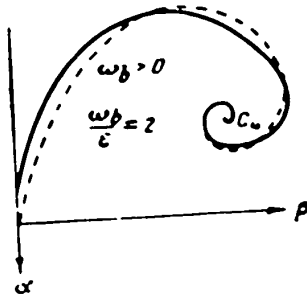


Fig.9.20 - Path of Motion of Vertex of Gyro Horizon during a Left Turn in the Case of Constant Correction Characteristics with Respect to Angle α and Proportional Correction Characteristic with Respect to Angle

path of the gyro vertex remains, in the case we are studying, the same in form as in the case of proportional characteristics alone, that is, it retains the form of a logarithmic spiral, but has a damping exponent half as great, and steady-position coordinates considerably smaller in modulus.

It follows from the spiral motion of the gyro vertex toward its steady position that the maximum values of the turning deviations will be less than twice the value of the deviation of the steady position of the gyro vertex C_4 ,

from the point O . In other words, for the maximum deviations of the tip along the $O\alpha$ and $O\beta$ axes, which we denote respectively by $(\alpha_B \max)_4$ and $(\beta_B \max)_4$, the inequalities

$$\left. \begin{aligned} |(\alpha_B \max)_4| &< 2 \frac{b_2}{a_1} \\ |(\beta_B \max)_4| &< 2b_2 \end{aligned} \right\} \quad (9.121)$$

will hold.

It follows from this, in particular, that we shall know the conditions corresponding to the 4th case we are now considering to be satisfied during all the motions of the gyro vertex if the zone of proportionality of the mixed characteristic for correction, with respect to angle β , satisfies the relation

$$\Phi_1 > 2b_2 \quad (9.122)$$

STAT

and for the correction with respect to angle α , the relation

$$\phi_1 < \gamma_0 - 2 \frac{b_1}{a_1}. \quad (9.123)$$

Let us now assume that the condition of eq.(9.123) is satisfied, while the zone of proportionality of the mixed characteristic of correction with respect to angle β

$$\phi_1 > b_2. \quad (9.124)$$

but that nevertheless its value does not assure the satisfaction of the conditions for the case under examination throughout the entire process of motion of the gyro vertex toward the steady position. In this case, within the limits of motion of the gyro vertex, determined by the relation

$$s < \phi_1. \quad (9.125)$$

motion will be known to take place along a spiral according to eq.(9.120), but beyond these limits, that is, for

$$s > \phi_1. \quad (9.126)$$

the vertex will pass over to a region corresponding to the conditions of the second case, that is, it will pass over into a cycle according to eq.(9.84) with its center at the point with coordinates $(\alpha_{B2}, \beta_{B2})$ defined by eqs.(9.80) and (9.82), of which the expression for α_{B2} may be rewritten, in this case, in the following form

$$\alpha_{B2} = - \frac{\phi_1}{a_1}. \quad (9.127)$$

After the situation becomes such that the inequality of eq.(9.126) is violated, and the inequality of eq.(9.125) now holds on any further motion of the gyro vertex, the reverse transition from the circular path to the spiral one takes place. If the gyro vertex after this again reaches the boundaries of transition from the spiral path to the circular one, then this now takes place, this time, in a position corresponding to a decreased radius of the circle.

Thus in the last analysis there is still a damping of the motion of the gyro vertex with its establishment in a position of rest corresponding to the pure spiral motion according to eqs.(9.115) and (9.116). The difference will only be that the

STAT

setting time, on account of the fact that the motion will take place, in part, in the absence of damping, will be accordingly lengthened.

If the zone of proportionality of mixed characteristic is alternately determined by the relation

$$\Phi_1 < h_2.$$

then, as will easily be seen from similar reasoning, the total path of the gyro vertex will necessarily consist of spiral and circular sections, but the motion will end, not in the establishment of the gyro vertex at some definite position of rest, but in the establishment of motion along a circle of radius

$$R \Phi_1 h_2.$$

It follows from this that the inequalities of eq.(9.121) constitute the maximum possible turning deviations, not only when the conditions of eq.(9.122) are satisfied, but also when the conditions of eq.(9.124) are satisfied.

Let us pass now to the study of the third case.

The equations of motion corresponding to this case are written in the following form (friction in the gimbals being neglected as in the preceding case):

$$\left. \begin{aligned} \dot{\alpha} + \epsilon_2 \alpha - \omega_2 \beta &= -\epsilon_2 \gamma_2 \\ \dot{\beta} + \omega_2 \alpha &= -\omega_2 \text{sign } \beta. \end{aligned} \right\} \quad (9.128)$$

On eliminating the variable β from the first equation by the aid of the second equation, we get

$$\dot{\alpha} + \epsilon_2 \alpha + \omega_2^2 \alpha = -\omega_2^2 b_1 \text{sign } \beta. \quad (9.129)$$

The integral of this equation will be

$$\alpha = A e^{-\frac{\epsilon_2}{\omega_2} t} \sin(m \omega_2 t + \vartheta) + \alpha_{ss}, \quad (9.130)$$

where

$$\alpha_{ss} = -b_1 \text{sign } \beta. \quad (9.131)$$

On substituting the solution eq.(9.130) in the first equation of eqs.(9.128), we get

$$\beta = Ae^{-\frac{1}{2}t} \left[-\frac{1}{2a_2} \sin(m\omega_2 t + \zeta) + m \cos(m\omega_2 t + \zeta) \right] + \beta_{as}, \quad (9.132)$$

where

$$\beta_{as} = \frac{\gamma_0 - b_1 \operatorname{sign} \dot{\beta}}{a_2}, \quad (9.133)$$

$$a_2 = \frac{\omega_0}{\epsilon_2}.$$

The locus of the points of the equilibrium positions with coordinates $(\alpha_{B3}, \beta_{B3})$ will be the curve defined by the equation

$$\beta \approx \frac{r_2}{\epsilon} - \frac{\epsilon_2}{\omega_{s1}} \alpha^2 \quad (9.134)$$

which is shown in Fig.9.19. It is assumed here that

$$\alpha_B \approx \tan \gamma_B = \frac{\omega_{s1}}{\kappa} \quad \text{and} \quad \operatorname{sign} \beta = 1, \quad \text{since } \beta > 0.$$

As will be seen from the solution so obtained, the motion of the gyro vertex will proceed in this case along a curve of the same form as in the preceding case, but with different coordinates of the steady position.

Let us now ascertain to what turning characteristics each of the four possible cases of the location of the gyro vertex in the steady state will correspond. Let us confine ourselves here to the case

$$\Phi_1 = \Phi_2 = \Phi, \quad \epsilon_1 = \epsilon_2 = \epsilon.$$

From eqs.(9.19) and (9.21) for the coordinates of the steady position with proportional characteristics, i.e., for the region of the first case, and from the conditions for the boundaries of this region, there result the following inequalities which become equalities on the boundaries of the region (cf.Fig.9.21):

$$\frac{\gamma_0}{1+a^2} > \gamma_0 - \Phi, \quad (9.135)$$

$$\frac{a\gamma_0}{1+a^2} < \Phi. \quad (9.136)$$

Let us take, here and hereafter:

STAT

or

$$\gamma_0 = \frac{V_{\infty}}{g}$$

$$\gamma_0 = \frac{V_0}{g} a. \tag{9.137}$$

Bearing this in mind, we obtain from the inequality of eq.(9.135):

$$1 > \frac{g}{V_0} \frac{1-a^2}{a^2} \tag{9.138}$$

and from the inequality of eq.(9.136):

$$1 > \frac{g}{V_0} \frac{1-a^2}{a^2} \tag{9.139}$$

Taking eq.(9.138) as an equality, we obtain from the inequality of eq.(9.139), for the boundary of this region along the $O\alpha$ axis:

$$a > 1 \text{ for } \phi < \phi_0 \tag{9.140}$$

Taking eq.(9.139) as an equality, we obtain the inequality of eq.(9.138) for the boundary of this region along the $O\beta$ axis:

$$a > 1 \text{ for } \alpha \geq \alpha_0 \tag{9.141}$$

If, as is usually done, we adopt an order of $2 - 3^0$ for the value of ϕ and a value of $\epsilon = 0.06$ l/sec, then we get the result that the vertex of the gyro can be in a stable position in the first region only in the case where the

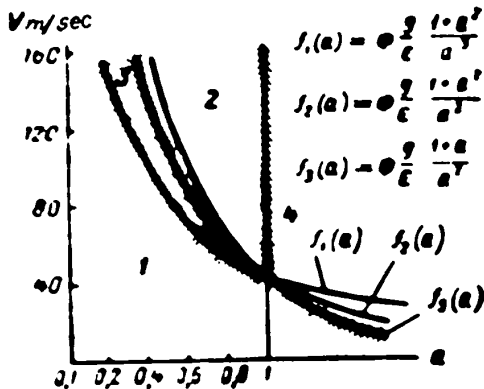


Fig.9.21 - Distributions of Regions of the Various Cases with a Mixed Correction Characteristic

aircraft speed is less than 12 - 18 m/sec.

Thus the first region may be considered practically excluded from the number of regions of possible position of the gyro vertex with a mixed correction characteristic.

From eqs.(9.80) and (9.82) for the coordinates of the center of the circle

STAT

described by the vertex of the gyro for constant correction characteristics, i.e., for the region of the second case, and under the conditions for the boundaries of this region, the following inequalities result:

$$b \cdot \gamma_0 \leq \dots \quad (9.142)$$

$$b \cdot \dots \quad (9.143)$$

Making use of eq.(9.137) and the expression $\omega_K = \varepsilon\Phi$ from the inequality of eq.(9.142), we get

$$\dots \quad (9.144)$$

From the inequality of eq.(9.143), putting $\omega_K = \varepsilon\Phi$ in the expression for b, we obtain directly

$$a \cdot 1 \quad (9.145)$$

Taking eq.(9.144) as an equality, and eq.(9.145) as an inequality, we get the conditions for the boundary of the second region along the Ox axis; taking eq.(9.145) as an equality, and eq.(9.144) as an inequality, we get the condition for the boundary of this region along the axis OR .

Thus the displacement of the gyro vertex in the second region is more probable than its displacement in the first region, but under the condition that $\omega_B < \varepsilon$ that is, under the condition that the angular velocity of the turn is sufficiently small.

From eqs.(9.115) and (9.117) for the coordinates of the steady position in the region of the fourth case, and the conditions for the boundaries of this region, the following inequality results:

$$b \cdot \gamma_n - \Phi \quad (9.146)$$

$$b \cdot \Phi \quad (9.147)$$

From the inequality of eq.(9.147) it follows directly that:

$$a \cdot 1 \quad (9.148)$$

Making use of eq.(9.137), we obtain from the inequality of eq.(9.146):

STAT

$$V \cdot \Phi \frac{\kappa}{a} \frac{1+a^2}{a^2} \quad (9.149)$$

Taking eq.(9.149) as an equality and eq.(9.148) as an inequality, we obtain the condition for the boundary of the fourth region along the axis $O\alpha$; taking eq.(9.148) as an equality and eq.(9.149) as an inequality, we get the conditions for the boundary of this region along the $O\beta$ axis.

It follows from this that the location of the steady positions of the gyro vertex in the fourth region is the most logical location.

From eqs.(9.131) and (9.133) for the coordinates of the steady position in the region of the third case, under the conditions of the boundaries for this region, there results the following inequalities:

$$\gamma_0 \cdot \Phi \cdot b. \quad (9.150)$$

$$\gamma_0 \cdot a \Phi \cdot b. \quad (9.151)$$

From the last two inequalities we obtain, after simple transformations:

$$a < 1.$$

Making use further of eq.(9.150), we get from the inequality of eq.(9.140):

$$V \cdot \Phi \frac{\kappa}{a} \frac{1+a^2}{a^2} \quad (9.152)$$

and from the inequality of eq.(9.151):

$$V \cdot \Phi \frac{\kappa}{a} \frac{1+a^2}{a^2} \quad (9.153)$$

It follows from this that the location of the gyro vertex in the third region, speaking generally, is possible, but in relatively narrow regions.

On the basis of the relations found for the boundaries of the regions it is easy to construct the distribution of these regions in the system of coordinates V and $a = \frac{\omega_B}{\varepsilon}$.

This construction is given in Fig.9.21 for $\varepsilon = 0.06$ l/sec and $\Phi = 0.1$. The latter value is taken, generally speaking, exaggerated, in order to make the construction graphically clearer.

STAT

By using the diagram on Fig.9.21 and the expression for the locus of the equilibrium positions in the four cases we are considering, it is easy to construct the general locus of steady positions of the gyro vertex with a mixed characteristic as ω_B varies from zero to infinity. In this case it is natural to assign definite values of the flying speed.

This locus is presented in Fig.9.22.

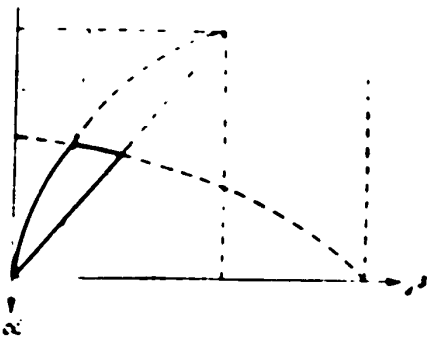


Fig.9.22 - Locus of Equilibrium Position of Tip of Gyrohorizon with Mixed Correction Characteristics at Various Angular Rates of the Angular Velocities of Turning and Constant Flight Speed

As for the effect of friction in the gimbals, as has already been elucidated, the motion of the gyro vertex in the general case consists of motion similar to those obtained with constant and proportional characteristics; therefore the influence of friction in the gimbals will be similar. In other words, with a left turn, the friction in the gimbals will encourage the damping of the motion of the gyro axis, while with a right turn the damping decreases. In motion in the second

region, however, it will favor the gradual slipping of the vertex of the gyro from the position of the center of the circle that would be described by the tip of the gyro in this region, if we neglect the friction in the gimbals.

Compensation of Turning Deviations of Gyrohorizon

It follows from the above that, in all four cases of the relations between the deviations of the gyro axes α and β , the angle of turn γ_B and the values of the zones of proportionality ϕ_1 and ϕ_2 , the motion of the gyro vertex is described by a differential equation of the second order. It is well known that, for a system described by a differential equation, initial conditions may be selected such that

the system shall remain mostly under the action of certain disturbances on it. From this it follows that the turning deviations of the gyro horizon at a definite turning velocity can be compensated by selecting the initial conditions for the coordinates of the gyro vertex. Such a method of compensating the turning deviations of the gyro horizon was first proposed by the Soviet engineer I.A. Timofeyev and the Soviet scientist Ya.N. Roytenberg.

The essence of this method is as follows: the rotor axis of the gyro is inclined by a definite angle β_0 with respect to the axis β forward in the direction of flight. This position of the gyro will correspond to zero mismatch of the correction system along axis $O\beta$. If the aircraft is making a turn, then the system of coordinates $O\alpha\beta$ participates in the rotation of constraint of the aircraft; while the vertex of the gyro is displaced, under the action of the correction system, along the axis $O\alpha$, since the sensitive element of the correction along the axis $O\alpha$ is deflected under the action of the centrifugal forces of inertia by the angle γ_B . If the velocity of the gyro vertex coincides with the velocity of constraint of that point of the coordinate system with which the gyro vertex coincided at the initial moment, then there will be no displacement of the gyro vertex with respect to the system of coordinates $O\alpha\beta$. But this will also mean the absence of turning deviations of the gyro horizon.

For a proportional characteristic of the system of correction along the $O\alpha$ axis, the velocity of the gyro vertex at the initial instant of the turn is determined by the action of the correction system along the axis of α , the sensitive element of which is deflected by γ_B :

$$\dot{\alpha} = \gamma_B \epsilon,$$

where $\tan \gamma_B = \omega_B \frac{V}{g}$.

The velocity of the point of the system of coordinates $O\alpha\beta$ coinciding with the gyro vertex is determined by the product $\omega_B \beta_0$.

On equating these quantities, we get the condition of compensation of the turn-

STAT

ing deviations with proportional characteristic of the correction system along the axis $O\alpha$:

$$\beta_0 = \frac{\gamma_0^2}{\omega_0^2} \quad (9.154)$$

For a constant characteristic of the correction system along the axis $O\alpha$, the velocity of the gyro vertex at the initial instant of the turn is determined by the quantity ω_{K2} . On equating it to the product $\omega_2 \beta_0$, we get the following condition of compensating of the turning deviations with a constant characteristic of the correction system along the $O\alpha$ axis:

$$\beta_0 = \frac{\omega_{K2}}{\omega_2} \quad (9.155)$$

Let us now determine, for these cases, the values of the residual turning deviations obtained in the case of a turn whose parameters do not satisfy the conditions of eqs.(9.154) or (9.155).

For proportional characteristics of correction, the equations of motion of the gyro vertex, eqs.(9.16), on the inclination of the gyro rotor axis along the β axis by the quantity β_0 , are rewritten in the form

$$\left. \begin{aligned} \dot{\alpha} + \epsilon \alpha - \omega_2 \beta &= -\epsilon \gamma_0 \\ \dot{\beta} + \epsilon(\beta - \beta_0) + \omega_2 \alpha &= 0 \end{aligned} \right\} \quad (9.156)$$

From a comparison of eqs.(9.156) and (9.16) it follows that eqs.(9.156) are obtained by replacing β in the second eq.(9.16) by $\beta - \beta_0$, which expresses the condition of equilibrium of the correction system for $\alpha = 0$ and $\beta = \beta_0$.

Performing the necessary operations, we obtain the following expressions for the residual turning deviations in connection with incomplete compensation or overcompensation:

$$\left. \begin{aligned} \Delta \alpha_{s1} &= \frac{\gamma_0 \omega_2 - \gamma_0}{1 + \epsilon^2} \\ \Delta \beta_{s1} &= \frac{\epsilon \gamma_0 \left(1 - \frac{\gamma_0}{\gamma_0}\right)}{1 + \epsilon^2} \end{aligned} \right\} \quad (9.157)$$

STAT

where $\gamma_{BO} = \beta_0 \alpha = \beta_0 \frac{\omega_P}{\epsilon}$, and γ_{BO} is the angle of bank for which the compensation is designed.

It will be seen from these expressions that the values of the turning deviations can be reduced by means of compensation, but, in this case, they cannot reach great values.

We remark that the condition of full compensation in the first case may be satisfied at various angular rates of turn. It is obvious, of course, that for each such angular velocity there will be only one value of the bank, that is, only one value for the linear turning velocity at which the condition of eq.(9.154), of full compensation of the turning deviation, is satisfied.

Let us determine the residual turning deviations for constant characteristics of the correction system. Let us write the equations of motion of the gyro vertex, eqs.(9.37) for the condition of the tilt of the rotor of the gyro rotor axis along the $O\beta$ axis by the quantity β_0' , that is, for the condition of equilibrium of the correction system at $\alpha = 0$ and $\beta = \beta_0'$:

$$\left. \begin{aligned} \dot{\alpha} - \omega_s \beta &= -\omega_s \text{sign}(\alpha + \gamma_s) \\ \dot{\beta} + \omega_s \alpha &= -\omega_s \text{sign}(\beta - \beta_0') \end{aligned} \right\} \quad (9.158)$$

If at the initial instant of a turn at angular velocity ω_{BO} the vertex of the gyro is at the point $(O_1 B_0')$, where $\beta_0' = \frac{\omega_k^2}{\omega_{BO}}$, then the condition of full compensation will be satisfied, and, according to the eq.(9.158), $\dot{\alpha} = 0$ at the initial instant of time. From the second eq.(9.158) we then get $\dot{\beta} = 0$ for this instant. The equilibrium positions for the vertex of the gyro by eq.(9.158) are determined by the quantities $\beta = \beta_0'$ and $\alpha = 0$, that is, they coincide with its initial positions. It follows from this that the vertex of the gyro will remain motionless.

If the angular velocity of the turn $|\omega_B| < |\omega_{BO}|$, then by the first eq.(9.107), $\dot{\alpha} < 0$ at the initial instant of time. This is explained by the fact that for $|\omega_B| < |\omega_{BO}|$, the velocity of motion of the gyro vertex under the action of the correction system, along the $O\alpha$ axis, the sensitive element of which is tilted by

the angle γ_B , is greater than the velocity of the motion of constraint of that point of the system of coordinates $\alpha\beta$, which at the initial instant of time coincided with the gyro vertex. As a result of the appearance of $\dot{\alpha} < 0$ for a left turn and $\dot{\alpha} > 0$ for a right turn, the vertex of the gyro begins to move along a straight line passing through the point β_0' parallel to the $O\alpha$ axis, toward lower values of the coordinate α with a left turn, and toward higher values of α with a right turn. We note that the velocity of this motion, equal to

$$\dot{\alpha} = -\omega_{K2} \cdot \beta_0'$$

will be less than the velocity of the motion in the absence of compensation equal to $-\omega_{K2}$, and that the smaller this given angular turning velocity is, and the less the given angular rate of turn ω_B differs from the angular rate of turn ω_{B0} for which the compensation is figured, the smaller will be the velocity of motion of the gyro.

In connection with the appearance of $\dot{\alpha} < 0$ in the equation for $\dot{\beta}$, obtained from the second equation of eq.(9.158),

$$\dot{\beta} = \omega_{K1} \alpha \cdot \text{sign}(\beta - \beta_0')$$

the positive term $\omega_{K1} \alpha$ will accumulate. However, the appearance of $\dot{\beta} > 0$ is at first impossible, since if $\beta > \beta_0'$ appears, the negative term ω_{K1} will appear with a jump in the expression for $\dot{\beta}$, and this negative term will at first exceed in modulus the positive term $\omega_{K1} \alpha$. In connection with this, $\dot{\beta}$ will change with a jump from a positive value to a certain negative value, and on account of this the value $\beta > \beta_0'$, which appears at first and can be made as small as is desired, will be liquidated. Things will proceed in this way until the condition

$$|\omega_{K1} \alpha| > |\omega_{K1}|$$

begins to be satisfied.

When this condition is satisfied the existence of a discontinuous function of $\beta > 0$ will be assured, which will mean the increase of $\beta > \beta_0'$.

Beginning at this instant of time, the vertex of the gyro will begin to move along a circle whose equation will be of the form:

$$(z - \alpha'_{B2})^2 + (\beta - \beta'_{B2})^2 = A^2 \tag{9.159}$$

where $\alpha'_{B2}, \beta'_{B2}$ are partial solutions of eqs.(9.158), defined by the expressions

$$\left. \begin{aligned} \alpha'_{B2} &= -\frac{u_{B1}}{u_n} \text{sign}(\beta - \beta_0) = -\frac{u_{B1}}{u_n} \\ \beta'_{B2} &= \frac{u_{B2}}{u_n} \text{sign}(\alpha + \alpha_0) = \frac{u_{B2}}{u_n} \end{aligned} \right\} \tag{9.160}$$

while A = radius of circle.

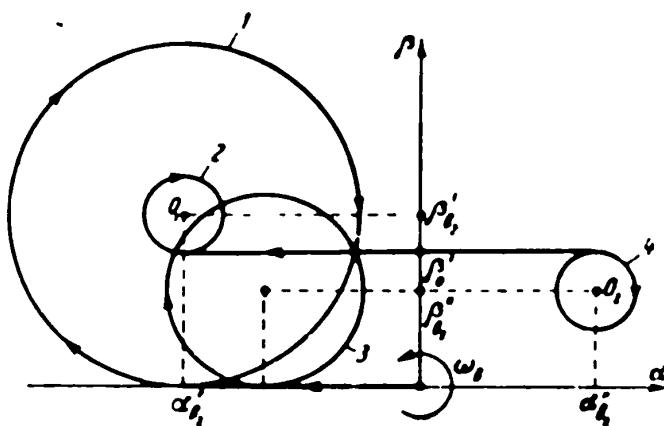


Fig.9.23 - Path of Motion of the Gyro Vertex during Turn at Constant Characteristics of Correction with Compensation of Turn Errors

To determine the radius of the circle, let us substitute in eq.(9.159) the expressions $\alpha'_{B2}, \beta'_{B2}$ and also the values of α and β corresponding to the point of the beginning of motion around the circle:

$$\alpha = \frac{u_{B1}}{u_n}, \quad \beta = \beta_0.$$

Then we get

$$A^2 = (\beta_0 - \beta'_{B2})^2$$

or

$$A = \frac{u_{B2}}{u_n} - \frac{u_{B1}}{u_n} \tag{9.161}$$



STAT

Figure 9.23 shows the path of motion of the gyro vertex for angular velocity $\omega_B > 0$ for the case of the absence of compensation for the turning deviations, the circle (1), and for the case of incomplete compensation for $|\omega_B| < |\omega_{BO}|$ and $\omega_B > 0$, the circle (2). From a comparison of these paths it follows that the maximum values of the turning deviations are decreased.

If the angular velocity of the turn $|\omega_B| > |\omega_{BO}|$, then, according to the first eq.(9.158), at the initial instant of time, $\dot{\alpha} > 0$ for a left turn and $\dot{\alpha} < 0$ for a right turn, since the rate of motion of the gyro vertex under the action of the correction system for the $O\alpha$ axis is less than the velocity of the motion of constraint of the point of the system of coordinates $O\alpha\beta$ coinciding at the initial instant of time with the vertex of the gyro. Owing to the appearance of $\dot{\alpha} > 0$ on a left turn and $\dot{\alpha} < 0$ on a right turn, the gyro vertex will begin to move along the straight line passing through the point β_0' parallel to the $O\alpha$ axis, toward the increase of the coordinate α on a left turn and toward the decrease of α on a right turn. On further examination, analogous to the preceding case, it may be shown that this motion will continue until the negative term $\omega_B \alpha$ in eq.(9.158) is greater than the positive term $\omega_{KL} \cdot \text{sign}(\beta - \beta_0')$. When this happens, the existence of a continuous function of $\dot{\beta} < 0$ will be assured, which will mean the decrease of $\beta < \beta_0'$.

Beginning at this instant of time, the gyro will commence to move along the circle whose equation will be of the form

$$(\alpha - \alpha_0')^2 + (\beta - \beta_0')^2 = A^2, \tag{9.162}$$

where

$$\left. \begin{aligned} \alpha_0' &= -\frac{\omega_{KL}}{\omega_B} \text{sign}(\beta - \beta_0') = \frac{\omega_{KL}}{\omega_B} \\ \beta_0' &= \frac{\omega_{KL}}{\omega_B} \text{sign}(\alpha + \gamma_0) = \frac{\omega_{KL}}{\omega_B} \end{aligned} \right\} \tag{9.163}$$

$$A = \beta_0 - \beta_0' = \frac{\omega_{KL}}{\omega_B} - \frac{\omega_{KL}}{\omega_B} \tag{9.164}$$

On Fig.9.15, the circle 3 represents the path of motion of the gyro vertex STAT

for $|\omega_B| < |\omega_{B0}|$ with $\omega_B > 0$, in the absence of compensation of the turning deviation, while circle (4) is for the case of its presence. Let us now determine the value of the residual deviation for mixed characteristics of the correction system under the condition (fourth case):

$$\alpha + \gamma_0 > \Phi_0, \quad \beta < \Phi_1.$$

The equations of motion of the vertex of the gyro, eq.(9.16), for this case, with a rotor axis inclined to the $O\beta$ axis by the quantity β_0 will be written in the following form:

$$\left. \begin{aligned} \dot{\alpha} &= \omega_0 \beta - \omega_0 \text{sign}(\alpha + \gamma_0), \\ \dot{\beta} &= -\omega_0 \alpha - \omega_0 (\beta - \beta_0). \end{aligned} \right\} \quad (9.165)$$

Let us find from these equations the equilibrium position of the gyro vertex in the case of incomplete compensation:

$$\left. \begin{aligned} \beta_{04} &= \frac{\omega_{02}}{\omega_0}, \\ \alpha_{04} &= -\frac{1}{\omega_0} \left(\frac{\omega_{02}}{\omega_0} - \frac{\omega_{01}}{\omega_0} \right). \end{aligned} \right\} \quad (9.166)$$

It will be clear from these expressions that the residual turning deviation along the axis $O\beta$ will be the same as in the absence of compensation, while along the $O\alpha$ axis it will be proportional to the degree of undercompensation or overcompensation.

By similar reasoning, the residual turning deviation might also be determined for the third case.

Let us now consider a different method of diminishing the turning errors, which leads to the cutting out of the lateral correction during a turn. We note that at the present time this method is widely used in practice.

Let us first discuss the case of proportional correction. With the lateral correction shut off, the equation of motion of the gyro vertex may be obtained from eqs.(9.13) by putting K equal to zero in the first of these equations.

STAT

Then we shall have

$$\left. \begin{aligned} \dot{\alpha} &= \omega_1 \beta + \epsilon \rho_1 \text{sign } \beta, \\ \dot{\beta} &= -\epsilon \beta - \omega_2 \alpha - \epsilon \rho_2 \text{sign } \alpha. \end{aligned} \right\} \quad (9.167)$$

The change of sign of $\dot{\alpha}$ takes place on the straight lines

$$\beta = -\frac{\epsilon}{\omega_1} \rho_1 \text{sign } \dot{\beta}, \quad (9.168)$$

while the change of sign of $\dot{\beta}$ takes place on the straight line

$$\beta = -\frac{\omega_2}{\epsilon} \alpha - \rho_2 \text{sign } \dot{\alpha}. \quad (9.169)$$

On intersecting, these straight lines form a quadrangle of repose, the four vertices of which are in turn the centers of spirals along which the motion of the

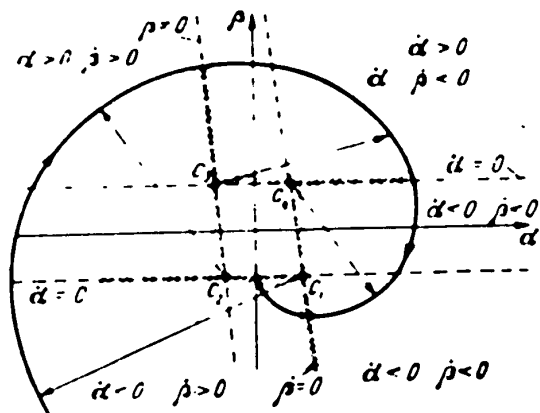


Fig.9.24 - Path of Motion of Gyro Vertex during Left Turn with Proportional Correction Characteristics and Lateral Corrector Turned Off

gyro vertex takes place. Figure 9.24 gives the construction of the path of the gyro vertex for a left turn, resembling what was previously constructed when we were considering turning errors on the disconnection of the lateral corrector. The gyro vertex arrives at the rectangle of repose. If, however, the gyro vertex is at the origin of coordinates at the beginning at the turn, then it will remain there.

It follows from the above that the steady values of the turning errors with corrector turned off are determined, for $p_1 = p_2 = p$ by the formulas

$$\beta_{\text{stat}} = -\frac{p}{a}, \quad (9.170)$$

$$\alpha_{\text{stat}} = p \frac{1+a}{a}, \quad (9.171)$$

Comparison of the formulas for the coordinates of the vertices of the quad-

STAT

range of repose with the lateral correction turned off, eqs.(9.170) and (9.171), and turned on, eqs.(9.39) - (9.44), show that turning off the lateral correction during a left turn considerably reduces the turning error.

Let us consider the behavior of the gyro with lateral correction turned off during a right turn. By eliminating α from eqs.(9.167), we get

$$\beta + \dot{\beta} + \omega_B^2 \beta = -\omega_B p_2 \text{ sign } \dot{\beta}. \quad (9.172)$$

In practice, usually $\frac{\varepsilon^2}{4} - \omega_B^2 < 0$, $a > \frac{1}{2}$.

Under these conditions, the equation will have the solution

$$\beta - \beta_0 = e^{-\frac{\mu}{2} t} (A \sin \mu t + B \cos \mu t), \quad (9.173)$$

where

$$\mu = \sqrt{\omega_B^2 - \frac{\varepsilon^2}{4}} = \omega_B \sqrt{1 - \frac{1}{4a^2}} < \omega_B. \quad (9.174)$$

$$\beta_0 = -\frac{p_2}{\omega_B} \text{ sign } \dot{\beta}. \quad (9.175)$$

Making use of the second eq.(9.167), we get

$$\alpha - \alpha_0 = \frac{1}{\omega_B} e^{-\frac{\mu}{2} t} \left[(B\mu - \frac{\varepsilon}{2} A) \sin \mu t - (A\mu + \frac{\varepsilon}{2} B) \cos \mu t \right], \quad (9.176)$$

where

$$\alpha_0 = -\frac{1}{\omega_B} [\beta_0 + p_1 \text{ sign } \dot{\alpha}] = \frac{1}{\omega_B} [p_1 \text{ sign } \dot{\beta} - \omega_B p_1 \text{ sign } \dot{\alpha}]. \quad (9.177)$$

Here α_B and β_B are the coordinates of the vertices of the quadrangle of repose.

We shall now show that, even with the correction turned off on a right turn, the vertex of the gyro comes into motion along the limit cycle. For this purpose let us discuss the case $p_1 = p_2 = p$. At the initial instant, let the vertex of the gyro be located at point A of the straight line $C_1 C_2$ (Fig.9.25) at distance r_{np} to the right of the vertex C_1 . The coordinates of the point A are determined by

$$\alpha_A = \alpha_0 + r_{np} = \frac{p}{\omega_B} (\text{sign } \dot{\beta} - a \text{ sign } \dot{\alpha}) + r_{np} = \frac{p(1-a)}{\omega_B} + r_{np} \quad (9.178)$$

STAT

$$\beta_2 = \beta_{B1} = - \frac{r_0}{a} \quad (9.179)$$

where α_{B1} and β_{B1} are the coordinates of the points C_1 . We observe that for a right turn $\alpha < 0$. In motion in the region (1), the coordinates of the vertex C_2 should be taken for α_B and β_B :

$$x_{B2} = \frac{r_0}{a} (\text{sign } \beta - \alpha \text{ sign } \beta) = \frac{r_0 (1 - \alpha)}{a} \quad (9.180)$$

$$\beta_{B2} = \beta_{B1} = - \frac{r_0}{a} \quad (9.181)$$

Then, putting $t = 0$, $\alpha = \alpha_A$, $\beta = \beta_A$, $\alpha_B = \beta_{B2}$, $\beta_B = \alpha_{B2}$, we find the integration constants

$$B = 0, \quad A = - \frac{r_0}{a} (r_{mp} - \frac{2p}{a}) \quad (9.182)$$

On substituting the values so found for A and B in the equations eq.(9.173) and eq.(9.176), we get

$$x - x_{B2} = (r_{mp} - \frac{2p}{a}) e^{-\frac{r_0}{a} t} \left[\frac{r_0}{2a} \sin \mu t + \cos \mu t \right] \quad (9.183)$$

$$\beta - \beta_{B2} = - \frac{r_0}{a} (r_{mp} - \frac{2p}{a}) e^{-\frac{r_0}{a} t} \sin \mu t \quad (9.184)$$

Let us determine the time of motion t_1 of the gyro vertex from the point A to intersection with the straight line C_2C_3 , whose equation will be:

$$\beta - \beta_{B2} = - \frac{r_0}{a} \quad (9.185)$$

since it passes through the point α_{B2} , β_{B2} , while its angular coefficient equals $(-a)$ according to eq.(9.169).

On substituting the time t in eqs.(9.183), (9.184), and (9.185), we find the equations for determining the time t_1 and the coordinates of the point $(\alpha_B$ and $\beta_B)$.

$$\left. \begin{aligned} x_B - x_{B2} &= (r_{mp} - \frac{2p}{a}) e^{-\frac{r_0}{a} t_1} \left[\frac{r_0}{2a} \sin \mu t_1 + \cos \mu t_1 \right] \\ \beta_B - \beta_{B2} &= - \frac{r_0}{a} (r_{mp} - \frac{2p}{a}) e^{-\frac{r_0}{a} t_1} \sin \mu t_1 \end{aligned} \right\} \quad (9.186)$$

STAT

$$\begin{aligned} \dot{y}_H &= \dot{y}_0 = -u. \\ \dot{x}_H &= \dot{x}_0. \end{aligned} \tag{9.186}$$



Fig.9.25 - Path of Motion of Vertex of Gyro on Right Turn with the Characteristics of the Correction Proportional and the Lateral Correction Shut Off

From eqs.(9.186) we find

$$\begin{aligned} \omega_0 \sin \mu t_1 &= u. \\ \dot{x}_0 \sin \mu t_1 + \dot{y}_0 \cos \mu t_1 & \end{aligned} \tag{9.187}$$

Or, since

$$u = \frac{\dot{y}_0}{t} \left(1 + \frac{t^2}{t_1^2} = \frac{t^2}{t_1^2} \right) \tag{cf.9.174}$$

we find

$$\operatorname{tg} \mu t_1 = \frac{t_1}{t}. \tag{9.188}$$

$$\cos \mu t_1 = -\frac{t}{2-t_1}. \tag{9.189}$$

$$\sin \mu t_1 = -\frac{t}{t_1}. \tag{9.190}$$

In eqs.(9.189) and (9.190) the minus sign has been used, since $\omega_B < 0$, while $t_1 > 0$.

Making use of eq.(9.189) and eq.(9.180), let us determine the coordinates of the point B:

$$y_B = y_{0B} + \left(r_{np} - \frac{2\dot{p}}{a} \right) e^{-\frac{t}{t_1}}. \tag{9.191}$$

$$x_B = x_{0B} - \frac{1}{a} \left(r_{np} - \frac{2\dot{p}}{a} \right) e^{-\frac{t}{t_1}}. \tag{9.192}$$

On further motion, the gyro vertex now enters region (2). On motion in region (2), the following coordinates for the vertex C_3 must be taken in eqs.(9.173) and (9.176):

$$x_{C3} = \frac{p}{a^2} (a-1). \tag{9.193}$$

$$\beta_{B3} = \beta_B. \quad (9.194)$$

To determine the constants of integration during motion in region (2), let us put, in eqs.(9.173) and (9.176):

$$t = 0, \quad z = z_B, \quad \beta = \beta_B, \quad z_3 = z_{B3}, \quad \beta_3 = \beta_{B3}.$$

Then we obtain

$$\beta_B - \beta_{B3} = B. \quad (9.195)$$

$$z_B - z_{B3} = -\frac{1}{\omega_3} \left(\frac{e}{2} B + \mu A \right). \quad (9.196)$$

On substituting the values of β_B , α_B , β_{B3} and α_{B3} in eqs.(9.195) and (9.196), we get

$$B = r_{sp} e^{-\frac{1}{2} \omega_3 t} - \frac{2\mu}{a} \left(1 + e^{-\frac{1}{2} \omega_3 t} \right) \quad (9.197)$$

$$\frac{1}{2\omega_3} B + \frac{\mu}{\omega_3} A = -\frac{2\mu}{a^2} \left(1 + e^{-\frac{1}{2} \omega_3 t} \right) + \frac{1}{a} r_{sp} e^{-\frac{1}{2} \omega_3 t}. \quad (9.198)$$

From eqs.(9.197) and (9.198), we find

$$A = \frac{e}{2\mu} B. \quad (9.199)$$

On substituting A and B in eqs.(9.173) and (9.176), we get the following equations of motions of the vertex of the gyro in regions (2):

$$\beta - \beta_{B3} = \left[r_{sp} e^{-\frac{1}{2} \omega_3 t} - \frac{2\mu}{a} \left(1 + e^{-\frac{1}{2} \omega_3 t} \right) \right] e^{-\frac{1}{2} \omega_3 t} \left(\frac{e}{2\mu} \sin \mu t + \cos \mu t \right) \quad (9.200)$$

$$z - z_{B3} = -\frac{1}{\omega_3} \left[r_{sp} e^{-\frac{1}{2} \omega_3 t} - \frac{2\mu}{a} \left(1 + e^{-\frac{1}{2} \omega_3 t} \right) \right] e^{-\frac{1}{2} \omega_3 t} \left[\left(\frac{e}{4\mu} - \mu \right) \sin \mu t + \cos \mu t \right]. \quad (9.201)$$

The time t_2 during which the gyro vertex passes from point B to point D, is determined from the condition

$$\beta - \beta_{B3} = 0.$$

Taking account of eq.(9.200), we get

$$\operatorname{tg} \mu t_1 = -\frac{b_0}{a_0} \quad (9.202)$$

By comparing eqs.(9.188) and (9.202), we get

$$\operatorname{tg} \mu t_1 = -\operatorname{tg} \mu t_2.$$

Whence

$$\mu t_1 + \mu t_2 = \pi. \quad (9.203)$$

It follows from eqs.(9.203), (9.189), and (9.190) that

$$\sin \mu t_1 = \sin \mu t_2 = -\frac{b_0}{a_0}. \quad (9.204)$$

$$\cos \mu t_1 = -\cos \mu t_2 = -\frac{a_0}{a_0}. \quad (9.205)$$

On substituting t_2 in eq.(9.201), we get, after simple transformations, the following expression for the coordinate x_D of the point D:

$$x_D = x_{03} = r_{np} e^{-\frac{1}{2}\mu t_1} + \frac{b_0}{a_0} \left(e^{-\frac{1}{2}\mu t_1} + e^{-\frac{3}{2}\mu t_1} \right). \quad (9.206)$$

Let us now require that the point D shall be at the distance r_{np} from the vertex C_3

$$x_D - x_{03} = -r_{np}. \quad (9.207)$$

Then, by virtue of symmetry, the motion from the third and fourth regions will proceed in the same manner as in the first and second regions. Therefore the gyro vertex will again travel toward point A, performing a motion along the closed cycle of period

$$T = 2(t_1 + t_2) = \frac{2\pi}{\mu} > \frac{2\pi}{\omega_0} = T_0.$$

On the basis of eq.(9.206) and eq.(9.207), we shall find the parameter of the limit cycle with lateral correction turned off during a right turn

$$r_{np} = -\frac{2b_0 r_{03}}{a_0} \frac{e^{-\frac{1}{2}\mu t_1} + e^{-\frac{3}{2}\mu t_1}}{1 - e^{-\mu t_1}}$$

STAT

or

$$r_{np} = -\frac{2a}{a} \frac{e^{\frac{\pi}{2} \frac{a}{r}} + 1}{e^{\frac{\pi}{2} \frac{a}{r}} - 1} \quad (9.208)$$

It can be shown that the limit cycle will be stable. In fact, if the point A_1 is at the distance $r_{np} \pm \Delta n$, from the vertex C_1 , then, after the first half-revolution, the vertex of the gyro will be at the point D_1 , whose coordinate α_{D1} is determined by eq.(9.206):

$$\begin{aligned} \alpha_{D1} - \alpha_{A1} &= -(r_{np} + \Delta r) e^{-\frac{\pi}{2} \frac{a}{r}} + \frac{2a}{a} (e^{\frac{\pi}{2} \frac{a}{r}} + e^{-\frac{\pi}{2} \frac{a}{r}}) = \\ &= -r_{np} \pm \Delta r e^{\frac{\pi}{2} \frac{a}{r}}. \end{aligned}$$

After the n -th half-revolution, the distance of the gyro vertex, when the straight lines C_1C_3 or C_3C_4 are intersected by the rectangle of repose C_1 or C_3 , will equal

$$\alpha_{Dn} - \alpha_{A1} = r_{np} \pm \Delta r e^{\frac{\pi}{2} \frac{a}{r}}$$

Thus

$$\lim_{n \rightarrow \infty} (\alpha_{Dn} - \alpha_{A1}) = r_{np}$$

Let us now determine the maximum errors, β_{max} and α_{max} , on motion along the limit cycle as well. It follows from Fig.9.25 that

$$\begin{aligned} \alpha_{max} &= \alpha_A = \alpha_{A1} + r_{np} \\ \beta_{max} &= \beta_B = \beta_{B1} + (r_{np} - \frac{2a}{a}) e^{-\frac{\pi}{2} \frac{a}{r}} \end{aligned}$$

By substituting the values of α_{D1} , β_{B2} and r_{np} , we find

STAT

$$\alpha_{\max} = \frac{p(1-a)}{a^3} - \frac{2p}{a} \frac{e^{\frac{1}{2}\pi} + 1}{e^{\frac{1}{2}\pi} - 1}, \quad (9.209)$$

$$\beta_{\max} = -\frac{p}{a} - \frac{2p}{a} \frac{e^{\frac{1}{2}\pi} + 1}{e^{\frac{1}{2}\pi} - 1}.$$

In the real range of angular velocities, $|a| > 1$. Let us determine the limit which α_{\max} and β_{\max} will approach as $a \rightarrow -\infty$. For this we remark that according to eq.(9.174) $\frac{\mu}{g} = \sqrt{a^2 - \frac{1}{4}}$, $t_1 \rightarrow 0$ and $t_2 \rightarrow 0$ as $a \rightarrow -\infty$, since the period of motion along the limit cycle approaches zero when the angular velocity increases without limit.

Then, by making use of the L'Hospital rule, we get

$$\lim_{a \rightarrow -\infty} \alpha_{\max} = \lim_{a \rightarrow -\infty} \beta_{\max} = -\frac{8}{\pi} p. \quad (9.210)$$

The values of α_{\max} and β_{\max} for $|a| > 1$ differ little from their values as $a \rightarrow -\infty$.

On comparing these values of the radii of the limit cycle of a right turn with lateral correction turned on (cf. eq.(9.61) and with that correction turned off eq.(9.210) we see that turning off the lateral correction of a right turn leads to the increase of the radius of the limit cycle. Figure 9.26 shows the limit cycles of maximum radius for a given rate of correction which are obtained on a right turn with correction turned off (curve 1), and with the lateral correction turned on (curve 2).

This does not mean that turning off the correction for a right turn is impermissible. For small values of the angular velocity on a right turn the turning deviations with correction turned off during the time of transition to the establishment of the limit cycle, the deviation will be less than with the corrector turned on. Moreover, if the gyro axis at the beginning of a right turn coincides with the

STAT

vertical ($\alpha_0 = \beta_0 = \alpha_0 = \beta_0 = 0$), then it will remain in this position (cf. eq. (9.167)) since there will be no cause that will operate to bring the gyro away from the vertical.

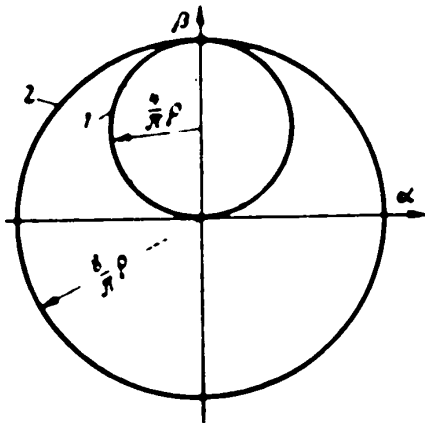


Fig.9.26 - Limit Cycles of Maximum Radius for a Given Rate of Correction with Proportional Characteristic with Lateral Correction Turned On (Curve 1) and with Lateral Correction Turned Off (Curve 2)

$n = \frac{L_p}{L_k}$ - ratio between moment of friction and moment of correction.

The equation of the path of the gyro vertex during a turn with lateral corrector turned off is the equation of the arc of a circle, as when the lateral corrector is on (eq. 9.91) but with its own values for the centers α_{B2} and β_{B2} :

$$(\alpha - \alpha_{B2})^2 + (\beta - \beta_{B2})^2 = R^2 \tag{9.213}$$

where

$$\alpha_{B2} = - \frac{\omega_k}{\omega_n} |\text{sign } \beta + n \text{ sign } \dot{\alpha}| \tag{9.214}$$

Let us now consider the motion of the vertex of the gyro during a turn with the lateral corrector turned off, in the case of a constant correction characteristic. The equations of motion for this case, with the same correction parameters on both axes and the same moments of friction in the axes of the gimbals, are obtained from eq.(9.75), if we reject the term $k_2 \text{ sign } (\alpha + \gamma_B)$ in the first equation:

$$\dot{\alpha} = - \omega_n \beta + \omega_n n \text{ sign } \dot{\beta} \tag{9.211}$$

$$\dot{\beta} = - \omega_n \alpha - \omega_n (\text{sign } \beta + n \text{ sign } \dot{\alpha}) \tag{9.212}$$

where $\omega_k = \frac{L_k}{I_1}$ - rate of correction;

$$\dot{\beta}_{02} = - \frac{\omega_B}{\omega_K} n \text{sign } \dot{\beta}. \tag{9.215}$$

R - radius of circle determined by the initial position of the gyro vertex.

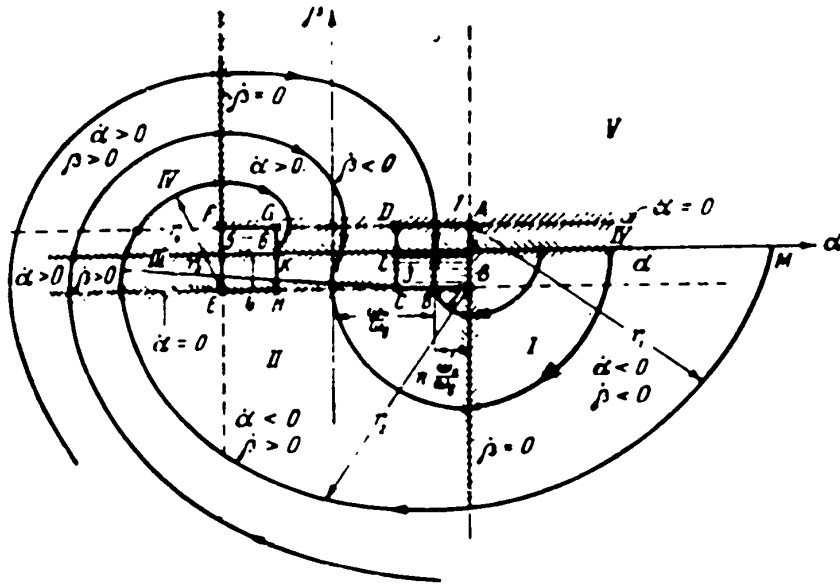


Fig.9.27 - Path of Motion of Vertex of Gyro during a Left Turn with Constant Correction Characteristics and Lateral Correction Turned Off

The coordinates of the centers of the circles lie on the corners of the squares ABCD and EFGH (Fig.9.27). The loci of the points of change of the centers of the circles lie on the straight lines:

- 1) $\dot{\beta} = 0$, i.e., $\omega_B \alpha + \omega_K (\text{sign } \beta + n \text{sign } \dot{\alpha}) = 0$ - the straight lines AB, CD, EF, and GH;
- 2) $\beta = 0$, i.e., the axis $O\alpha$;
- 3) $\dot{\alpha} = 0$, i.e., $\omega_B \beta + \omega_K n \text{sign } \dot{\beta} = 0$ - the straight lines AD, BC.

Let us first consider the behavior of the vertex of the gyro during a left turn: $\omega_B > 0$. Let it be situated at the point M on the axis $O\alpha$. For this point, $\omega_B \alpha > \omega_K$. For this reason it follows from eq.(9.212) that $\dot{\beta} < 0$, but in this case,

STAT

by eq.(9.211) we get the result that $\dot{\alpha} < 0$ as well the vertex of the gyro enters the region (1) (Fig.9.27), where $\beta < 0$, $\dot{\beta} < 0$, and $\dot{\alpha} < 0$, for which the center of the circle by eqs.(9.214) and (9.215) will be the point A with coordinates

$$\left. \begin{aligned} (\alpha_{01})_A &= \frac{\omega_B}{\omega_K} (1 + \pi), \\ (\beta_{01})_A &= \frac{\omega_B}{\omega_K} \pi. \end{aligned} \right\} \quad (9.216)$$

On the straight line AB the sign of $\dot{\beta}$ changes, since ω_B^{α} becomes less than ω_K . As a result of this, the coordinate β_{B2} of the center of the circle also changes. Thus the center of the circle for the region (2) becomes the point B with the coordinates

$$\left. \begin{aligned} (\alpha_{01})_B &= \frac{\omega_B}{\omega_K} (1 + \pi), \\ (\beta_{01})_B &= - \frac{\omega_B}{\omega_K} \pi. \end{aligned} \right\} \quad (9.217)$$

On the straight line BC the sign of $\dot{\alpha}$ changes, and the point C with the coordinates:

$$\left. \begin{aligned} (\alpha_{01})_C &= \frac{\omega_B}{\omega_K} (1 - \pi), \\ (\beta_{01})_C &= - \frac{\omega_B}{\omega_K} \pi. \end{aligned} \right\} \quad (9.218)$$

becomes the center of the circle for region (3). On the axis $O\alpha$ the sign of $\dot{\beta}$ changes and the point E, with the coordinates

$$\left. \begin{aligned} (\alpha_{01})_E &= - \frac{\omega_B}{\omega_K} (1 + \pi), \\ (\beta_{01})_E &= - \frac{\omega_B}{\omega_K} \pi. \end{aligned} \right\} \quad (9.219)$$

now becomes the center of the circle for region (4). On the straight line EF, the sign of $\dot{\beta}$ changes, and the point F, with the coordinates

STAT

$$\left. \begin{aligned} (\alpha_{01})_r &= -\frac{\omega}{\omega_0} (1 + \mu), \\ (\beta_{01})_r &= \frac{\omega}{\omega_0} \mu. \end{aligned} \right\} \quad (9.220)$$

now becomes the center of the circle for region (5). Finally, on the straight line AD the sign of α changes, and the point G, with the coordinates

$$\left. \begin{aligned} (\alpha_{01})_G &= -\frac{\omega}{\omega_0} (1 - \mu), \\ (\beta_{01})_G &= \frac{\omega}{\omega_0} \mu. \end{aligned} \right\} \quad (9.221)$$

now becomes the center of the circle.

By constructing the path of the gyro vertex, we satisfy ourselves that, as a result of the change in the centers of the circles, the radii of the circles diminish by jumps, both on account of the action of the moments of friction in the axis, and on account of the action of the longitudinal correcting moment. As a result, the vertex of the gyro reaches the square of repose ABCD or EFGH. We observe that the points of equilibrium of the gyro vertex will be the segment KL, the upper half of the square EFGH, the lower half of the square ABCD. In fact, after the vertex of the gyro reaches the boundaries of these half squares or the segment KL, this type of substitution of centers of the circle does take place, which would be expected to lead to a reversal of the sense of rotation of the gyro vertex with respect to the center of the circle, which is impossible. Physically this means that, on the appearance of a deviation of the gyro vertex from these boundaries, there appears from the halves of the square and from the segment KL in any direction a correcting moment and moments of friction of such sign as to return the vertex of the gyro to its previous position.

Thus on deviations from the segment KL we have $|\omega_K| > |\omega_B \alpha + \omega_K \eta|$ and therefore β and β will have different signs, by eq.(9.212), that is, any deviation along

STAT

the β axis that appears will be eliminated. On deviation from the side of the square FG upward, we will have

$$\begin{aligned} \gamma > 0, \text{ так как } |\omega_n| > \omega_n n, \\ \text{и } \gamma < 0, \text{ так как } -\omega_n \gamma - \omega_n n < 0. \end{aligned}$$

It follows from the above that the maximum value of the steady errors during a left turn with the correction turned off is determined by the formulas

$$\beta_{max} = \frac{\omega_n}{\omega_n} n, \tag{9.222}$$

$$\alpha_{max} = \frac{\omega_n}{\omega_n} (1+n). \tag{9.223}$$

From a comparison of Figs. 9.15 and 9.27 and of eqs. (9.98) - (9.101) and eqs. (9.222) - (9.223), it follows that turning off the lateral correction on a left turn considerably reduces the turning errors.

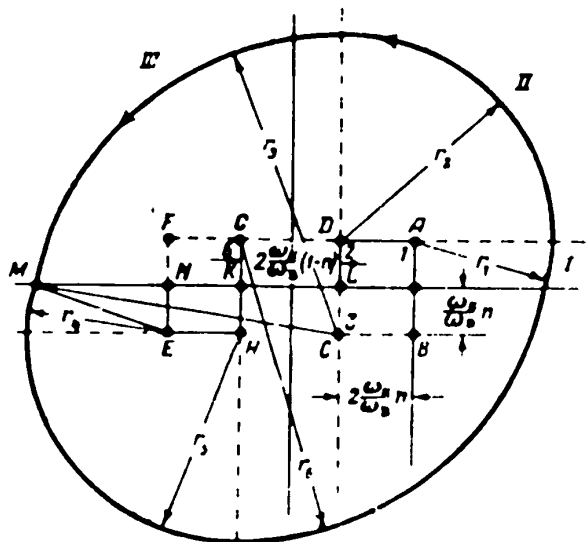


Fig. 9.28 - Limit Cycle on Right Turn with Constant Correction
Characteristics and Lateral Correction Turned Off

With a right turn it may be established by an analogous method that the centers of the circles here will be the vertices A, D, C, E, H, G, in succession. Om
STAT

constructing the path of the gyro vertex (cf. Fig. 9.28), we may make sure that the passage of the center of the circle from one corner of the square to the other corner leads to an increase to the radius of the circle, while the passage of the center of the circle from the corner of one square to the corner of another square leads to a decrease in the radius of the circle. The former transition is due to the change of signs of the moments of friction in the gimbals, the second transition is due to the change of sign of the longitudinal correcting moment. The action of these two opposite factors leads to the establishment of the limit cycle. Let us determine the radius of the circle r_1 with vertex at the point A for the limit cycle, at assigned values of ω_B , ω_K , and n . It is obvious that the limit cycle will become established at $r_4 = r_1$.

Let us write the obvious geometrical equalities:

$$r_1 = MN^2 + NE^2 = (ML - NL)^2 + NE^2 = \left(\sqrt{r_1^2 - \frac{3n^2}{4}} - 2\frac{n^2}{4n^2} \right)^2 + \frac{n^2}{4};$$

$$r_2 = r_1 + 2\frac{n^2}{4n^2} = r_1 + 4\frac{n^2}{4n^2};$$

$$r_4 = \left(\sqrt{\left(r_1 + 4\frac{n^2}{4n^2} \right)^2 - \frac{3n^2}{4}} - 2\frac{n^2}{4n^2} \right)^2 + \frac{n^2}{4}.$$

On equating r_4 and r_1 , after simple transformations we obtain the following equation for r_1 :

$$\left(\sqrt{r_1^2 - \frac{3n^2}{4}} \right)^2 (4n^2 - 1) + \left(\sqrt{r_1^2 - \frac{3n^2}{4}} \right) 4n (4n^2 - 1) + 16n^4 - 7n^2 + 1 = 0.$$

Whence we find:

$$r_1 = \frac{n^2}{4n^2} \left[-2n + \sqrt{\frac{3n^2 - 1}{4n^2 - 1}} \right].$$

STAT

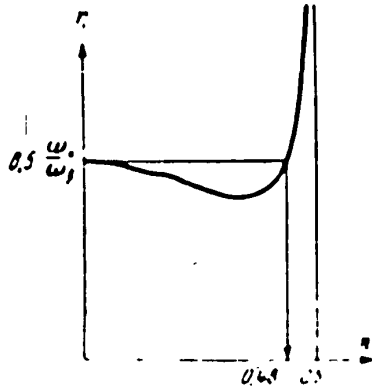


Fig.9.29 - Relation between Radius of Limit Cycle r_1 and $n = \frac{l_p}{l_k}$

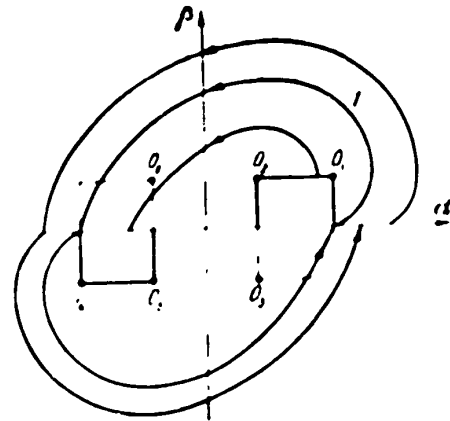


Fig.9.30 - Path of Motion of Gyro Vertex during Right Turn with Lateral Correction for $\frac{l_p}{l_k} = 0.48$

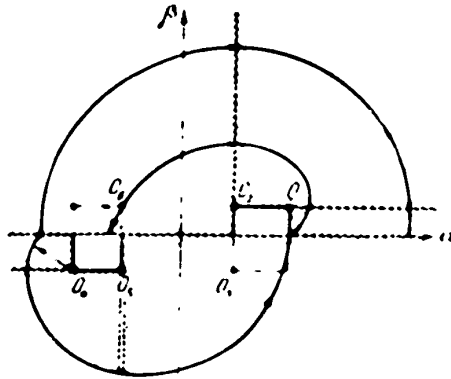


Fig.9.31 - Paths of Motion of Vertex of Gyro during Right Turn with Lateral Correction Off for $\frac{l_p}{l_k} < 0.48$

STAT

On Fig.9.29, r_1 has been plotted against the ratio $n = \frac{l_p}{l_k}$. For $n = 0.48$, the radius of the limit cycle equals half the side of the square $\frac{\omega_k}{\omega_\beta}$. In this case the limit cycle is the boundary cycle (Fig.9.30): all the paths that are inside it, are closed in the rectangles of repose for the segment KL, all the paths located outside the limit cycle, wind about that limit cycle. For $0 < n < 0.48$ $r_1 < \frac{\omega_k}{\omega_\beta}$, the limit cycle does not exist, since, for the closure of the cycle, it is necessary that $r_4 = r_1 > \frac{\omega_k}{\omega_\beta}$. In this case all the paths are closed in the rectangle of repose (Fig.9.31). When n increases from 0.48 to 0.5, the radius of the limit cycle increases from zero to infinity. For $n = 0.5$, the limit cycle does not exist, and there is a small region of the plane in which the paths meet and are closed in the zone of repose, while in the rest of the area, the paths are divergent. It follows from what has been said that when $n = 0.48$ is selected, the value of the steady turning errors with the lateral correction turned off on a right turn will be the same as for a left turn, and will be determined by the formulas eqs.(9.222) and (9.223). On comparing these quantities with the values of the maximum turning errors on a right turn with operating lateral correction, the conclusion may be drawn that turning off the correction when its characteristic is constant decreases the turning errors. All that need be done is to assure a ratio between moment of friction and moment of correction of not more than 0.48. In practice this ratio usually does not exceed 0.1 - 0.2.

Section 9.3. Ballistic Deviations

General Remarks

By ballistic deviations we shall mean here the displacements of the gyro axis due to the action of longitudinal accelerations on it. By the positional correction of ballistic deviations we shall mean deviations due to the action of accelerations on the pendulum serving as the sensitive member of the corrector of the frame whose axis of rotation is perpendicular to the direction of flight.

STAT

With oscillatory accelerations, oscillations of this pendulum will also take place. Since the influence of the oscillations of the sensitive member of the corrector has already been elucidated in Chapter 4, we shall confine ourselves here merely to elucidating the influences of the constant accelerations to which the aircraft is subjected during the course of some finite interval of time. We shall here consider that the pendulum of the corrector for the other frame is not subjected to disturbance.

In view of the foregoing, the expressions for the mismatches in the transmitters of the correction system, in the case of the longitudinal arrangement of the axis of the outer frame, may be written in the following form

$$\begin{aligned}\theta_2 &= \alpha, \\ \theta_1 &= \beta - \gamma \dot{V}.\end{aligned}$$

where

$$\gamma_1 = \arctg \frac{\dot{V}}{g} \approx \frac{\dot{V}}{g}.$$

We shall not take into account the moments of friction in the gimbals, since their influence in this case is not manifested in any new effect.

Let us also take into account, in the equations of motion of the gyroscope, the influence of the displacement of the aircraft with respect to the earth. Then the equations of motion of the gyroscope will take the form

$$\left. \begin{aligned}H\ddot{\alpha} &= f(\alpha); \\ H(\dot{\beta} + \frac{\dot{V}}{R}) &= f(\beta - \frac{\dot{V}}{R}).\end{aligned} \right\} \quad (9.224)$$

Ballistic Deviations with a Proportional Characteristic

In this case, the equations of motion eqs.(9.224) may be rewritten in the following form (putting, for simplicity, $k_1 = k_2 = k$):

STAT

$$\begin{aligned} \dot{\alpha} + \alpha z &= 0, \\ \beta + \epsilon \beta &= -z \left(\frac{V}{Rz} - \frac{V}{R} \right). \end{aligned} \quad (9.225)$$

The partial solutions of eq.(9.225) for $\dot{V} = \text{const}$, which represent the steady deviation in the case under study, are written in the following form:

$$\left. \begin{aligned} \alpha_V &= 0; \\ \beta_V &= -\left(\frac{V}{Rz} - \frac{V}{R} \right). \end{aligned} \right\} \quad (9.226)$$

that is, with a variable α there will be no deviation, but with a variable β there will be, and it will consist of the velocity deviation $\delta_V = -\frac{V}{Rz}$, with which we are already familiar, and the new ballistic deviation:

$$\delta_V = \frac{V}{R} \quad (9.227)$$

equal to the angle of deviations of deflection of a pendulum from the true vertical under the influence of the acceleration \dot{V} .

Let us confine ourselves in our further investigation to the equation with respect to the variable β . Its total integral is written in the form

$$\beta = B e^{-\epsilon t} - (\delta_V - \delta_1). \quad (9.228)$$

Let, for $t = 0$, $\beta = -\delta_V$. Then, for the arbitrary constant B we obtain

$$B = \delta_1 \quad (9.229)$$

Let us now introduce the variable $\Delta \delta_V^* = \beta + \delta_V$, which we shall call the current value of the ballistic deviation. Using this variable and the value found for the arbitrary constant, let us rewrite eq.(9.228) in the following form:

STAT

$$\Delta \delta_v = \delta_v (1 - e^{-t/T}). \quad (9.230)$$

Thus the current value of the ballistic deviation δ_v^* tends here to its steady value according to a law of increasing exponent with a time constant inverse in magnitude to the single velocity of precession ε , and consequently, the increase of deviation will be particularly intense at the initial instant of time, after which it will slow down. A value practically equal to δ_v^* , that is, equal to the deflection of the pendulum, is reached by $\Delta \delta_v^*$ after the lapse of the time

$$T_y \approx \frac{3}{\varepsilon}.$$

For $\varepsilon = 0.06$ 1/sec, $T_y = 50$ sec.

Under actual flying conditions, however, so prolonged a state of acceleration is improbable, or in other words, under actual flight conditions, the ballistic deviation will not reach its full value. It is therefore interesting to elucidate the ability of the gyroscope to accumulate ballistic deviations over the given time of action of the acceleration τ_v^* or in connection with the given increment of flight speed ΔV .

It is clear that, other conditions being equal, this ability will be less, the smaller the value of the unit rate of precession ε . On the other hand, at constant acceleration, the time of action of the acceleration will be determined by the expression

$$\tau_v^* = \frac{\Delta V}{\varepsilon}. \quad (9.231)$$

that is, will be inversely proportional to the acceleration.

At the same time, the limiting value to which the ballistic deviation tends will increase with increasing acceleration.

In order to elucidate the ultimate result of this contradictory influence of acceleration on the current value of the ballistic deviation in the case under

STAT

study, let us substitute in the solution eq.(9.230) the time τ_v according to eq. (9.231), and let us then expand this right side of eq.(9.230) into a series and transform the solution eq.(9.230) to the following form

$$\Delta \delta_v = \frac{\dot{V}}{\kappa} \left(\frac{\Delta V}{\dot{V}} - \frac{1}{2!} \frac{\dot{\Delta V}^2}{\dot{V}^2} + \frac{1}{3!} \frac{\dot{\Delta V}^3}{\dot{V}^3} - \dots \right). \quad (9.232)$$

It will be seen from the expression so obtained that the ballistic deviation increases in modulus with the increase in modulus of the increment of velocity ΔV , and that for a given ΔV it will be the larger, the larger in modulus the acceleration \dot{V} is, since in this case the terms in parenthesis in the right side of eq. (9.232) will be the closer to the quantity $\varepsilon \frac{\Delta V}{\dot{V}}$.

For the compensation of the ballistic error on account of the increment of the velocity deviation, the condition

$$\frac{V}{R} - \frac{\dot{V}}{\kappa} = 0.$$

must be satisfied.

Integration of this equation gives the following law of variation of velocity at which this compensation is observed:

$$V = V_0 e^{-\frac{\kappa}{R} t}.$$

Taking $\varepsilon = 0.06$ 1/sec, we find that the compensation of the ballistic error is possible only with an exponential law of increase of velocity with a time constant equal to 10 hrs. Thus the practical accomplishment of this compensation is unreal, owing to the different orders of magnitude of the ballistic and velocity deviations.

For a numerical evaluation of the ballistic deviation, let us take the case of the increment of velocity $\Delta V = 30$ m/sec with accelerations of 3 and 6 m/sec², taking $\varepsilon = 0.06$ 1/sec. We now obtain, by eq.(9.230), taking $t = \tau_v = \frac{\Delta V}{\dot{V}}$:

STAT

$$\Delta\beta_1 - 3.77/\text{sec} = 7.6;$$

$$\Delta\beta_1 - 4.6/\text{sec} = 8.8^\circ.$$

It will be clear that the errors obtained in this case will be rather considerable.

The Constant of the Correction Characteristic

As in the preceding case, it will be sufficient to consider only the equation of moment with respect to the variable β . In this case it will be rewritten in the following form:

$$\dot{\beta} - \omega_s \text{sign}(\beta - \gamma_1) = \frac{V}{R}. \quad (9.233)$$

According to this equation, at $\beta = 0$, precession of the inner frame occurs in the sense of matching the gyro axis with the position of the apparent vertical.

The influence of the flight speed V is manifested in this case in the slowing or acceleration of this precession to an insubstantial extent, and we shall therefore not take it into account.

The current value of the ballistic deviation is determined in this case by the expression

$$\delta_{\dot{\psi}} = \omega_s \tau_{\dot{\psi}} \text{sign } V',$$

where $\tau_{\dot{\psi}}$ is the time of action of the acceleration.

Or, taking $\dot{V} = \text{const}$ and expressing

$$\tau_{\dot{\psi}} = \frac{\Delta V'}{V'},$$

we get

$$\delta_{\dot{\psi}} = \omega_s \frac{\Delta V}{V}. \quad (9.234)$$

STAT

As will be clear, in this case the ballistic deviation will be proportional to the increment of velocity ΔV , and inversely proportional to the acceleration \dot{V} , that is, in contrast to the preceding case, it will be the smaller, the greater the acceleration with which the accumulation of the velocity increment ΔV takes place.

Let us take for \dot{V} those same data of the numerical example that were used above, and let us take $\omega_K = 6^\circ/\text{min}$, $\Delta V = 30 \text{ m/sec}$. In this case we get

$$\begin{aligned} \dot{\beta}_V &= 1 \text{ m/sec}^2 = 1^\circ \\ \dot{\beta}_V &= 0.5 \text{ m/sec}^2 = 0.5 \end{aligned}$$

As will be clear, with a constant characteristic, the ballistic deviations will be considerably smaller than with a proportional characteristic.

Let us determine the value of the constant acceleration \dot{V}_{Kp} , for which the ballistic deviation for an assigned ΔV reaches its maximum value β_{max} , equal to the angle of inclination of the apparent vertical $\frac{V_{kp}}{g}$:

$$\beta_{\text{max}} = \alpha = \frac{\Delta V}{V_{kp}}$$

since

$$t = \frac{\Delta V}{\dot{V}_{kp}}$$

From this we find:

$$\alpha = \frac{\Delta V}{V_{kp}} = \frac{\dot{V}_{kp}}{g} \quad (9.235)$$

$$\begin{aligned} \dot{V}_{kp} &= V_{kp} \frac{g}{\Delta V} \\ \beta_{\text{max}} &= \sqrt{\frac{\dot{V}_{kp} \Delta V}{g}} \quad (9.236) \end{aligned}$$

For $\dot{V} > \dot{V}_{Kp}$, the gyro axis will not succeed in getting as far as the position of the apparent vertical

STAT

$$\beta = \omega_s \frac{\Delta V}{V} < \beta_{max} = \omega_s \frac{\Delta V}{V_{sp}} \quad (9.237)$$

For $\dot{V} = \dot{V}_{Kp}$, the axis of the gyro will succeed in reaching the position of the apparent vertical

$$\dot{\beta} = \frac{V}{R} < \beta_{max} = \frac{V_{sp}}{R}$$

Thus, for an assigned value of ΔV , there is a critical value of the constant acceleration \dot{V}_{Kp} at which the ballistic deviation is maximum.

With a variable acceleration, the maximum ballistic deviation for an assigned ΔV is obtained in the case when the velocity of rotation of the apparent vertical is equal to the velocity of precession of the gyro. In this case the axis of the gyro will follow the apparent vertical as it is displaced. For this case, the equality

$$\omega_s t = \frac{V}{R},$$

will hold, since

$$\Delta v = \int_0^t V dt = \int_0^t g \omega_s t dt,$$

and

$$\Delta V = \frac{1}{2} g \omega_s t^2,$$

then the time of increment of velocity is determined from the formula

$$t = \sqrt{\frac{2\Delta V}{g \omega_s}}$$

Then the maximum value of the ballistic deviation is determined from the formula

STAT

$$\beta_{\text{ball}} = \alpha_{\text{ball}} \sqrt{\frac{2\Delta V \sigma_{\text{ball}}}{\kappa}} \quad (9.238)$$

that is, it is $\sqrt{2}$ times as great as at constant acceleration.

Mixed Correction Characteristic

If the acceleration \dot{V} is considerable, then the deflection of the apparent vertical from the true vertical on account of the action of the acceleration will be considerably greater than the zone of proportionality of the mixed characteristic. Consequently the behavior of the gyro will be determined mainly by the constant part of the mixed characteristic, that is, it will be about the same as for constant correction characteristics.

At low accelerations, when

$$\frac{\dot{V}}{\kappa} \leq \psi,$$

the behavior of the gyro will be the same as with a proportional characteristic. But, as already established, with a proportional characteristic, for a given acceleration, the ballistic deviation will be smaller the smaller the acceleration is.

Thus with a mixed characteristic the favorable aspects of both the proportional and constant characteristics of the correction are to a certain extent both used with respect to the ballistic deviation.

Section 9.4. Gyro Horizons with Electric Drive

At the present time gyro horizons with an electrically driven gyroscope rotor are widely used. Gyro horizons with a pneumatic drive, in view of the worsening of their characteristics in flight at high altitudes, are employed very rarely.

The indication system of the instrument is made in two versions: 1) in the form of a motionless aircraft silhouette, connected with the body of the instrument, and a movable line imitating the horizon, which is connected with the gyro; and

STAT

2) in the form of a movable aircraft silhouette, connected with the gyroscope, and a fixed horizon line.

The AGK-47B Gyro Horizon

The gyro horizons with corrector and electrically driven gyro rotor include the type AGK-47B gyro horizon, whose setup and operation are described below. The AGK-47B gyro horizon is a combination instrument, the single case of which contains not only a gyro horizon but also a turn indicator and a side-slip indicator. The instrument needs a triphase current, 36v, 400 cycles. The source of this current is usually a special PAG-1F transformer.

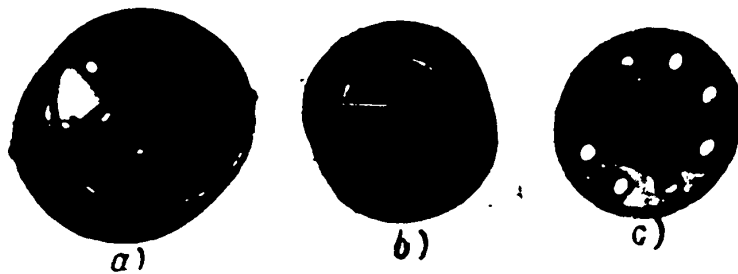


Fig.9.32 - Parts of Gyro Rotor of Gyro Horizon

The gyro horizon consists directly of a gyroscopic unit, a correcting unit, an arrester, and an indicating system.

The axis of rotation of the outer frame of the gimbals is located parallel to the transverse axis of the aircraft. The gyro motor casing, whose axis is parallel to the longitudinal axis of the aircraft, serves as the inner frame of the gimbals.

The gyro motor of the gyro horizon (Fig.9.32) is a triphase asynchronous electric motor. The stator of the gyro motor (Fig.9.32,c) is attached to the cover of the casing.

The rotor of the gyro motor (cf. Fig.9.32,b) consists of a massive steel fly-wheel into which a block of electrotechnical iron with a short circuited winding is

STAT

pressed. The rotor of the gyro motor is made in the form of a bell within which the stator is placed. This form of rotor makes it possible to obtain the maximum moment of inertia for the given dimensions and weight of the gyro motor (about 0.9 g-cm sec²). The rate of rotation of the rotor of the gyro motor is about 20,000 rpm.

The instrument uses a corrector consisting of a liquid level electrolytic switch of the corrector and two solenoids with cores. Its operation is described in Chapter 6.

In order to diminish the turning errors, the gyroscope axis is located not vertically but inclined forward in the direction of flight by 2°. For this purpose an inclined boss is provided at the bottom of the gyro motor casing, to which the sensitive correction element is attached by its base. Obviously bubbles in the level will be located symmetrically with respect to their contacts with the indicated inclination of the gyro axis.

The static balancing of the gyro units is effected with the cores in the middle position of the solenoids. The current is fed to the gyro motor and the correcting device through brushes and contact rings placed on the axes of the frames of the gimbals. The indicating system of the gyro horizon consists of a "horizon line" connected with the instrument casing, and of an aircraft silhouette, connected with the gyro unit.

For the bank readings on the instrument to correspond to the actual bank, the aircraft silhouette is connected with the inner frame of the gimbals through a gear drive with a gear ratio of 1 : 1. When the aircraft banks, the "horizon line", connected with the instrument case, rotates relatively to the initial position by the angular bank of the aircraft. The outer frame of the gyroscopic gimbals is also rotated by the angle of bank. If the aircraft silhouette were attached directly to the axis of the inner frame, then in this case it would be rotated with respect to the line of the "horizon" by the angle of bank in the direction opposite the actual bank of the aircraft, and consequently the instrument would yield the reverse read-

STAT

ings, but since the aircraft outline is connected with the axis of the inner frame of the gimbals through the above mentioned transmission, it would therefore turn

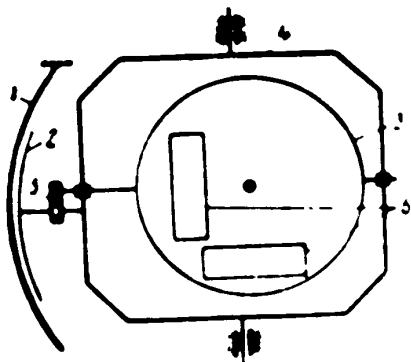


Fig. 9.33 - Indicating System of Gyro Horizon

1 - Horizon line; 2 - Aircraft silhouette; 3 - Inner frame of gimbals (Casing of gyro motor); 4 - Outer frame of gimbals; 5 - Gear drive; 6 - Solenoids

when the aircraft banks with respect to the "horizon line" by the angle of bank, in the direction corresponding to the actual bank of the aircraft. This is illustrated by Fig. 9.33.

In addition, a scale of longitudinal inclinations and a scale of banks are attached to the gyro unit. For convenient use of the instrument, the line of the horizon may be shifted with respect to the instrument case by means of a crank mechanism, whose handle is brought out on the face side of the instrument (Fig. 9.34).



Fig. 9.34 - Outer View of Gyro Horizon

1 - Handle for moving index of horizon;
2 - Arrester

STAT

A special mechanical device is used to arrest the gyro-unit. The maximum time necessary for arresting an operating instrument does not exceed 15 sec.

AGB-1 Bomber Gyro Horizon

The AGB-1 type electric gyro horizon is another example of the gyro horizon with radial correction (Fig.9.35), which is used on heavy aircraft. On the face part of the gyro horizon, a side-slip indicator is placed.



Fig.9.35 - a) External View of Type AGB-1 Gyro Horizon; b) Face View

- 1 - Front flange; 2 - Aircraft outline; 3 - Vertical pressure; 4 - Horizon line;
- 5 - Spherical screen; 6 - Bank scale; 7 - Ball of side-slip indicator; 8 - Scale division of side-slip indicator; 9 - Handle for blocking corrector switch;
- 10 - Handle of angle-of-attack mechanism

The gyro horizon consists of a gyroscopic unit, a correcting mechanism, an indicating system, a starting system, and a system for starting the corrector, and cutting out the corrector during turns.

Figure 9.36 gives a schematic diagram showing the arrangement of the gimbals on the aircraft. The axis of rotation of the outer frame of the gyroscope gimbals is located parallel to the longitudinal axis of the aircraft, while the axis of the

STAT

inner frame (the gyro motor casing) is parallel to the lateral axis of the aircraft. This arrangement of the gimbal axes allows measurement of the true angle of pitch

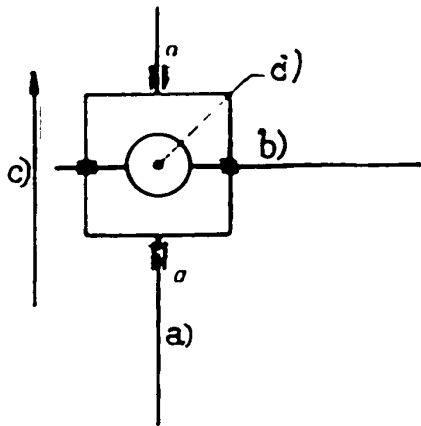


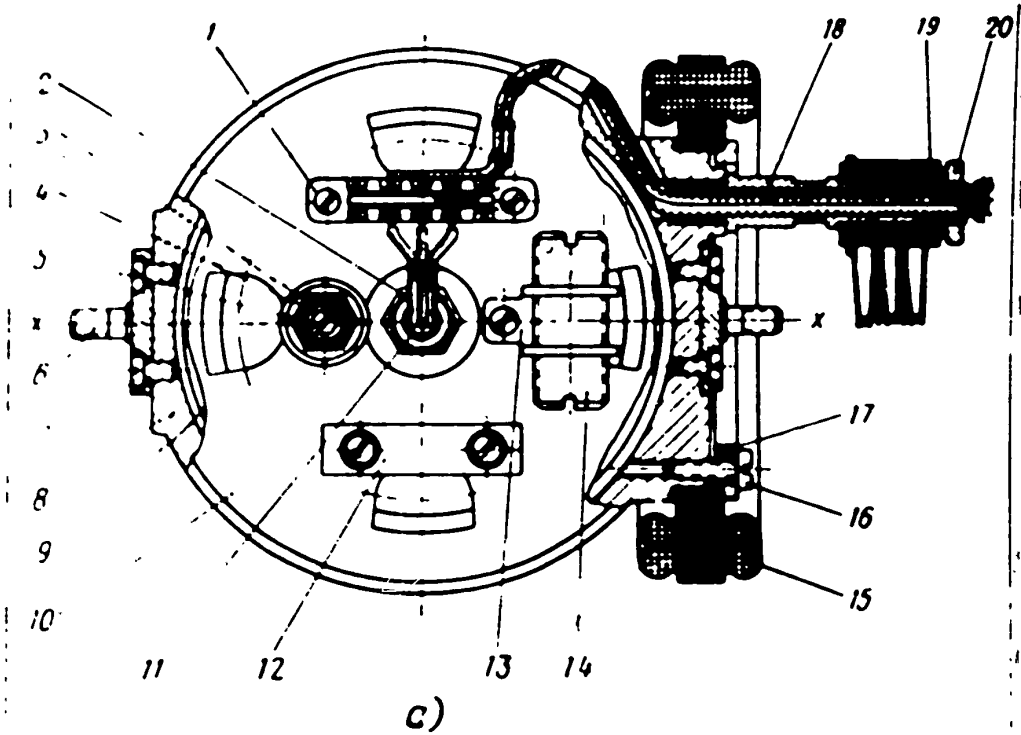
Fig.9.36 - Schematic Diagram of Arrangement of Gyro Horizon on Aircraft

a) Axis of measurement of angle of bank; b) Axis of measurement of angle of pitch; c) Direction of longitudinal axis of aircraft; d) Trace of gyro-scope axis

frame of the gimbals. The stator of the gyro motor (2) (Fig.9.38) is attached to the cover of the casing. The rotor (1) is a massive steel flywheel with the block (6) of electrotechnical steel and a short circuited winding, embracing the stator on the outside, pressed into it. The moment of inertia of the rotor is $1.9 \text{ g - cm - sec}^2$. The speed of the rotor is 21,000 - 23,000 rpm. The kinetic moment of the gyroscope amounts to about $4000 \text{ g - cm - sec}$. The motor of the rotor is triphase and synchronous, with one pair of poles and star-connected windings. It is fed by a triphase 36 volt 400 cycle alternating current. The line current of the motor

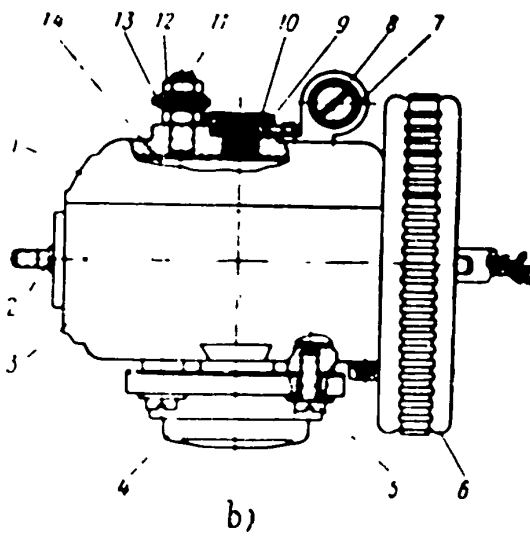
(dive or climb) during a bank, that is, it allows measurement of the angle between the longitudinal axis of the aircraft and the plane of the horizon, and measurement of the true angle of bank, the angle of rotation of the aircraft about its longitudinal axis when the angle of pitch is not zero. The range of measurement of the angles is $\pm 80^\circ$ in bank and $\pm 60^\circ$ in pitch. The principal feature of the gyro horizon is the high accuracy of its readings during a turn, which is obtained by cutting out the lateral correction of the gyroscope. The gyro unit of the instrument (Fig. 9.37) contains the gyro motor (Figs. 9.38 and 9.39) which is placed inside a casing. The casing is also the inner

STAT



a - View from above ;

- 1 - Junction box; 2 - Lock nut; 3 - Disc;
- 4 - Pin; 5 - Nut; 6 - Shaft of gyro unit;
- 7 - Screw; 8 - Body of gyro motor; 9 - Gyro motor;
- 10 - Cover of gyro motor; 11 - Bushing;
- 12 - Lead balancing weight; 13 - Bracket;
- 14 - Balancing screw; 15 - Rotor of electric motor of lateral corrector;
- 16 - Screw; 17 - Pressure reading;
- 18 - Stand; 19 - Contact group; 20 - Nut



b - Side view

- 1 - Cover of gyro motor; 2 - Axis of gyro unit;
- 3 - Body of gyro motor; 4 - Liquid switch;
- 5 - Screw; 6 - Rotor of electric motor;
- 7 - Balancing screw; 8 - Bracket;
- 9 - Bushing; 10 - Nut; 11 - Pin; 12 - Nut;
- 13 - Disc; 14 - Gyro motor

Fig.9.37 - Gyro Unit of Gyro Horizon

STAT

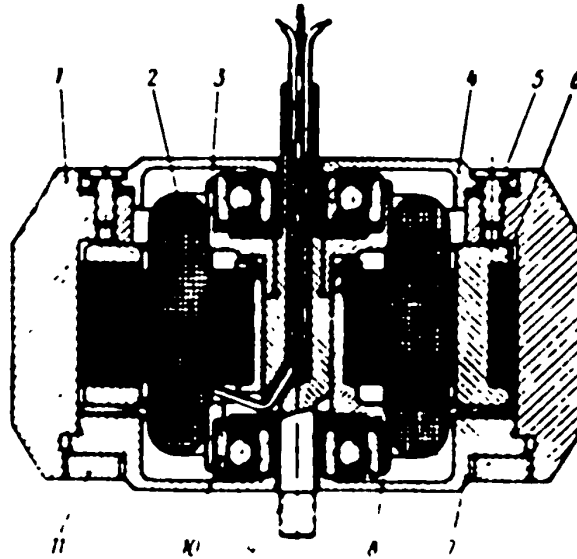


Fig.9.38 - Gyro Motor

- 1 - Gyroscope rotor; 2 - Stator of electric motor; 3 - Bushing;
- 4 - Cover of gyro motor; 5 - Screw; 6 - Electrotechnical steel block with short circuited winding; 7 - Cover of gyro motor; 8 - Bushing;
- 9 - Shaft of gyro motor; 10 - Bearing; 11 - Nut

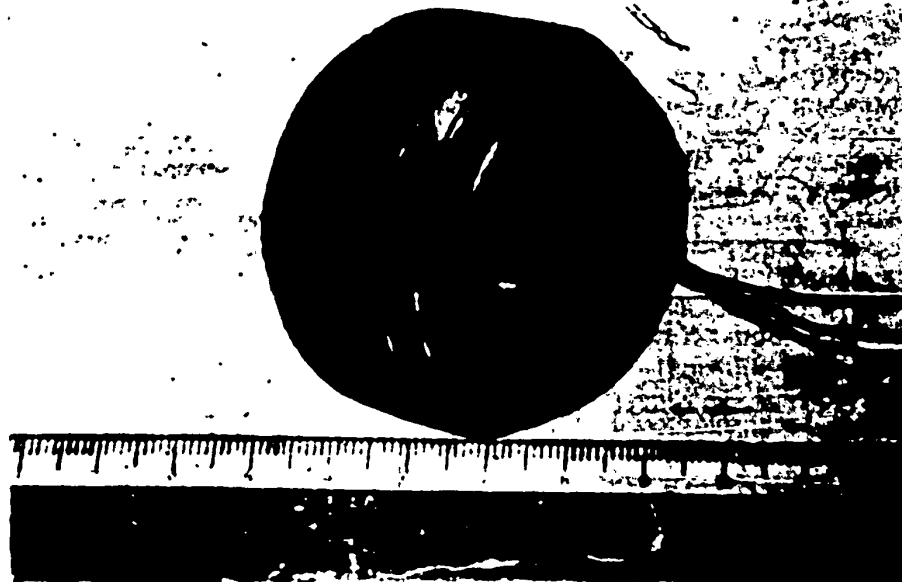


Fig.9.39 - Outside View of Gyro Motor

STAT

phase is about 0.35 amp. The time taken by the gyroscope to reach full speed is 2 min. During operation the gyro motor may be heated to not over 45° C. In the

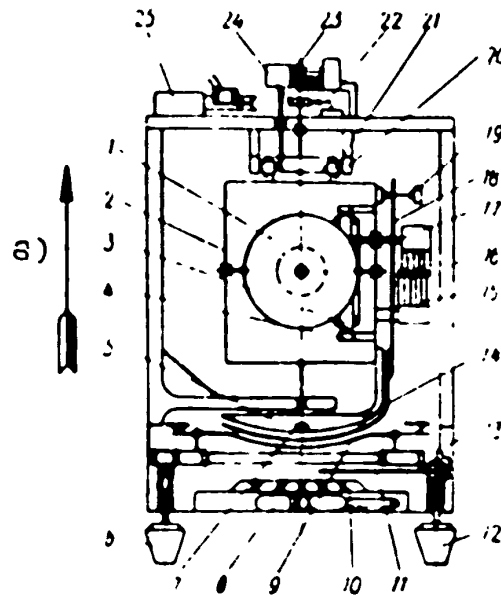


Fig.9.40 - Kinematic Scheme of Gyro Horizon

1 - Gyro unit; 2 - Gimbal frame; 3 - Rotor of lateral corrector electric motor; 4 - Stator of electric motor; 5 - Spherical screen; 6 - Handle of angle-of-attack mechanism; 7 - Vertical scale division; 8 - Side-slip indicator; 9 - Aircraft outline; 10 - Bank scale; 11 - Signal flag; 12 - Handle for blocking corrector switch; 13 - Front flange; 14 - Strip-horizon line; 15 - Current leads; 16 - Casing; 17 - Carrier; 18 - Lever; 19 - Bracket; 20 - Stator of electric motor of longitudinal corrector; 21 - Rotor of electric motor; 22 - Brushes of switch of lateral corrector; 23 - Leads; 24 - Cutout disc for lateral corrector; 25 - Bimetallic relay

a) Direction of flight

lower part of the gyro unit a pendulum switch is attached, forming the sensitive element of the corrector. In design and characteristics it does not differ from the sensitive element of the corrector of the AGK-47B gyro horizon (cf. Fig. 6.14). The

STAT

gyro-unit (1) (Fig.9.40) is suspended on bearings in the gimbal frame (2). The rotor of the electric motor of the lateral corrector (3) is rigidly connected to it.

The stator of the electric motor is attached to the gimbal frame (2), which is suspended on bearings in the body (16) of the instrument. In addition, the rotor of the longitudinal correction electric motor (21), the disc (24) for cutting out the lateral correction during a turn, the spherical screen (5) with vertical scale (7) for reading off the lateral bank, and three horizontal scales for reading off the angle of pitch (0 and $\pm 10^\circ$) are all rigidly attached to the frame (2).

The electric current is supplied to the gyro motor and the correction system by means of the moment-free power inputs (15) and (23). The moments of friction of these inputs are negligibly small, since the pointed contacts are located on the axis of rotation on the gimbals. The strip (14) with lever (18) reproduces the line of the horizon. The lever (18) is suspended in the brackets (19) attached to the frame (2). The tang (17), attached on the casing of the gyro unit enters the slot of the lever (18). In the horizontal position of the aircraft, the lever (18) with the strip (14) are perpendicular to the axis of the rotor to the rotor shaft of the gyro motor, and are consequently also in the horizontal plane. The aircraft outline (8) is connected with the instrument case (16) through a gear drive which is controlled by the lever (6) for setting the angle of attack. When the aircraft is inclined, the body and outer frame of the gimbals are also inclined with respect to the vertical shaft of the rotor of the gyro motor. These inclinations are reproduced by the strip-horizon (14) with respect to the aircraft outline (9). Figure 9.41 shows the readings of the gyro horizon during various maneuvers of the aircraft.

The electric motors of the longitudinal and lateral correctors consist of asynchronous biphasic electric motors (Fig.9.42). The operation of the correction system is described in Chapter 6 on pages 74-76. Three windings are placed in the rotor grooves: one excitation, winding and two control windings with the windings in opposite senses. The reversal of the correcting moment is effected by switching on

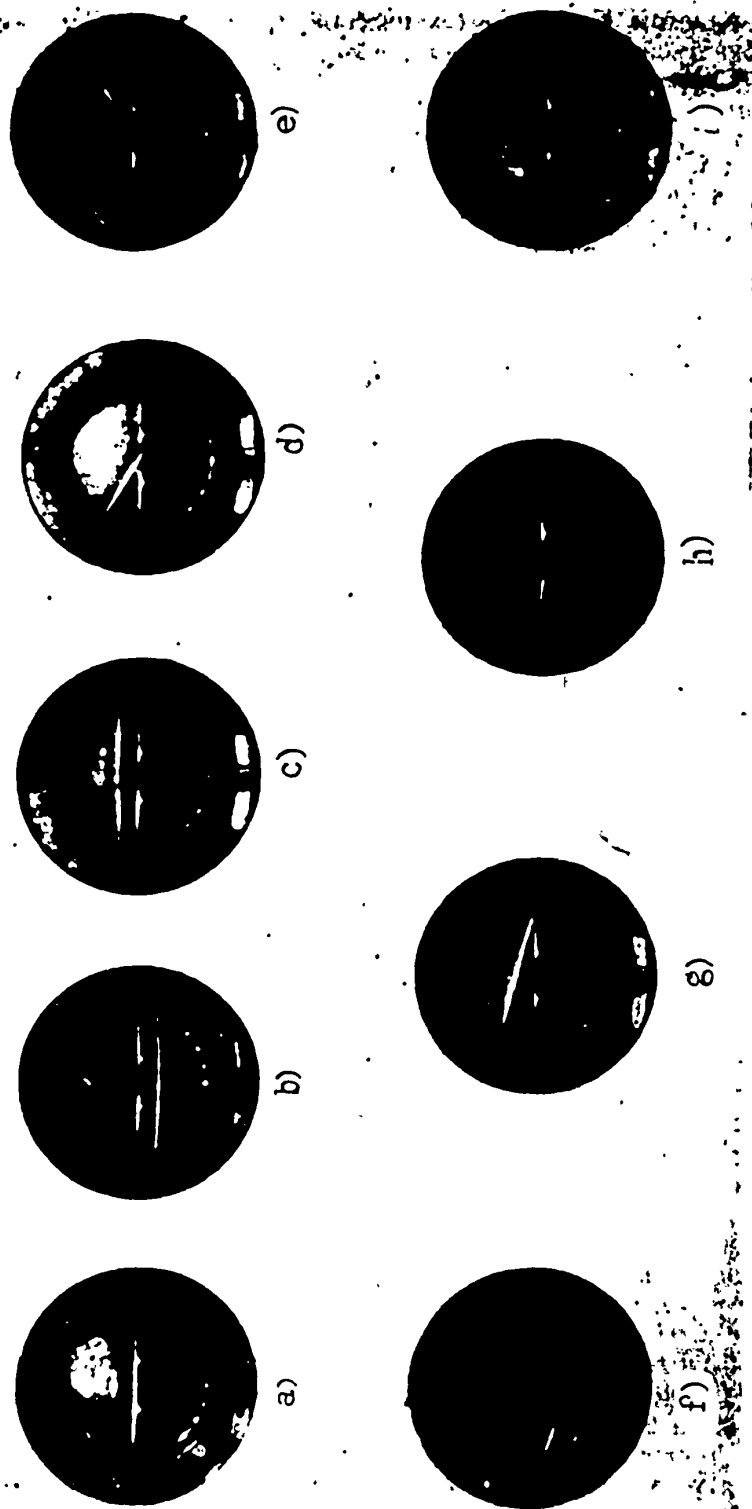


Fig.9.41 - Readings of Gyro Horizon during Various Maneuvers of Aircraft

a - Horizontal flight; b - Gaining altitude; c - Descent; d - Left turn;

e - Right turn; f - Left turn and gaining altitude; g - Left turn and descent;

h - Right turn and gaining altitude; i - Right turn and descent

one control winding or the other. The stator consists of a block of electrotechnical steel with grooves cast in aluminum alloy and forming a short-circuited stator winding.

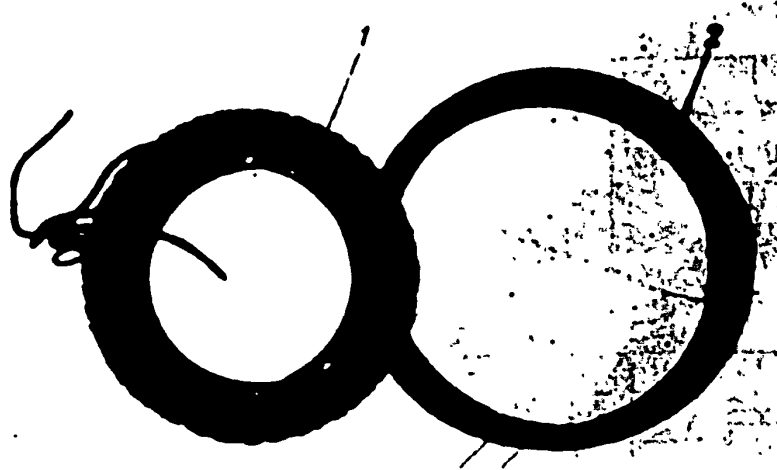


Fig.9.42 - Outer View of Electric Correction Motor

1 - Rotor; 2 - Stator

The maximum torque developed by the electric motor is 7 - 9 g - cm, and the diameter of its rotor is 61 mm. The resistance of the excitation winding is 5.2 ± 0.5 ohms and that of each of the control windings is 420 ± 50 ohms.

Figure 9.43 gives the electrical circuit of the gyro horizon. The current is supplied to the gyro motor (1) from the series converter PAG-1F through the terminals ABC of the plug connector of the gyro horizon. The central contact of the liquid switch (2) is connected to phase A of the gyro motor. The excitation windings of the electric motors (3) and (4) of the correction are connected in series with the phase windings B and C of the electric motor of the gyroscope. This method of connecting the windings increases the torques of the correcting motors on starting the instrument by 2 - 2.5 times as a result of the starting currents of the gyro motor flowing through them. This considerably shortens the time required for the

STAT

gyroscope to reach the vertical operating position on starting.

The lateral correcting motor (4) is turned off, during a bank, by the contact disc (5), located on the shaft of the outer frame of the gimbals. When the aircraft banks by more than $7 - 9^{\circ}$, the lateral correction is cut out. Two current-carrying sectors on this disc, with angles up to 18° , are electrically connected with the common lead-out (8) of the electric correcting motor (4). In horizontal flight, the brushes (9), connected with the body of the instrument, are located in the middle of the sectors of the disc (5). In this case, the control winding and the motor (4) are connected with phase B and develop the normal correcting moments. If the bank of the aircraft exceeds 9° , then the brushes (9) break contact with the current carrying sectors of the disc (5), and the motor (4) is switched off.

The corrector cutoff is blocked during the period of starting the instrument by means of the bimetallic relay (7) and the mechanism (6), which are connected with the object of duplication.

At the instant of starting the instrument, the bimetallic relay is in the closed state and the control windings of the electric motor (4) are connected to the contact of this relay to phase B. In this case the lateral corrector of the gyroscope operates at any lateral inclinations of the gyroscope. At the same time the starting mechanism (6), whose closed contacts duplicate the bimetallic relay (7), is turned on. This duplication allows the instrument to be started even if the bimetallic relay should fail for some reason, or if the pilot should forget to turn on the starter mechanism (6).

The winding on the bimetallic relay, with a resistance of 1500 ± 50 ohms, becomes heated, and in $45 - 180$ sec after the current is turned on, it breaks the circuit connecting the phase B with the terminal G of the snap connector. During this time the gyro spindle is able to establish itself in the vertical position, owing to the forced operation of the correction mechanism.

To assure stability of the operating time of the bimetallic relay in an ambient

temperature range from $+50^{\circ}$ to -60° C, two bimetallic plates are installed in it. When the temperature of the air varies, both plates are flexed parallel to each other, maintaining the contact force constant at 25 to 30 g. When the heating winding is switched onto one of the bimetallic plates, this plate becomes heated and deformed. The contact pressure continuously weakens, and after 40 - 150 sec, the contacts are separated.

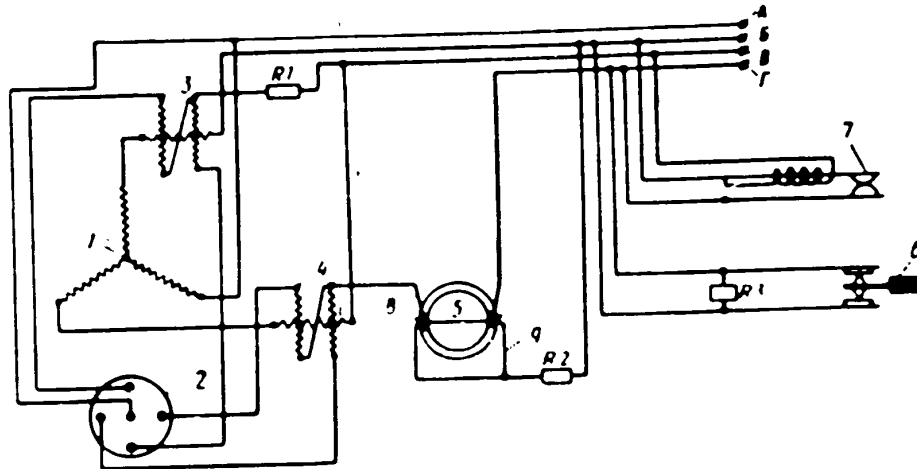


Fig.9.43 - Electrical Circuit of Gyro Horizon

a - Gyro motor winding; 2 - Liquid pendulum switch; 3 - Electric motor for longitudinal corrector; 4 - Electric motor for lateral corrector; 5 - Disc for cutting out corrector; 6 - Mechanism for blocking corrector cutout; 7 - Bimetallic relay; 8 - Common leadout of control winding; 9 - Brushes;

R_1, R_2, R_3 - Resistors

The signal flag (11), connected with the handle (12), appears in the zone of visibility of the front part of the instrument (Fig.9.44,a) when the cutoff of the lateral correction is blocked. When the block is removed, that is, when the switch is in a neutral position, the signal flag disappears (Fig.9.44,b).

The resistors $R_1 \approx 500$ ohms and $R_2 \approx 240$ ohms serve to produce the necessary torque characteristics for the correction motors. The resistor $R_3 - 5.1$ ohms is a

STAT

spark arrester in the circuit of the brushes (9) and the disc sectors (5). The terminal G of the snap connector serves to test the operating time of the relay (7) and the angle of cutoff of the lateral corrector. With this object a voltmeter is connected between the terminals B and G. If the brushes (9) are on the current carrying sectors of the disc (5), then the voltmeter will show a voltage drop of about 1.8 volts across resistor R_2 . When the brushes are displaced away from sectors, the voltmeter shows the full phase voltage of about 36 - 40 volts.

Figure 9.45 shows the design of the instrument.

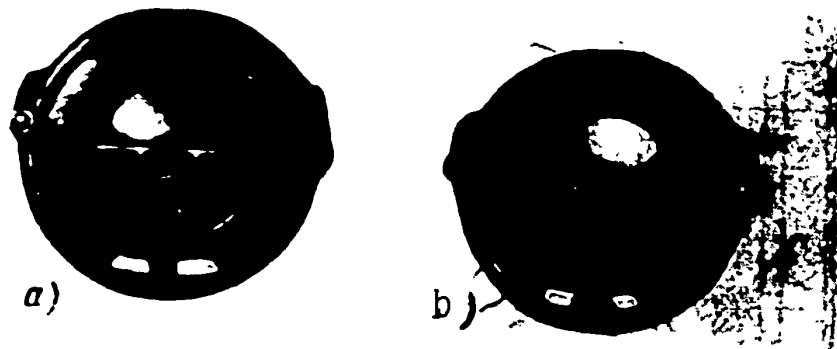
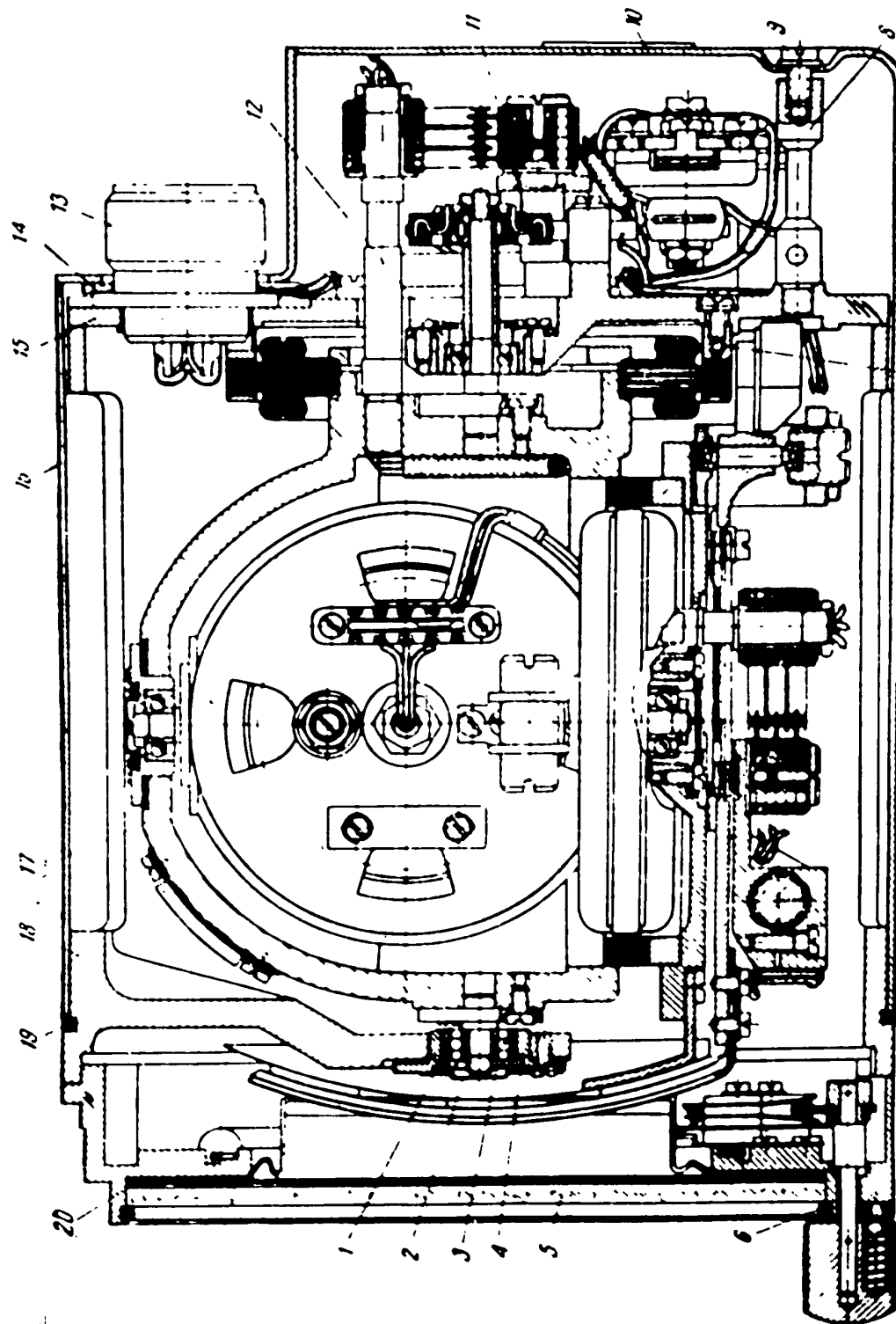


Fig.9.44 - Front View of Gyro Horizon before Starting (a)
and After Establishment of the Gyro (b)

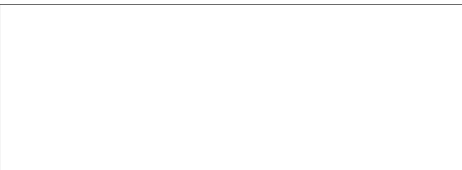
The technical characteristics of the gyro horizon are as follows:

1. Errors in determining bank and pitch in rectilinear flight, not over 1° .
2. Error in readings due to turns lasting up to 6 min and with banks from 10 to 80° , amount to 1 - 2° .
3. Errors in readings arising on additional turns of aircraft by 30 - 60° with banks of 5 - 7° , reach 4° .
4. Direct current used by instruments when supplied by the PAG-1F converter, 2.5 amp.
5. Alternating current used by each phase not more than 0.4 amp.

STAT



21



STAT

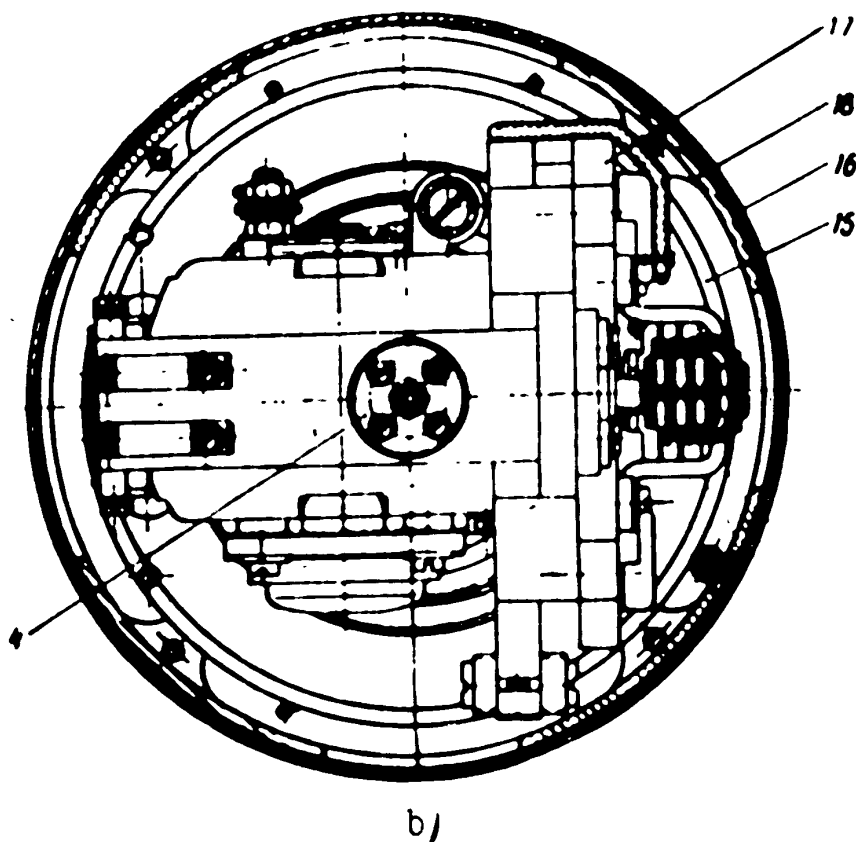


Fig.9.45 - General View of AGB-1 Gyro Horizon

a - Top view; b - Side view

1 - Bearing; 2 - Special disc; 3 - Nut; 4 - Body plug; 5 - Glass; 6 - Ring;
 7 - Stator of longitudinal corrector electric motor; 8 - Stand; 9 - Screw;
 10 - Pin; 11 - Disc; 12 - Plug; 13 - Plug yoke; 14 - Washer; 15 - Rear cover;
 16 - Casing; 17 - Gimbal connection; 18 - Body; 19 - Gasket; 20 - Gasket

6. Time to prepare instrument for use: at ambient temperatures of $+20 - +50^{\circ}\text{C}$, not more than 3 min, and at -60°C not more than 6 min. (An aircraft with a gyro horizon is allowed to take off only after the lapse of this period of preparation of the instrument.)

7. Maximum altitude of instrument, up to 20,000 m.

8. Weight of instrument, not over 2 kg.

9. Instrument is vibration proof for horizontal vibration with accelerations up to 0.6 g, and for vertical vibration with accelerations up to 1.5 g in the frequency range of 10 to 80 cycles.

The mechanism of the gyro horizon is covered by the casing (16) (Fig.9.45) with the rubber washer (19), keeping the instrument dustproof. With this same object, gaskets are placed between the casing (16) and the socket yoke (13). The gyro unit is balanced by means of lead weights and balancing screws. The axial play of the gimbal connection (17) is accomplished by gaskets inserted between the plug (4) and the body (18) of the instrument. The face side of the instrument is covered by the glass (5) attached to the front cover by the split ring (6).

The installed diameter of the gyro horizon is 110 mm, the length of the body is 156 mm. The attachment to the instrument board is accomplished by four M5 x 15 screws screwed into locking nuts of the front flange.

The AGI-1 Fighter Gyro Horizon

In stunt flying, the shaft of the gyro rotor may coincide with the shaft of the outer frame. In this case the gyro will lose one degree of freedom and will therefore lose its stability and will be blocked thereby interfering with the normal operation of the gyro horizon. Various devices are used to prevent the coincidence of these axes.

Figure 9.46 shows another version of this device in a gyro vertical with stop.

On the casing (5) of the gyro rotor is installed the rod (2) with the disc (3) at the end. Through the outer axis of the gimbals is passed the stop (1) which, STAT

when the axis of the gyroscope rotor dangerously approaches the shaft of the inner frame, will make contact with the disc (3). The force acting on the disc will produce a moment whose vector is directed along the axis of the inner frame of the

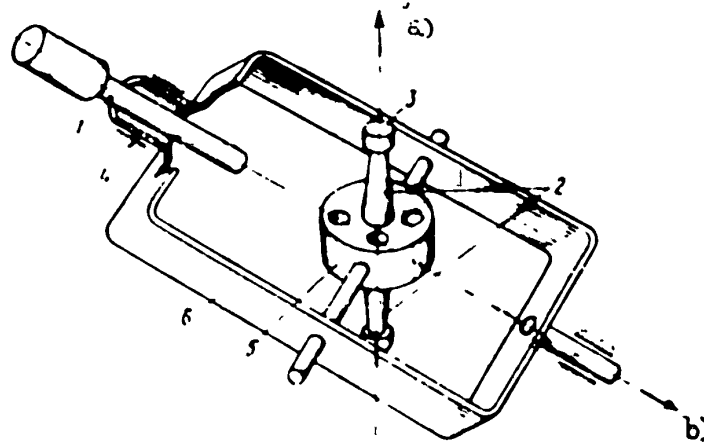


Fig.9.46 - Gyro Vertical with Stop

1 - Stop; 2 - Rod; 3 - Disc; 4 - Hollow gimbal shaft; 5 - Casing;
6 - Outer frame

a) Axis of gyroscope rotor; b) Longitudinal axis of aircraft

gimbals. The precession due to this moment is directed in such a way that the disc (3) slides along the surface of the rest of the stop (1) and runs around it, thus eliminating the coincidence between the gyroscope spindle and the outer frame of the gimbals. Obviously the stop (1) will force the gyroscope spindle to deflect from the vertical by a certain angle, which is a shortcoming of this device.

Another example of a device that eliminates the superimposition of the axes, is the gyro horizon in which the axis of the gyroscope rotor does not lie in the plane perpendicular to the axis of the inner frame of the gimbals and of the outer frame passing through its axis, but is inclined by angle of 3° with respect to this plane.

The type AGI-1 gyro horizon for a fighter aircraft is an improved example of such designs (Fig.9.47).

STAT

In this gyro horizon, the angle between the axis of the gimbals and the axis of the gyroscope rotor is automatically held at 90° during any maneuvers of the aircraft, as a result of which the gyroscope maintains its maximum stability constant. For this purpose, the gyro unit (1) (Fig.9.48) and the gimbals (2) are suspended on bearings in the servo frame (3), which is automatically maintained by the electric motor (6) in a position such that the axis II-II shall be perpendicular to the principal axis of rotation of the gyro. The sensitive element registering any disturbance in the mutually perpendicular position of the axes, and which switches on the actuating electric motor (6) to restore the mutually perpendicular position of the axes, consists of the switch (4) attached to the outer gimbals (2), and the sliding contact (5), connected with the gyro unit. The rate of actuation of the servo frame is taken considerably greater than the maximum angular velocity of the banking maneuvers of the aircraft, thanks to which the mutually perpendicular position of the axes and the maximum stability of the gyro are maintained during any maneuvers of the aircraft whatsoever.

The readings of bank and pitch of the aircraft are measured from the position of the aircraft outline (7), which is connected with the body of the instrument, with respect to the spherical scale (8) connected with the gyro unit. Consequently, the scale (8) for reading off the longitudinal and lateral banks does not vary its position with respect to the ground. The angle of pitch is measured about the horizontal axis II-II, the angle of bank is measured about the axis I-I located parallel to the longitudinal axis of the aircraft. This position of the axes of the gyro system allows measurements of the true angles of pitch and bank. The spherical scale (8) is painted in colors: the upper hemisphere is colored brown, the lower blue. When the aircraft dives, the aircraft outline enters the upper hemisphere; this hemisphere has numbered scale divisions for reading off the angles of pitch from 0 to 360° . The accuracy of the reading of the angles of bank decreases as the angle of pitch increases.

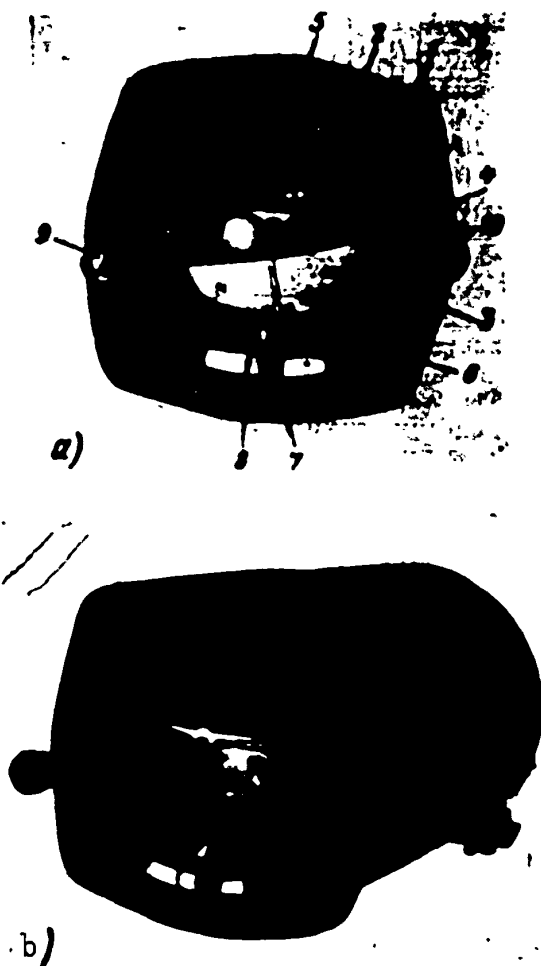


Fig.9.47 - a) Outer View of Gyro Horizon, Type AGI-1, for Fighter Aircraft; b) Face View

- 1 - Body; 2 - Aircraft outline;
- 3 - Spherical scale; 4 - Index-horizon;
- 5 - Pitch scale; 6 - Bank scale;
- 7 - Sideslip indicator; 8 - Index of sideslip indicator; 9 - Handle for shifting aircraft outline; 10 - Starting button

Thus, for instance, with an angle of pitch up to 70° , the error in bank does not exceed 3° ; with an angle of pitch of 75° the error amounts to $3 - 4^\circ$; with an angle of pitch of 80° the error reaches 6° . In a vertical dive or climb (angle of pitch $\pm 90^\circ$), the longitudinal axis of the aircraft coincides with the direction of the principal axis of the gyro, and the gyro horizon loses its sensitivity to the angle of bank. Consequently, in diving or climbing at angles of around $80 - 90^\circ$, the bank cannot be followed with the gyro horizon.

To eliminate the turning errors, the AGI-1 gyro horizon, like the AGB-1 gyro horizon, is provided with a cutout for the corrector, on turns with an angle of bank of more than 13° . Owing to this cutout, the error after a turn does not exceed 3° .

The electrical circuit as given by Fig.9.49 for the AGI-1 gyro horizon has much in common with the circuit of Fig.9.43. The electric motor (1) of the gyroscope, the liquid

STAT

pendulum switch (2), and the electric correction motors (3) and (4), are the same as in the AGE-1 gyro horizon. The power supply for the electric circuit of the gyro

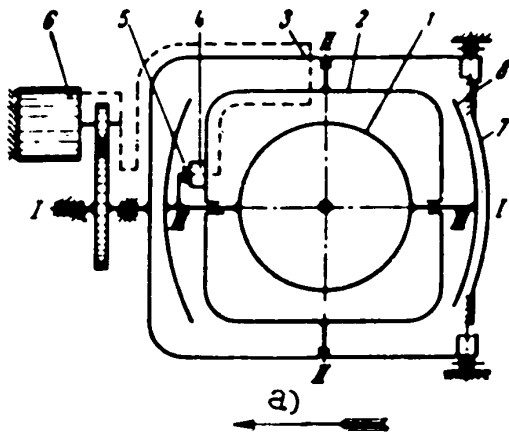


Fig.9.48 - Schematic Kinematic Diagram
of AGI-1

1 - Gyro unit; 2 - Gimbals; 3 - Servo frame; 4 - Switch for electric motor; 5 - Contact of switch; 6 - Electric actuating motor; 7 - Aircraft outline; ε - Spherical scale

a) Direction of flight

switch (5). The contact of the switch, connected with the case of the gyro motor, is connected to the phase B and feeds this phase to the first or second control winding of the motor (6), depending on the side to which the outer gimbal axis of the gyroscope deflects from the perpendicular position to the shaft of the rotor of the gyro horizon. The electric motor (6) actuates the servo frame and restores the perpendicular position between the axes. The switch (7), located on the outer shaft of the gimbal, switches the ends of the control windings of the electric motor (6) and provides the correct sense of rotation of the electric motor in the case of the

horizon is through the terminals ABC from a type PAG-1F converter. The excitation windings of the correction motors (3) and (4) are connected in series with the phases of the electric motor of the gyroscope, which provides for the forced state of operation of these motors on starting the instrument. The operation of the correction system of the gyroscopes is the same in AGI-1 and AGE-1. The excitation winding of the actuating motor of the servo frame (frame (3) in Fig.9.48) is connected between phases A and B. The middle point of the control windings is connected to phase A. The ends of the control windings are brought out to the

STAT

actuation of the servo frame when making a Nesterov loop.

The ballast resistor 10 limits the rate of precession of the gyroscope in the longitudinal direction to 3 - 5.5 °/min. At temperatures below -35°C this resistor

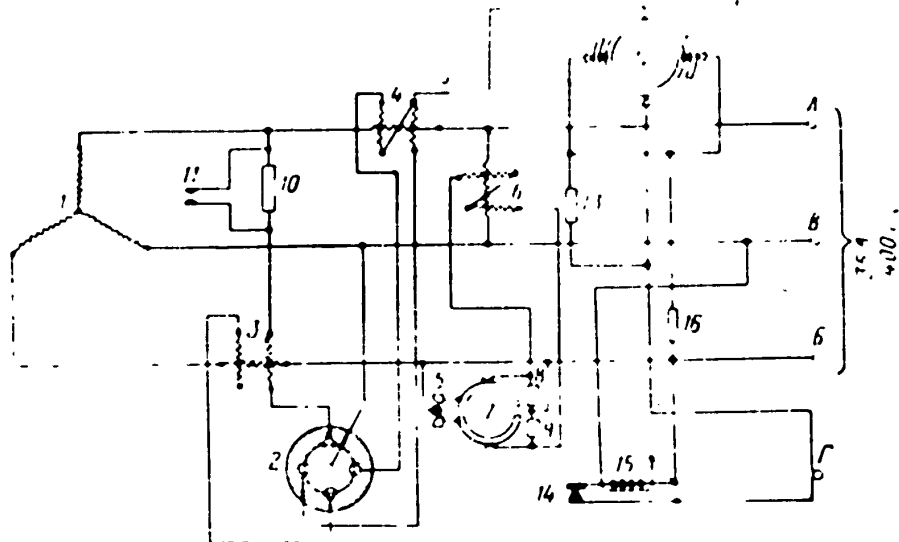


Fig.9.49 - Schematic Electrical Diagram of AGI-1

1 - Electric motor of gyroscopes; 2 - Liquid pendulum switch; 3 - Longitudinal correction electric motor; 4 - Electric motor of lateral correction; 5 - Switch of electric motor of actuation of servo frame; 6 - Electric motor of actuation of servo frame; 7 - Switch; 8 and 9 - Spark arresting resistors of 3300 ohms (0.25 w); 10 - Ballast resistor, 300-430 ohms (0.5 w); 11 - Bimetallic switch; 12 - Cutout of corrector on turns; 13 - Spark arrester resistor, 5100 ohms (0.25 w); 14 - Bimetallic relay; 15 - Heating element; 16 - Ballast resistor, 100 ohms (1 w)

is closed by the bimetallic switch (11), thus accelerating the starting of the instrument under low temperature conditions.

The cutoff switch for the lateral corrector (12), operates when the aircraft banks more than 13°. The ballast resistor (16) limits the current in the control windings of the electric motor and of the lateral corrector. The rate of precession

of the gyroscope in the lateral direction is as high as $3.5 - 7$ °/min.

In starting the instrument, the corrector cutoff switch (12) is blocked by the bimetallic time relay (14), and the control windings of the electric motor (4) of the lateral corrector are connected to the terminal B through the closed contacts of relay (14), regardless of the initial position of the gyro unit or the magnitude of the angle of bank. In 40 - 150 sec after the heating element (15) is turned on, it causes deformation of one of the bimetallic plates of relay (14), thus separating the contacts, unblocking the corrector cutoff switch, and bringing the gyro horizon from the starting into the operating state. The heating element is always energized after that, and a clearance of the order of 0.4 - 0.8 mm is established between the contacts of relay (14).

The terminal G in the snap connector is used, as in the gyro horizon AGB-1, for testing the operating time of the relay (14) and the angle of bank at which the correction is switched off.

Figure 9.50 gives a structural diagram of the AGI-1 gyro horizon. The gyro motor (1), with liquid pendulum switch, is suspended on bearings in the gimbal (4). On the shaft of the gyro unit is attached the spherical scale (6), the cut-in switch (5) for the mutually perpendicular position of the axes, and the rotor of the electric motor (2) for the longitudinal correction. The stator of this electric motor is located on the frame (4).

The frame (4) is suspended on bearings attached in the servo frame (7).

The stator of the electric motor (3) of the lateral corrector is mounted in the servo frame (7), while the rotor is attached to the frame (4). The servo frame suspended in the body rests on its front part on the three supporting bearings (8) and in the rear part on one radial ball bearing. The electric actuating motor is attached to the instrument case and is connected with the servo frame through a reducer with a gear ratio of 1 : 16.3. On the rear part of the instrument, on the shaft of the servo frame, is mounted the switch (15), cutting out the corrector

STAT

during turns.

To shorten the starting time of the instrument the push-button mechanism (10) is employed to switch on the power supply of the gyro horizon.

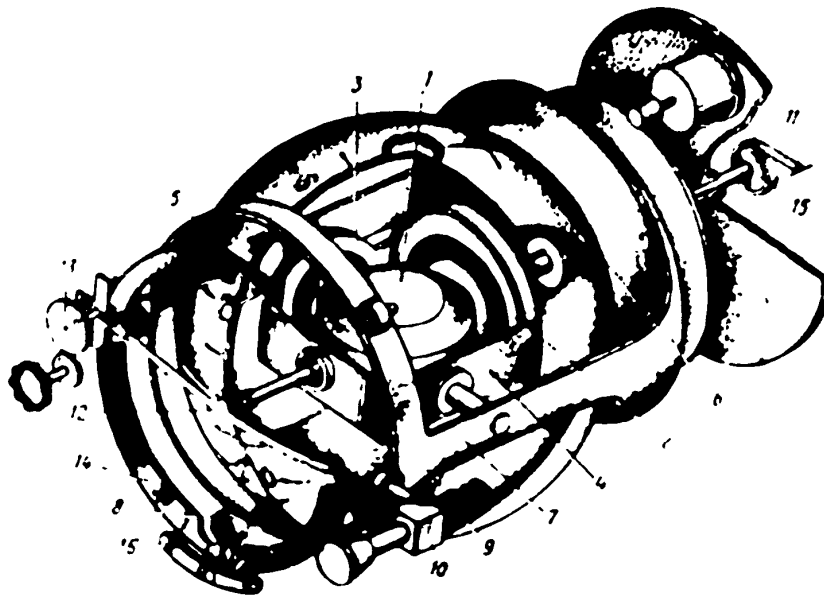


Fig.9.50 - Structural Diagram of AGI-1

1 - Gyro motor with liquid pendulum switch; 2 - Electric motor for longitudinal corrector; 3 - Electric motor for lateral corrector; 4 - Gimbal frame; 5 - Switch for setting axes in mutually perpendicular position; 6 - Spherical scale; 7 - Servo frame; 8 - Support bearings of servo frame; 9 - Cam surface of servo frame; 10 - Push-button mechanism; 11 - Electric motor operating servo frame; 12 - Aircraft outline; 13 - Mechanism for shifting aircraft outline; 14 - Lateral banking scale; 15 - Cutout switch for corrector on turns; 16 - Side slip indicator

When the button (10) is pressed, the force is transmitted through a bearing on the face side of the servo frame, made in the form of the cam (9). The profile of the face cam is so selected as to assure the setting of the servo frame from any arbitrary position to its normal horizontal position. The displacement of the air-vertical plane is effected by means of the mechanism (13) STAT

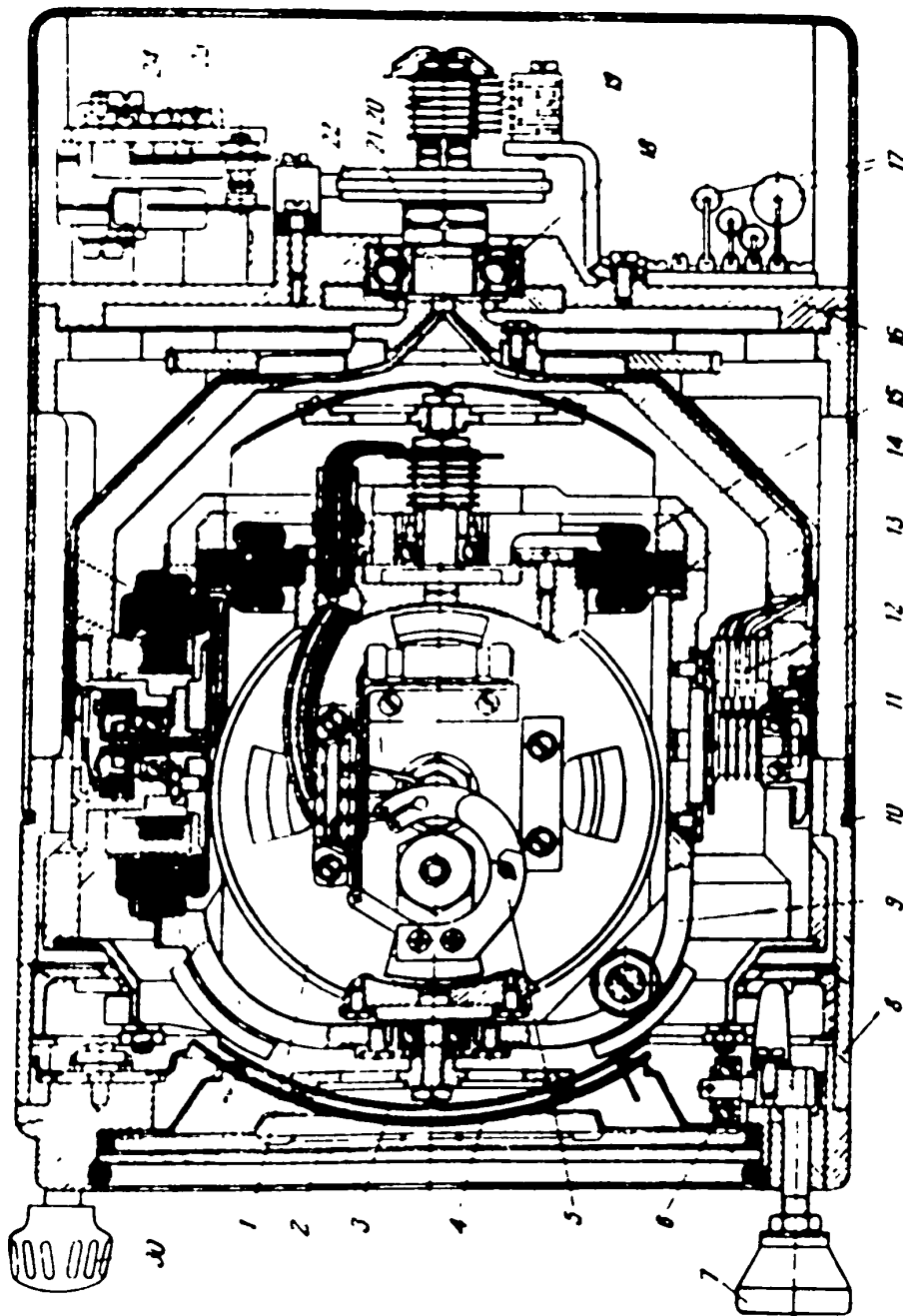


Fig.9.51 - General View of AGI-1 (View from Top)

1 - Gyro unit; 2 - Glass; 3 - Spherical scale; 4 - Aircraft outline; 5 - Bimetallic switch; 6 - Ball bearing of push-button starting mechanism; 7 - Starting push-button; 8 - Instrument casing; 9 - Gimbal frame; 10 - Rubber gasket; 11 - Ball bearing; 12 - Brush unit and contact rings; 13 - Unit of servo frame; 14,15 - Stator and rotor of electric motor for longitudinal correction; 16 - Unit of plate; 17 - Spark-suppressor and ballast resistors; 18 - Bearing of shaft of servo frame; 19 - Unit of current-carrying brushes; 20 - Current-collector rings; 21 - Spindle of servo frame; 22 - Disc of corrector cut-off; 23 - Casing; 24 - Mechanism of bimetallic time relay; 25,26 - Rotor and stator of electric motor for lateral corrector; 27 - Ball bearing; 28 - Ring with supporting bearings for servo frame; 29 - Unit of front flange; 30 - Handle of mechanism for shifting aircraft outline

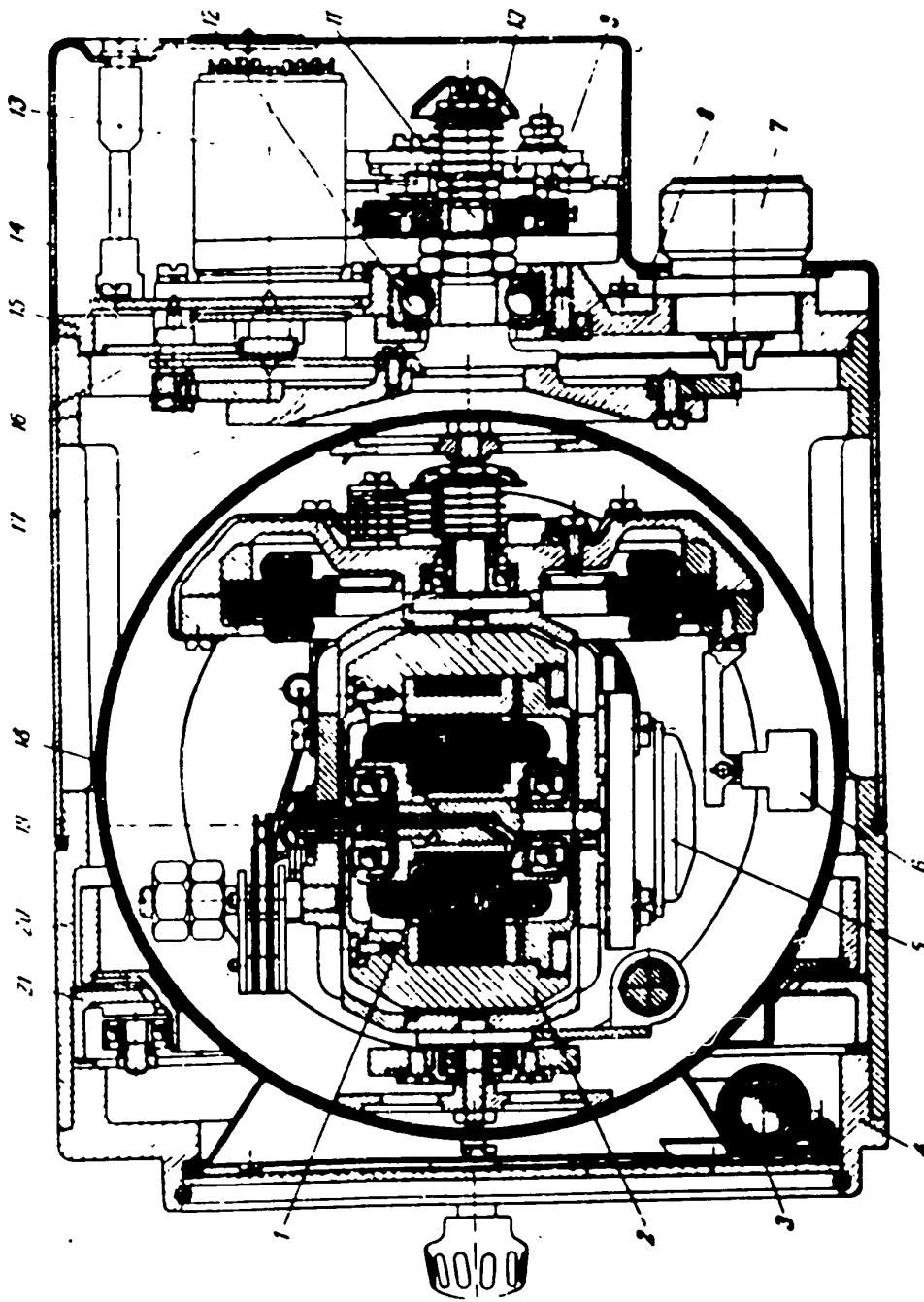


Fig.9.52 - General View of AGI-1 (Side View)

- 1 - Stator of electric motor of gyroscope; 2 - Rotor of electric motor and gyroscope; 3 - Side-slip indicator; 4 - Attachment of front flange; 5 - Liquid pendulum switch; 6 - Starting pendulum;
- 7 - Yoke for snap connector; 8 - Rubber gasket; 9 - Disc of correction cutout; 10 - Collector;
- 11 - Shaft of servo frame; 12 - Bearing; 13 - Electric motor actuating servo frame; 14 - Casing;
- 15 - Attachment of plate; 16 - Reducer; 17 - Attachment of servo frame; 18 - Spherical scale;
- 19 - Rubber gasket; 20 - Case of instrument; 21 - Ring with bearings

STAT

whose handle is located in the left part of the front flange of the body.

The angles of bank are read off on scale (14), the angles of pitch on the spherical scale (6). The side-slip indicator (16) is placed at the bottom of the front flange of the case.

Figures 9.51, 9.52 and 9.53 show the structure of gyro horizon AGI-1.

The technical data of the gyro motor and pendulum liquid switch are the same as those of the analogous units of the AGB-1. The longitudinal corrector motor develops a torque of not less than 7 γ - cm. The DC resistance of its excitation winding is 5 ohms \pm 0.5 ohm; the DC resistance of each control winding is 180 ohms \pm 18 ohms. The electric motor for the lateral corrector develops a torque of about 5.5 γ - cm; the direct current resistance of these windings is: excitation winding, 12.5 ohms \pm 1 ohm; and for each control winding, 300 ohms \pm 30 ohms.

The heating element of the bimetallic time relay has a DC resistance of 1500 ohms \pm 50 ohms. The electric motor operating the servo frame is standard, of type DID-0.5. Its maximum static torque is about 5.5 γ - cm. Its idling speed is not less than 13,000 rpm. The direct current resistance of the excitation winding is 70 ohms \pm 7 ohms. The resistance of each control winding is 260 ohms \pm 26 ohms.

Principal Characteristics of AGI-1 Gyro Horizon

1. Error of readings of angles of pitch and bank in state of horizontal flight, 1°.
2. Errors of instrument:
 - a) after turn with bank of over 15°, not over 3°;
 - b) after stunt flying, not over 5°.
3. Range of measurement of angles of pitch and bank, unlimited.
4. Power supply of instrument, triphase, 36 v, 400 cycle alternating current.
Alternating current (line) drawn, not over 0.6 amp.
5. Altitude performance of instrument to 20,000 m.
6. Temperature range of operation from +50°C to -60°C.

STAT

7. Weight of instrument not over 2.6 kg.

8. Time when instrument ready for operation after switching on:

at temperatures from $+50^{\circ}$ to -30°C 2 min

at temperatures from -30° to -60°C 3 min

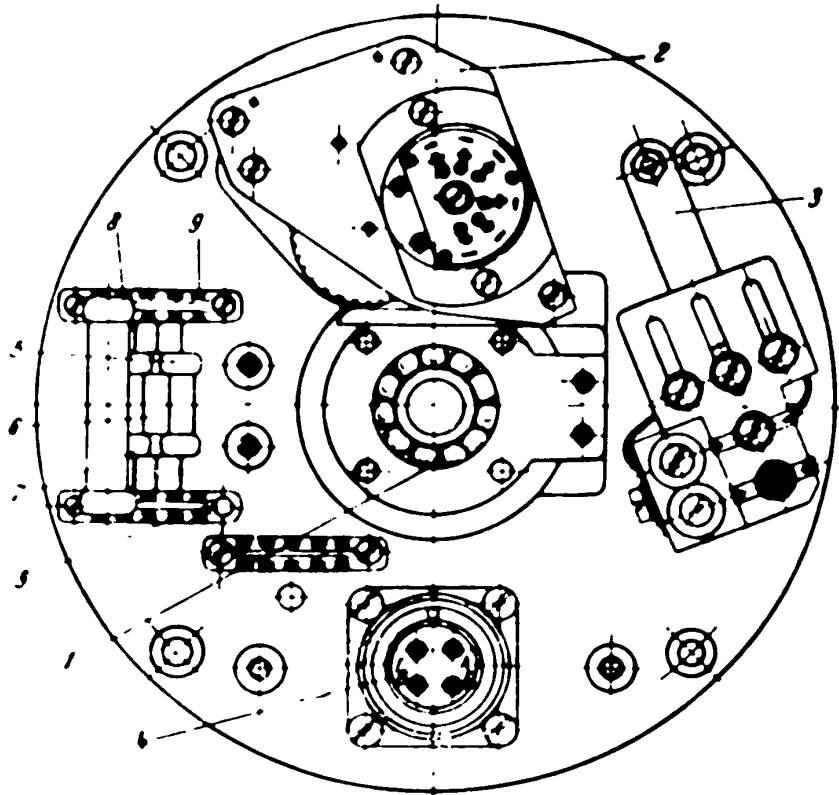


Fig.9.53 - Plate Unit (Rear View)

1 - Bearing; 2 - Electric actuating motor with reducer; 3 - Bimetallic relay;
4 - Yoke of plug connector; 5, 6, 7 - Spark-suppressor resistors; 8 - Ballast
resistor, 100 ohms (1 w); 9 - Assembly boxes

The instrument allows supervision of the state of horizontal flight, bringing the aircraft into horizontal flight on loss of spatial orientation in bank and pitch, and allows supervision of the accuracy of execution of all maneuvers by an

hunt maneuvers.

STAT

During night flights, the colored luminescent coating of the indicating elements of the gyro horizon provides easily perceived orientation in bank and pitch.

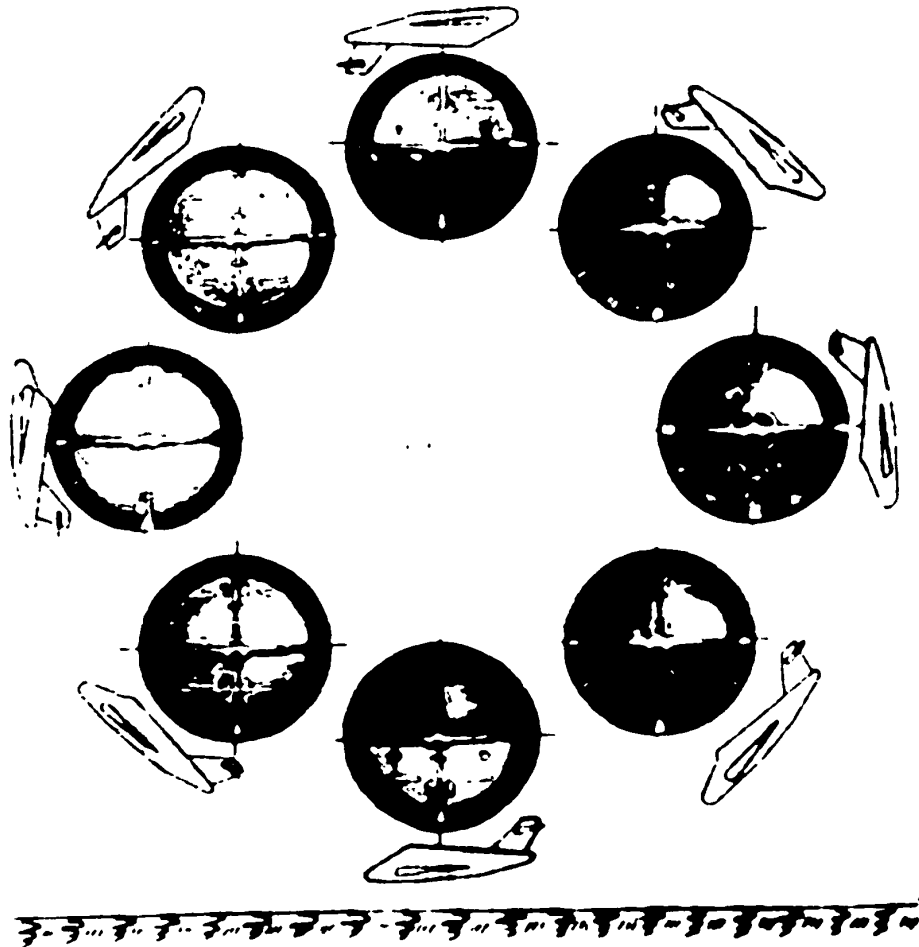


Fig. 9.54 - Readings of AGI-1 Gyro Horizon in Performing a Nesterov Loop

Figures 9.54, 9.55, and 9.56 give examples of the readings of the gyro horizon during execution of various maneuvers.

The AGI-1 gyro horizon is installed on a shock absorbing mounting with an allowable load factor of 1.3 g. The instrument board should be located perpendicular to the longitudinal axis of the aircraft with an accuracy of $\pm 1^\circ$. The gyro horizon is attached to the instrument board by four M5 x 15 screws with half-round

STAT

heads.

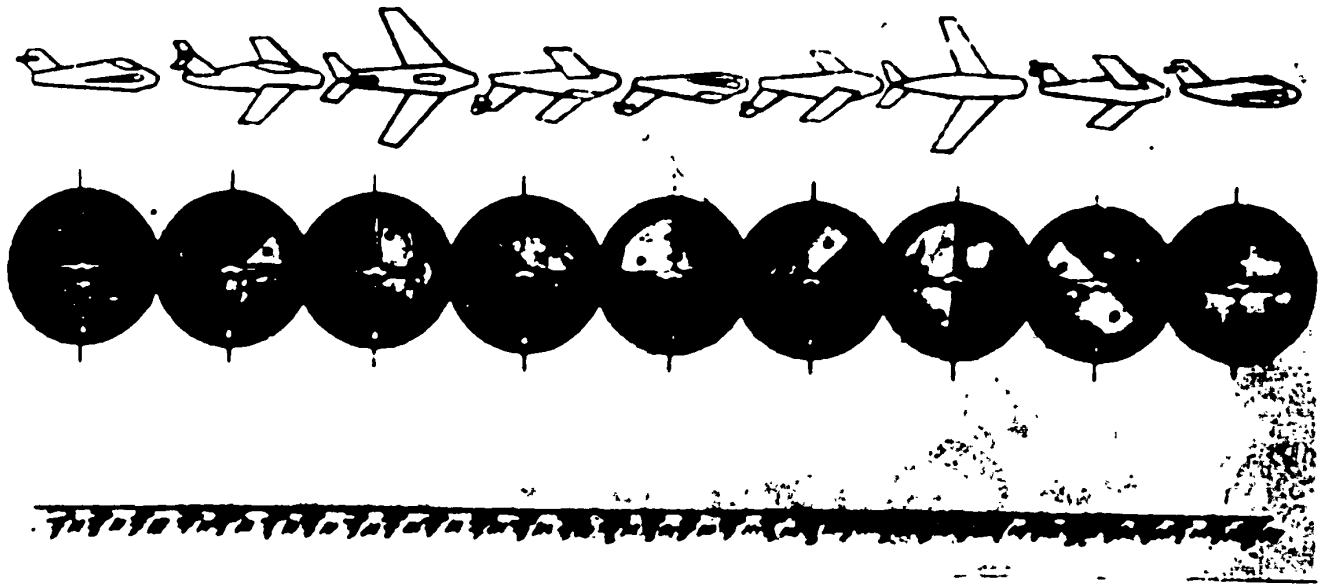


Fig.9.55 - Readings of AGI-1 Gyro Horizon during a Right Barrel Turn

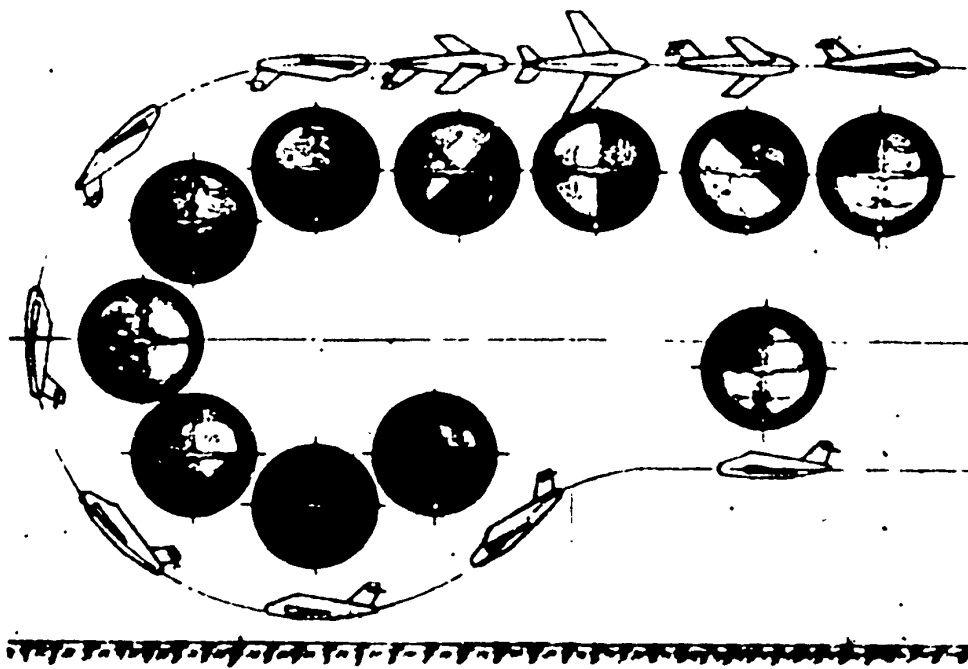


Fig. 9.56 - Readings of AGI-1 Gyro Horizon during a Nesterov Half Loop

STAT

The PAG-1F converter supplying the gyro horizon with power should have a 15 amp fuse for the starting current and a 3 amp fuse for the operating current.

STAT

CHAPTER 10

DEVIATIONS OF COURSE GYROSCOPES

Section 10.1. The Directional Gyro (GPK)General Remarks

A course gyroscope whose outer frame has a constant precession designed to compensate the effect of the earth rotation, while the inner frame has a radial correction with one characteristic or another, accomplished either with a pendulum or by the position with respect to the outer frame, is called a directional gyro. Usually the outer frame, that is, the frame which is not corrected, is used as the working frame in the directional gyro, that is, the frame used to attach the compass card, or for connection with the corresponding transmitter of the autopilot. Its position is oriented before it is turned on by rotating the arrested gyroscope by means of the corresponding handle until the readings of the directional gyro card agree with the readings of the magnetic compass card. After this has been accomplished, the arrester is released. By virtue of the properties of gyroscopic rigidity, for a limited period of time, of the order of 10 - 15 min, the directional gyro will indicate, with a certain degree of accuracy, the course of the aircraft, that is, it will serve as a compass. When this period of time has elapsed, the readings of the directional gyro are again verified from the readings of the magnetic compass and the appropriate corrections made in its position on the basis of these readings.

This principle of utilization of the directional gyro is connected with the

STAT

fact that the exact holding of the aircraft course still does not mean the exact holding of the assigned route line, owing to the influence of drift, which is always known only approximately. This circumstance forces periodic checks, every 10 - 15 min, of the actual maintenance of the assigned route, followed by the appropriate corrections to the assigned course. When this is done the position of the directional gyro is incidentally corrected.

We shall consider that, at the initial instant, the corresponding correction has been made, and that in connection with this correction the spin axis is located, at the initial instant, sufficiently close to the plane of the meridian. Its non-coincidence with this plane and its subsequent deflection from it by the angle of shift of the outer frame will be what will characterize the deviation of the directional gyro.

Deviation of Directional Gyro in Rectilinear Flight

The starting equations of motion will, as before, be the equations of precession

$$\left. \begin{aligned} Hq &= L_x \\ -Hp &= L_y \end{aligned} \right\} \quad (10.1)$$

For p and q we have, respectively (cf. eq.(2.36) and eq.(2.37):

$$\left. \begin{aligned} p &= -\beta - \left(\omega_1 + \frac{V}{R} \sin K \right) \alpha + \frac{V}{R} \cos K \\ q &= \alpha - \left(\omega_1 + \frac{V}{R} \sin K \right) \beta + \left(\omega_1 + \frac{V}{R} \frac{\sin K}{\cos \varphi} \right) \sin \varphi \end{aligned} \right\} \quad (10.2)$$

where ω_1 = horizontal component of angular velocity of earth rotation, $\omega_1 = \omega_e \cos \varphi$;

ω_e = angular velocity of earth rotation;

V = flight speed;

K = course of aircraft;

STAT

φ = latitude of place;

R = radius of earth.

The expressions for the moments L_x and L_y will be taken in the following form:

$$\begin{aligned} L_x &= k_2 + L_1 \operatorname{sign}(\dot{\beta} - \dot{\psi}_1), \\ L_y &= -f(\beta) \cdot \dot{L}_1 \operatorname{sign}(\dot{\alpha} - \dot{\psi}_1), \end{aligned} \quad (10.3)$$

where k_2 - the moment, constant in magnitude and direction, designed to compensate the effect of the earth rotation;

$\dot{\psi}_n$ - component of angular velocity of rotation of aircraft about the axis of the outer frame, i.e., along the normal axis of the aircraft; since the axis of the outer frame of the directional gyro is located parallel to the normal axis of the aircraft, then, for horizontal flight, $\dot{\psi}_n$ will represent the angular velocity of yawing of the aircraft;

$f(\beta)$ - moment of correction of inner frame;

$\dot{\psi}_x$ - component of angular velocity of rotation of aircraft about the axis of the inner frame Ox .

The form of the expression selected for L_x and L_y thus take into account the influence of friction in the suspension, not only in connection with the rotation of the gyro about the axes of the gimbals, but also in connection with the rotation of the aircraft about these axes. The actual picture of the origin of the moments of friction in the axes is precisely what is connected with the sign of the resultant velocity of rotation of the corresponding bearing and the spindle lying in it, with respect to each other.

On substituting eqs.(10.2) and (10.3) in (10.1), we get

$$\left. \begin{aligned} H \left[\dot{\alpha} - \left(\omega_1 + \frac{V}{R} \sin K \right) \dot{\beta} + \left(\omega_3 + \frac{V}{R} \frac{\sin K}{\cos \varphi} \right) \sin \varphi \right] &= \\ &= k_2 + L_1 \operatorname{sign}(\dot{\beta} - \dot{\psi}_1); \\ H \left[\dot{\beta} + \left(\omega_1 + \frac{V}{R} \sin K \right) \dot{\alpha} - \frac{V \cos K}{R} \right] &= -f(\beta) - \\ &- L_1 \operatorname{sign}(\dot{\alpha} - \dot{\psi}_1). \end{aligned} \right\} \quad (10.4)$$

STAT

We shall consider in the future that the characteristic of correction $f(\beta)$ is proportional. Then eq.(10.4) may be rewritten in the following form:

$$\left. \begin{aligned} \dot{\alpha} &= \left(\omega_1 + \frac{V}{R} \sin K \right) \beta + \Omega_1, \\ \dot{\beta} &= - \left(\omega_1 + \frac{V}{R} \sin K \right) \alpha - \Omega_2, \end{aligned} \right\} \quad (10.5)$$

where

$$\Omega_1 = \frac{L}{H} \left(\omega_3 + \frac{V \sin K}{R \cos \varphi} \right) \sin \varphi + \frac{L}{H} \text{sign}(\dot{\beta} - \dot{\psi}_x), \quad (10.6)$$

$$\Omega_2 = \frac{V \cos K}{R} - \frac{L}{H} \text{sign}(\dot{\alpha} - \dot{\psi}_x). \quad (10.7)$$

Let us confine ourselves to a qualitative analysis of the paths of the vertex of the gyro, by constructing the field of tangents to these paths.

On dividing one of eqs.(10.5) by the other, we get

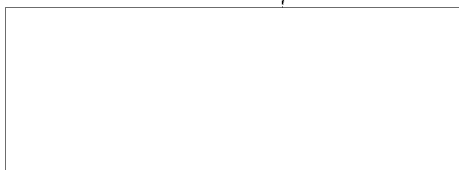
$$\frac{d\alpha}{d\beta} = - \frac{\left(\omega_1 + \frac{V}{R} \sin K \right) \beta + \Omega_1}{\left(\omega_1 + \frac{V}{R} \sin K \right) \alpha + \Omega_2}. \quad (10.8)$$

The equation so obtained is the equation of the slopes with respect to the axis $O\beta$ of the tangents to the paths of the vertex of the gyro.

Let us find the locus of points at which the tangents to the paths have one and the same inclination ν . As already mentioned, such loci are called isoclinic. For this purpose it is sufficient to equate the right side of eq.(10.8) to the quantity ν . On doing this, and solving the equation so obtained with respect to α , we get the required equation of the isoclines in the following form:

$$\alpha = \frac{\omega_1 + \nu}{\omega_1 + \frac{V}{R} \sin K} \beta + \frac{\Omega_2 - \nu \Omega_1}{\omega_1 + \frac{V}{R} \sin K}. \quad (10.9)$$

where



STAT

$$\omega_i = \omega_1 + \frac{v}{R} \sin \lambda_i.$$

It follows from this equation that the isoclines will be straight lines.

Let us find further the coordinates of the intersection of the isoclines for tangents of two different slopes, v_1 and v_2 . For this purpose it is sufficient to solve simultaneously the two equations obtained after substituting in the equation of isocline eq.(10.9) a v equal respectively to v_1 and v_2 , i.e., the equations

$$\left. \begin{aligned} \alpha + \frac{\omega_1 + v_1 \epsilon}{v_1 \omega_1} \beta &= \frac{\omega_2}{\omega_1} - \frac{v_2}{v_1 \omega_1}, \\ \alpha + \frac{\omega_1 + v_2 \epsilon}{v_2 \omega_1} \beta &= \frac{\omega_2}{\omega_1} - \frac{v_1}{v_2 \omega_1}. \end{aligned} \right\} \quad (10.10)$$

Whence the coordinates of the intersections of the required intersection of the isoclines α_0 and β_0 are determined by the expressions

$$\alpha_0 = \frac{\omega_2}{\omega_1} + \frac{\epsilon}{\omega_1} \frac{\omega_1}{\omega_1}, \quad (10.11)$$

$$\beta_0 = -\frac{v_1}{\omega_1}. \quad (10.12)$$

It follows from these expressions that the coordinates of the points of the intersection of isoclines do not depend on the slope of the tangents to which these isoclines refer, and, in particular, that with unvaried values of Ω_1 , Ω_2 , ω_1 and ϵ , all the isoclines will intersect in a single point.

This circumstance very greatly simplifies the problem of constructing the field of tangents to the paths of the vertex of the gyro; in order to determine the slope of the tangents to a path at a given point, it is sufficient to draw a straight line connecting this point with the point of intersection of the isocline, prolong the straight line to the intersection with the $O\beta$ axis, and determine the tangent of the angle between this line and the $O\beta$ axis.

STAT

Let us assume that this tangent is equal to μ_i . Then, in order to determine the angle between the $O\beta$ axis and the tangents to the paths v_i , to which the isocline so drawn relates, we have, by eq.(10.9), the following equation:

$$\mu_i = - \frac{\omega_i \dot{v}_i}{v_i \dot{\omega}_i} \quad (10.13)$$

whence, by solving this equation with respect to v_i , we obtain

$$v_i = - \frac{\omega_i}{\mu_i \dot{\omega}_i + \dot{\omega}_i} \quad (10.14)$$

Let us now return to the expressions for the coordinates of the point of intersection of the isoclines.

Equation (10.11) for α_0 consists of two terms, of which the second is of an order which is $\frac{\varepsilon}{\omega_1}$ times higher than the order of the second, since $\frac{\Omega_1}{\omega_1}$ and $\frac{\Omega_1}{\omega_2}$, are of about the same order. The quantity $\frac{\varepsilon}{\omega_1}$ is of the order of one thousand, if we have in mind for ε the usual order of 0.05 to 0.10 l/sec. It follows from this that in the expression for α_0 , the first term can, with a high degree of accuracy, be neglected by comparison with the second term. Moreover, the coordinate β_0 will be so much greater in modulus than the coordinate α_0 , that, in the neighborhood of small values α and β , to which the theory here developed relates exclusively, the slopes of the isoclines will be relatively greater in modulus.

For isoclines I (Fig.10.1) $\beta = \beta_0$, the inclination to the $O\beta$ axis equals 90° , and, consequently, according to eq.(10.13), the angle between the $O\beta$ axis and the tangent to the path will be equal to 0° (cf.Fig.10.1).

With increasing angle between the positive semiaxis $O\beta$ and the isocline, μ_i takes a negative value, which gradually diminishes in modulus as this angle increases. In connection with this, the inclinations of the tangent to the $O\beta$ will increase.

At points with isoclines having an inclination equal to $\tan^{-1} \mu'$, where

$$\mu' = -\frac{\varepsilon}{\omega_1} \quad (10.15)$$

the inclinations of the tangents to the path will be equal to 90° . It is easy to see that there will only be one such isocline, namely the one that is obtained by joining the point of intersection of the isoclines to the origin of coordinates (if in eq.10.11 we neglect the first summand).

We shall call this isocline the boundary isocline (isocline 3 in Fig.10.1).

We remark that it follows, from what has been said of the order of magnitude of $\frac{\varepsilon}{\omega_1}$, that the boundary isocline will in practice coincide with the axis $O\alpha$.

In this way the motion of the vertex of the gyroscope from the points lying above the boundary isocline with which we have been dealing up to now, may be characterized as motion toward the boundary isocline, or, practically, motion toward the $O\alpha$ axis.

At the points lying below the boundary isocline, the inequality

$$|\mu| > \frac{\varepsilon}{\omega_1} \quad (10.16)$$

will obviously hold, and therefore the slopes of the tangents to the path of these points will be less than 90° . In other words, the motion of the gyro from these points will also be directed toward the boundary isocline, that is, practically toward the $O\alpha$ axis. It follows that, under any initial conditions, the motion of the gyro vertex along the boundary isocline will ultimately be established.

We remark that it follows from what has been said on the relation between ε and ω_1^0 , and from the form of eq.(10.14), that at all points, except for the immediate neighborhood of the boundary isoclines, the tangents to the paths, and consequently the paths themselves will be close to lines parallel to the $O\beta$ axis.

For the velocity of the motion of the gyroscope vertex, U , in this case, we

STAT

get, by eq.(10.5):

$$U = \sqrt{(\omega_1 \beta + \Omega_1)^2 + (\omega_2 - \omega_1 \alpha - \omega \beta)^2} \quad (10.17)$$

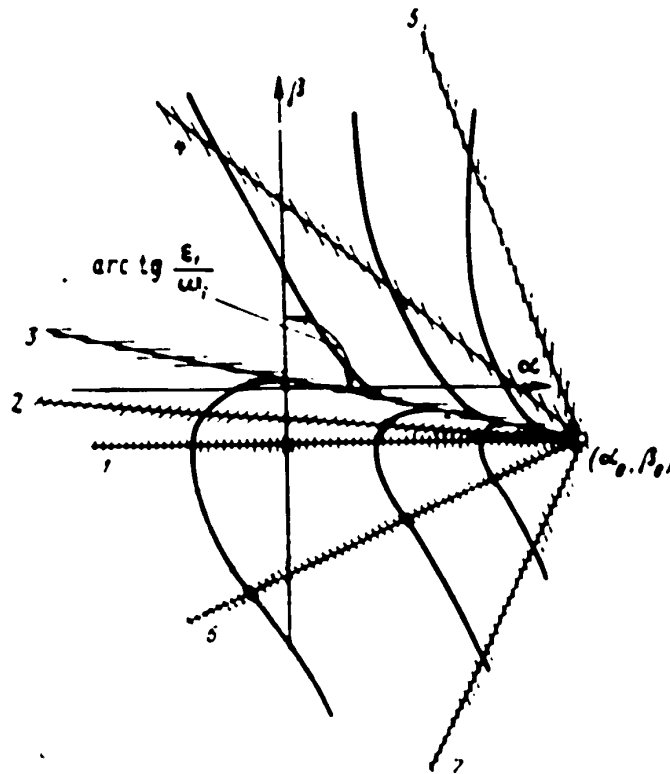


Fig.10.1 - Paths of Motion of Top of Directional Gyro without Allowing for Friction in the Gimbals, with Proportional Characteristic

By the condition of eq.(10.15), on motion along the boundary isocline,

$$\dot{\beta} = -\frac{\alpha}{\mu} \quad (10.18)$$

On substituting this value of β in eq.(10.17), and bearing eq.(10.15) in mind, we obtain

$$U = \sqrt{(\Omega_1 - \omega_1^2 \alpha)^2 + \Omega_2^2} \quad (10.19)$$

STAT

or

$$U \approx \sqrt{\Omega_1^2 + \Omega_2^2}. \quad (10.20)$$

In this case, the components of the velocity along the O_α and O_β axes will be respectively:

$$U_\alpha \approx \Omega_1, \quad (10.21)$$

$$U_\beta \approx \Omega_2. \quad (10.22)$$

In the subsequent argument we shall assume friction in the gimbals to be absent.

Then the projections of the velocity U on the O_α axis will be determined, according to eqs.(10.6) and (10.21), by the expressions

$$U_\alpha = \frac{h_2}{H} - \left(\omega_1 + \frac{V \sin \lambda}{R \cos \varphi} \right) \sin \varphi. \quad (10.23)$$

that is, it will be determined by the difference between the precession of the gyro owing to the action of the moment of compensation, and the precession due to the vertical component of the earth rotation.

If, in particular,

$$\frac{h_2}{H} = \left(\omega_1 + \frac{V \sin \lambda}{R \cos \varphi} \right) \sin \varphi. \quad (10.24)$$

then we get

$$U_\alpha = 0$$

Consequently, if in this case, at the initial instant of time, the gyro axis was brought into the plane of the meridian, then it will remain in that plane, that is, the directional gyro will perform its function for an indefinitely long time.

STAT

Obviously such a condition, for a given value of k_2 , will be satisfied only for some definite latitude at which eq.(10.24) will hold. At other latitudes however, $U_\alpha \neq 0$, will already hold, and with the passage of time the gyro vertex will depart from the position originally given it with respect to the earth.

In particular, if $k_2 = 0$, then the gyro vertex will depart from the originally assigned position at the rate

$$U_\alpha = - \left(\omega_1 + \frac{V \sin A}{R \cos \varphi} \right) \sin \varphi$$

Let us now elucidate the role of friction in the gimbals.

Let us do this at first, assuming the absence of compensation of the earth rotation, and not taking into account the role of the aircraft rotation.

In this case the expressions for Ω_1 and Ω_2 will take the following form:

$$\Omega_1 = \frac{L_1}{H} \text{sign } \dot{\beta} - \left(\omega_1 + \frac{V \sin A}{R \cos \varphi} \right) \sin \varphi; \quad (10.25)$$

$$\Omega_2 = \frac{L_2}{H} \text{sign } \dot{\alpha} + \frac{V \cos A}{R} \quad (10.26)$$

Since, usually

$$\frac{L_1}{H} > \left(\omega_1 + \frac{V \sin A}{R \cos \varphi} \right) \sin \varphi, \quad \frac{L_2}{H} > \frac{V \cos A}{R}$$

it follows that the signs of Ω_1 and Ω_2 will be determined by the signs of the angular velocities $\dot{\beta}$ and $\dot{\alpha}$ respectively.

In connection with this, the point of the intersection of the isoclines will be, according to eqs.(10.11) and (10.12), for $\dot{\beta} > 0$, in quadrant IV of the plane $O\alpha\beta$ (Fig.10.2), and for $\dot{\beta} < 0$, in quadrant II. We have the following rules based on eq.(10.5) to determine the signs of $\dot{\beta}$ and $\dot{\alpha}$:

STAT

$$\dot{\alpha} = 0 \left\{ \begin{array}{l} \text{for } \dot{\beta} = 0, \text{ if } |\beta| > \left| \frac{c_1}{c_2} \right|, \\ \text{for } \dot{\beta} \geq 0, \text{ if } |\beta| < \left| \frac{c_1}{c_2} \right|, \\ \text{for } \dot{\beta} > 0, \text{ if } \beta = - \left| \frac{c_1}{c_2} \right|, \\ \text{for } \dot{\beta} < 0, \text{ if } \beta = \left| \frac{c_1}{c_2} \right|. \end{array} \right. \quad (10.27)$$

$$\dot{\beta} = 0 \left\{ \begin{array}{l} \text{for } \dot{\alpha} = 0, \text{ if } \left| \beta + \frac{a_1}{a_2} \alpha \right| > \frac{c_1}{c_2}, \\ \text{for } \dot{\alpha} = 0, \text{ if } \left| \beta + \frac{a_1}{a_2} \alpha \right| < \left| \frac{c_1}{c_2} \right|, \\ \text{for } \dot{\alpha} < 0, \text{ if } \beta + \frac{a_1}{a_2} \alpha = - \left| \frac{c_1}{c_2} \right|, \\ \text{for } \dot{\alpha} > 0, \text{ if } \beta + \frac{a_1}{a_2} \alpha = \frac{c_1}{c_2}. \end{array} \right. \quad (10.28)$$

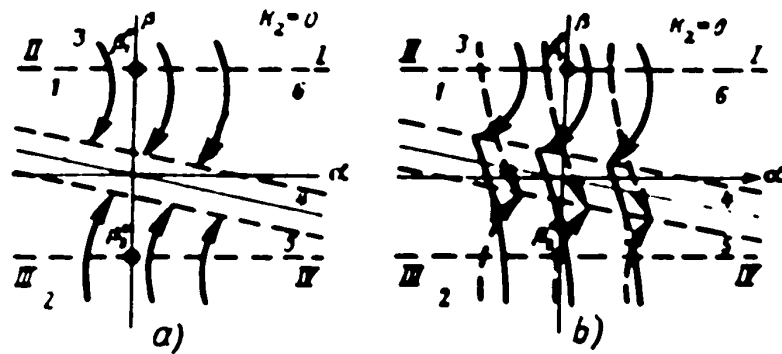


Fig.10.2 - Path of Motion of Vertex of Directional Gyro, Allowing for Friction in Gimbals, with Proportional Characteristic of Correction of Inner Frame

Under all these conditions, Ω_1 and Ω_2 are determined by eqs.(10.25) and (10.26).

Thus the coordinate plane $O\alpha\beta$ is divided, with respect to the determination of the sign of $\dot{\alpha}$, into the regions (1), (2), and (3) (cf.Fig.10.2). The sign of $\dot{\beta}$ in

STAT

region (1) will be determined by the sign of β , and in regions (2) and (3), by the sign of $\dot{\beta}$. With respect to the determination of the sign of $\dot{\beta}$, the coordinate plane is divided into the regions (4), (5), and (6). In the region (4), the sign of $\dot{\beta}$ will be determined by the sign of $\dot{\alpha}$, in the regions (5) and (6), by the sign of $\beta + \frac{\omega_1}{\varepsilon_1} \alpha$. In this case, the motion of the vertex, from points located in the region (5), will be directed toward the boundary of this region, to the right; the motion from points located in the region (6), will be directed toward the boundary of this region to the left.

We remark that both these boundaries will move parallel to the boundary isocline and will be separated from it by a distance equal to $\frac{\Omega_2}{\varepsilon}$ along the $O\beta$ axis. For $V = 0$, this distance will be exactly equal to the angle of repose of the inner frame.

Let us assume that the vertex of the gyroscope moves in the region (6) and reaches its boundary at some point of that boundary. It is easy to see that at this point the motion of the vertex will stop. For, if we assume that that motion continues to exist under the same condition with respect to $\dot{\alpha}$ as it did before this point was attained, that is, that $\dot{\alpha} < 0$, this will mean that $\dot{\beta}$ will change its sign in the region (4), since, by hypothesis, in the region (4), for $\dot{\alpha} < 0$, $\dot{\beta} > 0$. But the change of sign of $\dot{\beta}$ will mean the change of sign of $\dot{\alpha}$ as well, according to the condition of region (1), and, consequently, the restoration of the conditions for the maintenance of $\dot{\beta} < 0$. Thus the assumption that the conditions of motion in region (4) are maintained leads to a contradiction, which means that such motion cannot take place.

We reach analogous results by analysing the motion of the vertex of the gyro from points located in region (5).

Thus, instead of moving along the boundary isocline, as it did when we did not allow for friction in the gimbals, the vertex of the gyroscope will now remain at one fixed position or another (depending on the initial conditions) with respect to

STAT

the given direction, and separated from it by a quantity equal approximately to the angle of repose of the inner frame.

It is easy to understand the physical origin of this fact: it is a result of the fact that the precession of the gyro owing to friction in the axes of the inner frame exceeds in modulus the vertical component of the earth rotation. In this case the general picture of the phenomena may be treated as follows: the rotation of the gyro with respect to the body of the aircraft, owing to the vertical component of the earth rotation, lead to the appearance of a moment of friction about the axis of the outer frame. This moment will lead to precession of the inner frame, which will mean the appearance of a moment of friction about the axis of that frame. The moment of friction about the axis of the inner frame causes precession of the outer frame in the same sense as the rotation of the plane of the meridian owing to the vertical component of the earth rotation. Since the rate of this latter precession is higher than that of the vertical component of the earth rotation, it follows that the gyro will overtake the plane of the horizon, i.e., that it will, in the last analysis, follow this plane.

Thus there will be no visible drift of the gyro with respect to the plane of the horizon.

This behavior of the gyroscope is fully maintained even when the action of the moment of compensation for the influence of the earth rotation is taken into account. To speak strictly, this compensation in the case described completely loses its practical meaning, since even without it a gyroscope, affected by friction in the bearings, would follow the plane of the meridian.

Let us assume now that an oscillatory rotation of the aircraft is observed, yielding an oscillatory component on the axis of the inner frame $\dot{\psi}_x$, which is so great in modulus that we may put, for any instant of time:

$$\text{sign} (\dot{\beta} - \dot{\psi}_x) = -\text{sign} \dot{\psi}_x$$

STAT

Under this assumption, Ω_1 and Ω_2 are represented in the following form:

$$\Omega_1 = -\frac{L_{11}}{H} \text{sign } \dot{\psi}_x - \left(\omega_3 + \frac{V \sin K'}{R \cos \varphi} \right) \sin \varphi. \quad (10.29)$$

$$\Omega_2 = -\frac{L_{12}}{H} \text{sign } (\dot{\alpha} - \dot{\psi}_1) + \frac{V \cos K'}{R}. \quad (10.30)$$

Under the same condition

$$\frac{L_{11}}{H} > \left(\omega_3 + \frac{V \sin K'}{R \cos \varphi} \right) \sin \varphi$$

we get the result that the sign of Ω_1 , and consequently, also the position of the point of intersection of the isoclines, is determined by the sign of $\dot{\psi}_x$. Since the latter, by hypothesis, varies periodically, the direction of motion of the vertex of the gyro will also vary periodically. In this case the component of velocity of this motion along the $O\alpha$ axis, which is, according to eq.(10.21), practically equal to Ω_1 , will be greater in modulus on motion to the left than on motion to the right. Thus, while the conditions of motion are maintained, the vertex of the gyro will advance with each cycle of oscillations $\dot{\psi}_x$ in the direction in which it would advance in absence of friction in the gimbals.

In order to find the path of the vertex of the gyro, let us substitute $\dot{\psi}_x$ for $\dot{\beta}$ in the conditions of eq.(10.27), and change the signs of the inequalities, as a result of which we get the conditions of motion for the given case. So long as the vertex of the gyroscope does not reach the boundaries of the region (4), the conditions of motion will under all circumstances be maintained. Let the vertex of the gyroscope descend on this boundary under the condition $\dot{\psi}_x > 0$ (cf. Fig. 10.2, b, heavy lines of path). Consequently, it will have $\dot{\alpha} < 0$ in this case. Thus it will pass into region (4). In this case, so long as the sign of $\dot{\psi}_x$ does not change, nothing else will change, that is, the same conditions of motion that existed on the boundary will be maintained even after it is crossed. As a result, the vertex of the gyroscope will approach the upper boundary of region (4) and will travel along this

STAT

boundary until the sign of $\dot{\psi}_x$ changes, since this would have happened in the total absence of friction in the suspension.

If, under the same condition, $\dot{\psi}_x > 0$, then the vertex of the gyro will move upward on the boundary of region (4), after which, so long as the sign of $\dot{\psi}_x$ does not change, it will also travel along the upper boundary of region (4). With a change of sign of $\dot{\psi}_x$, the sign of $\dot{\alpha}$ will change accordingly; in this case the motion will take place along the dashed path lines and along the lower boundary of region (4).

Under the conditions described, the practical meaning of using a compensation for the influence of the earth rotation is already restored.

We remark that this reasoning remains about the same under any assumptions with respect to the components of the aircraft rotation on the axis of rotation of the outer frame $\dot{\psi}_\eta$. Only the sign of $\dot{\beta}$ will depend on this component when the vertex of the gyroscope moves in the region (4). The law of this relation is determined by substituting $\dot{\alpha} - \dot{\psi}_\eta$ for $\dot{\alpha}$ in the conditions of eq.(10.28).

In this case the character of the motion in region (4) is somewhat modified with respect to the angle β , but the character of the motion still remains as before with respect to angle α .

Under practical flight conditions, there will always be oscillations of the aircraft. The effect of the influence of these oscillations on the role of friction in the gyroscope gimbals that has here been described will therefore, in general, manifest itself rather markedly in actuality. However, owing to the fact that the oscillations of the aircraft are not strictly cyclical, this effect is to some extent disturbed, so that ultimately the friction in the gimbals leads to the accumulation of a certain error with the passage of time. In the aggregate, this error, taken together with the error due to undercompensation or overcompensation of the effect of the earth rotation, does lead to the necessity of systematically correcting the position of the directional gyro.

If, in the relations obtained for the case under study, of a proportional

STAT

characteristic $f(\beta)$, we put:

$$\Omega_1 = \begin{cases} -\frac{A_1}{H} \text{sign } \dot{\beta} + \frac{V \cos \kappa}{R} - \frac{L_n}{H} \text{sign}(\dot{\alpha} - \dot{\psi}_q) & \text{for } |\beta| > \theta_{\Delta 1} \\ \frac{V \cos \kappa}{R} - \frac{L_n}{H} \text{sign}(\dot{\alpha} - \dot{\psi}_q) & \text{for } |\beta| < \theta_{\Delta 1} \end{cases} \quad (10.31)$$

then all these relations will be found to be suitable for the case of the constant characteristic as well.

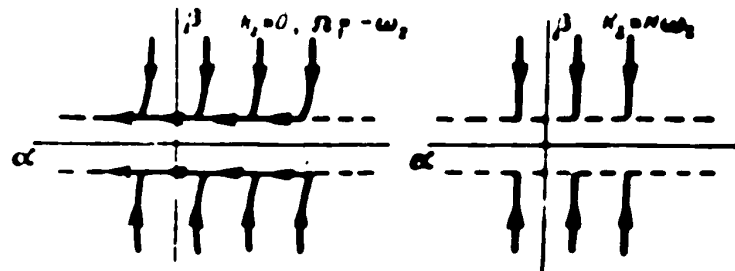


Fig.10.3 - Path of Motion of Vertex of Directional Gyro, without Allowing for Friction in the Suspension, with a Constant Hysteresis Characteristic of Inner Frame Correction

Thus we obtain:

for the coordinate of the point of intersection of the isoclines

$$\alpha_0 = \frac{L_1}{H_1} \quad (10.32)$$

$$\beta_0 = -\frac{L_1}{H_1} \quad (10.33)$$

for the relation between the slope of the isocline and that of the tangents related to this isocline

$$\mu_1 = \frac{1}{\nu_1} \quad (10.34)$$

STAT

It follows from this last relation that the tangents to the paths will here always be directed perpendicular to the isoclines, i.e., the paths will be parts of circles drawn from the point with the coordinates (α_0, β_0) . Thus if friction is neglected, the field of paths will have the form given in Fig.10.3 and ultimately the motion of the gyro vertex will be established parallel to the $O\alpha$ axis along the boundary of the zone of insensitivity of the correction system of the inner frame at the velocity:

$$U_x = \frac{k_1}{H} \left(\omega_0 + \frac{V \sin K}{R \cos \varphi} \right) \sin \varphi. \quad (10.35)$$

The picture will be roughly similar even when the friction is taken into account. The vertex of the gyro will stop at the boundary of the zone of insensitivity of the inner frame correction system, if we consider that there are no oscillations of the aircraft. If, however, we consider that oscillations of the aircraft yielding the component ψ_x do occur, then a resultant motion along the $O\beta$ axis will appear.

If the characteristic $f(\beta)$ is constant, but there is a hysteresis state, then we must put:

$$\Omega_x = \begin{cases} \frac{k_1}{H} \operatorname{sign} \dot{\beta} + \frac{V \cos K}{R} + \frac{L_n}{H} \operatorname{sign} (\dot{\alpha} - \dot{\psi}_x) \operatorname{sign} |\dot{\beta}| > \theta_{\Delta 1}, \\ \frac{k_{\Delta 1}}{H} \operatorname{sign} \dot{\beta} + \frac{V \cos K}{R} + \frac{L_n}{H} \operatorname{sign} (\dot{\alpha} - \dot{\psi}_x) \operatorname{sign} |\dot{\beta}| \leq \theta_{\Delta 1}. \end{cases} \quad (10.36)$$

In this case, the motion of the vertex of the gyro from points corresponding to positive values of β exceeding in modulus the zone of hysteresis, will continue through the zone of hysteresis without change until the boundary of the condition of hysteresis on the side of the negative values of β is reached (Fig.10.4). On this boundary, the sign of $\dot{\beta}$ will change owing to the change of sign of the moment of correction.

Thus in the zone of hysteresis the vertex of the gyro will perform oscillations. These oscillations will be rather strictly cyclical. It follows that in

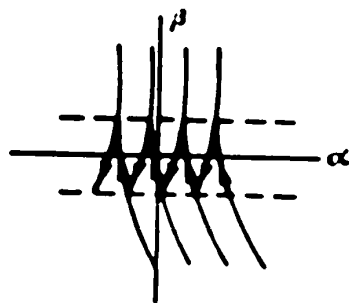


Fig.10.4 - Path of Motion of Vertex of Directional Gyro, Allowing for Friction in the Gimbals, with a Constant Hysteresis Characteristic of Correction of Inner Frame

Under actual aircraft flight conditions the oscillations of the aircraft will be superimposed on these oscillations of the gyro.

We must consider those cases as most real where the frequency of the aircraft oscillations considerably exceeds the frequency of the natural oscillations of the gyro. It would be expected in this connection that the behavior of the gyroscope with respect to the variation of the variable α would on the whole be determined by the aircraft oscillations, that is, that they would be roughly the same as with a constant hysteresis-free characteristic.

The Deviations of the Directional Gyro in a Turn

Since the axis of the inner frame of the directional gyro is parallel to the normal axis of the aircraft, it follows that in a turn this axis will describe a cone about the local vertical, having a vertex angle double the angle of bank or turn. In this connection the plane of the card attached to the outer frame will also rotate about the vertical. As a result of the rotation, the plane of the card

this case, even without the participation of aircraft oscillations, the conditions will still be assured under which friction in the gimbals is no longer capable of preventing the apparent drift of the gyro at the rate given by eq.(10.35). Thus the useful role of friction in this case is paralyzed.

This fact was first noted in the works of A.M.Letov.

Under actual aircraft flight con-

STAT

will bank differently toward the plane of the horizon, which will lead, for purely geometrical reasons, to the appearance of the special error in reading off the course, which is termed the Cardan error.

Let us determine this error, using the constructions proposed by G.O.Fridlender for this purpose (Bibl.15).

Let us take the instant of time of the turn when the aircraft had the instantaneous value of the course, defined by the arc, equal to ψ (Fig.10.5).

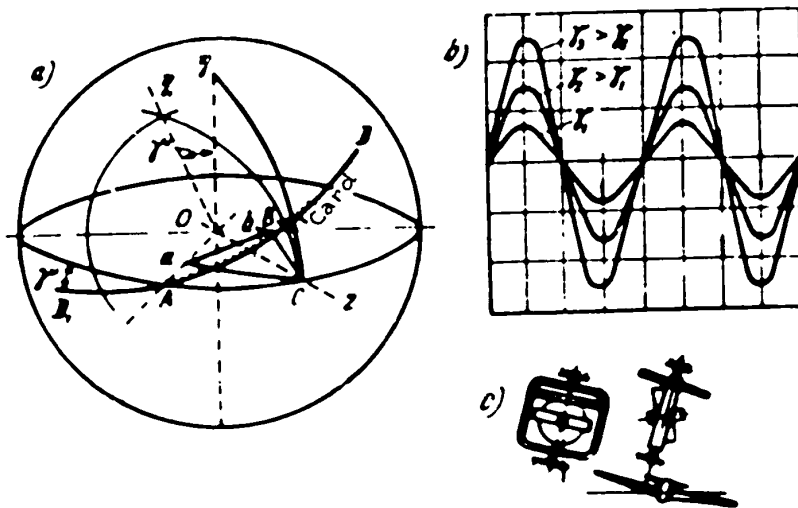


Fig.10.5 - Cardan Error of Directional Gyro: arc AC = ψ - Actual Course; AB = ψ_1 - Course Reading; $O\eta z$ - Plane of Meridian; aOb , aOc and abc are All Right Triangles

Let the bank of the aircraft corresponding to the given turn be equal to γ . Under the influence of this bank, the axis of the outer frame takes the position $O\eta_1$, and the plane of the card the position AD. The arc AB on the card, connecting the course mark A with the plane passing through the axis of the inner frame $O\eta_1$ and the axis of the rotor O_z , will determine the course reading ψ_1 .

We remark that the point B on the card corresponds to the zero course mark. In the absence of bank, and with the rotor axis in the horizontal position, this is the prolongation of the rotor axis. If the rotor axis also lies

STAT

in the meridian in addition to this, then the point B will also lie in the meridian. Let us now give our attention to the fact that a banking of the card by the angle γ , with the course corresponding to Fig.10.5, will lead to a departure of the zero course mark from the plane of the meridian, and that therefore the course reading ψ_1 will differ from the actual course ψ . Now let us produce through the point C a plane perpendicular to the longitudinal axis of the aircraft. This plane will intersect the axes OA and OB at the points a and b. It is easy enough to see that the angle aOb will be equal to the arc AB = ψ_1 , and the angle aOC to the arc AC = ψ .

Since, by construction, $ab \perp aO$ and $aC \perp aO$, then, consequently, we have from the right triangles aOb and aOC:

$$\begin{aligned} \operatorname{tg} \psi_1 &= \frac{ab}{aO}, \\ \operatorname{tg} \psi &= \frac{aC}{aO}, \end{aligned} \quad (10.37)$$

whence

$$\frac{\operatorname{tg} \psi_1}{\operatorname{tg} \psi} = \frac{ab}{aC}.$$

Let us now give our attention to the triangle abC. Its angle b is a right angle, like the angle between the plane of the card DD_1 and the plane passing through the axis of the outer frame $O\eta_1$ and the rotor axis Oz , while the angle a is equal to the angle of bank γ , as the angle between the plane of the card and the plane of the horizon.

Consequently, we have, from the triangle abC:

$$\frac{ab}{aC} = \cos \gamma.$$

Making use of this relation, let us rewrite eq.(10.37) in the following form:

$$\operatorname{tg} \psi_1 = \cos \gamma \operatorname{tg} \psi. \quad (10.38)$$

STAT

Whence, for the value of the Cardan error

$$\Delta \phi = \phi - \phi_1$$

we have

$$\operatorname{tg} \Delta \phi = \frac{\operatorname{tg} \psi (1 - \cos \gamma)}{1 + \operatorname{tg}^2 \psi \cos \gamma}$$

Figure 10.5c is a diagram of the Cardan error as a function of the value of the instantaneous course.

The absence of the Cardan error on the cardinal directions (0, 90, 180 and 270°) is explained by the fact that on these directions, as shown in Fig.10.5,c, the zero course mark remains in the plane of the meridian.

As already indicated, the inner frame correction most often used is for the mutually perpendicular positions of the rotor axis and the outer frame axis. This correction tends, during a turn, to match the rotor axis with the position of the zero course mark. Since this position, on all courses except the four cardinal directions, will leave the meridian plane on account of banking, the rotor axis will, to the same extent, owing to the action of the correction system for mutually perpendicular frames, likewise tend to leave the meridian plane.

As a result of this, an error of the directional gyro, now no longer merely a reading error, but an actual one, will accumulate. We shall term this the shift error. S.S.Tikhmenev, as well as P.V.Bromberg and D.S.Pel'por have studied this error and have shown that with intense correction this error may become substantial. G.O.Fridlender subsequently studied it and showed that for the standard directional gyro, with a low rate of correction, this error is small and does not go beyond the limits of instrumental error.

Section 10.2. Remote Gyro Magnetic Compass

The remote gyro magnetic compass is one of the directional gyroscopic instru-

STAT

ments in which, for the purpose of correcting the readings, remote magnetic compasses are used. It must be remarked at once, however, that in contrast to other types of remote gyro magnetic compasses, the magnetic compass is here used, not for correcting the gyro in azimuth, but to correct the device from which the signal transmitted to the indicators is taken. The gyroscope itself is not corrected in azimuth, that is, it is a free gyroscope. Consequently, the gyroscope used is in principle no different from the gyroscopes employed in directional gyros.

Let us consider in greater detail the arrangement and operation of the units entering into the set. The set includes: a magnetic compass-transmitter, a gyro unit, an amplifier, indicators (one or two), a converter, a matching button, a rectifier, and a junction box.

The gyro unit (Fig.10.6) consists of a directional gyro not corrected in azimuth. On the shaft of the outer frame of the gimbals is rigidly attached the circle potentiometer (1). A 27-v direct current is fed to the potentiometer at two diametrically opposite points through the contact rings (2). On a special brush-holder (3), placed on a bracket in the upper part of the gyro unit, are rigidly attached the three brushes (4) contacting the ring potentiometer. The brushes are 120° apart. It is obvious that the potential of each brush is determined by its position with respect to the points of the current lead-in.

The voltages taken by the brushes from the potentiometer of the gyro unit are fed to the indicators of the instrument and are responsible for their readings.

If we consider the operation only of the gyro unit with the indicators, (without the magnetic transmitter), then it will be easily seen that in this case the instrument constitutes a remote directional gyro. In fact, on the gyro, uncorrected in azimuth, is attached a potentiometer (in the ordinary directional gyro its scale is attached to the gyro), while on the instrument case are attached brushes making contact with the potentiometer (in the ordinary directional gyro, the course mark is placed on the glass of the face side of the instrument). A variation of the course

of the aircraft leads to a displacement of the brushes
ment case with the aircraft, with respect to the pote

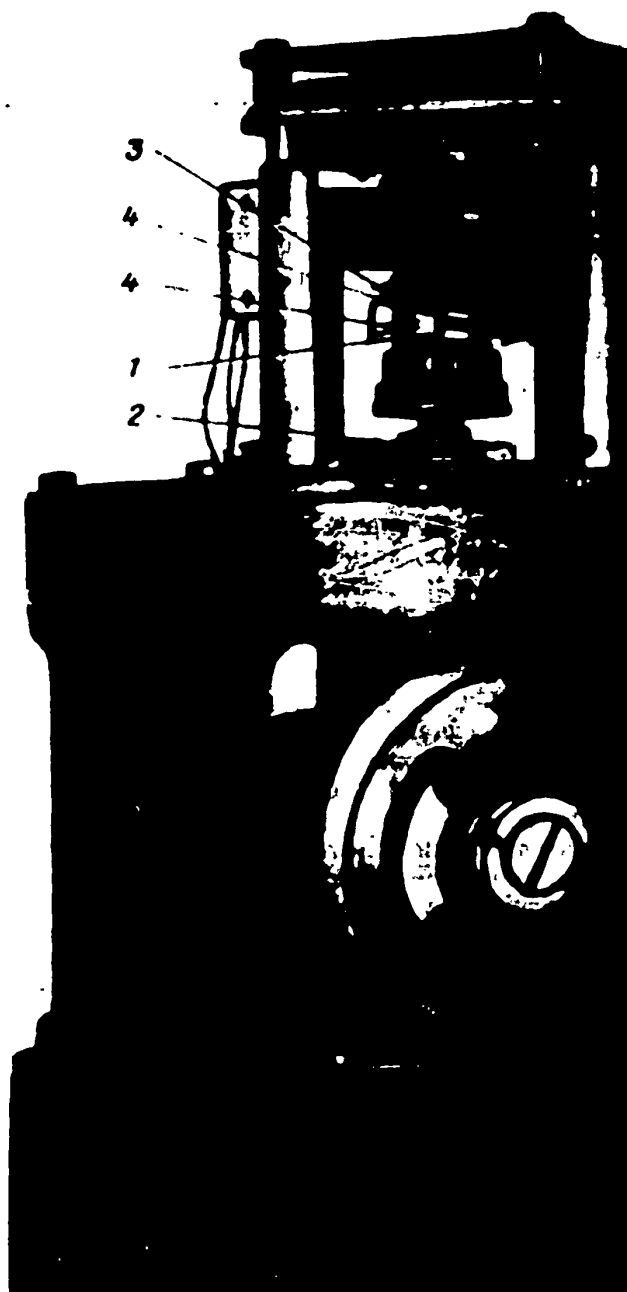


Fig.10.6 - Gyro Unit of Remote

the shaft of the outer frame of the gyroscopic suspe
brushes relative to the potentiometer in turn causes
STAT

ted through the instru-
er, which is attached to

the indicators. But the departure of the gyroscope in azimuth, as will be clear, leads to the displacement of the position of the brushes on the potentiometer, and, consequently, to the variation of the instrument readings. This variation of the readings represents the ordinary error of the directional gyro due to the drift of the gyroscope.

Thus on prolonged use of the instrument, it would be necessary to correct its readings periodically. This could be accomplished, either by rotating the entire gyroscopic unit (and with it the potentiometer), as is usually done in directional gyros, or by rotating the brushes with respect to the potentiometer. But since the instrument we are considering is not a directional gyro but a gyro magnetic compass, it must indicate the aircraft course without human intervention for the periodic liquidation of the errors due to the gyroscope drift.

In order to have the readings of the indicators correspond to the course of the aircraft, a one-one relation between the voltages taken off by the brushes and the course is necessary. In other words, the position of the brushes with respect to the points of the current lead-in must be completely determinate for each course. Thus arises the necessity for correcting the position of the brushes on the potentiometer of the gyro unit by means of a magnetic compass.

A magnetic transmitter (Fig.10.7) is used to correct the position of the brushes of the potentiometer of the gyro unit.

On the axis of the magnetic system (1) of the compass transmitter are rigidly attached three brushes (2), sliding along the ring potentiometer (3). The angles between these brushes are equal to 120° . The potentiometer is attached to the body of the transmitter. The potentiometers of the gyro unit and the magnetic transmitter are the same.

The potentiometer has its output leads at two diametrically opposite points.

The brushes of the potentiometer of the magnetic transmitter are connected electrically with the brushes of the potentiometer of the gyro unit, and as a result

The displacement of the
e in the readings of

the potentials taken off by the brushes of the potentiometer of the gyro unit are transmitted to the potentiometer of the magnetic transmitter. The voltage between

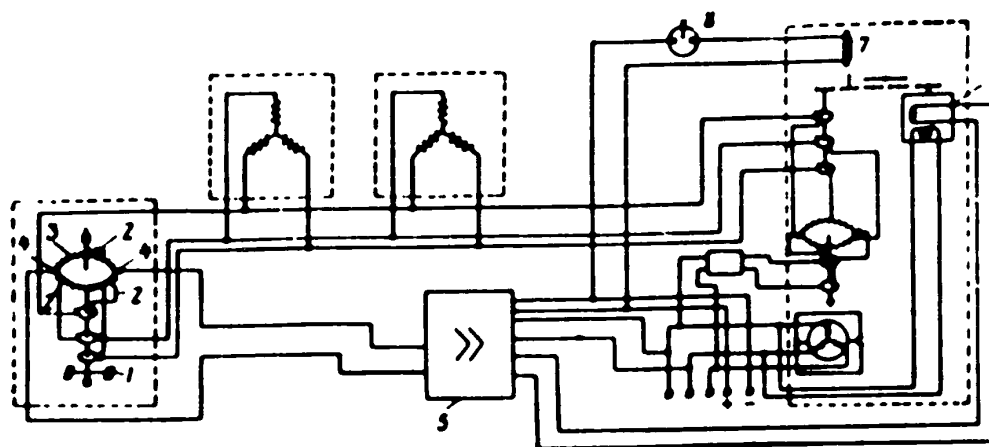


Fig.10.7 - Electrical Circuit of Remote Gyro Magnetic Compass

the points of the output (4) of the potentiometer of the magnetic transmitter is obviously determined by the position of the brushes on the given potentiometer with respect to the output points, that is, by the aircraft course, and by the potentials taken off from the potentiometer of the gyro unit, that is, by the position of the brushes and the potentiometer of the gyro unit.

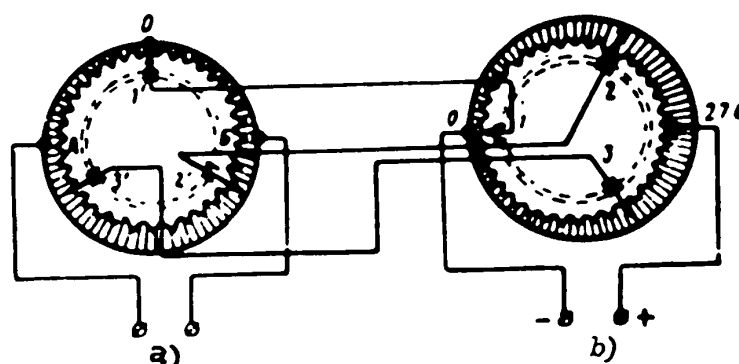


Fig.10.8 - Distribution of Potential on Potentiometers of Distant Transmission

a) 27 v; b) Feed, 27 v

The voltage from the points of lead-out of the potentiometer of the magnetic transmitter is fed to the amplifier (5), and from the amplifier output to the actuating motor (6) located in the upper part of the gyro system. If this voltage is not equal to zero, then the actuating motor of the gyro unit is brought into rotation, and its rotation is transmitted to the brushholder through a reducer with a high gear ratio. The sense of the rotation depends on the sign of the voltage fed to the amplifier.

Thus, in rotating, the actuating motor displaces the brushes on the potentiometer of the gyro unit, which leads to a change in their potentials, and, consequently, to variations in the readings of the indicators. The displacement of the brushes of the gyro unit will continue until the voltage between the lead-out points of the potentiometer of the magnetic transmitter becomes equal to zero. From a consideration of the distribution of the potentials on the potentiometers of the gyro units and the magnetic transmitter (Fig. 10.E), it will be clear that for a given position of the brushes on the potentiometer of the magnetic transmitter, that is, on a given course, the voltage between the lead-out points will be equal to zero at a completely determinate position of the brushes on the potentiometer of the gyro unit. To put it more precisely, the position of the brushes on the potentiometer of the gyro unit with respect to the lead-out points differs in this case from the position of the brushes on the potentiometer of the magnetic transmitter with respect to the lead-out points by a constant angle equal to 90° .

Since the position of the brushes on the potentiometer of the magnetic transmitter is determined by the course of the aircraft, it follows from what has been said above that the position of the brushes on the potentiometer of the gyro unit will also be determined by the course of the aircraft. Consequently, the voltages taken from the potentiometer of the gyro unit and fed to the indicators will likewise be determined by the course of the aircraft.

In this way, it may be stated, in short, that the brushes of the potentiometer

of the gyro unit follow the position of the brushes on the potentiometer of the magnetic transmitter.

When the aircraft makes a turn, (we assume that before the turn the brushes were in the matched state) the brushes in the gyro unit will rotate with respect to the potentiometer by an angle equal to the angle of turn of the aircraft, and the indicators will show, without a lag, the new course and the angle by which the aircraft has turned.

If the magnetic system of the transmitter during a turn were not entrained, and there were no turning error, then the brushes in the transmitter would rotate with respect to the potentiometer by the same angle of turn, and the system of the brushes would still remain in the matched state. But the entrainment and turning error of the magnetic system of the transmitter lead to mismatching in the position of the brushes, and the brushes of the gyro unit will begin to be displaced along the potentiometer, tending once more to reach the matched state. This leads to the appearance of error in the instrument readings. It will be easily seen that this error will be determined by the rate of displacement of the brushes along the potentiometer of the gyro unit and by the duration of the turn. This rate is low and amounts on the average to $2 - 3^{\circ}$ a minute. Consequently, during a minute of turn, the instrument can accumulate an error not exceeding 3° , while the entrainment of the magnetic system may have the value of several tens of degrees.

It is well known that in rectilinear flight the magnetic system of a compass undergoes oscillation. In view of the low rate of matching of the brushes of the gyro unit, these oscillations will not be able to be transmitted to the indicators, and the indicators will therefore show the mean compass course.

The drift of the gyroscope in azimuth does not lead to the appearance of substantial errors in the instrument readings. The rate of drift of the gyroscope in azimuth does not exceed 1° a minute, and, consequently, the mismatching in the position of the brushes due to the drift of the gyroscope (to the rotation of the

potentiometer of the gyro unit) will be liquidated by the rotation of the brushes of the gyro unit, whose rate of displacement is greater than the rate of drift of the gyro. The brushes of the gyro unit "overtake" the potentiometer, which drifts together with the gyro.

For the rapid matching of the brushes, for example in starting up the instrument, when the angle of mismatch may reach 180° , the gear ratio in the reducer is changed, thus providing a rate of matching of the brushes equal to 20° a second. The gear ratio of the reducer is varied by means of the electromagnet (7) (cf. Fig. 10.7), mounted in the upper part of the gyro unit. The electromagnet is turned on by pressing the matching button (8) (cf. Fig. 10.7).

The gyroscope used in the remote gyro magnetic compass has a correction system based on the mutually perpendicular position of the rotor axis and the axis of the outer frame. The operation of this correction system is described in Chapter 6 on page 101.

The gyro motor is a triphase asynchronous motor with short circuited rotor. The rotor speed is about 22,000 rpm. The case of the gyro unit is air-tight. Its inner cavity is filled with nitrogen. This protects the parts of the instrument from corrosion and assures normal operation of the gyroscope correction system at any altitude.

STAT

CHAPTER XI

VELOCITY AND ACCELERATION VELOCITY GYROSCOPES

Section 11.1. Principle of Operation

By velocity gyros we mean gyros intended to detect and measure the angular velocity of rotation.

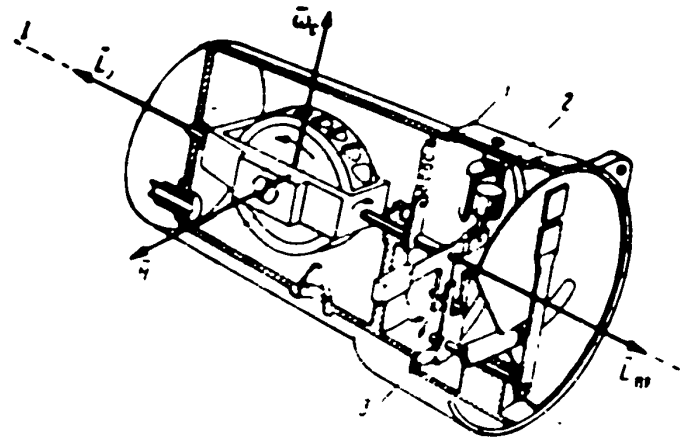


Fig.11.1 - Diagram of Turn Indicator

I - Axis of inner frame

1 - Counteracting (centering) spring; 2 - Damper; 3 - Indicating system for $\bar{\omega}_c$, vector of angular velocity being measured; \bar{L}_j - Applied gyroscopic moment; \bar{L}_{np} - Counteracting moment

These instruments are also often called "precession gyroscopes", and certain types of these instruments are termed turn indicators or damping gyroscopes.

One of the most widely used types of velocity gyros is the turn indicator, which indicates the angular velocity of an aircraft turn, and is a part of the set of piloting-navigational instruments. It consists of a gyro with two degrees of freedom; one of rotation of the rotor and the other rotation of the suspension, with the degree of freedom of the suspension limited by the centering spring and damper (Fig.11.1).

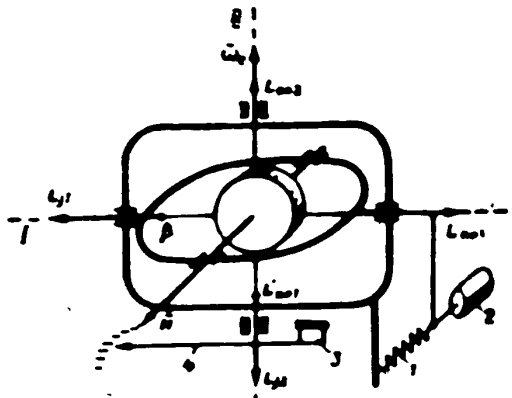


Fig.11.2 - Diagram of Acceleration-Velocity Gyroscope

I and II - Axis of suspension

1 - Counteracting spring of inner frame;

2 - Damper; 3 - Counteracting spring of outer frame; 4 - Indicating system;

H - Kinetic moment; $\bar{\omega}_c$ - Vector of angular velocity being measured; \bar{L}_{y1} - Acting

(gyroscopic) moment about axis of inner

frame, \bar{L}_{np1} - Counteracting moment about axis of inner frame; \bar{L}_{y2} and \bar{L}_{np1} - Effective moments about axis of outer frame;

\bar{L}_{np2} - Counteracting moment about axis of

It may also be treated as a gyro with three degrees of freedom, whose outer frame is the case of the instrument, which is connected with the aircraft. In the literature, the following explanation of the principle of action of the turn indicator is usually given.

Its action is based on the utilization of the gyroscopic moment. The direction of the axis of the lacking degree of freedom is matched with the axis about which the angular velocity is to be measured. Thus rotation about this axis will be imparted by constraint to the rotor. Under the action of the moment of gyroscopic reaction so arising, the frame of the suspension will rotate until the acting gyroscopic moment is balanced by the counteracting moment of the

spring. This takes place at a completely determinate angle of shift of the frame of the suspension, which is a measure of the gyroscopic moment as well, and consequently, also of the angular velocity of rotation of the rotor due to the appearance of this gyroscopic moment.

The damper, as usual, is intended to extinguish the oscillations of the frame.

This method of explaining the principle of operation of the turn indicator has the shortcoming that here the moment of gyroscopic reaction, constituting the moment of the forces of inertia, appears as the cause of the rotational motion of the frame.

Another method of explaining the operation of the turn indicator is as follows.

When the case rotates at the angular velocity ω_c (cf. Fig. 11.1), a moment whose vector coincides with the vector ω_c acts on the gyro through the bearings of the frame. This moment causes precession of the gyro, tending to match the vector of kinetic moment with the vector of external moment. As a result the frame rotates about the axis. The tension of the spring due to the rotation of the frame produces a moment causing precession of the gyroscope in the sense of rotation of the aircraft. In the steady state, the moment of the spring produces a rate of precession equal to the rate of rotation of the aircraft. In this case the moment of pressure from the bearings on the gyroscopes disappears. In the quantitative aspect, both these treatments of the principle of operation of the velocity gyroscope are naturally analogous.

The acceleration-velocity gyroscope (cf. diagram on Fig. 11.2) is intended to measure both angular velocity and angular acceleration. This is accomplished, in contrast to the velocity gyroscope, by not completely depriving the acceleration-velocity gyroscope of its freedom of rotation about the axis of measurement, since the connection with the casing is not rigid but elastic.

At constant rate of rotation of the aircraft about the measurement axis, this connection assures the establishment of precisely the same constant rate of rotation of the gyro about the same measurement axis. The inner frame of the gyro will react

STAT

to this velocity in exactly the same way as in the ordinary velocity gyro, by rotation by an angle corresponding to the given value of the angular velocity of rotation of the aircraft.

In this case, in the steady state, the spring of the outer frame will not be deformed, but the moment of the spring of the inner frame produces a precession of the gyroscope, in the sense of rotation of the aircraft, at an angular velocity equal to the angular rate of turn. A peculiarity of this device is that the moment of the spring of the inner frame and the gyroscopic moment balancing it are the internal moments for the unit outer frame-inner frame-rotor. They therefore do not produce deformations of the spring of the outer frame, which is connected with the instrument casing, and consequently also with the aircraft.

When the angular rate of turn varies, the angle of deflection of the inner frame must obviously also vary, since it is precisely this angle that is the measure of the angular rate of turn. The more rapidly the angular rate of turn varies, the more rapidly will the inner frame rotate about its axis, i.e., the rate of rotation of the inner frame will be proportional to the angular acceleration of the aircraft when the angular rate of turn varies. In this rotation the gyroscopic moment manifests itself. Its vector is directed along the axis of the outer frame. The modulus of this gyroscopic moment, however, will be proportional to the rate of rotation of the inner frame, that is, proportional to the angular acceleration of the aircraft. Obviously this gyroscopic moment will modify the motion of the gyroscope about the axis of the outer frame with respect to the aircraft until the moment from the spring of the outer frame balances it. In this case the outer frame will deflect from its normal position with respect to the casing (the aircraft) by an angle proportional to the gyroscopic moment, and consequently, to the angular acceleration of the aircraft.

If we use, instead of two springs, as in the acceleration-velocity gyro (cf. Fig.11.2), only one spring (Fig.11.3), which is able to produce moments both about

the axis of the inner frame and about the axis of the outer frame, then the deflection of the outer frame will now be proportional not only to the angular acceleration, but will also be a function of the angular rate of turn.

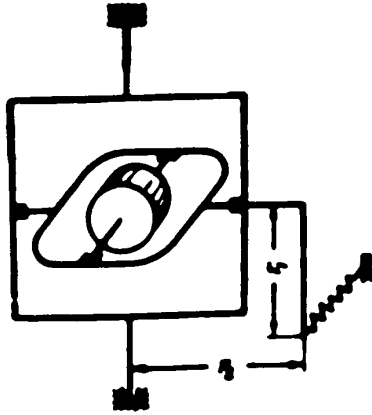


Fig.11.3 - Diagram of
Acceleration-Velocity Gyroscope with One
Counteracting Spring

For this purpose the spring must be attached at one end to the inner frame, and at the other end to the instrument casing. Let us have a steady turn; then the inner frame will rotate about its axis. In this case the spring will be stretched. The tension of the spring will produce a moment not only about the axis of the inner frame, but also about the axis of the outer frame. This will produce a deflection of the outer frame by an angle which is

a function of the angle of deflection of the inner frame, that is, a function of the angular rate of turn.

Naturally, when the aircraft rotates at an angular acceleration, the angle of deflection of the inner frame will vary. In this case a gyroscopic moment will arise, thereby producing an additional deflection of the outer frame with respect to the aircraft by an angle such that this gyroscopic moment will be balanced by the spring.

Thus the angle of deflection of the outer frame will be proportional both to the angular velocity, and to the angular acceleration, in a definite ratio between them. This ratio depends on the ratio of the arms r_1 and r_2 , that is, on the design parameters of the device.

STAT

Section 11.2. Motion of Frame of Velocity Gyroscope

Equations of Motion

In this case we shall start out from the complete equations of motion of the gyroscope and shall reject in them only the terms characterizing the influence of the centripetal accelerations, rewriting them in the following form:

$$\begin{aligned} I_{\text{eq } x} \frac{dp}{dt} + Hq &= L_x, \\ I_{\text{eq } y} \frac{dq}{dt} - Hp &= L_y, \end{aligned} \tag{11.1}$$

where $I_{\text{eq } x}$ and $I_{\text{eq } y}$ are the equatorial moments of inertia of the gyro with respect to the Ox and Oy axes respectively.

As already pointed out, a velocity gyro may be treated as a gyro with three degrees of freedom, the outer frame of which is the casing of the instrument. For turn indicators and velocity gyroscopes of autopilots, the casings are rigidly connected with the aircraft. In essence, it is the aircraft that performs the role of the outer frame for these instruments.

It follows from this that, in eq.(11.1), q is determined by the projection of the angular velocity of the aircraft about the axis of measurement ω_c on the axis Oy ; the equatorial moment of inertia $I_{\text{eq } y}$ is determined by the moment of inertia of the aircraft itself with respect to the axis of measurement; and L_y is determined by the moments acting on the aircraft about that same axis. In other words, the second of the eqs.(11.1) will relate practically to the rotations of the aircraft, that is, to what is, essentially, the assigned object of measurement and does not need any investigation in this case. In this case the second term of the left side of this equation, representing the gyroscopic moment which arises in connection with the rotation of the gyro about the Ox axis, shows what the influence of the motions of the gyro will be on the motion of the aircraft. It is perfectly clear that this influence, in view of the smallness of the value of this gyroscopic moment by com-

parison with the moment of inertia of the aircraft itself, will be negligibly small. Consequently, the second of eqs.(11.1) may be simply rejected.

Let us take the original system of earth-bound coordinate axes $O\xi\eta\xi$, which we shall orient in the following manner (Fig.11.4): we match the axis $O\xi$ with the axis of measurement, the axis $O\eta$ with the axis of rotation of the gyro frame, and thereby, with one of the axes of the aircraft. This latter procedure means that the system of axes $O\xi\eta\xi$ will rotate about the axis of measurement, that is, about the axis $O\xi$, at the angular rate of turn of the aircraft ω_c .

Let the other two axes of the aircraft, which we shall denote by $O\xi_c$ and $O\xi_c$, deviate from the $O\xi$ and $O\xi$ axes respectively by the angle of bank γ . According to the arrangement of the instrument (cf.Fig.11.1), to the neutral position of the gyroscope frame, and, accordingly, to the zero reading, will correspond the position in which the system of gyroscope axes $Oxyz$ will coincide with the system of aircraft axes, $O\xi_c\eta\xi_c$, respectively. We shall denote by the letter β the angle of deviation of the gyroscope from this position owing to rotation about the axis of the frame and shall consider that sense to be positive that brings the rotor axis of the gyroscope Oz closer to the axis $O\xi$. It is this angle β that, in this case, will be the measure of the angular velocity ω_c .

The moments acting on the gyroscope will consist of the moments produced by the deformation of the spring and the resistance of the damper, as well as the moment produced by the friction in the bearings of the shaft of the frame.

We shall consider for simplicity that rotation at the angular velocity ω_c about the vertical is the only rotation of the aircraft, that is, that the aircraft is performing a turn in the horizontal plane.

Then, on the basis of the above, we may write the following expressions

$$q = \omega_c \cos(\gamma - \beta). \quad (11.2)$$

$$L_s = k_s \beta + m_d \dot{\beta} + L_1 \operatorname{sign} \dot{\beta}. \quad (11.3)$$

$$\dot{\beta} = -p. \quad (11.4)$$

STAT

where

k_{sp} - coefficient of rigidity of the spring, which we shall take as constant;

m_d - coefficient of damping;

L_{p1} - moment of friction acting about the axis of the frame.

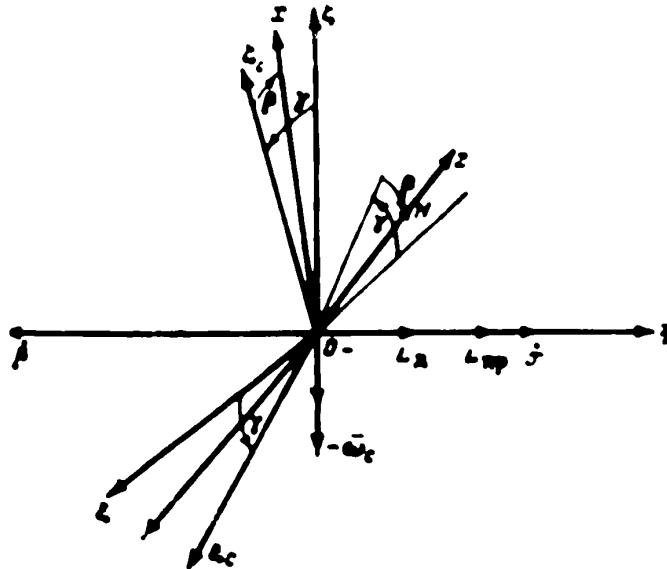


Fig.11.4 - Position of Axes of Velocity Gyro

Consequently, omitting hereafter the second subscript in the symbol for the equatorial moment of inertia, the equation of motion of the gyroscope frame is now written in the following form:

$$I_{\cdot} \cdot m_d \beta \cdot k_{sp} \beta = H \omega_c \cos (\gamma - \beta) - L_{\cdot 1} \text{ sign } \beta \quad (11.5)$$

or, replacing $\sin \beta$ by the value of β in radians, and replacing $\cos \beta$ by unity, which is permissible, since β usually does not exceed $10 - 20^\circ$:

$$I_{\cdot} \cdot m_d \beta \cdot (k_{sp} - H \omega_c \sin \gamma) \beta = H \omega_c \cos \gamma - L_{\cdot 1} \text{ sign } \beta. \quad (11.6)$$

Influence of Damping and of Rigidity of Centering Spring

We shall consider

$$\omega_c = \text{const}$$

and shall omit, in the right side, the term characterizing the influence of friction, having in mind a subsequent return to the consideration of the influence of the dependence of ω_c on the time and the influence of friction.

Let us rewrite eq.(11.6), under these assumptions, in the following form

$$\ddot{\beta} + 2D\omega_0\dot{\beta} + \omega_0^2\beta = \omega_c^2\beta^* \quad (11.7)$$

where

$$D = \frac{m_A}{2\sqrt{I_0(k_{sp} - H\omega_c \sin \gamma)}} \quad (11.8)$$

$$\omega_0^2 = \frac{k_{sp} - H\omega_c \sin \gamma}{I_0} \quad (11.9)$$

$$\beta^* = \frac{H\omega_c \cos \gamma}{k_{sp} - H\omega_c \sin \gamma} \quad (11.10)$$

If we assume that the condition

$$D < 1$$

is satisfied (on the bases stated below, which are in fact usually satisfied), then the solution of eq.(11.7) will be a function of the following form:

$$\beta = B e^{-D\omega_0 t} \sin(\omega_1 t + \delta) + \beta^* \quad (11.11)$$

where

$$\omega_1 = \omega_0 \sqrt{1 - D^2} \quad (11.12)$$

B and δ are arbitrary constants.

After a sufficient interval of time has passed, the term depending on the time in this solution, and expressing the influence of the inertia of the frame, will vanish, and then:

$$\beta = \beta^* \quad (11.13)$$

In this way, the value of β^* is the steady value of the angle of shift of the gyroscope frame, which also results directly from eq.(11.7) if we put $\ddot{\beta} = \dot{\beta} = 0$ in

STAT

it.

If we put $\gamma = 0$, then we get

$$\beta^{\circ} = \frac{H}{k_{sp}} \omega_c. \quad (11.14)$$

that is, at a constant value of H and k_{sp} , the steady value of β will be directly proportional to the angular velocity being measured.

The variation of the value of k_{sp} , speaking generally, takes place in connection with the influence of the temperature on the modulus of elasticity of the material of which the spring is made. This variation, however, is so insignificant that it may be neglected in practice.

It is easier to hold the value of H constant, or, in other words, to hold the rate of rotation of the rotor constant, if electric energy is used to maintain this rotation, and more difficult when the energy of an air jet is used for this purpose, mainly owing to the effect of the flight altitude on the rate of flow of the source of this energy.

We remark that the dependence of the angle of shift of the frame on the measured angular velocity by eq.(11.14) is obtained under the assumption that this angle is small. For large angles this relation loses its linear character. Thus, in those cases where it is essential to maintain the linearity of $\beta(\omega_c)$ (for example for the velocity gyros used in autopilots), the range of possible angles of shift of the gyroscope frame on account of the corresponding selection of the rigidity of the frame is limited to a few degrees (of the order of $5 - 6^{\circ}$).

The velocity gyro most widely used in aviation is the so-called "turn indicator", designed to measure the angular velocity of a turn. In this gyro the range of possible angles of shift of the frame is of the order of 30° , in other words, the condition that the angles β shall be small is here deliberately abandoned, and, consequently this instrument cannot be used as a real measuring instrument for angular velocity. It is not, in fact, so used as a rule, and even lacks a numbered scale

for this purpose, but is used as an indicator making it possible to estimate the approximate intensity of a turn from the amount of deflection of the pointer.

As follows from eq.(11.10), β^* also depends on the angle of bank γ , and, for $\gamma \neq 0$, β^* depends nonlinearly on ω_c . Although the turn indicator is also an indicator instrument, it is still desirable to have, as far as possible, a linear relation between the angle of deflection of the pointer and the angular velocity of the turn. For regular turns, this relation will be close to linear where $H > 0$, i.e., when the vector of the kinetic moment of the rotor of the turn indicator is directed along the left wing. As a matter of fact, for a right turn:

$$\bar{L} \gamma = -c \bar{V}.$$

Figure 11.4 shows the position of the axes of the gyro for a right turn. With a bank by the angle γ the aircraft axis will be tilted by the angle γ . Owing to the banking of the aircraft, the gyroscope axis will rotate by the angle γ , and then, under the action of the moment \bar{L} , coinciding with the vector $\bar{\omega}_c$, the rotor axis will then turn in the opposite sense by the angle β , if the kinetic moment is directed along the left ring.

For a static state it follows from eq.(11.5) (for $L_{pl} = 0$):

$$\beta = \frac{H}{k_{sp}} = c \cos(\gamma - \beta). \quad (11.15)$$

For $H > 0$, γ and β are subtracted, for $H < 0$, they are added. For this reason, for $H > 0$ the factor $\cos(\gamma - \beta)$ in eq.(11.15) is close to unity and the relation $\beta(\omega_c)$ is close to linear.

Let us now dwell on the characteristics of the transient state.

Let us take the initial conditions corresponding to the state of rest: for $t = 0$, $\beta = 0$, $\dot{\beta} = 0$.

The arbitrary constants for these initial conditions are defined as follows:

$$B = -\frac{\beta^*}{\sin \delta},$$

$$\operatorname{tg} \delta = \frac{\sqrt{1-D^2}}{D}.$$

From the latter relation, in particular, the following relations result:

$$\begin{aligned} \sin \delta &= \sqrt{1-D^2}, \\ \cos \delta &= D. \end{aligned} \quad (11.16)$$

Making use of the relations so found, we obtain the following form for the solution eq.(11.11):

$$\beta = \beta^* \left[1 - \frac{1}{\sqrt{1-D^2}} e^{-D\omega t} \sin(\omega_0 t + \delta) \right]. \quad (11.17)$$

Let us find the time τ after which the deviation β from the steady value β^* shall not exceed a certain sufficiently small and assigned quantity $\Delta\beta$, that is, the time after which the following condition

$$(\beta^* - \beta) \leq \Delta\beta. \quad (11.18)$$

will be satisfied.

We shall call this time the damping time.

On substituting the value of β by eq.(11.18) in eq.(11.17), and putting the damping time τ which is being sought, instead of t , we obtain

$$\frac{\beta^*}{\sqrt{1-D^2}} e^{-D\omega\tau} \sin(\omega_0\tau + \delta) \leq \Delta\beta. \quad (11.19)$$

Obviously the condition eq.(11.19) will be known to be satisfied if the condition

$$\frac{1}{\sqrt{1-D^2}} e^{-D\omega\tau} = m. \quad (11.20)$$

is satisfied, where $m = \frac{\Delta\beta}{\beta^*}$ = assigned ratio between the deviation of β from the steady value and this steady value itself.

STAT

From eq.(11.20), we have

$$\tau = \frac{1}{D\omega_0} \ln \frac{1}{m} \cdot \frac{1}{1-D^2} \quad (11.21)$$

Thus the damping time τ is a function of two parameters, ω_0 and D (considering that the value of m is assigned), while it depends monotone on ω_0 , that is, with increasing ω_0 , τ decreases over the entire range of measurement of ω_0 , while its dependence of D is of extremal character, that is, with increasing D , beginning with zero, τ at first decreases, but then, beginning at a certain value less than unity, again increases.

The former circumstance expresses the well known fact that the higher the frequency of the natural oscillations of the moving system of a measuring instrument, the smaller will be the distortions of its readings due to the natural inertia of this moving system.

The second circumstance expresses the role of the damping of the oscillations of the moving system in the distortions of the readings of the measuring instrument: this damping plays a favorable role only within certain limits, and over-damping is in this sense as unfavorable as insufficient damping. In particular, we get the result that it is most favorable in this sense to use a damping such that aperiodic damping is not yet reached, but that the moving system still retains a certain degree of oscillation, since the condition $D < 1$, corresponding to the shortest damping time, is the condition that the roots of the characteristic equation, eq.(11.6), shall remain complex.

On finding the derivative of τ with respect to D , and setting it equal to zero, we obtain the following equation for determining the external value of D :

$$m = \frac{1}{1-D^2} \cdot e^{D^2-1} \quad (11.22)$$

Figure 11.5 shows the graph of:



STAT

$$f(D) = \frac{1}{1-D^2} e^{mD} - 1 \tag{11.23}$$

from which it will be seen that, for example, for $m = 0.03$, which is entirely sufficient for us to consider the damping of the gyroscope frame to have already taken place, the extremal value of D will be approximately 0.90.

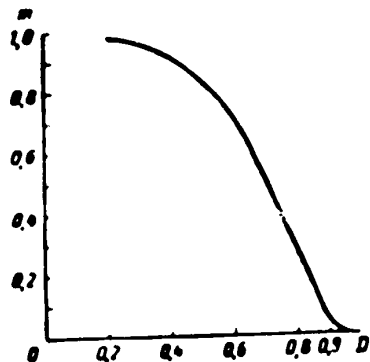


Fig.11.5 - Determination of Optimum Value of Damping Parameter

On substituting the value of m according to eq.(11.22) in eq.(11.21), we get the following expression for the minimum damping time (for a given ω_0) which we shall denote by τ_{min}

$$\tau_{min} = \frac{1}{\omega_0} \frac{D_{ext}}{1-D_{ext}^2} \tag{11.24}$$

where D_{ext} is a root of eq.(11.22) for the given m .

In particular, for $m = 0.03$, we get

$$(\tau_{min})_{m=0.03} = \frac{1.75}{\omega_0} \tag{11.25}$$

Bearing eq.(11.12) in mind, eq.(11.24) may be rewritten in the following form:

$$\tau_{min} = \frac{1}{\omega_e} \frac{D_{ext}}{\sqrt{1-D_{ext}^2}}$$

or

$$\tau_{min} = \frac{D_{ext}}{2\pi \sqrt{1-D_{ext}^2}} T_e \tag{11.26}$$

where $T_e = \frac{2\pi}{\omega_e}$ = period of natural oscillations of gyroscope frame in the presence of damping. In this case to mean the "period" of oscillations in this case to mean the

STAT

interval of time between two successive passages of the function through zero.

It is easy to see that τ_{\min} , the minimum damping time, is usually less than T_e , the "period" of the natural oscillations of the frame in the presence of damping.

In particular

$$(\tau_{\min})_{m=0.03} = 0.33T_e.$$

Let us find the relation between τ_{\min} and the instant of time t_1 when the frame of the gyro first passes through the position corresponding to the value

$$\vartheta = \vartheta^*.$$

To determine the instant of time t_1 , we have, on the basis of eq.(11.17), the equation

$$\omega_d t_1 + \delta = \pi.$$

From this we obtain:

$$t_1 = \left(0.5 - \frac{\delta}{2\pi}\right) T_e \quad (11.27)$$

Thus

$$\frac{\tau_{\min}}{t_1} = \frac{D_{ext}}{2\pi \sqrt{1 - D_{ext}^2} \left(0.5 - \frac{1}{2\pi} \arctg \frac{\sqrt{1 - D_{ext}^2}}{D_{ext}}\right)} \quad (11.28)$$

where the root of eq.(11.22) for the given value of m should be substituted for D_{ext} .

In particular, for $m = 0.03$

$$\frac{\tau_{\min}}{t_1} = 0.77.$$

that is, the damping in this case may be considered to be practically completed. STAT

somewhat before the gyroscope frame passes for the first time through the position corresponding to $\beta = \beta^*$. But this means that it will pass through this position practically no more than once. It is precisely on this condition, the maintenance of the oscillatory motion of the frame only to such an extent that the frame shall only pass the necessary position once, that the damping is regulated.

From the relation so derived it is easy to obtain the condition for selection of the coefficient of rigidity of the spring k_{sp} and the coefficient of damping m_d that shall assure an assigned damping time.

On the basis of eq.(11.24), and bearing in mind eq.(11.9) as well, after putting $\gamma = 0$ in it, we obtain the condition for the selection of the coefficient of rigidity of the spring, k_{sp} :

$$k_{sp} = \frac{I_e}{\tau_{zad}^2} \frac{D_{ext}^2}{(1 - D_{ext}^2)^2} \quad (11.29)$$

On the basis of eq.(11.8), likewise putting $\gamma = 0$ in it, and making use of eq. (11.29), we get

$$m_d = \frac{2}{\tau_{zad}} I_e \frac{D_{ext}^2}{1 - D_{ext}^2} \quad (11.30)$$

In particular, for $\tau_{zad} = 0.3$ sec, $I_e = 0.5$ g-cm-sec² and $D_{ext} = 0.90$, corresponding to the value $m = 0.03$, we get

$$\begin{aligned} k_{sp} &= 125 \text{ g cm,} \\ m_d &= 14.2 \text{ g cm/sec.} \end{aligned}$$

These relations are not hard to attain in a design, and it consequently becomes possible to assure a sufficiently short damping time.

Let us dwell in conclusion on the questions of the influence of ω_c on the variation and influence of the moment of friction about the axis of the frame. As

STAT

has been shown, it is not hard to make the damping time of the moving system of the order of 0.1 - 0.3 sec. At the same time, the minimum order of the period of possible oscillations of the angular velocity of the aircraft may be taken at 1 to 5 sec. It is obvious that, with such ratios between the damping time of the moving system and the period of variation of the measured quantity, the distortions in the instrument readings due to the natural oscillations of the instrument can be neglected, with an accuracy sufficient for practical purposes.

On the other hand, as we have also shown, the damping of a moving system is accomplished in a time equal approximately to one half-period of oscillations of this moving system. Consequently, with a high degree of accuracy, we may neglect the effect of the moment of friction about the axis of the frame during the transient state, and confine ourselves only to the elucidation of this influence on the state of the readings of the instrument.

It follows from eq.(11.5) that, allowing for friction, the steady value of the angle of shift of the frame β^* is determined by the following expression (considering that the angle of bank $\gamma = 0$):

$$\beta_e^* = \beta^* - \Delta\beta, \text{ sign } \beta. \quad (11.31)$$

where $\Delta\beta_p = \frac{L_p l}{k_{sp}}$ - angle of repose.

If we take $L_{p1} = 1$ g-cm and $k_{sp} = 100$ g-cm, then we get

$$\Delta\beta_p = 0.5^\circ.$$

Let us now convert this error into the error of the readings of angular velocity.

Considering that the rotation of the frame can commence only after the gyroscopic moment begins to exceed the moment of friction about the axis of the frame, we get to determine the threshold of sensitivity of the gyroscope with respect to the angular velocity ω_{cp} , the following expression:

STAT

$$\alpha_c = \frac{L_{p1}}{H} \quad (11.32)$$

Putting $L_{p1} = 1 \text{ g-cm}$ and $H = 500 \text{ g-cm-sec}$, we get

$$\alpha_c = 0.1^\circ/\text{sec}.$$

Its value corresponds roughly to the threshold of sensitivity of the turn indicator.

With increasing kinetic moment, this threshold may be lowered correspondingly and it is, in fact, lower in velocity gyros with an electrically actuated rotor.

Section 11.3. Motion of Acceleration-Velocity Gyro

S.S.Tikhmenev and A.M.Letov have investigated the motions of the acceleration-rate gyro.

Of the published works devoted to this question, we may cite the paper by D.S. Pel'por (Bibl.12).

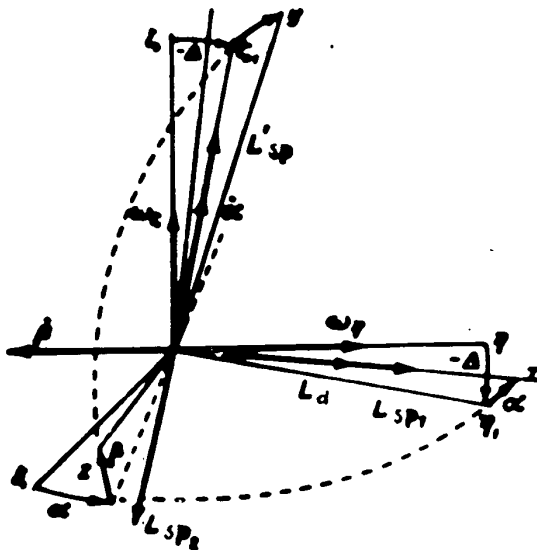


Fig.11.6 - Position of Axes of Acceleration-Velocity Gyro during Turns of Aircraft

Let us take the system of coordinate axes $O\zeta_1\eta_1\xi_1$ (Fig.11.6) rotating together with the aircraft at the angular velocities ω_ζ and ω_η , of which we are to measure ω_ζ and its first derivative $\dot{\omega}_\zeta$. Let us orient the axis of the outer frame with respect to the $O\zeta_1$ axis, which deviates from the $O\zeta$ axis in the plane $O\zeta\eta$ by the constant angle Δ . The purpose of this deviation will be explained later. The axis $O\eta_1$, lying in the same plane $O\zeta\eta$, at the angle Δ to the $O\eta$ axis, characterizes that position of the axis of the inner

STAT

frame at which there will be no deformation of the spring of the outer frame. The deviation of the Ox axis from $O\eta_1$ axis and the corresponding deformation of the spring centering the outer frame, is determined by rotating the gyro about the axis of the outer frame by the angle α . It will be this angle α that will, on the other hand, be the measure of the total effect of the action of the measured angular velocity ω_z and of the first derivative $\dot{\omega}_z$. The deviation of the rotor axis Oz in the plane $Oz\zeta_1$ and, correspondingly, of the axis Oy from the axis $O\zeta_1$ by the angle β , determines the impairment of the equilibrium of moments with respect to the axis of the inner frame Ox .

Let us confine ourselves to the study of the motion of the gyroscope, neglecting the influence of the ordinary moments of inertia on these motions, that is, taking account only of the action of the gyroscopic moments of inertia. This is entirely satisfactory for our purpose, since the influence of the ordinary inertial moments is manifested only when rapidly varying quantities are being measured.

Accordingly, as the starting equations of motion, let us take the ordinary equations of precession:

$$\left. \begin{aligned} Hq &= L_x \\ -Hp &= L_y \end{aligned} \right\} \quad (11.33)$$

As follows from the design of the instrument (cf. Fig. 11.2) and from its orientation, according to Fig. 11.5, the moments L_x and L_y are represented by the following expressions (if we neglect the moment of friction about the axis of the inner frame and assume, as usual, that the angles α and β are small):

$$\left. \begin{aligned} L_x &= k_1 \beta + m_1 \theta \\ L_y &= -k_2 \alpha - k_3 \theta \end{aligned} \right\} \quad (11.34)$$

where the constants k_1 , m_1 , k_2 are positive, and the constant k_3 may be either positive or negative, depending on whether the point of attachment of the spring of the

inner frame is below or above the axis of this frame. We remark that $k_3 = ik_1$, where i - is the gear ratio.

In eq.(11.34) the moment of deformation of the spring of the inner frame due to the rotation of the gyro about the axis of the outer frame is not taken into account, in view of the smallness of this deformation by comparison with the deformation due to the rotation of the gyro about the axis of the inner frame.

The projections of the angular velocities p and q are expressed in the following way (under the same condition that the angles α and β shall be small):

$$\left. \begin{aligned} p &= \dot{\beta} + \omega_r \cos \Delta - \omega_r \sin \Delta, \\ q &= \dot{\alpha} + \omega_r \cos \Delta + \omega_r \sin \Delta. \end{aligned} \right\} \quad (11.35)$$

Thus eqs.(11.33) are rewritten in the form:

$$\begin{aligned} H(\dot{\alpha} + \omega_r \cos \Delta + \omega_r \sin \Delta) &= k_1 \beta + m_1 \dot{\beta}, \\ H(\dot{\beta} - \omega_r \cos \Delta + \omega_r \sin \Delta) &= -k_2 \alpha - k_3 \beta. \end{aligned}$$

or

$$\left. \begin{aligned} \dot{\alpha} - \varepsilon_1 \dot{\beta} - M \dot{\beta} &= -\omega_r \cos \Delta - \omega_r \sin \Delta, \\ \dot{\beta} + \varepsilon_2 \alpha + \varepsilon_3 \beta &= \omega_r \cos \Delta - \omega_r \sin \Delta, \end{aligned} \right\} \quad (11.36)$$

where

$$\begin{aligned} \varepsilon_1 &= \frac{k_1}{H} ; \quad \varepsilon_2 = \frac{k_2}{H} ; \quad \varepsilon_3 = \frac{k_3}{H} ; \\ M &= \frac{m_1}{H}. \end{aligned}$$

Eliminating the variable β , we get

$$\begin{aligned} \ddot{\alpha} + (\varepsilon_2 + M\varepsilon_3) \dot{\alpha} + \varepsilon_1 \varepsilon_3 \dot{\alpha} &= -\dot{\omega}_r (\cos \Delta + M \sin \Delta) - \omega_r (\varepsilon_2 \cos \Delta + \\ &+ \varepsilon_1 \sin \Delta) + \dot{\omega}_r (M \cos \Delta - \sin \Delta) + \omega_r (\varepsilon_1 \cos \Delta - \varepsilon_3 \sin \Delta). \end{aligned} \quad (11.37)$$

STAT

As will be seen, the right side of the equation so obtained depends not only on the angular velocity $\omega\zeta$ and its first derivative $\dot{\omega}\zeta$, which are to be measured, but also on the angular velocity and angular acceleration about the axis $O\eta$.

If, in particular, we put $\Delta = 0$, as a result of which the equilibrium position of the axis of the inner frame will coincide with the axis $O\eta$, then eq.(11.37) is rewritten in the following form:

$$\ddot{\alpha} + (\varepsilon_2 + M\varepsilon_1)\dot{\alpha} + \varepsilon_1\varepsilon_2\alpha = -\dot{\omega}\zeta - \varepsilon_2\omega\zeta + M\dot{\omega}\eta + \varepsilon_1\omega\eta. \quad (11.38)$$

The quantities ε_1 and ε_2 are of about the same order of magnitude, since both of them depend on the coefficient of elasticity of one and the same spring of the inner frame, and differ from each other only on account of the difference in the kinematic linkages between this spring and the inner and outer frames. It follows from this that the influence of $\omega\zeta$ and $\omega\eta$ on the right side of eq.(11.38) will be of the same order. As for the compatibility of the influences of $\dot{\omega}\zeta$ and $\dot{\omega}\eta$, this will be determined by the commensurability of the constant M with unity.

If we put

$$\operatorname{tg} \Delta = M = \frac{k_1}{k_2}, \quad (11.39)$$

then the coefficients of $\dot{\omega}\eta$ and $\omega\eta$ on the right hand side of eq.(11.37) will be equal to zero, the coefficients of $\dot{\omega}\zeta$ and $\omega\zeta$ are simplified, and eq.(11.37) is rewritten in the following form:

$$\ddot{\alpha} + (\varepsilon_2 + M\varepsilon_1)\dot{\alpha} + \varepsilon_1\varepsilon_2\alpha = -\frac{1}{\cos \Delta}(\dot{\omega}\zeta + \varepsilon_2\omega\zeta). \quad (11.40)$$

Thus, on satisfying the condition of eq.(11.39), we obtain the right side of the equations of motion of the outer frame depending only on $\omega\zeta$ and $\dot{\omega}\zeta$.

We shall henceforth consider that the condition of eq.(11.39) is satisfied.

Let us find the solution of eq.(11.40) for the special case corresponding to constant angular acceleration $\dot{\omega}\zeta$, equal to

$$\dot{\omega}_z = \text{const} = a. \quad (11.41)$$

On substituting in eq.(11.40), the value of $\dot{\omega}_z$ according to eq.(11.41), we now rewrite it in the following form:

$$z \cdot 2D\omega_0 \dot{a} + \omega_0^2 a = b + a_1 t, \quad (11.42)$$

where

$$b = \frac{a + \varepsilon_2 \omega_0}{-\cos \Delta}.$$

$$a_1 = \frac{a \varepsilon_2}{-\cos \Delta}.$$

$$D = \frac{\varepsilon_2 + M \varepsilon_1}{2 \sqrt{\varepsilon_1 \varepsilon_2}}.$$

$$\omega_0 = \sqrt{\varepsilon_1 \varepsilon_2}.$$

The integral of eq.(11.42) will be the function

$$a = A e^{-D\omega_e t} \sin(\omega_e t + d) + \frac{1}{\omega_0^2} \left[b - \frac{2Da_1}{\omega_0} + a_1 t \right], \quad (11.43)$$

where $\omega_e = \omega_0 \sqrt{1 - D^2}$.

With a sufficiently high value of the frequency of the undamped natural oscillations ω_0 and a value of D close to unity, the first term of the solution eq. (11.43) may be neglected, in which case we obtain

$$a = \frac{1}{\omega_0^2} \left[b - \frac{2Da_1}{\omega_0} + a_1 t \right]. \quad (11.44)$$

For a sufficiently large value of ω_0 and the value of D sufficient to assure damping in the course of one or two oscillations, the angle of deviation of the outer frame may be considered proportional to the total effect of the action of the measured angular velocity and of its first derivatives.

It is clear from the expressions for ω_0 that on account of the rather great coefficients of elasticity of the spring centering the outer frame, the value of ω_0 may be made rather great. In this case, the selection of the necessary value of D may be assured by selecting an appropriate value for the coefficient of damping of the oscillation of the inner frame M.

CHAPTER XII

FUNDAMENTAL CONCEPTS IN THE THEORY OF GYROSCOPIC POWER

STABILIZATION

Section 12.1. Principles of Power Gyroscopic Stabilization

If, as is usually done, we neglect the nutational motions of the gyroscope, then we may consider that the application of an external disturbing moment to any frame of a gyroscope with three degrees of freedom will not lead to any rotation of the gyroscope about the axis of this frame, but will lead to the appearance of precession about the axis of the other frame, that is, about the axis crossing the direction of the vector of the disturbing moment (Fig.12.1). Both these two phenomena are interrelated: precession about the axis intersecting the action of the disturbing moment leads to the appearance of a moment of gyroscopic reaction, balancing the applied disturbing moment. By virtue of this balancing, there will be no cause for the appearance of motion about the axis of action of the disturbing moment.

Thus we obtain a rather peculiar picture of the phenomena inherent only in the gyroscope: owing to the dynamic effect of the precessional motion about one of the axes of the gyro (since the phenomenon of gyroscopic reaction is indeed a dynamic phenomenon) a resistance to the disturbing factor about its other axis is produced. The action of these disturbing factors in this way is completely balanced.

Let us now assume that the precessing frame of the gyroscope is corrected. In this case, already on account of the kinematic effect of this precessional motion,

STAT

that is, owing to the appearance of the corresponding mismatch in the signal transmitter of the corrector, a moment of correction is applied to the gyroscope.

According to the principle of correction, this moment will be applied, not to the

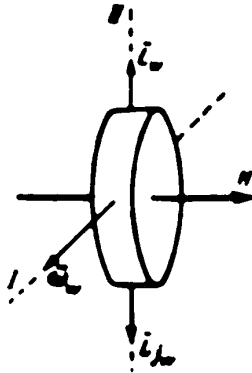


Fig.12.1 - Action of Disturbing Moment on the Gyroscope

I, II - Axis of suspension; L_w -

Disturbing moment; ω_w - Precession due to disturbing moment; L_{jw} - Gyroscopic moment

frame whose position is disturbed, but to the other frame, or in other words, precisely to the frame to which the disturbing moment is applied. This correcting will obviously be directed opposite to the moment of disturbance, since it must produce the opposite motion of the disturbed frame (Fig.12.2).

As a result of this, the disturbed frame itself is relieved of load, the accumulation of disturbance of the other frame stops, and the liquidation of its already accumulated disturbance begins, of course, only in the case where the moment of correction is ade-

quate, or exceeds the moment of disturbance. We remark that, while this liquidation is taking place, the moment of gyroscopic reaction connected with it will already balance the excess of the moment of correction over the moment of disturbance.

Thus a system of correction of positional gyros may be treated as a system of balancing the disturbing moments, at first by means of the dynamic effect of the precession about the axis diagonal to the direction of the disturbing moment, that is, on account of the gyroscopic reaction from this precession, and then, on account of the appearance of a moment of correction in connection with this precession.

If both frames of the gyro are working, or in other words, if the axis of both frames are used as the measurement axes for the angular deviations of the object,

STAT

then, naturally, disturbances of both frames are equally undesirable. As has been established above, one of the methods of reducing these disturbances is to limit the maximum allowable rates of correcting precession to quantities of the order of degrees per minute. But a reduction of the rate of precession means a corresponding

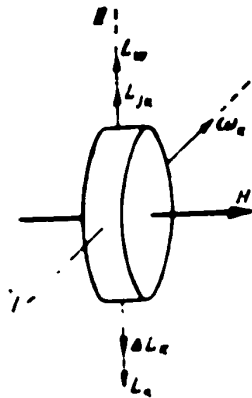


Fig.12.2 - Relieving Action of Moment of Correction

I, II - Axis of suspension;

L_w - Disturbing moment; L_k - Correcting moment included on account of the kinematic effect of precession; ΔL_k - Residual moment of correction; ω_k - Correcting precession

reduction of dynamic effect as well, since the moment of the gyroscopic reaction is determined from the magnitude of the product of the kinetic moment by the angular velocity of precession, while the magnitude of the kinetic moment may be considered as assigned by dimensional considerations. It is this reduction that also means a reduction in the correction moments. It is clear that, on the whole, this means also a corresponding reduction in the magnitude of the disturbing moments which could be balanced. It is precisely this circumstance that is expressed in the usual requirement that must be met by gyroscopic systems with two axes of measurement, which is that the reac-

tions on the gyroscope on the part of its couplings with the indicating system and the automatic control system shall be limited to the maximum extent.

The situation will be different if only one gyro frame is a working frame, that is, if the gyro is designed to measure the angular deviations of the object about the axis of only one of its frames. Thus, this is the case, for example, in directional gyros, where it is only the outer frame of the gimbals that serves as a work-

ing frame, and it is on this frame that the card is attached. The position of the inner frame, however, is not used directly for measurement purposes, and in this sense the inner frame may be considered as nonworking. The only demand that it must meet is to assure the maintenance of the rotor axis in the most favorable position, which is a position sufficiently close to perpendicularity of this axis with respect to the axis of the outer frame, that is, the working frame. It is precisely this object that is served by the correction of the inner frame. It is clear that in this case the boundaries of the allowable velocities of the correcting precession of this frame may already be considerably expanded, which will mean the corresponding increase of the dynamic effect of this precession, and thereby the expansion of the limits for the disturbing moments acting on the outer frame.

As a result of this, in this case, even without any substantial increase in the kinetic moment of the gyro, the load that can be allowed on the single working frame is considerably greater than can be allowed where both frames are working frames. This will allow the use of such a gyro, no longer merely as an indicator, but also as a direct power stabilizer. It is hardly necessary to say, of course, that the rate of precession of the working frame, if its correction is a rate of precession in this case, must still maintain the former condition of definite limitation. This will also imply a corresponding limitation of the moments designed for the correction of the working frame by comparison with the moments designed for the correction of the nonworking frame.

Thus, in the case where only one of the axes of the gimbals is used as an axis of measurement in the positional gyro with radial correction, the other axis of gimbals may be considered as the axis of precession, which performs the function of relieving the load on the axis of measurement, and thereby, also the function of the power stabilization of the gyro about this axis. This stabilization is produced, either on account of the gyroscopic moment due to this precession, or on account of the corresponding moment of the system of correction, the switching on

of which is a consequence of the same precession.

We shall henceforth call this precession the stabilizing precession.

Starting out from this treatment, the moments of a correction system may be subdivided into relieving and correcting. The former moment is the moment of correction of the nonworking frame, the latter the moment of correction of the working frame.

On the basis of the above it will be easy to get the idea of a gyroscopic device in which the principle of power stabilization about the axis of measurement would be realized even where the instrument had not one axis of measurement, but several of them. It would obviously be sufficient for this purpose that each axis of measurement should have its own axis of stabilizing precession and the appropriate devices for producing relieving and correcting moments. This can be assured only in the case where the sensitive system of the instrument has not one gyroscope but several gyroscopes, as many, in fact, as there are axes of measurement, with a system of suspension of these gyros such that each of them, in association with its axis of measurement, forms a system of a gyro with three degrees of freedom.

Section 12.2. Systems of Devices with Power Gyroscopic Stabilization

Figure 12.3 gives a diagram of one of the possible versions of the gyro vertical using power gyroscopic stabilization.

The sensitive system used in this device is a two-gyro platform placed in a suspension with two degrees of freedom. The axes of this suspension, I and II, are the axes of measurement of the instrument. Each of the gyros has two degrees of freedom with respect to the platform, and is arranged in it in such a way that, together with one of the measurement axes, more specifically, the one whose Roman numeral is the same as the Arabic numeral of the gyro involved, it forms a gyro system with three degrees of freedom.

We remark that with respect to the axis of measurement I and the gyro (1), precisely this relation is maintained with complete accuracy, while with respect to the STAT

measurement axis II and the gyro (2), it is maintained only approximately, but the more exactly, the smaller the angle of shift of the platform with respect to the axis I.

The gyro (1) may be called the stabilizing gyro of the measurement axis I. In accordance with what has been said above, the relieving signal transmitter C_1 , on the precession of the gyro, switches on the device L_1 to impose the relieving moment on the gyro.

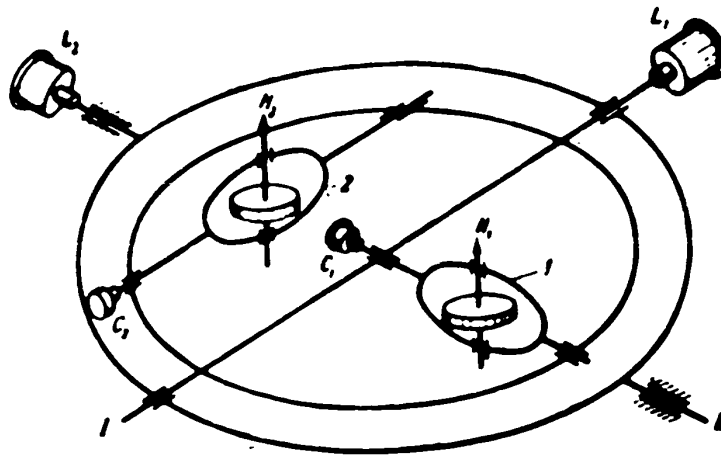


Fig.12.3 - Diagram of Gyro Horizon with Power Stabilization

I, II - Measurement axes;

1, 2 - Stabilizing gyros; H_1 , H_2 - Kinetic moments of stabilizing gyros;

C_1 , C_2 - Relieving signal transmitters; L_1 , L_2 - Relieving moment transmitters.

The axis of stabilizing precession for the measurement axis II will be the axis of precession of the gyro (2) with respect to the platform. Consequently, the gyro (2) will serve as the stabilizing gyro of the measurement axis II. The relieving signal transmitter of the platform with respect to the measurement axis II must be connected with the axis of the frame of this gyro, while the measurement axis itself, is connected with the relieving moment transmitter of the platform with respect to

STAT

the same axis.

All this is shown in the diagram of Fig.12.3.

Figure 12.4 gives a diagram of another version of a similar device, but in this case with three measurement axes, that is, one designed to determine the angular deviations of the object about all three of its axes. We shall henceforth term such a device a universal positional instrument.

The sensitive system used in this instrument is now a three-gyro platform, mounted in a suspension with three degrees of freedom. The axes, I, II, and III of this suspension are used as the measurement axes.

As in the preceding case, the gyros have two degrees of freedom with respect to

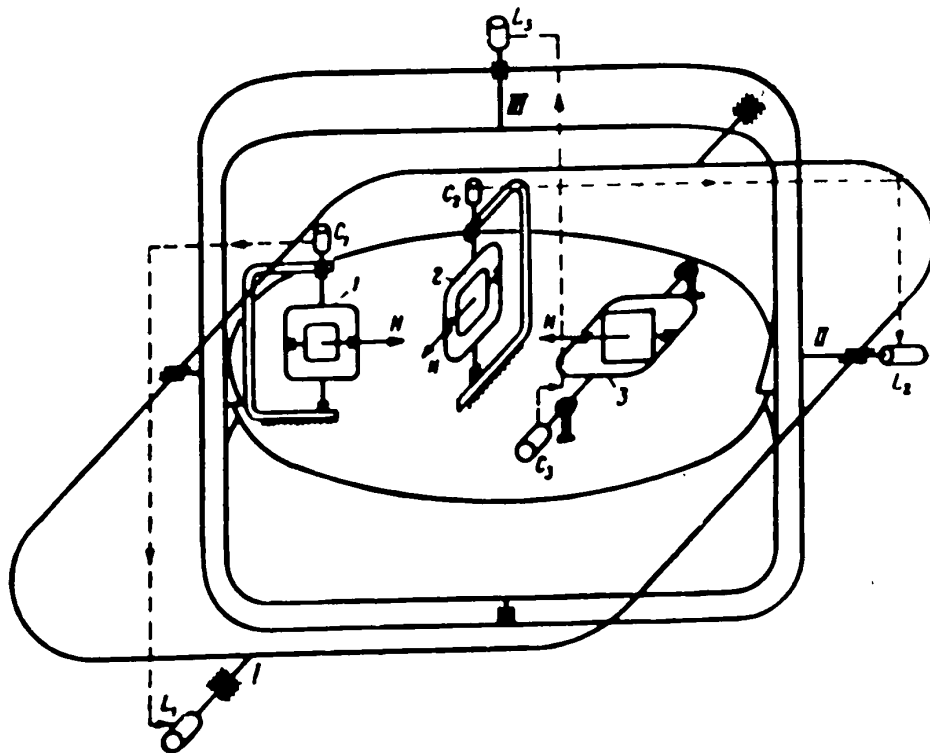


Fig.12.4 - Diagram of Universal Positional Instrument with Power Stabilization

I, II, III - Measurement axes; 1, 2, 3 - Stabilizing gyros; C_1 , C_2 , C_3 - Relieving signal transmitters; L_1 , L_2 , L_3 - Relieving motors

the platform, and are so arranged in it that, together with one of the measurement

STAT

axes, they form a gyro system with three degrees of freedom, either exactly (measurement axis I and gyro 1), or approximately with accuracy to small angles of shift of the platform about its axis. Likewise, by analogy to the preceding instrument, the relieving moment transmitters are connected with the corresponding axes of measurement, while the relieving signal transmitters are connected with the axis of precession of the corresponding stabilizing gyros.

In both of these devices, the friction in the axis of precession of the stabilizing gyros will produce the corresponding precession of the platform, thus forming a certain error in the position of this platform. In general, the situation here will be exactly the same as in ordinary (that is, single-gyro) gyroscopic instruments, where an error in the position of the outer frame is formed owing to the friction about the axis of the inner frame under certain conditions. The axes of precession of the stabilizing gyros, in this device, are precisely the axes of the "inner frames" with respect to the measurement axes as axes of the "outer frames". In other words, we may consider that the power stabilization described gives an advantage only in the sense of eliminating the influence of friction and of all other loads acting about the axis of measurement. But friction and the other harmful moments acting about the axis of precession of the stabilizing gyros will still continue to exert their influence.

We must point out still another shortcoming of these versions, if only on the example of the diagram of the gyro horizon shown in Fig.12.5. It resides in the fact that each stabilizing gyro in this diagram will only react to a load about its own measurement axis and only so long as this gyro does not deviate from the position in which the gyro rotor axis and the measurement axis stabilized by it are perpendicular to each other. But as soon as such a deviation takes place, the stabilizing gyro will now also react to a load about the other axis of measurement, with which its rotor axis will now form a certain angle different from zero. Although this additional reaction will not lead to any substantial disturbances in the

operation of the instrument, it is nevertheless undesirable.

This can be avoided by using, for each axis of measurement, not one stabilizing gyro, but a pair of them with oppositely directed kinetic moments. Since, owing to

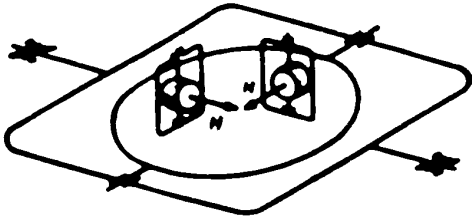


Fig.12.5 - Diagram of Gyro Horizon with Two Gyros having Horizontal Axes of Rotation

this latter circumstance, under the influence of a load about the axis of measurement, the stabilizing gyros of a given pair will precess in opposite senses, their reaction to a load about the other axis of measurement will be directed opposite to each other.

An example of such a device is the multigyroscope vertical described and studied in detail by Ya.N.Roytenberg (Bibl.13). Figure 12.6 gives a diagram of this vertical.

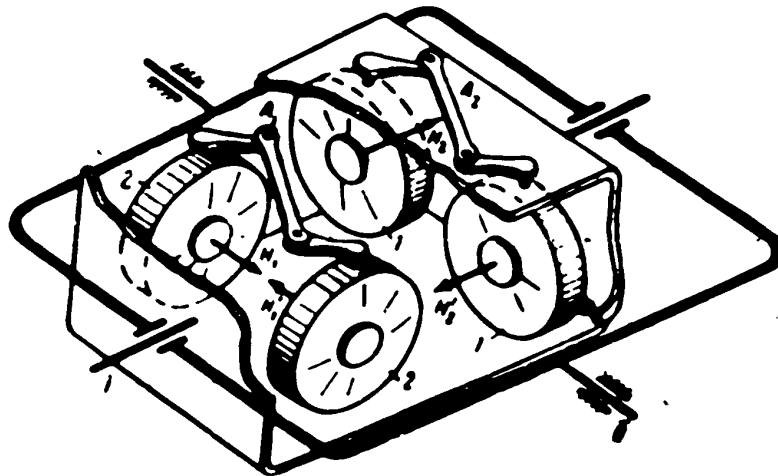


Fig.12.6 - Diagram of Gyro Horizon with Power Stabilization by I, II - Measurement axes; 1, 1; 2, 2 - Paired stabilizing gyros; A_1, A_2 - Antiparallelograms

It will be seen that the axis of precession of the stabilizing gyros of each

STAT

given pair are connected by antiparallelograms. The device provides a system of load relief for the axis of measurement, that is, for the connection with the axis of one of the stabilizing gyros of the relieving signal transmitter of the corresponding measurement axis, and for the connection of the relieving moment transmitter with the axis of measurement.

As for the correction of the platform, Ya.N.Roytenberg in his study (Bibl.13) assumed for this purpose the presence of a displacement of the center of gravity of the whole device with respect to the center of the suspension, and, in addition, also assumed the presence of an elastic coupling between the stabilizing gyros and the platform.

B.V.Bulgakov and Ya.N.Roytenberg (Bibl.2) have investigated another version of the scheme of the system of the power gyro horizons, likewise based on the use of a pair of gyros for each axis of measurement, this pair being connected by antiparallelograms, with their kinetic moments in opposite senses, but, in contrast to the preceding system, using a platform correction.

Figure 12.7 gives the system of the Bulgakov gyro horizon. On the whole it contains the elements already known, which require no additional explanation. Let us therefore confine ourselves to the most important remarks to be made with respect to the system of correction of the platform.

The horizontal pendulums k_1 and k_2 are the sensitive elements of this correction system.

For convenience of further discussion we shall denote the signal transmitters of the correction by the same subscripts as the subscripts of the pendulum with which they are connected as sensitive elements of the corrector.

By analogy, let us denote the correction moment transmitters by the subscripts of the same gyros with whose axis of precession the moment transmitters are connected.

If the signal transmitters C_{K1} , C_{K2} are connected respectively with the correc-

STAT

tion moment transmitters L_{K1} , L_{K2} , then the behavior of the gyro horizon will be the usual behavior of a gyro horizon with radial correction, with the additional effect given by power stabilization about the axis of measurement.

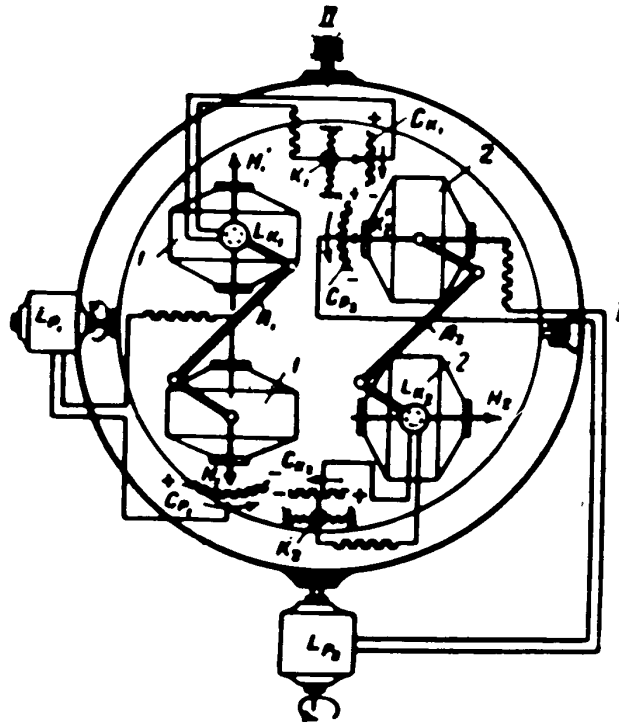


Fig.12.7 - Diagram of Bulgakov-Roytenberg Gyro Horizon

I, II - Measurement axes; H_1 , H_1' , H_2 , H_2' - Kinetic moments of stabilizing gyros; C_{p1} , C_{p2} - Relief signal transmitters; L_{p1} , L_{p2} - Relief moment transmitters; C_{K1} , C_{K2} - Correction signal transmitters; L_{K1} , L_{K2} - Correction moment transmitters

As shown above, one of the disadvantages of correcting gyro horizons is the impossibility of freeing them from ballistic deviations. A gyro magnetic type of gyro horizon is more advantageous in this respect, for here it is possible to compensate the ballistic deviations.

Bulgakov and Roytenberg have shown, however, that the condition of compensation of the ballistic deviations may also be obtained in the gyro horizon system

STAT

proposed by them. For this purpose it is necessary to change the connections between the signal transmitters and the correction moment transmitters: the signal transmitter C_{k1} is connected with the moment transmitter L_{k2} , while the signal transmitter C_{k2} is connected with the moment transmitter L_{k1} . As a result of this substitution, the behavior of the gyro horizon will now correspond to that of an undamped gyro pendulum. But, for the undamped gyro pendulum, it is well known that it is possible (cf. Chapter III of this book) to select a period of precession such that the ballistic deviations shall be completely compensated. A period equal to 84.4 min is such a period.

It is very simple here to obtain the necessary damping as well. For this purpose it is necessary, together with the connection we have just indicated between the signal transmitters and the moment transmitters, to maintain the former connections as well. In other words, for this purpose each signal transmitter must be connected to both moment transmitters.

Thus in the Bulgakov gyro horizon the advantages of power gyroscopic stabilization can be combined with the advantages of compensation of the ballistic deviations, which is of particularly great importance in aviation.

Section 12.3. The Build-Up State of the Power Gyro Horizon

Although multigyro systems have long been known, serious theoretical studies devoted to such systems have appeared only in recent years, and, more particularly, in the USSR. B.V. Bulgakov has played a leading role here as in a number of other topics in the applied theory of modern gyroscopy. The studies of Ya.N. Roytenberg, which we have already mentioned, also deserve notice. The studies of these authors are used as the base for the theories and propositions to be set forth below.

Let us bind to the platform of the gyro horizon the system of coordinate axes $Oxyz$, of which the axis Oz will be the polar axis of the platform, and the axes Ox and Oy , its equatorial axes. Of these last two axes, let us match the axis Ox with the axis of measurement I , i.e., with the axis of the inner frame of the platform

STAT

suspension.

Let us orient the earth bound system of coordinates $O\xi\eta\zeta$ as usual for the gyro horizon, that is, let us match the axis $O\xi$ with the true vertical, the axis $O\eta$ with

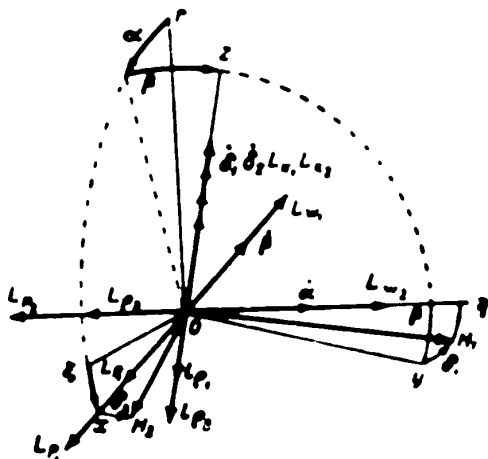


Fig.12.8 - Position of Axes of Power
Gyro Horizon

$O\xi\eta\zeta$ - System of earth bound coordinate axes; $Oxyz$ - Platform-bound axes; $O\eta$ and Ox - Axes of measurement; H_1, H_2 - Kinetic moment of stabilizing gyros; δ_1, δ_2 - Angles of precession of stabilizing gyros with respect to platform; L_{K1}, L_{K2} - Relieving moments; $L_{\rho 1}, L_{\rho 2}$ - Correcting moments; $L_{\rho 1}, L_{\rho 2}$ - Moments of friction in bearings of axes of suspension of platform; $l_{\rho 1}, l_{\rho 2}$ - Moments of friction in bearings of axes of stabilizing gyros

position of the gyros, will be laid off in the equatorial plane: δ_2 , from the equatorial axis Ox ; δ_1 , from the equatorial axis Oy .

the flight path, considering the axis of measurement II to be matched at the same time with this flight path, that is, the axis of the outer frame of the platform suspension is matched with the flight path.

The position of the system of platform-bound coordinates with respect to the earthbound system of coordinate is determined, as usual, by the angles α and β , of which the former will be the angle of rotation of the platform about the axis of the outer frame of its suspension, and the latter the angle of rotation of the platform about the axis of the inner frame of its suspension (Fig.12.8).

The position of the gyros (1), (2) with respect to the platform will be determined by us respectively by the angles δ_1, δ_2 . These angles, in accordance with the

We shall consider, further, that the axes of precession of both gyros are matched with the polar axis of the platform Oz.

As a result of this, the following vectors are arranged along the axis Oz: the angular velocities of precession of the gyros with respect to the platform, $\dot{\delta}_1, \dot{\delta}_2$; the moments of correction L_{k1}, L_{k2} ; the moments of friction of the axes of precession of the gyros, l_{p1}, l_{p2} .

The relieving moments L_{p1} and L_{p2} will act about the axis of suspension of the platform I and II in the sense that will respectively bring about the elimination of the angles δ_1 and δ_2 .

We shall consider that about these same axes of the platform suspension there act the disturbing moments L_{w1}, L_{w2} in the sense opposite the corresponding relieving moments.

The remaining quantities presented in Fig.12.8 need no explanation.

Neglecting, as usual, the nutational motions, the required equations of motion of the gyro horizon are obtained by us by setting the sum of the outer of the external and gyroscopic moments equal to zero, that is, from the equations

$$\left. \begin{aligned} L_x + L_{jx} &= 0. \\ L_y + L_{jy} &= 0. \\ L_z' + L_{jz}' &= 0. \\ L_z'' + L_{jz}'' &= 0. \end{aligned} \right\} \quad (12.1)$$

where L_x, L_y - sums of projections of external moments on platform axis Ox, Oy;

L_{jx}, L_{jy} - sums of projections of gyroscopic moments on these same axes;

L_z', L_z'' - moments of external forces acting about the axes of precession 1 and 2, respectively;

L_{jz}', L_{jz}'' - gyroscopic moments acting about these same axes.

From Fig.12.7 we have, in the absence of the gyros 1' and 2', and retaining, as usual, our assumption that the angles α and β are small,:

STAT

$$\left. \begin{aligned} L_x &= L_{p1} - L_{g1} + L_r \operatorname{sign} \dot{\beta}, \\ L_y &= L_{p2} - L_{g2} - L_r \operatorname{sign} \dot{\alpha}. \end{aligned} \right\} \quad (12.2)$$

$$\left. \begin{aligned} \dot{L}_x &= L_{a1} - l_r \operatorname{sign} \dot{\delta}_1, \\ \dot{L}_y &= L_{a2} - l_r \operatorname{sign} \dot{\delta}_2, \\ L_{jx} &= H_1 \dot{\delta}_1 - H_2 \dot{\delta}_2 \dot{\delta}_2, \\ L_{jy} &= -H_2 \dot{\delta}_2 + H_1 \dot{\delta}_1 \dot{\delta}_1, \\ \dot{L}_{jx} &= H_1 \dot{\beta}, \\ \dot{L}_{jy} &= H_2 \dot{\alpha}. \end{aligned} \right\} \quad (12.3)$$

In the third and fourth expression of eq.(12.3), the last terms express the effect of the additional reaction of the stabilizing gyros in the case of their deviation from the axes of the equilibrium position in response to a load about axes of measurement that "do not belong to them".

Hereafter we shall omit these terms, both because they are small by comparison with the first terms, and also because these terms might in general be wiped out, as stated above, if we use for each axis not one stabilizing gyroscope but two of them with their kinetic moments oppositely directed, as shown in Fig.12.7.

We shall take the characteristics of the correction and relieving moments as proportional, and shall consider that each correcting moment depends not on a single angle of disturbance of the platform, but on both angles, as proposed by Bulgakov and Roytenberg.

As a result we get

$$\left. \begin{aligned} L_{p1} &= S_1 \delta_1, \\ L_{p2} &= S_2 \delta_2, \\ L_{a1} &= k_1 \beta + C_1 \alpha, \\ L_{a2} &= k_2 \alpha - C_2 \beta. \end{aligned} \right\} \quad (12.4)$$

where S , k , and C are constants; the minus sign before C_2 is taken for reasons that

will be clear later.

On the basis of eqs.(12.4), (12.3) and (12.2), the equations of motion of the gyro platform are now rewritten in the following form

$$\begin{aligned} H_1 \dot{\delta}_1 + S_1 \delta_1 + L_1 \text{sign } \dot{\beta} - L_{w1} &= 0; \\ -H_2 \dot{\delta}_2 - S_2 \delta_2 - L_2 \text{sign } \dot{\alpha} + L_{w2} &= 0; \\ H_1 \dot{\beta} + k_1 \beta + C_1 \alpha - l_1 \text{sign } \dot{\delta}_1 &= 0; \\ H_2 \dot{\alpha} + k_2 \alpha - C_2 \beta - l_2 \text{sign } \dot{\delta}_2 &= 0. \end{aligned}$$

We shall consider, further, that

$$H_1 = H_2 = H; \quad k_1 = k_2 = k; \quad S_1 = S_2 = S; \quad C_1 = C_2 = C.$$

Bearing all this in mind, by dividing all the equations by H and using the following notation

$$\frac{k}{H} = \varepsilon; \quad \frac{S}{H} = \lambda; \quad \frac{C}{H} = \mu; \quad \frac{L_w}{S} = \omega; \quad \frac{L_p}{S} = \Delta; \quad \frac{l_p}{k} = \rho.$$

we get

$$\left. \begin{aligned} \dot{\delta}_1 + \lambda \delta_1 &= \lambda \omega_1 - \lambda \Delta_1 \text{sign } \dot{\beta}; \\ \dot{\delta}_2 + \lambda \delta_2 &= \lambda \omega_2 - \lambda \Delta_2 \text{sign } \dot{\alpha}; \\ \dot{\beta} + \varepsilon \beta + \mu \alpha &= \varepsilon \rho_1 \text{sign } \dot{\delta}_1; \\ \dot{\alpha} + \varepsilon \alpha - \mu \beta &= \varepsilon \rho_2 \text{sign } \dot{\delta}_2. \end{aligned} \right\} \quad (12.5)$$

The first two equations of eqs.(12.5) are the equations of precession of the gyros with respect to the platform. As follows from their form, at $L_{w1} = L_{w2} = 0$, $\omega_1 = \omega_2 = 0$, δ_1 and δ_2 will approach the values

$$\begin{aligned} \delta_{10} &= \mp \Delta_1, \\ \delta_{20} &= \mp \Delta_2. \end{aligned}$$

by an exponential law.

For a sufficiently large value of S , Δ_1 and Δ_2 will be small, and we may consider that, in this case, the values of δ_1 and δ_2 will always differ only little from zero.

For an L_{w1} and L_{w2} different from zero and constant in value, δ_1 and δ_2 will approach the values

$$\delta_1 = w_1 + \Delta_1;$$

$$\delta_2 = w_2 + \Delta_2.$$

by the same law

Thus the disturbing moments acting on the platform about the axes of its suspension, will lead to the establishment of non-null values of δ_1 and δ_2 , which is of no importance with respect to the measuring demands that the instrument must meet. Moreover, at a large value of S , the values of w_1 and w_2 may be made sufficiently small.

For L_{w1} and L_{w2} of the variables, the values of δ_1 and δ_2 will also vary accordingly. This again will be of no practical importance. Moreover, for a large value of S , the limits of these variations of δ_1 and δ_2 may be sufficiently restricted.

The second two equations (12.5) are the equations of precession of the platform. Let us assume $C = 0$, whence it follows that $\mu = 0$ as well. This condition corresponds to the connection of the signal transmitters with the moment transmitters of the corrector according to the principles of the ordinary corrector.

Then these equations are rewritten in the following form:

$$\begin{aligned} \dot{\beta} + \epsilon\beta &= \epsilon\rho_1 \text{sign } \delta_1, \\ \dot{\alpha} + \epsilon\alpha &= \epsilon\rho_2 \text{sign } \delta_2. \end{aligned} \quad (12.6)$$

If we take the moments of friction about the axes of precession of the stabilizing gyros as equal to zero: $\rho_1 = \rho_2 = 0$, then, in this case, the disturbances α and β of the platform will approach zero values by an exponential law, according to

STAT

the form of eq.(12.6), regardless of whether any load moments act on the platform or not.

In fact, the moments of friction about these axes of precession will not be equal to zero, and, consequently, there will arise a corresponding error in the position of the platform. But the position of the platform, as before, will not depend on the load on it.

Let us now assume that, on the contrary, $C \neq 0$, $k = 0$, which will correspond to a permutation of the connections between the signal transmitters and the moment transmitters of the correction by comparison with the preceding case.

In this case the equations of motions of motions of the platform are rewritten in the following form:

$$\begin{aligned}\dot{\beta} + \mu z &= \lambda \rho_1 \operatorname{sign} \dot{\delta}_1, \\ \dot{\alpha} - \mu \beta &= \lambda \rho_2 \operatorname{sign} \dot{\delta}_2.\end{aligned}$$

where

$$\mu = \frac{I_p}{C}.$$

This equation corresponds exactly to the equations of motion of the undamped gyropendulum, and for this reason it is possible to select a period of precession such that compensation of the ballistic deviations is accomplished. The condition of compensation of the ballistic deviations is written in the following form:

$$\mu = \sqrt{\frac{R}{L}}. \quad (12.7)$$

If we select μ according to eq.(12.7) and still hold $k \neq 0$, that is, if we maintain the equations of motions of the platform according to the form of the last two equations of eqs.(12.5), then we get something like a damped gyro pendulum in which, with the proper selection of k , the conditions of the compensation of the

ballistic deviations may be maintained to a sufficient degree.

BIBLIOGRAPHY

1. Bulgakov, B.V. - Applied Theory of the Gyroscope. GONTI, 1939.
2. Bulgakov, B.V. and Roytenberg, Ya.N. - Contribution to the Theory of the Power Gyroscopic Horizon. Izv. AN SSSR, Otd. tekhn. nauk, No. 3 (1948).
3. Bulgakov, V.V. and Tikhmenev, S.S. - Theory of Sperry Gyro Horizon with Pendulum Airblast Corrector. Uch. zap. Mosk. Gos. Univ. No. 7 (1937).
4. Braslavskiy, D.A., Logunov, S.S., Pel'por, D.S. - Calculation and Design of Aviation Instruments. Oborongiz, 1954.
5. Bromberg, P.V., Pel'por, D.S. - Theory of Aviation Verticals. Publishing Department, BNT, 1948.
6. Zhukovskiy, N.Ye. - Complete Collected Works. Lectures, No. 2. 1939.
7. Krasovskiy, A.A. - Vibrational Linearization of Certain Nonlinear Systems. Avtom. i Telemekh. No. 1 (1948).
8. Krylov, A.N. - General Theory of Gyroscopes. AN SSSR, 1932.
9. Kudrevich, B.I. - Additional Questions in the Theory of the Gyro Compass and Gyro Vertical. Voenmorizdat, 1945.
10. Levental', Ye.B. - Effect of Vibrations of Pendulum Shutters. Techn. Indust. No. 7 (1939).
11. Ol'man, Ye.V., Solov'yev, Ya.I., Tokarev, V.P. - Autopilots. Oborongiz, 1946.
12. Pel'por, D.S. - The Damping Gyroscope. Vest. inzh. i tekhn. No. 4-5 (1946).
13. Roytenberg, Ya.N. - The Multigyro Vertical. Prikl. matem. i mekh. 10 (1) (1946).
14. Solov'yev, Ya.I. - Gyroscopic Instruments and Autopilots. Oborongiz, 1947.
15. Fridlender, G.O. - The Cardan Error of the Directional Gyro. Techn. Indust. No. 8 (1940).

STAT